



HAL
open science

Toxicologie pulmonaire de nanoparticules biodégradables : effets cytotoxiques et inflammatoires sur cellules épithéliales et macrophages

Nadège Grabowski

► **To cite this version:**

Nadège Grabowski. Toxicologie pulmonaire de nanoparticules biodégradables : effets cytotoxiques et inflammatoires sur cellules épithéliales et macrophages. Médecine humaine et pathologie. Université Paris Sud - Paris XI, 2013. Français. NNT : 2013PA114845 . tel-01016697

HAL Id: tel-01016697

<https://theses.hal.science/tel-01016697v1>

Submitted on 1 Jul 2014

HAL is a multi-disciplinary open access archive for the deposit and dissemination of scientific research documents, whether they are published or not. The documents may come from teaching and research institutions in France or abroad, or from public or private research centers.

L'archive ouverte pluridisciplinaire **HAL**, est destinée au dépôt et à la diffusion de documents scientifiques de niveau recherche, publiés ou non, émanant des établissements d'enseignement et de recherche français ou étrangers, des laboratoires publics ou privés.

UNIVERSITÉ PARIS-SUD 11

ECOLE DOCTORALE :

INNOVATION THÉRAPEUTIQUE : DU FONDAMENTAL A L'APPLIQUÉ

PÔLE : PHARMACOTECHNIE ET PHYSICO-CHIMIE PHARMACEUTIQUE

DISCIPLINE :

Pharmacotechnie et Biopharmacie

ANNÉE 2013 - 2014

SÉRIE DOCTORAT N° 1254

THÈSE DE DOCTORAT

soutenue le 13/12/2013

par

Nadège GRABOWSKI

Toxicologie pulmonaire de nanoparticules biodégradables
Effets cytotoxiques et inflammatoires
sur cellules épithéliales et macrophages

Directeur de thèse : Elias FATTAL Pr. (UMR CNRS 8612)
Co-directeur de thèse : Hervé HILLAIREAU M.C.U. (UMR CNRS 8612)

Composition du jury :

Présidente du Jury : Saadia Kerdine-Romer Pr. (INSERM U996)
Rapporteurs : Jorge Boczkowski D.R. (INSERM U955)
Françoise PONS Pr. (UMR CNRS 7199)
Examineurs : Didier Bazile Chercheur (Sanofi-Aventis, Vitry-Sur-Seine)
Stéphanie Briancon Pr. (UMR CNRS 5007)

A Elodie, petit ange, rappelée à Dieu à l'aube de ta vie.

Pas un jour ne passe sans que j'aie une pensée pour toi.

A ma mamie Hélène, qui m'a fait grandir, et qui me manque tant.

A mon père, parti trop tôt,

Sans avoir pu m'apprendre tout ce qu'un père apprend à sa fille.

A mon papi Jean, qui m'a transmis le gène de la science.

*A tous les doctorants,
Les déjà diplômés, ceux en souffrance et les futurs
Au-delà des domaines et des sujets de recherche*

*A tous les chercheurs qu'il m'a été donné la chance
de rencontrer au cours de ces trois années*

La thèse

Un jour, quelqu'un m'a dit, « Une bonne équipe commence par la solidarité », et c'est exactement ce que j'ai appris au cours de ces trois années...

Beaucoup nous demande « Qu'es-ce que la thèse » ? Nous répondons rapidement que c'est un rassemblement d'expériences en labo, de recherches biblio, et puis de rédaction, mais finalement, en réalité, la thèse est avant tout une expérience humaine qui rassemble les doctorants de toutes disciplines, peu importe leur domaine et leur sujet de recherche.

Le doctorat nous pousse dans nos retranchements, nous amène à dépasser nos limites. Au cours des ces 3, 4, voire 5 années, nous traversons des périodes de doutes, lorsque les manip ne donnent rien, nos capacités et connaissances sont sans arrêt remises en question. Et pourtant, la joie finie par prendre le dessus, quand enfin nous obtenons quelque chose d'exploitable, et que notre nom fait son entrée dans la communauté scientifique. Mais, plus que les connaissances que nous acquérons, c'est une formidable aventure humaine. Nous tissons des liens exceptionnels avec les gens qui nous entourent, doctorants actuels ou déjà diplômés, des liens, qui nous le savons, survivront aux années. Nous créons des liens fraternels au-delà de nos origines et de nos attentes pour nos vies futures, unis par la difficulté que le projet nous impose, et que seuls les gens qui le vivent ou qui l'ont vécu comprennent.

A la question que tous les étudiants de master qui franchissent la porte du laboratoire nous posent « Recommencerais-tu ? », il ne faut penser qu'à la finalité, et à la joie du travail accompli pour leur répondre « oui », et leur donner l'envie de tenter cette expérience, qui nous a, sans aucun doute, construit pour le restant de notre vie de chercheur, mais aussi pour notre vie personnelle.

Remerciements

Pour commencer, je tiens à remercier chaleureusement mon très cher directeur de thèse, le Pr Elias Fattal de m'avoir donné l'opportunité de conduire mon doctorat au sein de son unité, et de son équipe des « Fragiles » après m'avoir acceptée en master 2. J'ai pu me construire un métier et un avenir. Le labo fut ma maison, l'équipe ma famille au cours de ces presque 4 années, que nous allons prolonger un peu !

Je souhaite également remercier tout aussi chaleureusement le Dr Hervé Hillaireau, mon encadrant direct au cours des ces années de doctorat, qui ont fait suite à mon master. Les longues discussions scientifiques, sa rigueur scientifique, et tout son savoir faire ont fait de moi une jeune chercheuse, et je m'efforcerais de transmettre à mon tour toutes ces qualités (probablement dans la recherche privée !).

Je remercie également le Dr Nicolas Tsapis, pour toutes les connaissances scientifiques dont il m'a fait part, sa précieuse aide dès qu'un problème se présent au laboratoire, ou sur un ordinateur, et surtout pour son coaching pendant la rédaction (il faudrait songer à créer une PME...).

Je remercie également les Pr Saadia Kerdine-Römer et Marc Pallardy, pour m'avoir permis de réaliser les manip d'immunologie au sein de leur unité, et de m'avoir en quelque sorte enseigné cette matière. Merci Saadia d'également de prendre part à mon jury de thèse.

Je voudrais remercier le Pr Françoise Pons et le Dr Jorge Boczkowski d'avoir accepté d'être les rapporteurs de ce manuscrit, qui rassemble les résultats obtenus au cours de ces années. Mr Boczkowski vous m'aviez déjà fait l'honneur de participer à mon comité de mi-thèse, j'espère que la suite des travaux a pris une bonne tournure !

Je tiens également à remercier le Pr Stéphanie Briançon et Dr Didier Bazile d'être les rapporteurs de ce travail. Pr Briançon, je tenais à ce que vous preniez part à ce jury, pour « boucler la boucle » !

Je souhaite également remercier le Dr Juliette Vergnaud qui m'a beaucoup aidé au cours de ces années, avec de longues discussions que j'ai beaucoup appréciées. Je te remercie également d'avoir relu une partie de ces travaux, ton œil extérieur m'a été très utile !

Je souhaite remercier Simona Mura et Letícia Aragão Santiago, avec qui j'ai eu la chance de travailler au cours de ce projet. Ces nanoparticules de PLGA n'ont plus aucun secret pour

nous !! Osons croire à la science, et imaginons les administrées à des patients lorsqu'un de nos successeurs les aura chargées d'une molécule active efficace !

Je souhaite adresser un très grand merci à Amélie Dufay-Wojcicki, Nadia Abed et Valentina Agostoni, avec lesquelles j'ai pu discuter pendant de nombreuses heures de mes manips, et qui m'ont fait partager tout leur savoir en biologie, immuno et toutes ces autres sciences qui étaient pour moi un grand mystère ! Je tiens également à remercier Odile Diou et Bénédicte Sacko-Pradines qui furent là dès le début, Giovanna Giacalone pour sa bonne humeur et son rire qui habite les couloirs, et Violeta Rodriguez (et ton petit accent que tu ne dois jamais abandonner !). Nous sommes devenues plus qu'amies, nous sommes une famille, et votre présence m'a permis de faire face aux difficultés de la thèse.

Je tiens à remercier toutes les personnes qui sont passées un jour par l'UMR, et avec lesquelles nous avons beaucoup partagé, à la bière du jeudi soir, celle du vendredi soir, et celle du samedi soir ! Il y a eu tous ceux qui ont vécu au sein de l'équipe V (The best of course !) Patricia, Thaïs, Chantal, Nathalie, Mounira, Ludivine M, Gopan, Naïla, Inah, Minh, Regina, Romain, Ambre, Walhan, Christian et tous les autres, Ludivine B. mon alliée de culture cellulaire, Bettina, Bénédicte, Dario, Laura, Hubert, Olivier, Silvia, Resmi, Zoltàn et Ahmet « the cyclon guys », Claire, Dunja, Daniel ; la team de la tour B Katia, ma compagne de TP, Elise, Floriane, Hélène, Christelle, Claudio et Junior « the best friends », ainsi que les gens que j'ai eu l'occasion de rencontrer à ULLA, Zeina, qui par la suite fut toujours présente pour m'accueillir dans son labo, et pour discuter de mes manips, Massaba, Evelia, Bret. J'adresse une pensée à ceux que j'aurai bien malgré moi oublié de citer.

Je voudrais également remercier les personnels statutaires de l'UMR, Patricia Livet, la psy de l'unité, toujours prête à m'écouter et à activer mon badge 1632 – l'extension de ma poche- et faire accepter ma voiture sur le parking le week end, Dominique Martin pour son sourire matinal et quotidien accompagné de son « Bonjour ma bichette », Hélène Chacun et Christian Ducas pour leur bonne humeur, et Sylvie Zemmour qui à toujours passé mes commandes urgentes... en urgence !

Enfin cette thèse n'aurait pu être sans toutes les cellules THP-1 et A549 que j'ai entretenues en musique, et malmenées au cours des expériences, ni mon petit joujou préféré, le cytomètre ! Merci à Youtube pour les longues heures d'écoute de Maurice El Medioni, El Gusto, Chopin et Beethoven, tout au long du traitement des données et de la rédaction !

Et comme on le dit si bien, gardons le meilleur pour la fin, je souhaite remercier tous les membres de ma famille et en particulier ma mère, ma sœur et ma grand-mère pour leur soutien au cours de toutes ces années d'études et de vie. Sans elles, je ne serais pas qui je suis, et je ne serais pas où je suis. Maman, tu es mon modèle, tu as fait face à tout ce que la vie t'a fait subir, et tu t'es toujours sortie la tête haute. Mamie, je ne sais pas si la génétique le prouvera un jour, mais tu m'as transmis le gène de la science lorsque nous avons observé ensemble ce pou au microscope que tu avais dérobé à la fac !

Remerciements	5
Table des matières	9
Abréviations	11
Introduction générale	15
Travaux antérieurs	19
Evaluation and characterization of lung toxicity of biodegradable nanoparticles	21
Introduction	21
1. Structure of the respiratory tract	23
1.1. Anatomy	23
1.2. Histology	24
2. Clearance mechanisms in lungs	26
3. Nanoparticles for lung drug delivery	27
3.1. Nanoparticles	27
3.2. Administration modes in lung delivery	28
3.2.1. Delivery under liquid form	29
3.2.2. Delivery under solid form: Trojan microparticles	29
3.3. Fate of nanomedicine after pulmonary	32
3.3.1. <i>In vivo</i> biodistribution	32
3.3.2. Translocation	34
3.3.3. Mechanisms of cellular uptake <i>in vitro</i> and <i>in vivo</i>	34
4. Toxicity endpoints	36
4.1. Cell integrity	36
4.2. Apoptosis detection	38
4.3. DNA damage – Genotoxicity	38
4.4. Oxidative stress assay	39
4.4.1. Reactive Oxygen Species	40
4.4.2. Reactive Nitrogen Species	40
4.4.3. Superoxide Dismutase	41
4.4.4. Glutathione	41
4.5. Inflammatory response	42
4.5.1. Cytokine assay	42
4.5.2. Complement activation	43
4.5.3. Polymorphonuclear counting in bronchoalveolar lavages	43
4.6. Mucus interactions	43
5. Models for lung nanotoxicology: <i>in vitro</i> , <i>ex vivo</i> , <i>in vivo</i>	44
5.1. <i>In vitro</i> cell culture for nanoparticle toxicity studies	45

5.2. Co-culture of lung cells in nanotoxicology	47
5.3. <i>Ex vivo</i> models	50
5.3.1. Isolated perfused lungs	50
5.3.2. <i>Ex vitro</i> mucus models	52
5.4. <i>In vivo</i> models	52
5.5. Compared <i>in vitro</i> / <i>ex vivo</i> / <i>in vivo</i> nanotoxicity studies	53
Conclusion	55
Travaux expérimentaux	74
Chapitre 1: Toxicité de nanoparticules de PLGA de charge de surface variée vis-à-vis de cellules épithéliales alvéolaires pulmonaires humaines	77
Article 1: Toxicity of surface-modified PLGA nanoparticles towards lung alveolar epithelial cells	80
Chapitre 2 : Le recouvrement de surface des nanoparticules de polymère joue un rôle clef dans la toxicité vis à vis de macrophages dérivés de monocytes humains	106
Article 2: Surface-coating mediates the toxicity of polymeric nanoparticles towards human-like macrophages	109
Chapitre 3 : Co-culture de cellules épithéliales alvéolaires pulmonaires humaines et de macrophages : Un outil <i>in vitro</i> pertinent et efficace en nanotoxicologie	134
Article 3: Evaluation and characterization of lung toxicity of biodegradable nanoparticles	137
Discussion générale	167
Conclusions et perspectives	190

Abbreviations / Abréviations

7-AAD	: 7-Aminoactinomycin D
AF488	: AlexaFluor 488
AM	: Alveolar macrophage / Macrophage alvéolaire
ANR	: Agence Nationale de la Recherche
ANSES	: Agence Nationale de la Sécurité Sanitaire, de l'Alimentation, de l'Environnement et du travail
AT	: Alveolar type / Type alvéolaire
ATP	: Adenosine triphosphate
BAL	: Broncho Alveolar Lavage / Lavage Broncho-alvéolaire
BALF	: Broncho Alveolar Lavage Fluid
BALT	: Bronchial Associated Lymphoid Tissue
BSA	: Bovine Serum Albumin
CBA	: Cytometric Beads Array
CDX	: Cluster of differentiation number X
CFSE	: 5-(and 6)-Carboxyfluorescein diacetate succinimidyl ester
Chol	: Cholesterol
CLSM	: Confocal Laser Scanning Microscopy
CS	: Chitosan / Chitosane
DAPI	: 4',6'-diamidino-2-phénylindole
DCF	: 2',7'-dichlorofluorescein
DCP	: Dicetylphosphate
DMSO	: Dimethylsulfoxyde
DOPE	: 1,2-Dioleoyl-sn-glycero-3-phosphoethanolamine
DPI	: Dry Powder Inhaler
DPPC	: 1,2-dipalmitoyl-sn-glycero-3-phosphocholine
DTPA	: Diéthylène triamine pentaacétique acid
ELISA	: Enzyme-Linked ImmunoSorbent Assay
FBS	: Fetal Bovine Serum / Sérum de veau fœtal
FDA	: Food and Drug Administration
FITC	: Fluorescence IsoThioCyanate
FL-	: Fluorescence Channel
FSC	: Forward scatter
g	: Gravity / Gravité
GPR	: Glutathione reductase
GPX	: Glutathione peroxidase
GSH	: Reduced Sulfhydryl form glutathione
GSSG	: Oxidized disulfide form glutathione
GST	: Glutathion S-transferase
GS-TNB	: Glutathion derivat (see TNB)
H ₂ DCFDA	: 2',7'-dichlorodihydrofluorescein diacetate
HSPC	: hydrogenated soy phosphatidylcholin
ICAM-	: Intracellular Adhesion Molecule
IFN	: Interferon
IL-X	: Interleukine-X
IPL	: Isolated Perfused Lung
LDH	: Lactate dehydrogenase / Lactate déshydrogénase
LPS	: Lipopolysaccharide

MCP-	: Monocyte chemoattractant Protein
MDI	: Metered Dose Inhaler
MFI	: Mean Fluorescence Intensity
MTS	: 3-(4,5-dimethylthiazol-2-yl)-5-(3-carboxymethoxyphenyl)-2-(4-sulfophenyl)-2H-tetrazolium
MTT	: 3-[4,5-dimethylthiazol-2-yl]-3,5 diphenyl tetrazolium bromide
<i>n</i>	: Number of independent trial
na	: Not applicable / Non applicable
NADPH	: Nicotinamide Adenine Dinucleotide Phosphate-oxidase
NBT	: Nitroblue tetrazolium / Bleu de tetrazolium
nd	: Not determined / Non déterminé
NIR	: Near Infra Red / Proche Infra Rouge
NMR	: Nuclear Magnetic Resonance
NPs	: Nanoparticles / Nanoparticules
NT	: Non treated / Non traitées
<i>p</i>	: Statistic value / Valeur statistique
PBS	: Phosphate Buffer Saline
PC	: Phosphatidylcholine
PE	: Pycoerythrin
PEG	: Polyethylene Glycol
PEI	: Polyethylenimine
PF68	: Pluronic F68 (Poloxamer 188)
PI (IP)	: Propidium Iodide / Iodure de propidium
PLA	: Polylactic acid
PLGA	: Poly(lactide-co-glycolide)
PMA	: Phorbol 12-myristate 13-acetate
PMN	: PolyMorphoNuclear
PS	: Polystyrene / Polystyrène
PVA	: Polyvinyl alcohol / Alcool Polyvinylique
Rhod	: Rhodamine
RNS	: Reactive Nitrogen Species / Espèces Réactives de l'Azote
ROS	: Reactive Oxygen Species / Espèces Réactives de l'Oxygène
SCG	: Single Cell Gel
SD	: Standard deviation / Ecart Type
SLN	: Solid Lipid nanoparticle
SOD	: Superoxide dismutase
SSC	: Side-scatter curves
TB	: Trypan Blue / Bleu trypan
TEER	: Trans Epithelial Electric Resistance
TEM	: Transmission Electronic Microscopy
TNB	: 5-thio-2-nitrobenzoic acid
TNF-	: Tumor Necrosis Factor
WST	: Water soluble Tetrazolium salts
XTT	: 2,3-bis-(2-methoxy-4-nitro-5-sulfophenyl)-2H-tetrazolium-5-carboxanilide

Introduction générale



La nanotoxicologie, nouvelle sous-discipline de la toxicologie, a pour but d'étudier la toxicité de nanoparticules vis-à-vis de l'organisme. L'évaluation de cette toxicité est réalisée par le suivi de plusieurs paramètres, tels que la viabilité cellulaire, la réponse inflammatoire, le stress oxydant ou encore les dommages induits à l'ADN. Parmi les nanoparticules développées, celles conçues pour des nanomédicaments doivent faire l'objet d'études très poussées. Composé de nanoparticules auxquelles sont associées une ou plusieurs substances actives (anticancéreux, antibiotique, protéine, gène), le nanomédicament est capable de transporter ces dernières jusqu'aux cellules/tissus cibles, afin d'augmenter l'efficacité du traitement tout en diminuant la toxicité. Néanmoins, peu d'études se concentrent sur la nanotoxicité de ces vecteurs qui doivent pourtant être le plus inertes possibles vis-à-vis de l'organisme, tout en libérant la substance active au site d'action.

Parmi les différentes voies d'administration des nanomédicaments, la voie pulmonaire est prometteuse car elle présente de nombreux avantages. En effet, en plus d'être non-invasive (comparée à la voie parentérale), les traitements peuvent être délivrés pour des applications locales (traitement de l'asthme ou de la broncho-pneumopathie chronique obstructive) ou systémiques (traitement du diabète). Dans cette dernière perspective, le passage systémique s'effectue grâce aux échanges constants entre les alvéoles et la circulation sanguine. En outre, en raison de la faible activité enzymatique qui règne dans les poumons, les molécules fragiles sont peu dégradées contrairement à d'autres tissus. Enfin, à l'inverse de certains traitements administrés par voie orale, l'effet de premier passage hépatique est évité.

Au sein de l'équipe *Vectorisation pharmaceutique de Molécules Fragiles* de l'*Institut Galien Paris-Sud*, un projet de recherche soutenu par l'ANSES (« Emerging Risks »), l'ANR (2009 CESA) et le Fond Pour la Recherche Respiratoire se concentre sur les études de toxicité pulmonaire *in vitro* et *in vivo* de nanoparticules polymères qui pourraient être utilisées comme vecteurs de substance active. Les nanoparticules sont formulées à base d'un polymère biodégradable et l'ajout de différents polymères stabilisants permet de moduler la charge de surface, sans en modifier la taille. La toxicité *in vitro* vis-à-vis de cellules bronchiques a été précédemment étudiée par Simona Mura et la toxicité *in vivo* (chez la souris) par Letícia Aragão Santiago, chacune au cours de leur stage post-doctoral. L'objectif de ce projet de thèse est d'évaluer la toxicité *in vitro* de nanoparticules vis-à-vis de cellules épithéliales alvéolaires et de macrophages en mono et en co-culture.

La première partie de ce manuscrit consiste en une revue de l'état de l'art de la toxicologie pulmonaire des nanoparticules biodégradables, et sera publiée sous forme d'un chapitre dans le livre « Targeted Drug Delivery Concept and Design », dans la partie « Nanotoxicology and Regulatory Issues » (Elsevier).

La seconde partie, découpée en trois chapitres rédigés sous forme d'articles de recherche, fait état des travaux expérimentaux menés au cours de ce projet de thèse. Le premier chapitre qui étudie la toxicité des nanoparticules vis-à-vis de cellules épithéliales pulmonaires alvéolaires (A549) a récemment été publié. Le deuxième chapitre s'intéresse à la toxicité de ces mêmes nanoparticules vis-à-vis de macrophages humains (différenciés des monocytes THP-1). Le troisième et dernier chapitre décrit l'établissement d'un modèle de co-culture de cellules épithéliales pulmonaires alvéolaires et de macrophages et démontre son intérêt en nanotoxicologie.

Au cours d'une discussion générale, tous les résultats *in vitro* et *in vivo* actuellement obtenus dans le cadre de ce projet nanotoxicologie sont mis en parallèle et discutés, afin de dégager des conclusions générales sur les facteurs modulant la toxicité des nanoparticules.

Travaux antérieurs



La nanotoxicologie est une sous-discipline émergente de la toxicologie relative aux effets délétères des nanoparticules (Donaldson *et al.*, 2004). Les travaux décrits dans le présent chapitre sont centrés sur la nanotoxicologie pulmonaire. Par définition une nanoparticule est un assemblage d'atomes qui possède au moins l'une de ses dimensions dans le domaine du nanomonde ($1 \text{ nm} = 10^{-9} \text{ m}$). Les nanoparticules peuvent être d'origine naturelle, mais le plus souvent elles sont créées par l'homme, de manière intentionnelle ou pas (Andujar *et al.*, 2009). L'exposition pulmonaire qui constitue la voie d'exposition la plus importante peut dans ce sens constituer un danger pour l'être humain si les particules inhalées s'avèrent posséder des effets néfastes. Au niveau de l'arbre pulmonaire, on distingue une forte barrière physiologique qui fait face à la pénétration de petites particules. En effet, les nanoparticules inhalées ont de fortes chances d'être piégées dans la couche de mucus, qui, grâce à l'action de la clairance mucociliaire, seront entraînées vers la sortie. Si l'on se place sur un plan galénique, la voie pulmonaire est très prometteuse pour l'administration des médicaments (Patton and Byron, 2007). Parmi ses nombreux avantages, nous pouvons citer sa grande accessibilité et le fait qu'elle soit non invasive. De plus, grâce à la fine épaisseur des tissus alvéolaires qui sont très vascularisés, les traitements envisagés peuvent être, certes locaux (cancer, mucoviscidose ou tuberculose par exemple), mais également systémiques (diabète). Par ailleurs, les nanomédicaments, composés d'un principe actif et d'un nanovecteur, peuvent être administrés par inhalation ou nébulisation. C'est pour cette raison que nous avons consacré cette revue de la littérature à l'évaluation et la caractérisation de la toxicité pulmonaire des nanoparticules biodégradables qui contrairement aux nanoparticules manufacturées sont peu décrites.

Au cours de ces travaux bibliographiques, l'anatomie et l'histologie de l'arbre pulmonaire ainsi que ses mécanismes de défense sont présentées dans une première partie. Dans une seconde partie, les nanoparticules qui peuvent être utilisées pour l'administration pulmonaire sont détaillées ainsi que les modes d'administration et leur biodisponibilité cellulaire et tissulaire. La toxicité peut être évaluée selon de nombreux paramètres, présentés et expliqués dans une troisième partie. Les tests présentés ont fait l'objet d'études de nanotoxicité concernant principalement les nanoparticules non-biodégradables, mais sont néanmoins transposables aux nanoparticules biodégradables. Enfin, le système pulmonaire humain étant complexe, de nombreux modèles *in vitro*, *in vivo* et *ex vivo* sont utilisés pour le mimer, en partie ou en totalité. Les résultats obtenus après application de nanoparticules biodégradables sur ces différents modèles sont discutés.

En conclusion, nous montrons comment l'ensemble de ces données contribuent à montrer une relative innocuité des nanoparticules biodégradables utilisables par voie pulmonaire.

Evaluation and characterization of lung toxicity of biodegradable nanoparticles

Nadege Grabowski, Hervé Hillaireau, Juliette Vergnaud, Elias Fattal

To be published in Targeted Drug Delivery Concept and Design

Issue « Nanotoxicology and Regulatory Issues »

(Book – Elsevier)

Introduction

The term Nanotoxicology was introduced in 2004 by Donaldson and co-workers (Donaldson *et al.*, 2004) and defined as “a new frontier in particle toxicology relevant to both the workspace and general environment and to consumer safety”. The concept was aiming to create a new sub-discipline in toxicology, meeting specific aspects of nanoparticle toxicity and modifying the existing tests to adapt them to the evaluation of risks associated to nanoparticles (Figure 1).

Nanoparticles are nowadays being used in a large variety of manufactured products, such as electronic components, textile or cosmetics (Mu and Sprando, 2010). In addition, very promising applications in medicine have been highlighted in diagnostic and therapeutic. For such purposes, nanoparticles can enter the organism using different routes such as inhalation, oral ingestion, dermal or parenteral route. Despite a high number of promises for therapeutics and diagnosis, nanoparticles are potentially able for each of these routes of administration to induce adverse effects and toxicity. Among all the tissues susceptible to be affected by nanoparticle interaction are the lungs which have been widely explored, mostly for inorganic nanoparticles (Choi *et al.*, 2009). A large number of *in vitro* and *in vivo* studies have reported cytotoxic effects, inflammatory and oxidative stress responses from lung cells after exposure to particulate matter, silica (Lin *et al.*, 2006), titanium dioxide (Wang *et al.*, 2008, Bhattacharya *et al.*, 2009), gold and silver (Bachand *et al.*, 2012) nanoparticles. The involuntary inhalation of these materials through accidental exposure represents therefore a high source of toxicity. Nevertheless, the pulmonary route is also an interesting non invasive route of administration for drug delivery (Patton *et al.*, 2004). Both local and systemic treatments can be considered taking advantage of the lungs' large absorption surface area (around 140 m²), and high vascular permeability with continuous exchanges between alveoli

and blood (Patton, 1996). In addition, the weak enzymatic activity present in lungs is relevant for administration of poorly stable drugs (peptides / proteins). Administration of drug loaded nanoparticles can lead to several advantages. Ideally, nanoparticles will not only protect drug against degradation and transport it to target cells, but also allow a sustained drug release, decreasing the frequency of administration and subsequent risk of side effects (Sung *et al.*, 2007). Nanomedicine can be delivered to the lungs by nebulization of an aqueous nanoparticle suspension or aerosolization of a dry powder of nanoparticles. However, because of their small size, solid nanoparticles are eliminated by the mucociliary clearance and only low amounts reach the alveoli. Diverse processes have been employed to transform nanoparticles into ephemeral microparticles that can first go deeper into the lungs and secondly turn into nanoparticles once in contact with biological fluids (Tsapis *et al.*, 2002).

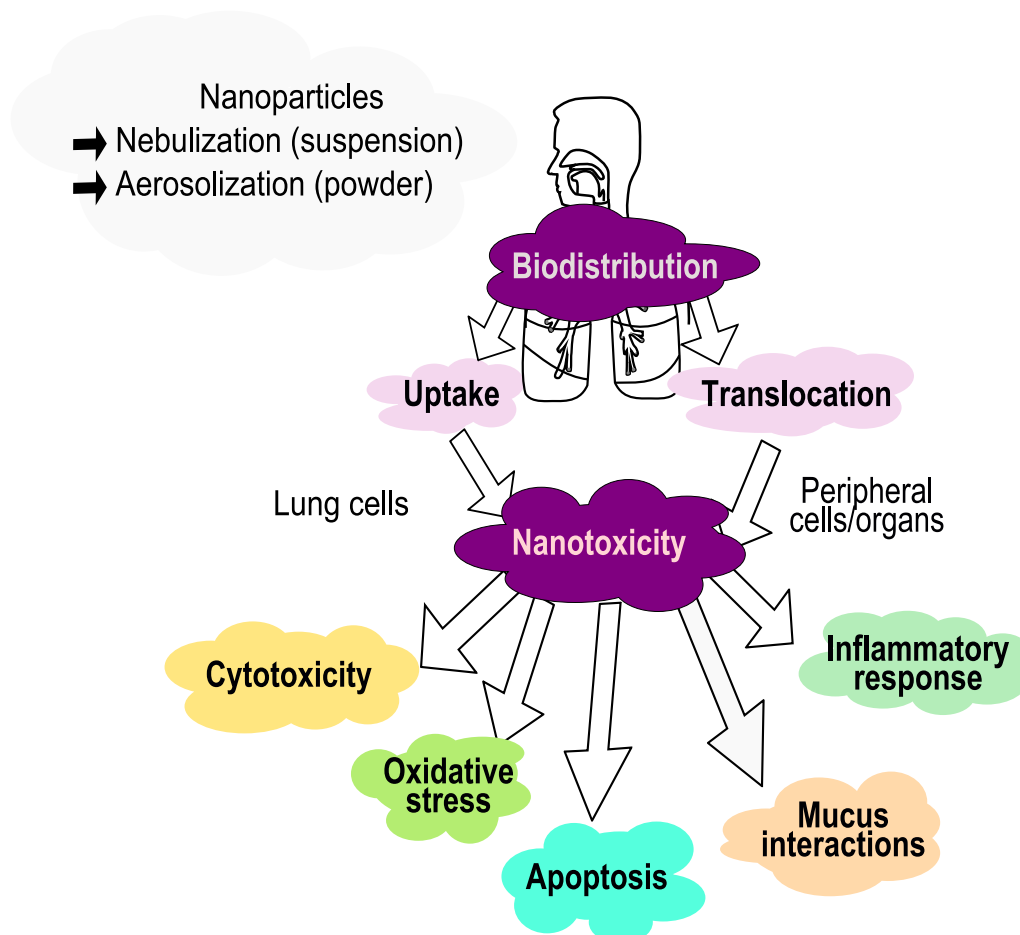


Figure 1. General roadmap to assess lung nanotoxicology.

A large variety of nanoparticles can be used to prepare nanomedicines (Mansour *et al.*, 2009). Polymer-based nanoparticles, solid lipid nanoparticles (SLN) and liposomes have all been

investigated for lung delivery of antibiotics, anti-inflammatory, antineoplastic compounds or hormones. However, a small number of nanoparticles have been so far proposed as tool to lung cancer diagnosis by local delivery (Yang *et al.*, 2010, McIntire *et al.*, 1998).

The question of whether nanomedicines are safe remains debated. For this purpose, toxicity studies should be carried out *in vitro*, *in vivo* or *ex vivo* after exposure to nanomedicine. Toxicity encompasses different mechanisms, from cellular viability, to inflammatory response, oxidative stress induction and DNA damage that should be deeply investigated.

In the present chapter, the pulmonary tract architecture and its strong defense barriers are firstly presented. Secondly, nanoparticles used for lung delivery, and their administration modes are detailed. The toxicity tests used to investigate toxicity of nanoparticles and the large variety of pulmonary tract models developed so far are then illustrated by their application for the evaluation of nanoparticle toxicity.

1. Structure of the respiratory tract

1.1. Anatomy

The respiratory tree is in charge of bringing oxygen to the body and removing carbon dioxide through continuous gas exchanges with blood circulation. The lung volume is included in the range of 2.5 (children) to 7 liters (adults) depending on the size lung (Weibel and Gomez, 1962). According to the model proposed by Weibel (Weibel and Gomez, 1962), the respiratory tree is a hierarchical and symmetric network, divided into 24 generations, beginning with the trachea (generation 0) and ending with alveolus (generation 23). Each airway is divided into two airways increasing the specific surface, to carry the air up to alveolar ducts where gas exchanges occur. During each breath, inhaled air is transported to the conductive zone (generations 0 to 4), including the trachea and bronchus that divides into two distal bronchi (dichotomy), in order to reach the respiratory zone. As reviewed by Shelly *et al.* (Shelly *et al.*, 1988), the temperature and the moisture of alveolar gases are essential parameters in normal lungs to maintain physiological conditions. Conditions of optimal inhaled air were determined as 100 % of humidity, and a temperature closed to the body (Tsuda *et al.*, 1977), modulated by the nose and the upper respiratory tract.

While the conductive zone represents 10 % of the lung volume, the respiratory zone represents the lasting 90 % (Weibel and Gomez, 1962). The respiratory zone is composed of

300 million alveoli and 14 million alveolar ducts. The average alveolar diameter in human lungs is in the range of 250 to 290 μm , among the lung volume. With an average diameter of 400 to 450 μm , 3-4 generations of alveolar ducts are terminating in alveolar sacs that have exactly the same structure. In addition, 3 generations of respiratory bronchioles, with an average diameter of 500 μm , are proximal to alveolar ducts. Blood vessels follow exactly the same pattern than the bronchial tree, with similar dimensions. The pulmonary arteries divide into 28 generations, with an average diameter of 15 to 25 μm . In the respiratory zone, 277 billions of capillary segments, with an average diameter of 8.3 μm create a total tissue-blood interface (or alveolar capillary surface) of 60 to 80 m^2 .

1.2. Histology

The bronchial epithelium is pseudostratified and is composed of four cell types: basal cells, ciliated cells (allowing mucus elimination), goblet cells (secreting mucus) and Clara cells (producing mucus, pulmonary surfactant proteins and cytokines, and involved in epithelium regeneration) (Figure 2). The epithelium thickness is close to 60 μm and covered with 2-10 μm of an airway fluid (Patton and Byron, 2007, Rubin, 2002). The latter is composed of 2 layers cleared by ciliary beating, the mucus, and the periciliary fluid (consisting of water layer that cover cilia cells on apical surface) separated by a surfactant layer (Matsui *et al.*, 1998). Mucus from healthy human lungs is nonhomogeneous and viscous (rheology of a crossed linked gel) with a pH ranging from 7 to 8.5. Biochemical analyses have shown that human mucus samples are mostly made of water, containing 7 % solids, 8 to 20 % mucins and less than 1 % DNA. Secreted mucins (glycoproteins) form a 3-dimensional polymer meshwork able to trap particles (Rubin, 2002), with pores from 10 to 100 nm (Schuster *et al.*, 2013). Mucins are made of 70-80 % carbohydrates, 20 % proteins and 1-2 % sulfates. 8 proteins encoded as MUC are present in mucus layer, with a large majority of MUC5AC (~80 %) and MUC5B (~20 %) (Rubin, 2002) expressed by goblet cells and glandular mucous cells respectively (Groneberg *et al.*, 2002). In terminal bronchus, the epithelium has a cuboid shape with a thickness of 10 μm , is covered with 3 μm of airway fluid and is composed of ciliated and Clara cells (Patton and Byron, 2007).

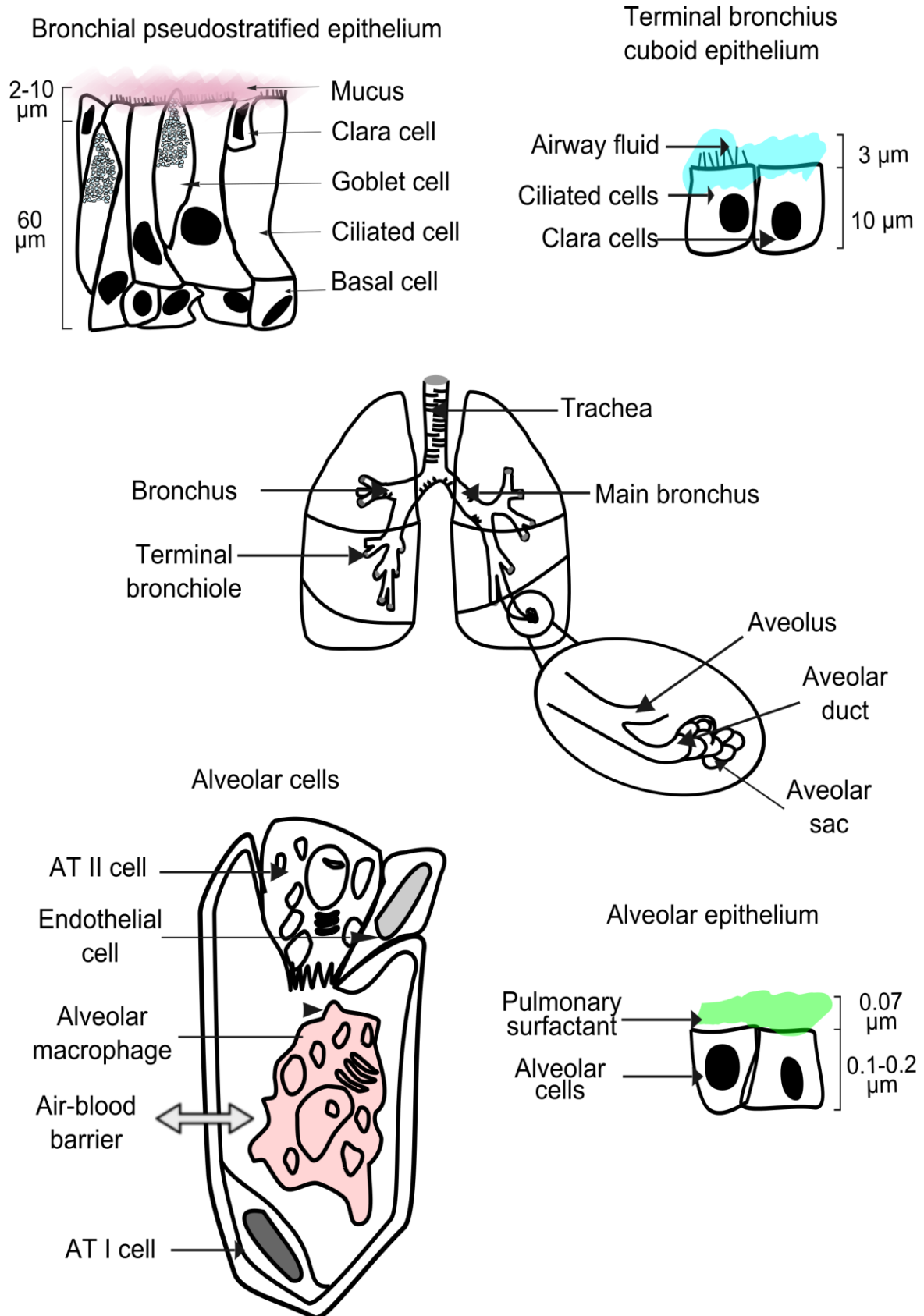


Figure 2. Structure of the respiratory tract and cellular composition of human lung bronchial / terminal bronchial and alveolar epithelia. (ATI/II, Alveolar Type I/II cells).

Alveolar type I cells (8 %) involved in gas exchanges co-exist with alveolar macrophages (3-5 %, up to 19 % in smoker subjects), alveolar type II cells (16 %, cover 7 % of the alveolar surface), capillary endothelial cells (30 %) and cells in the interstitial spaces (37 %) (Sherman and Ganz, 1992, Crapo *et al.*, 1982) (Figure 2). The alveolar macrophages perform phagocytosis of foreign particles or pathogens. The endothelial cells, lining lung blood vessels, are highly metabolic and are involved in the circulation of bioactive substances such as peptides, lipids, and prostaglandins. Alveolar type II cells produce lung surfactant components and are involved in the regeneration of type I pneumocyte cells by differentiation. In alveolar ducts, the thickness of the epithelium is around 0.1 to 0.2 μm and covered with 0.07 μm of pulmonary surfactant (Patton and Byron, 2007). The pulmonary surfactant is composed of lipoproteins, 90 % of which are phospholipids and 10 % are surfactant proteins (SP), secreted by type II alveolar cells (Sherman and Ganz, 1992): SP-A (the most abundant), SP-B, SP-C, SP-D. SP-B and SP-C, very small and hydrophobic proteins, reduce the surface tension at the air-liquid interface of the lung, that is essential to avoid collapse. SP-A and SP-C, members of collectin family, participate to the innate immunity, before induction of an antibody-mediated response (Wright, 1997, Sherman and Ganz, 1992). SP-A and SP-C, present also in non-pulmonary sites, are involved in viruses and bacteria uptake by phagocytes (Wright, 2005), and SP-A was shown to be involved in the uptake of nanoparticles covered with different polymers (Ruge *et al.*, 2011).

2. Clearance mechanisms in lungs

Defense mechanisms are both immunological and physiological. The Bronchial Associated Lymphoid Tissue (BALT) plays a major role in the immune response to all kind of antigens, with a local response faster and more protective than those initiated by the systemic system (Randall, 2010). Absent in the lungs of healthy newborn babies, the BALT starts its development after meeting the first antigens. Generally located along the bronchial airways and the airway bifurcations, the BALT contains essentially B lymphocytes, dendritic cells, macrophages, T lymphocytes and M cells (Microfold). M cells present the antigen to dendritic cells that participate in maintaining the alert BALT.

A major clearance mechanism is also achieved physiologically by the mucociliary escalator. Between 2 and 24 h after inhalation, most of the foreign particles are expectorated, with a rate closed to 5 mm/min in peripheral zone and 20 mm/min in trachea (Samet and Cheng, 1994). The second clearance pathway consists in phagocytosis performed by resident alveolar

macrophages (around 10 macrophages per alveoli – 500 millions of alveoli). Particles are then enzymatically degraded or driven out by the mucociliary clearance, or brought to trachea-bronchial lymphatic canals by translocation. Phagocytosis is modulated, not only by particle size, but also by particle geometry (Sahay *et al.*, 2010). Some inhaled particles can be metabolized thanks to detoxification enzymes, such as cytochrome P450, but compared to the other organs such as the liver, this pathway is negligible (Labiris and Dolovich, 2003).

3. Nanoparticles for lung drug delivery

3.1. Nanoparticles

Nanoparticles have been extensively used for lung drug delivery for the administration of a large variety of drugs (anticancer, anti-psychotic, antibiotic, peptide, protein or nucleic acid) that have been loaded into lipid or polymeric nanoparticles (Figure 3) (for review see Beck-Broichsitter *et al.*, 2012, Mansour *et al.*, 2009, Sung *et al.*, 2007). Nanoparticles can induce both local and systemic delivery after release of the encapsulated drug. Major successes were obtained with lipid or polymer nanoparticles. For instance, uni or multilamellar liposomes ranging from 400 nm to 1 μm made from the self organization of glycerophospholipids or non ionic surfactants were produced for lung delivery. One of their major advantages for pulmonary administration is their biocompatibility due to their natural origin and their lipid composition quite often close to the one of the lung surfactant. Liposomes were used to deliver peptides and proteins to the lung (Li *et al.*, 2011) and were already investigated in phase II clinical trials to deliver amikacin (Weers *et al.*, 2009) or ciprofloxacin (Bruinenberg *et al.*, 2010). Furthermore, several studies investigated the potential of solid lipids nanoparticles (SLN) composed of a solid lipid core (dispersed in water) and a shell of stabilizers (soy lecithin or poloxamer) (Schwarz *et al.*, 1994). SLN have shown a great potential for insulin delivery towards lung (Liu *et al.*, 2008).

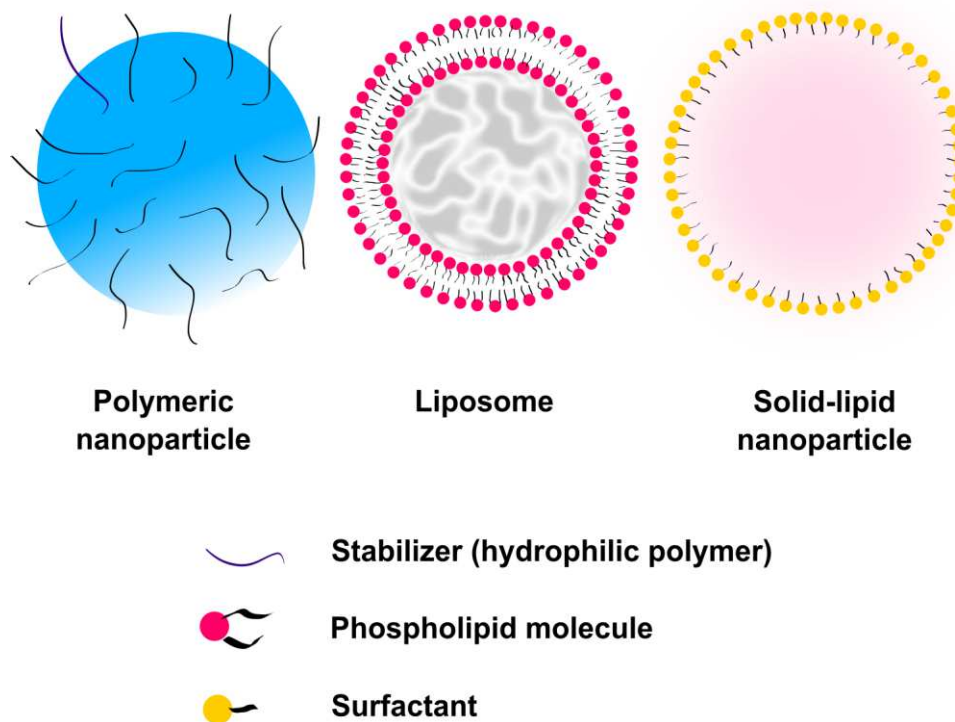


Figure 3. Nanoparticles used for the lung drug delivery.

Last but not least, polymeric nanoparticles are of great interest for lung drug delivery (Ungaro *et al.*, 2012) since they can be tailored from a range of biodegradable polymers, such as poly(lactic acid) (PLA), poly(lactide-co-glycolide) (PLGA), chitosan (Huang *et al.*, 2002), gelatin or alginate (Yang *et al.*, 2010). Stabilizers like polyvinyl alcohol (PVA), chitosan or poloxamers are often required, in order to obtain spheres in the size range of 100 to 250 nm. However, their presence at the surface can modify the cell-nanoparticle interactions and must therefore be carefully investigated. For instance, a large amount of PVA significantly decreases cellular uptake (Sahoo *et al.*, 2002) or the presence of chitosan modulates dendritic cell recognition (Bivas-Benita *et al.*, 2004b). Other surface modification such as PEGylation (using polyethylene glycol (PEG)) of polymeric nanoparticles has been shown to decrease the time of mucus layer crossing (Schuster *et al.*, 2013).

3.2. Administration modes in lung delivery

Nanomedicines can be delivered to the lung by two modes, under liquid (using nebulizers or Metered Dose Inhalers – MDIs) or solid form (using Dry Powder Inhalers – DPIs). Knowing the administration mode is crucial before conducting a nanotoxicity study, since nanoparticle

biodistribution will be different according to their mode of entry, which might impact the type of cells that will be first in contact with nanoparticles.

3.2.1. Delivery under liquid form

Nebulization is the easiest administration mode to deliver aqueous suspensions of nanoparticles or liposomes around 200 nm (Zaru *et al.*, 2007), but it is not convenient for the delivery of large particles (0.3 μm to 3 μm) that can provoke nasal obstructions or be filtered by the nasal mucosa (Schwab and Zenkel, 1998). To achieve nebulization, two devices are available: nebulizers (delivery under controlled rate) and MDIs. The MDI is a pressured device that allows the delivery of uniformed doses of suspension / solution to the patient (Nowacki *et al.*, 1985). Droplets are formed under pressure and further inhaled by the patient. MDI were originally developed to deliver anti-asthmatic treatments. Although there is a little number of applications of MDI for the delivery of nanoparticles, they have demonstrated an interest for the delivery of chitosan nanoparticles to the deep lung (Sharma *et al.*, 2012). On the contrary, nebulization is the preferred mode that in most cases is achieved *in vivo* in small animals (rats and mice) with a specific device, as example the MicroSprayTM aerosolizer (Penn-Century for liquid) which was firstly used to deliver an aerosol of fluorescent nanoparticles to mice (Bivas-Benita *et al.*, 2005). No mortality was induced by the technique, and one day after administration, mice showed full recovery (Bivas-Benita *et al.*, 2005).

3.2.2 Delivery under solid form: the example of Trojan microparticles

Reproducible doses of solid particles can be delivered using DPI (Newhouse, 1992). A special veterinary device is available, called Dry Powder InsufflatorTM Pulmonary Aerosol Kit (Penn-Century for solid) for *in vivo* studies in small animals (Ohashi *et al.*, 2009). However, solid nanoparticles are never used as such in DPI because they are too small to be delivered directly in deep lung regions (*i.e.* alveolar ducts), being eliminated mainly by the mucociliary clearance. To overpass this constraint, different methods have been employed to deliver nanoparticle micro-aggregates that turn into the native nanoparticles once reaching the target (Figure 4). Tsapis *et al.* have proposed to spray-dry nanoparticles into controlled micro-aggregates, called Trojan microparticles (Tsapis *et al.*, 2002) that deliver the initial nanoparticles once in contact with biological fluids. Similarly, insulin was loaded into chitosan nanoparticles (Grenha *et al.*, 2005) and rifampicin (Tomoda *et al.*, 2008), TAS-103

(anticancer drug) (Tomoda *et al.*, 2009), or dexamethasone (Gómez-Gaete *et al.*, 2008) were associated to PVA-coated PLGA nanoparticles. The nanoparticles were spray dried in the presence of trehalose (Tomoda *et al.*, 2008, Tomoda *et al.*, 2009) or 1,2-dipalmitoyl-sn-glycero-3-phosphocholine (DPPC) and haluronic acid (Gómez-Gaete *et al.*, 2008) forming microparticles ranging from 2 to 5 μm . For such aerodynamic diameter values, the deposition in deep lung is favored (Grenha *et al.*, 2005). The efficacy of the decomposition of microparticles into nanoparticles in contact with water is dependent on the spray-dried optimal temperature and the ratio of primary nanoparticles (Tomoda *et al.*, 2008). The size of microparticles is in addition dependent on the diameter of primary nanoparticles. Conversely, when the spray-drying process is performed at optimal temperature, the fine particle fraction is 20 to 30 times higher than those of primary nanoparticles, and is almost not affected by the ratio and the size of primary nanoparticles (Tomoda *et al.*, 2009). However, compared to primary nanoparticles, the drug was released more rapidly. Indeed, during the spray dried process, samples can become amorphous that accelerate the moisture absorption and thus the drug release (Zeng *et al.*, 2007). Shi *et al.* have formed PLGA nanoparticle flocs (Shi *et al.*, 2007). In this process, PLGA nanoparticles were pre-formulated by emulsion / solvent extraction with two oppositely charged polyelectrolytes (PVA vs poly(ethylene-maleic anhydride)) and then mixed in water under controlled rate. Following electrostatic interactions, flocs were formed with a large superstructure which were then freeze-dried to obtain a dried powder formulation. To be delivered in deep lungs, tobramycin was loaded in pre-formulated PLGA nanoparticles embedded into microparticles after a bath in lactose aqueous solution (Ungaro *et al.*, 2012). Microparticles were finally freeze dried to be intratracheally delivered to rats. Last, but not least, the use of large porous effervescent microparticles to deliver ciprofloxacin (Ely *et al.*, 2007) or doxorubicin (Al-Hallak *et al.*, 2012, Kim *et al.*, 2012) to the lung was reported. Primary drug-loaded polymeric nanoparticles (polycyanoacrylate, PLGA) were spray dried with, among other excipients, lactose (charge), ammonia (to ensure pH to 8) that were mixed to citric acid and sodium carbonate that cause effervescence in contact with water. Results have shown that the shape, the size, the density and the fine particle fraction of microparticles are mediated by amounts of lactose, PEG, leucine (Ely *et al.*, 2007) and bicarbonate (Yang *et al.*, 2009b). Moreover, thanks to the effervescence of the mixture, the release rate of the ciprofloxacin was demonstrated higher than with lactose microparticles.

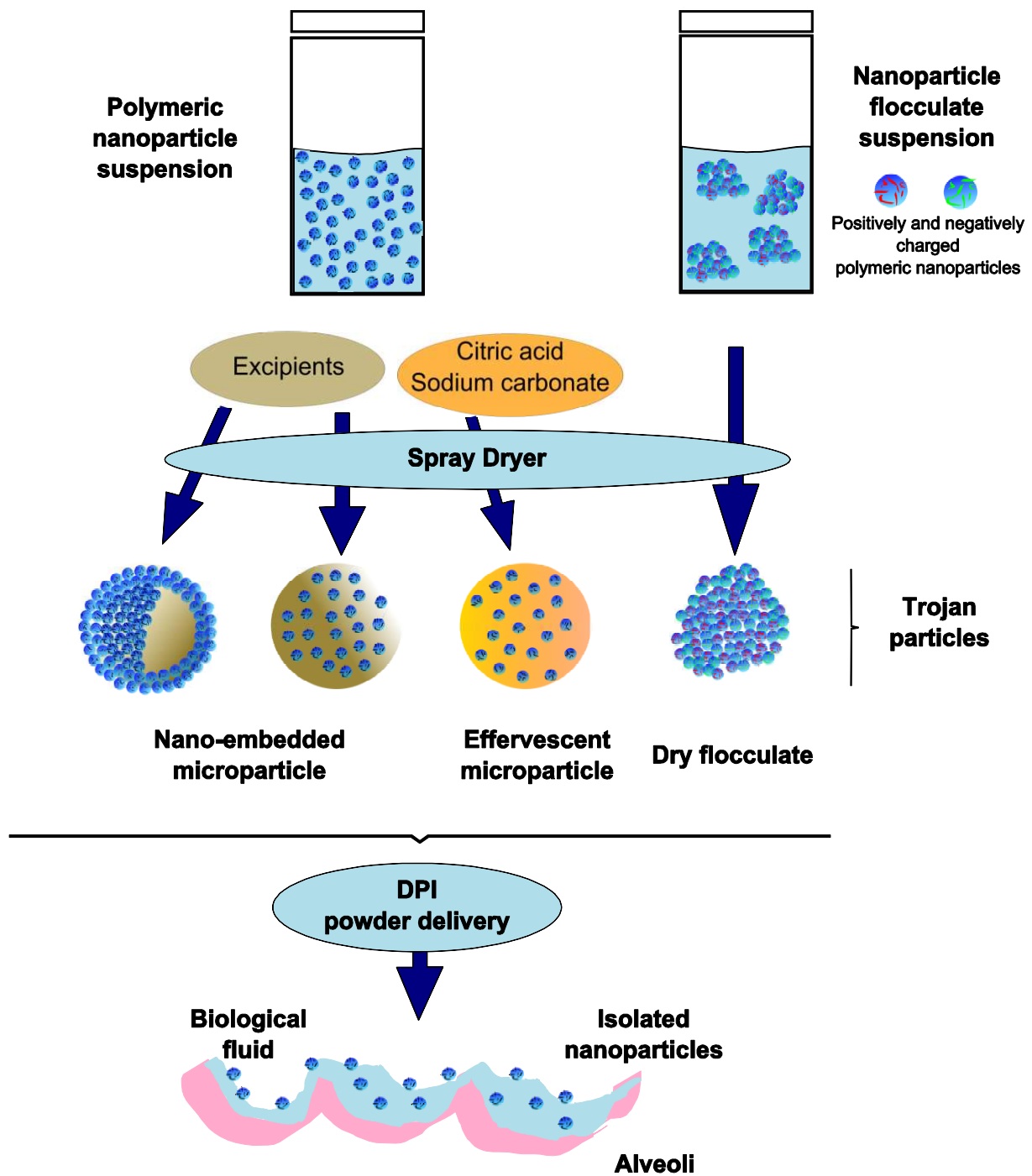


Figure 4. Modified nanoparticles for an aerosol delivery. To form nano-embedded microparticles, the main used excipient is lactose, but the use of mannitol, gum Arabic, 1,2-dipalmitylphosphatidylcholine (DPPC), hyaluronic acid, polyvinyl alcohol or whey protein is reported (for review see Anton *et al.*, 2012).

Recently, several *in vitro* studies have proposed to spray powders within cell cultures using as receptor the cascade impactor, described in the European pharmacopoeia, which is designed to mimic the respiratory tract. Under pressure, a breath is simulated. Bronchial or epithelial

cells have been cultivated on Transwell[®] at the air-liquid interface and, once the confluence was reached, they were incorporated to the impactor system and exposed to dry powder. The complex system allowed studying the effect of active drugs (Hein *et al.*, 2011) or diesel particles (Cooney and Hickey, 2011) that reached cell cultures by impaction.

Trojan particles have several advantages, such as reduction of the delivered dose, increasing the drug bioavailability, controlling the release, reducing the toxicity, and as a result improving the therapeutic index and patient compliance (Anton *et al.*, 2012).

3.3. Fate of nanomedicine after pulmonary delivery

3.3.1. *In vivo* biodistribution

Biodistribution studies have been performed after nanoparticle delivery in several animal species (mainly mice and rats), and tissue distribution has been limited to the pulmonary regions or extended to peripheral organs. Fluorescent or radio-labeled nanoparticles have been mostly utilized for this purpose.

Ungaro *et al.* (Ungaro *et al.*, 2012) have administered to rats, through the Dry Insufflator device[™], spray dried / PLGA nano-embedded microparticles (in lactose) containing rhodamine. After administration, animals were anesthetized, the abdominal cavity incised and lung perfused, firstly with phosphate buffer and then with formaldehyde. Respiratory tissues were removed, cut into thin slices to be observed and analyzed by fluorescence microscopy (Ungaro *et al.*, 2010). The results have demonstrated that *in vivo* nanoparticle distribution was mediated by surface recovering (Ungaro *et al.*, 2012). Indeed, microparticles were found in trachea, bronchia and bronchioles when primary nanoparticles were stabilized with PVA, whereas microparticles were mainly found in alveolar ducts when primary nanoparticles were stabilized by chitosan (Figure 5).

Other biodistribution studies have shown that after lung delivery into healthy or tumor-bearing mice, nanoparticle fate differs. Indeed, when fluorescent gelatin nanoparticles were delivered by nebulization, healthy mice rapidly eliminated nanoparticles towards kidneys, whereas tumor-bearing mice retained them in lungs, until 24 h (Tseng *et al.*, 2008). Moreover, 30 min after administration, most of the nanoparticles were found in association with epithelial cells lining the trachea. Gelatin nanoparticles were also identified in blood vessels, heart, spleen, brain and liver. After aerosolization of effervescent microparticles (Al-Hallak *et*

al., 2012, Kim *et al.*, 2012) containing radio-labeled nanoparticles loaded with doxorubicin, the latest were disseminated in the lung whereas the heart, a tissue sensitive to the toxicity of doxorubicin, remained free of nanoparticles.

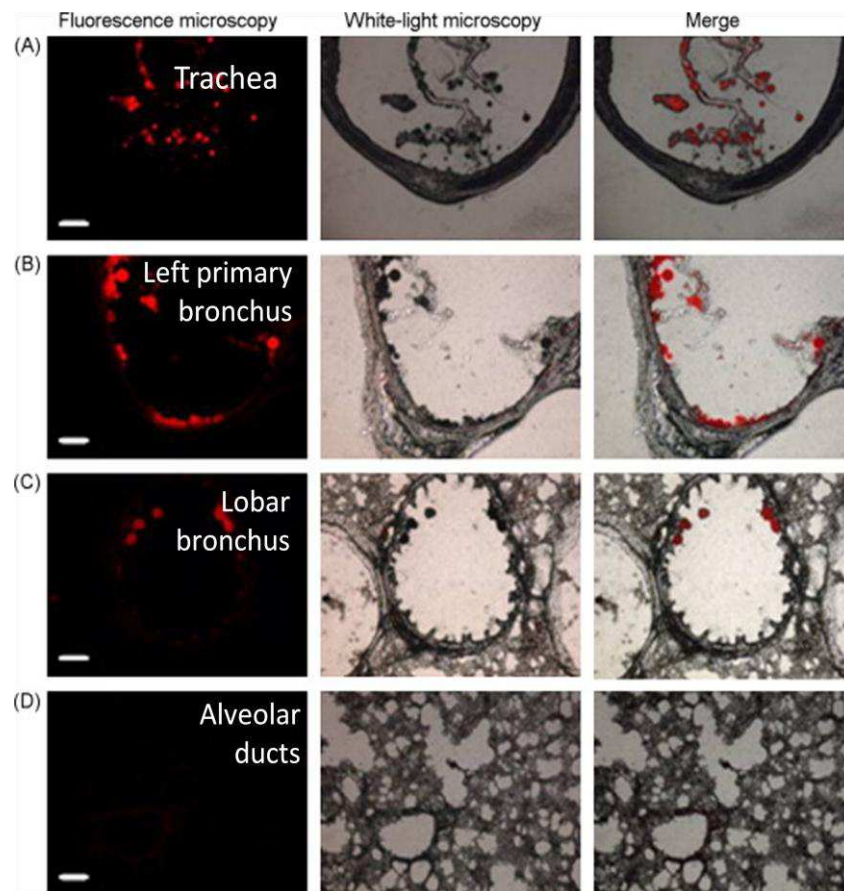


Figure 5. *In vivo* biodistribution of Rhodamine-PLGA nano-embedded microparticles in rat lungs. Photomicrographs show localization of fluorescent nanoparticles (red) in section of trachea (A), left primary bronchus (B), lobar bronchus (C) and alveolar ducts (D). (Modified from Ungaro *et al.*, 2010).

Finally, free or SLN-loaded radio-labeled amikacin (170 nm, spherical) were delivered to rats by nebulization or intravenous (*iv*) administration (Varshosaz *et al.*, 2013). While after lung delivery of SLN, sustained concentrations were obtained in the lungs, with all other conditions, the rate of amikacin reaches a maximum 30 min following the delivery, after which it started to be cleared. Moreover, 6 h after delivery of SLN by pulmonary route, a significant amount of amikacin was found in the stomach, most likely because the animal swallowed exhaled SLN. As far as the amikacin rate in blood is concerned, the delivery of SLN, either by pulmonary route or *iv.* administration, led to lower drug concentration than after the administration of free drug.

3.3.2. Translocation

It is suggested that a small fraction of nanoparticles that are not trapped in alveolar macrophages or in lung epithelial cells have the potential to cross the lung blood-air barrier to reach extrapulmonary spaces and blood circulation (Muhlfeld *et al.*, 2008). Kunzli and co-workers (Kunzli and Tager, 2005) have reviewed the impact of inhaled air nanoparticles on the cardio-vascular system. Adverse effects, such as heart rate, blood pressure or inflammatory state, were attributed to nanoparticle translocation from lung to the blood circulation. A strong *in vivo* comparative studies including inorganic (silica, quantum dots) / organic (polystyrene, human serum albumin) hybrid nanoparticles have demonstrated that translocation is size and surface-dependent, whereas the composition of the core (organic / inorganic) does not have an influence (Choi *et al.*, 2010). Regarding the size, it was shown that below 34 nm, nanoparticles rapidly translocate from the alveolar space to the lymph nodes, followed by a second translocation towards the bloodstream. Secondly, zwitterionic, anionic and polar nanoparticles are able to translocate, whereas cationic nanoparticles are probably trapped by epithelial cells or macrophages which slow down the translocation. Finally, zwitterionic nanoparticles with an aerodynamic diameter under 6 nm can be found in lymph nodes within 3 min after exposure. After 30 min they start accumulating in the kidney before being excreted (Choi *et al.*, 2010).

3.3.3. Mechanisms of cellular uptake *in vitro* and *in vivo*

Cellular uptake results from the ability of nanoparticles to cross cell barriers. Nanomedicines are generally taken up by cells following endocytosis mechanisms, either phagocytosis or pinocytosis. Phagocytosis is generally performed by phagocytic cells such as macrophages, whereas pinocytosis is performed by all kind of cells. Pinocytosis mechanisms can be clathrin-dependent endocytosis or clathrin-independent endocytosis. This last pathway is classified as caveolae-dependent endocytosis, clathrin and caveolae-independent endocytosis and macropinocytosis (Sahay *et al.*, 2010, Hillaireau and Couvreur, 2009). To address the question of uptake by endocytosis, a simple method consists in performing uptake studies simultaneously at 37 °C and 4 °C (Figure 6). A nanoparticle uptake at 4 °C similar to the one at 37 °C, characterizes a non-energy dependent mechanism such adsorption whereas differences of uptake results from endocytosis. Then, to determine the endocytosis pathways, various chemical (amiloride, chlorpromazine, genestein or filipin) or biological (AP180 or caveolins) inhibitors can be used to block one or more pathways (Iversen *et al.*, 2011). For

instance, genestein can inhibit several tyrosine kinases that inhibit caveolae pinching, or caveolin can stabilize receptors in caveolae. Some endocytosis mechanisms are clathrin-independent and cholesterol-dependent (such as macropinocytosis).

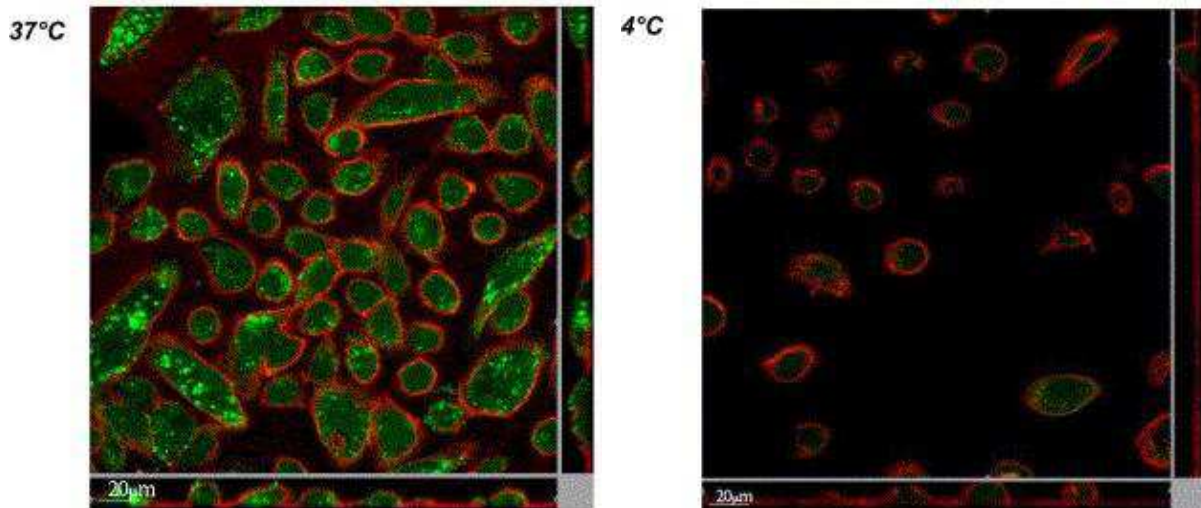


Figure 6. Confocal microscopy imaging (section showing interior of cells) of primary pulmonary epithelium cells after exposure to gelatin nanoparticles at 37°C and 4°C. The cell membrane is bounded with TRITC-concanavalin is coded red and nanoparticle of gelatin bound with FITC is coded green, at 37 °C and 4 °C. (Modified from Brzoska *et al.*, 2004).

In order to visualize nanoparticle trafficking within cells and their exact location, two microscopic modes may be used, which are confocal laser scanning microscopy (CLSM) as well as transmission electronic microscopy (TEM). In the first case, fluorescent nanoparticles are required. For that reason, polymeric nanoparticles can be loaded with fluorescent compounds, such as 6-coumarin (Panyam *et al.*, 2003) or for ensuring greater stability, covalently labeled with rhodamine (Mura *et al.*, 2011b) or fluorescein derivatives (Huang *et al.*, 2002), or near infra-red emitting fluorescent probe (Reul *et al.*, 2012). For more accuracy and complete details, each cell compartment, *i.e.* endoplasmic reticulum, endosome, golgi apparatus, lysosome, mitochondria, nucleus or plasma membrane, can be labeled with specific commercial fluorophores (Cell Staining Simulation Tool Life Technologies). In the case of transmission electronic microscopy, nanoparticles must be electron dense. Otherwise, it is not possible to discriminate between nanoparticles and cell vesicles. For this purpose, in one study, polymeric nanoparticles have been loaded with osmium tetroxide, to be detectable (Panyam *et al.*, 2003).

The quantification of the *in vitro* (Cartiera *et al.*, 2009) cellular uptake is performed by flow cytometry but some studies use radioactivity sampling or fluorescence intensity measurements (Yang *et al.*, 2009a, Ohashi *et al.*, 2009).

Nanoparticle cellular fate after pulmonary delivery is a crucial point to be investigated when carrying out toxicity analyses. Indeed, the same type of nanoparticle can be taken up by all the previously described ports of entry. Clearance of radioactive-labeled ultrafine nanoparticles was followed after rat intratracheal intubation (Semmler *et al.*, 2004, Semmler-Behnke *et al.*, 2007). The nanoparticles were mostly retained in lungs up to 6 months after exposure, and the clearance was mainly performed by excretion. The small fraction of free nanoparticles found in bronchoalveolar lavages is mostly associated with alveolar or epithelial cells. Translocation into the circulation and accumulation in other organs was also reported, but nanoparticle levels in the extrapulmonary spaces quickly decreased within 7 days (Semmler-Behnke *et al.*, 2007). According to the size, nanoparticles were either retained by epithelium or sequestered by alveolar macrophages, beyond the epithelium.

4. Toxicity endpoints

The term toxicity is very large and embraces several parameters (Figure 7). This section should provide an overview of the different *in vitro*, *in vivo* or *ex vivo* tests reported in the literature to study nanoparticle-related toxicity.

4.1. Cell integrity

Cell integrity can routinely be restimated by trypan blue, eosin or acridine orange which are stains that selectively color damaged cells (Tennant, 1964). MTT (3-(4,5-dimethylthiazol-2-yl)-2,5-diphenyltetrazolium bromide) assay, or equivalents [MTS (3-(4,5-dimethylthiazol-2-yl)-5-(3-carboxymethoxyphenyl)-2-(4-sulfophenyl)-2H-tetrazolium), XTT (2,3-bis-(2-methoxy-4-nitro-5-sulfophenyl)-2H-tetrazolium-5-carboxanilide), WST-1 (Water Soluble Tetrazolium salts)] (Mosmann, 1983) are widely used to assess the *in vitro* metabolic activity of cells. In these tests, the tetrazolium dye is reduced to formazan purple crystals in living cells by Nicotinamide Adenine Dinucleotide Phosphate-Oxidase-(NADPH) dependent oxidoreductase enzymes. The measurement of the absorbance of the colored solution is directly related to the cellular metabolic activity.

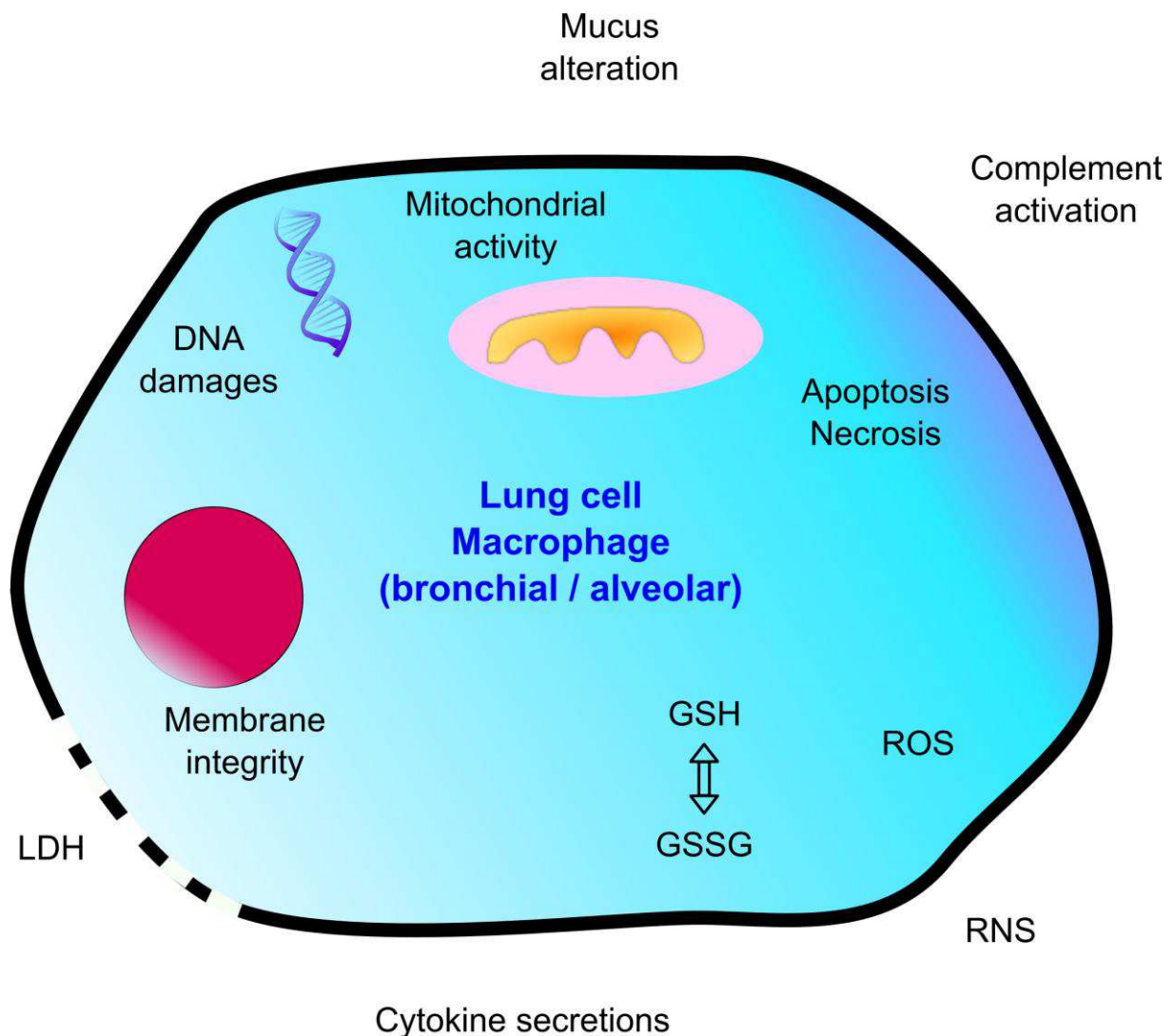


Figure 7. Nanotoxicology can be expressed by several endpoints: evaluation of mitochondrial activity evolution, membrane integrity, inflammatory response, oxidative stress. Tests are performed in supernatants, or inside lung cells (*GSH / GSSG*: glutathione sulfhydryl / oxidized disulfide forms, *ROS*: Reactive oxygen species, *RNS*: Reactive Nitrogen Species, *SOD*: Super Oxide Dismutase), apoptosis / necrosis detection, analyses of the complement activation, and DNA damage.)

Membrane integrity can also be evaluated by different methods. One of the most commonly used tests is the lactate dehydrogenase (LDH) assay, suitable for both *in vitro* and *in vivo* models (Dailey *et al.*, 2006). When cell membrane gets disrupted, the intracellular LDH is released in extracellular medium. This release, which is quantified by an indirect enzymatic assay, correlates to an enhancement of membrane permeability. The LDH released reduces NAD^+ into NADH which catalyzes the reduction of a tetrazolium salt to form a formazan crystal with an absorbance wavelength of 540 nm. By the use of a different principle, the Live/dead[®] test – or equivalent – also allows investigating membrane integrity. To achieve these tests, cells are collected and put in contact with two fluorescent probes able to link

nucleic acids, i) one red-orange, generally propidium iodide (or 7-Aminoactinomycin D (7-AAD)), an intercalating agent, able to penetrate cells with damaged membrane, and ii) one green, such as the acetomethoxy derivate of calcein or Syto[®] 24, able to penetrate all cells. Cells can then be observed by microscopy, or the intracellular fluorescent level can be determined by flow cytometry.

4.2. Apoptosis detection

Apoptosis corresponding to programmed cell death is generally opposed to necrosis that is “accidental” cell death (Kerr *et al.*, 1972). In apoptotic cells, membrane phospholipids undergo a “flip-flop” event in which phosphatidylserine molecules are translocated to the outer leaflet, to be recognized by macrophages, without disruption of the membrane in the early stages (Fadok *et al.*, 1992), whereas the necrotic cell membrane is disrupted. Quantification of apoptotic cells can be performed by detecting caspase-3, an activated protease in apoptotic cells (Jänicke *et al.*, 1998), or by flow cytometry after staining of phosphatidylserines with annexin V, an anticoagulant (Koopman *et al.*, 1994). To discriminate apoptotic cells from necrotic and intact cells, annexin V, coupled with FITC (green fluorescence) is combined with propidium iodide (or 7-AAD) (red fluorescence) (VanEngeland *et al.*, 1996). Annexin V is added in cell culture medium for a short time. Detached cells are pooled with harvested cells (in case of adherent cells), and propidium iodide (or 7-AAD) is added. Intact, early apoptotic, necrotic and late apoptotic cells are respectively untagged, fluorescent in green channel, fluorescent in red channel, simultaneously fluorescent in both green and red channels. Quantification of each cell population is performed by flow cytometry. Fluorescent microscopy can give supplementary morphology-based information concerning the cellular viability of epithelial or bronchial cells. Indeed, apoptotic cells are characterized by membrane blebbing.

4.3. DNA damage - Genotoxicity

Nanoparticles can penetrate inside cells, causing damage to DNA by single or double strands breaking. The single cell gel assays (SCG) also called “comet assay” are able to detect DNA single strand breaks, alkali labile sites or incomplete excision repair sites with a strong sensitivity to determine the lower DNA damage (Singh *et al.*, 1988). However these tests require the extraction of single-strand DNA, obtained after different steps including: i) cells

loading into an agarose gel slice, ii) treatment with a lysis solution and iii) DNA unwinding with an alkaline buffer (Tice *et al.*, 2000). The staining is generally achieved after a neutralization step with fluorescent compound such as ethidium bromide, propidium iodide or 4',6'-diamidino-2-phénylindole (DAPI), or non fluorescent dye such as the silver nitrate. Quantitative analysis can be performed by determining the proportion of cells with altered migration onto the agarose gel, or by classifying them according to the length of migration. The ability of lung cancer cells to form colonies is another relevant endpoint of cytotoxicity and genotoxicity (Shoemaker *et al.*, 1985). A very small amount of treated cells were seeded on plates in order to perform single cell forming colonies. After a long incubation period (few days), cells were fixed to finally count colonies after trypan blue staining (Jantzen *et al.*, 2012).

4.4. Oxidative stress assay

Oxygen is required for all aerobic organisms, but it is also a strong oxidant molecule that can be responsible for undesirable oxidations in cells. This hazardous phenomenon is called oxidative stress (Sies, 1997) and can be caused by free radicals, reactive oxygen species (ROS) or reactive nitrogen species (RNS), that are superoxide anion ($O_2^{\cdot-}$), hydroxyl radical (OH^{\cdot}), nitric oxide (NO^{\cdot}), peroxy radical (ROO^{\cdot}), hydrogen peroxide (H_2O_2), ozone (O_3), hypochlorite anion (ClO^-), peroxyxynitrite (NO_3^-), and also copper and iron ions (Cu^{2+} , Fe^{3+}) that catalyze Haber-Weiß and Fenton reactions (Sorg, 2004) (Figure 8). In physiological conditions, reactive species are neutralized by antioxidants, such as super oxide dismutase (SOD), catalase, glutathione peroxidase (GPX), reductase (GPR) and S-transferase (GST), ascorbic acid (vitamin C), retinoids (vitamin A), carotenoids, tocopherols (vitamin E), and selenium. However, when the organism is exposed to hazardous compounds like pollutants, ultraviolet, tobacco smoke or nanoparticles, the oxidant / antioxidant balance is destabilized, and ROS and RNS are formed.

As it was widely shown in the literature, lungs are the site of several oxidative stress reactions (MacNee, 2001, Li *et al.*, 2008, Repine *et al.*, 1997). For instance, one of the causes of emphysema or acute respiratory distress syndrome is related to oxidant release in alveolar tissues or pulmonary endothelium (Babior, 2000), and SOD plays an antioxidant key role in asthma and in chronic obstructive pulmonary disease (Tsukagoshi *et al.*, 2000).

4.4.1. Reactive Oxygen Species

To quantify intracellular located ROS, before exposure to nanoparticles, cells are shortly incubated with 2',7'-dichlorodihydrofluorescein diacetate (H₂DCFDA) that penetrates inside cells (LeBel *et al.*, 1992) and which upon cleavage of the acetate group by intracellular esterase is converted into 2',7'-dichlorofluorescein (DCF) that expresses a high fluorescent intensity after ROS oxidation. Quantification is achieved by flow cytometry.

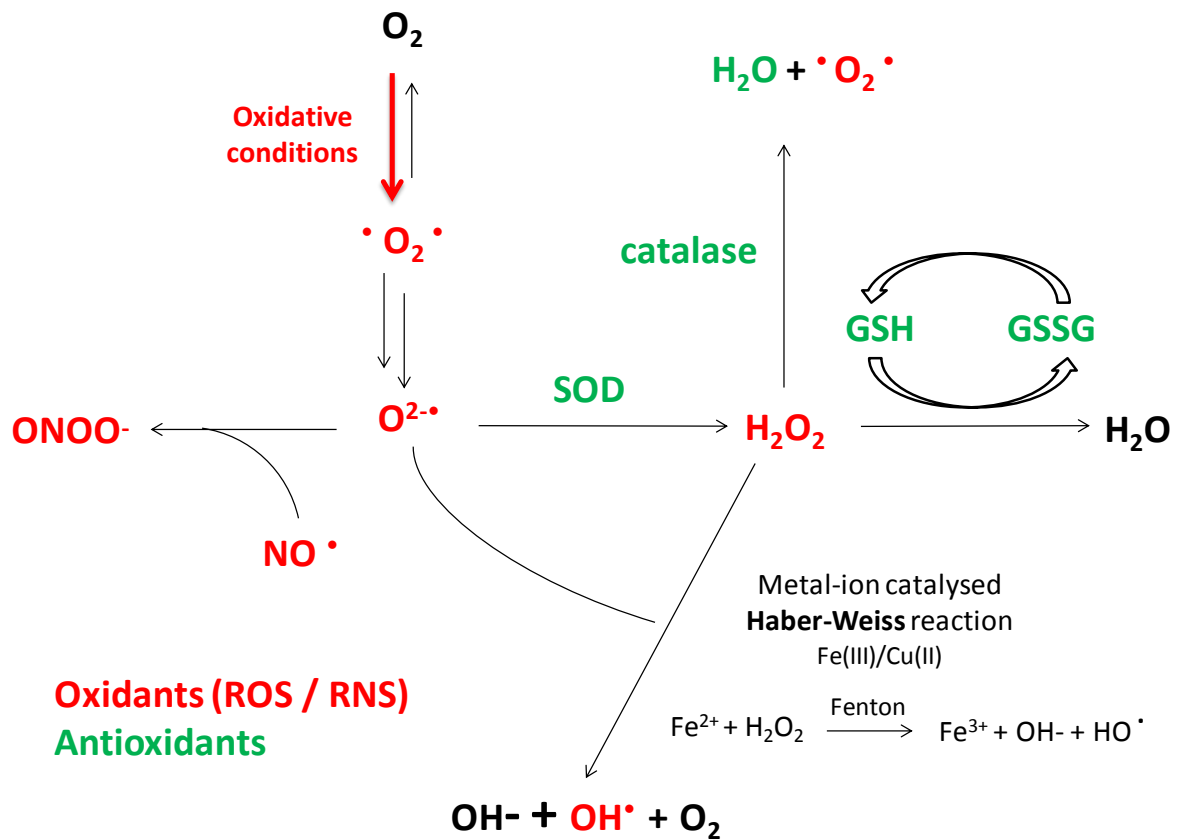


Figure 8. Oxidants (in red) and anti-oxidants (in green) species involved in oxidative stress reactions. ROS = Reactive Oxygen Species, RNS, Reactive Nitrogen Species; SOD, Super Oxide Dismutase; GSH/GSSH, reduced sulfydryl / oxidized disulfide glutathione (Modified from Sorg, 2004).

4.4.2. Reactive Nitrogen Species

Contrary to ROS, cells release RNS in the extracellular medium. The most common method to quantify them is the Griess reagent (Green *et al.*, 1982, Hensley *et al.*, 2003) containing sulfanilic acid and α -naphthylamine in acetic acid. In presence of RNS, a pink compound that absorbed at a wavelength of 560 nm will be formed. However, this method has a poor

sensitivity, the nitrite concentration being detectable in the range of 1 to 5 μM . The 2,3-diaminonaphthalene is also able to react with nitrites forming a fluorescent compound (excitation at 355 nm and emission at 460 nm) allowing the detection of lower nitrite concentrations (from 0.02 to 10 μM) (Nussler *et al.*, 2006). Moreover, this method can quantify the nitrates, by pre-converting them into nitrites with NADPH.

4.4.3. Superoxide Dismutase

The SOD catalyzes the dismutation of super oxide radicals ($\text{O}_2^{\bullet-} + \text{O}_2^{\bullet-} + 2\text{H}^+ \rightarrow \text{O}_2 + \text{H}_2\text{O}_2$) (McCord and Fridovich, 1969). Its increase in the extracellular medium characterizes the presence of superoxide radical that is immediately neutralized by the enzyme. To quantify SOD, superoxide radical anions are formed *in situ*. They are either neutralized by the SOD, if it is present in the extracellular medium, or they react with nitroblue tetrazolium forming colored nitroblue tetrazolium-formazan (NBT-formazan) (absorbance at a wavelength of 540 nm) (Beauchamp and Fridovich, 1971, Sun *et al.*, 1988). In presence of SOD, production of NBT-formazan is inhibited and the quantity of SOD is accessible by a colorimetric assay.

4.4.4. Glutathione

Physiologically, glutathione exists within the cell under, both, the reduced sulfhydryl form (GSH) and the oxidized disulfide form (GSSG). In healthy cells, GSSG is quickly reduced by glutathione reductase into GSH, but in presence of high number of free radicals, GSSG cannot be reduced. GSH can react with the 5,5'-dithio-bis(2-nitrobenzoic acid) (DTNB) to form the 5-thio-2-nitrobenzoic acid (TNB) (absorbance at a wavelength of 412 nm) and a glutathione derivate (GS-TNB) (Rahman *et al.*, 2007). The addition of glutathione reductase allows the reduction of GS-TNB into GSH, and the reduction of GSSG into two molecules of GSH. The total quantity of glutathione is $[\text{GDH}]_{\text{total}} = [\text{GSH}] + 2[\text{GSSG}]$. To determine the exact amount of each glutathione form, a second assay can be performed: the excess of 2-vinylpyridine reacting with GSH is neutralized by triethanolamine. GSSG assay is then performed as previously described.

4.5. Inflammatory response

4.5.1. Cytokine assay

The immune system is composed of the innate system that is non-specific and the acquired system that is antibody mediated. After even a slight perturbation in lungs, the immune response is activated and regulated (amplitude and duration) thanks to low molecular weight proteins, called cytokines, released in response to cellular signals (Kelley, 1990). Cytokine denomination includes chemokine, interleukine (IL), growth factor and interferon (IFN). Every cytokine – that can be secreted in cascade – can cause multiple effects on growth and differentiation (mitosis, chemotaxis, angiogenesis, cytoskeleton arrangement, immunomodulation and extracellular production) in a large variety of cells, even at low concentration (Kelley, 1990, Galley and Webster, 1996). Pro-inflammatory chemotactic chemokines (IL-8, Monocyte Chemoattractant Protein (MCP)-1) are able to attract primarily neutrophils and cells of the innate immune system, regulate cell trafficking (Deshmane *et al.*, 2009), and can be produced by macrophages or alveolar type-II epithelial-like cells (Sallusto *et al.*, 2000, Cromwell *et al.*, 1992). By regulating the migration and infiltration of monocytes, MCP-1 is also involved in various diseases (Polito and Proud, 1998). The tumor necrosis factor- α (TNF- α), IL-1, IL-6, mostly secreted by alveolar macrophages, are involved in pulmonary diseases; TNF- α increase transitory, with high levels in a short time, but will cause important injuries in lung and fever or tachycardia (Kelley, 1990).

The inflammatory response can be quantified by assaying released cytokines in extracellular medium. Cytokines have been historically quantified by ELISA (Enzyme Linked Immunosorbent Assay) based on cytokine recognition with specific antibodies linked to an enzyme detected by a colorimetric reaction. However by ELISA, only one cytokine per sample can be quantified. More recently new methods have been developed to quantify several cytokines (until 30) simultaneously (duPont *et al.*, 2005). Among them, BDTM CBA (Cytometric Beads Array – BD Biosciences) (Tarnok *et al.*, 2003, Morgan *et al.*, 2004), Luminex[®] system (Invitrogen), BioPlex cytokine assays (Bio Rad) were successfully used. Such systems use calibrated beads of different sizes and fluorescence wavelengths that specifically recognize cytokines. The final addition of antibodies that also recognize each cytokine allows quantifying the amount of each cytokine. These methods lead to important improvement and a higher sensitivity compared to ELISA tests (duPont *et al.*, 2005, Djoba Siawaya *et al.*, 2008).

4.5.2. Complement activation

The complement system is a multiple-component triggered enzyme cascade which attracts phagocytes to micro-organisms increasing capillarity, permeability and neutrophil chemotaxis and adhesion (Galley and Webster, 1996). As previously shown, epithelial lining fluid contains the complement system proteins (Robertson *et al.*, 1976). In one example of complement activation determination, bovine heat-inactivated serum exposed to nanoparticles was loaded into the bottom of 96-well neuroprobe chemotaxis chamber, equipped with polycarbonate filter with 5 μm pores. Murine macrophages were placed at the top of the insert, in serum free media. The positive control employed was rich in chemotaxis complement proteins C3a (recognized by phagocytes that will process to engulfment of nanoparticles) and C5a (chemotaxis for polymorphonuclear). After incubation, the insert was removed and cells were stained with Romanowsky reagent (mixture of eosin and methylene blue). Absorbance measurement allows the assessment of the amount of macrophages passed through the filter, which number was function of complement activation.

4.5.3. Polymorphonuclear counting in bronchoalveolar lavages

Polymorphonuclear (PMN) are locally recruited in lungs and an increased number characterizes a disorder. By collecting the bronchoalveolar lavages (BAL) on animals, cells can be characterized and counted on a hemacytometer. After nanoparticle lung delivery, BAL are withdrawn from anesthetized animals. Bronchoalveolar lavage fluids (BALF) are then stained with Romanowsky reagent to estimate the number of PMN present.

4.6. Mucus interactions

As the mucus is a strong defense barrier in the pulmonary tract, interactions with inhalable nanoparticles are important, and different parameters can be investigated to characterize mucus alterations. To begin with, an overproduction of mucus is synonym of airway inflammation. Four mucins are generally quantified: MUC2, MUC5AC, MUC5B and MUC19. The quantification of these proteins or their respective mRNA expression can give essential information about the mucus state. The quantity of mucin in BALF can be obtained by ELISA (Lin *et al.*, 1989, Phillips *et al.*, 2006) or electrophoresis (Spurr-Michaud *et al.*, 2007). Both methods use multiple anti-mucin antibodies, specific of each mucin proteins. To investigate the passage of insoluble fluorescent particles across the mucus layer, artificial

mucus composed of water, DNA, egg yolk emulsion, mucin, pentetic acid (DTPA), NaCl, KCl and cell culture medium (RPMI) (Yang *et al.*, 2011) can be prepared and then coated on a gelatin layer (Ungaro *et al.*, 2012). The measurement of the turbidity of the gelatin layer is related to the quantity of particles able to cross the mucus layer. On the other hand, the muco-adhesion of particles can be estimated by mixing them with a known mucin solution (Zaru *et al.*, 2007). The suspension is then centrifuged, and supernatant isolated to quantify the free mucin by a Bradford assay. Finally, mucus layer can be labeled with fluorescent wheat germ agglutinin, to be observed in confocal microscopy, after incubation with fluorescent particles (Mura *et al.*, 2011a).

Taken this into account, it is obvious that complete studies are required to deeply understand nanoparticle effects, firstly because all toxicity endpoints are linked, and secondly because eventual interferences of nanoparticles with the assay can lead to false results (Wörle-Knirsch *et al.*, 2006). All tests have shown their interest to evaluate the toxicity of non-biodegradable nanoparticles (Hoet *et al.*, 2004) and are subsequently relevant for investigating the safety of biodegradable nanoparticles. For example, titanium dioxide nanoparticles were proved to induce DNA damage (Trouiller *et al.*, 2009), oxidative stress (Bhattacharya *et al.*, 2009) and inflammatory response (Park *et al.*, 2009), and apoptosis (Shi *et al.*, 2010). However, these tests have to be taken with caution. For instance artifacts MTT test were reported (Simon-Deckers *et al.*, 2008).

5. Models for lung nanotoxicology: *in vitro*, *ex vivo*, *in vivo*

The complexity of the respiratory tract explains the high number of *in vitro/in vivo/ex vivo* models available to mimic all physiological or histological conditions present in lungs (Table 1). Several reviews draw a complete list of *in vitro* (primary cultured cells; human and animal cell lines isolated from human cancer or transformed from normal cells; cell co-cultures), *ex vivo* (isolated perfused lung – IPL) and *in vivo* (rodents such as rats, guinea pigs or mice; larger animals such as rabbits, dogs, monkeys and sheep) models that can be used to assess pulmonary toxicity (Sakagami, 2006, Fisher and Placke, 1987). Most of these models were used to study the impact of non-biodegradable nanoparticles – also called manufactured or engineered nanoparticles–, and only some of them were applied to study effect of nanoparticles used as drug carriers in lung drug delivery.

Table 1. *In vitro*, *ex vivo* and *in vivo* models used for nanotoxicity studies

Models		Organ / Origin	
<i>In vitro</i> cells			
Epithelial			
Bronchial	Primary NHBE (<i>primary cells</i>)	Isolated from bronchial spaces – Human or rodents	
	Beas-2B	Transformed from normal human lung	
	16HBE14o-	Transformed from normal human lung	
	Calu-3	Human lung adenocarcinoma; derived from metastatic site: pleural effusion	
Alveolar type II	A549	Human lung adenocarcinoma	
	RLE-6 TN	Rat lung	
	Primary AT I/II	Isolated from alveolar spaces – Human or rodents	
Lymph node	H2009	Human lung	
Endothelial			
	NCI H441	Human lung adenocarcinoma	
	Primary	Isolated from human or murine BAL	
	NR8383	Rat lung	
<i>Ex-vivo</i>			
	Isolated perfused lung	Rat Rabbit	
<i>In vivo</i>			
Small rodent	Rat	Winstar, Dawley-Sprague	
	Mice Guinea pig	Balb/c	
Mammal	Sheep		
	Dogs	Beagle	

AT I/II, Alveolar type I/II epithelial cells; BAL, Bronchoalveolar lavages.

5.1. *In vitro* cell culture for nanoparticle toxicity studies

A lot of cell lines used to investigate potential effects after particle exposure are commercially available (Phelps *et al.*, 1996). The majority of these cell lines are established from cancer tissues and others are immortalized with Epstein-Barr viral co-infection. In most cases, cell lines are well characterized and present the advantage to be not expensive and easy to use. However, to stay as close as possible to the physiological response, the use of primary cells can be performed as a second approach. Handling these cells is however more complicated than the use of cell lines since they have to be well characterized after sampling and before

their use. Moreover, their stability is generally limited to a small number of passages. To mimic the lung, human or murine epithelial cells (bronchial, alveolar, lymph nodes), endothelial cell lines and murine macrophages are available. Human primary macrophages can be obtained from BAL or by monocyte differentiation.

The delivery to the bronchus can be studied on bronchial epithelial cell lines, such as 16HBE14-o cells, human bronchus cells (Dombu *et al.*, 2012, Brzoska *et al.*, 2004) or Calu-3 cells (Bivas-Benita *et al.*, 2004a), isolated from a human lung carcinoma (Fogh *et al.*, 1977). These both cell lines can be cultured at the air-liquid interface, to form a confluent monolayer with good trans-epithelial electrical resistance (TEER) values, due to polarized tight junctions (Foster *et al.*, 2000) and a dense mucus layer (Fiegel *et al.*, 2003). Using these models, good correlations with *in vivo* results were shown (Mathias *et al.*, 2002). Gelatin and human serum albumin nanoparticles were prepared and stabilized with glutaraldehyde to deliver drug or gene into primary lung cells (isolated from lobectomies) or 16HBE14o- cells (Brzoska *et al.*, 2004). Previous confocal microscopy observations have evidenced that nanoparticles were taken up according to an endocytic mechanism. Then, toxicity studies on both cell types, have shown that membrane integrity was not affected (LDH), even after the highest tested concentration (50 µg/mL), and no IL-8 secretions were detected. Another study has investigated the potential gene delivery polyethylenimine (PEI) coated PLGA nanoparticles (Bivas-Benita *et al.*, 2004a). Nanoparticle uptake was observed within Calu-3 cells with a lysosomal co-localization. The uptake level was shown to be PLGA / PEI ratio-dependent, as demonstrated by the levels of gene expression.

Beas-2 B cells, isolated and modified from normal human bronchial cells (Reddel *et al.*, 1988), were widely used to study the effect of non-biodegradable nanoparticles such as the inflammatory response after particulate matter exposure (Steerenberg *et al.*, 1998), the oxidative stress after exposure to silica nanoparticles (Eom and Choi, 2009) and complete toxicity studies (oxidative stress, apoptosis, gene expression, DAPI staining) after exposure to titanium dioxide nanoparticles (Park *et al.*, 2008). In most of these studies the model was relevant to demonstrate toxicity properties of the tested particles.

Major studies that focused on alveolar conditions used the A549 cell line. These cells are isolated from a human carcinoma (Lieber *et al.*, 1976) and constitutes a good model of type II pneumocytes (Rothen-Rutishauser *et al.*, 2012, Foster *et al.*, 1998), giving the possibility to test, after exposure to biodegradable nanoparticles, several previously detailed toxicity

endpoints. As an example, the uptake of fluorescent chitosan nanoparticles was shown to be an endocytosis-mechanism initiated by adsorptive steps (Huang *et al.*, 2002), while the SLN (loaded with paclitaxel) endocytosis was PEG or folate coating-mediated (Yuan *et al.*, 2008). The low cytotoxicity of SLN based on 6-lauroxyhexyl lysinate and complexed to DNA allowed to induce a similar rate of gene transfection comparable with those obtained with Lipofectamine (commercial reagent) (Li *et al.*, 2011). Finally, liposomes loaded with ciprofloxacin have shown a good antibacterial effect without leading to LDH release (Chono *et al.*, 2006). Moreover, after exposure of A549 cells to inorganic nanoparticles, apoptosis detection, cell proliferation assay, ROS quantification and inflammatory response were observed (Choi *et al.*, 2009).

To expand alveolar condition studies, human primary alveolar type II cells were isolated after lung resection of carcinoma (Witherden *et al.*, 2004). Such cells express an alveolar cell-type phenotype and can be immortalized (O'Hare *et al.*, 2001) showing an increased internalization of latex beads (Kemp *et al.*, 2008).

5.2. Co-culture of lung cells in nanotoxicology

Co-culture systems have provided significant advances in cell biology. Indeed, by mixing different cell types (2 or more), interactions occur and culture conditions are closer to physiology than classic *in vitro* cell line models. Co-culture models can be established with direct or indirect contact between the cells (Figure 9). Models with indirect contact require the use of a device such as Transwell[®] inserts equipped with porous membranes allowing communication between different cell types placed in wells. Each cell type is then seeded on each side of the insert. To mimic pulmonary tract, a large variety of cells have been used: bronchial, alveolar, epithelial, fibroblast, dendritic and macrophages. However, in each case the relevance of co-cultures needs to be validated by deep comparisons between cells in mono- and in co-culture.

Bronchial conditions were reproduced by a co-culture of 16HBE14o- cells or human primary bronchial cells (apical compartment) with lung fibroblast cells Wi-38 (basolateral compartment) at the air liquid interface (Pohl *et al.*, 2009). The use of primary cells has shown interest. Indeed, in co-culture with fibroblastes, primary bronchial cells (which are continuously differentiated) mimic the structure of a native polarized bronchial epithelium

showing mucus-producing, basal and ciliated cells. Such model was used from 3 weeks to 3 months (Pohl *et al.*, 2009).

EpiAirway™ (MatTek Corporation) and MucilAir™ (Epthelix), two commercial differentiated pulmonary epithelium, are available to perform toxicity tests after exposure to chemical compounds (Constant *et al.*, 2011a) or manufactured nanoparticles (Constant *et al.*, 2011b, Hayden *et al.*, 2011). Composed of human primary cells isolated from trachea, bronchus and nose, MucilAir™ device is cultivated at the air-liquid interface and presents characteristics of airway tissues (available for healthy or damaged conditions). Indeed, the device contains basal, ciliated and mucosal cells and displays a regular ciliary beating, tight junctions, ion transport and metabolic activity. The epithelium remains in homeostasis state for more than one year, thus, long term studies after single or repeated exposure can be performed. After 28 days repeated exposure to chemical compounds, cytochrome expression was modulated (Constant *et al.*, 2011a). After delivery of nanoparticles on apical surface, trans-epithelial resistance, LDH and cytokine released were quantified (Constant *et al.*, 2011b). It was shown that the epithelium has the potential to recover after low nanoparticle concentration exposure. EpiAirway™ and MucilAir™ present an interesting potential to drive environmental studies, as the ones responding to EU regulations in the REACH programme (BéruBé *et al.*, 2010).

Alveolar conditions were simulated by different co-culture models. For example, the indirect co-culture of A549 cells or NC H441 with primary human pulmonary microvascular endothelial cells allowed developing a model of an alveolo-capillary barrier (Hermanns *et al.*, 2004). This model has been used to study environmental cadmium exposure side-effects and has shown that whereas viability of epithelial cells largely decreases, the viability of endothelial cells remains unaffected (Papritz *et al.*, 2010). To investigate the predominant role of resident macrophages following air particulate exposure, lung alveolar epithelial cells, [A549 (Wottrich *et al.*, 2004, Jantzen *et al.*, 2012), L132 (Abbas *et al.*, 2009), RLE-6N (Wang *et al.*, 2002)], were co-cultured with macrophages [differentiated from THP-1 monocytes (Stříž *et al.*, 2001, Wottrich *et al.*, 2004), Mono Mac 6 (Wottrich *et al.*, 2004) or human (Abbas *et al.*, 2009) / murine (Wang *et al.*, 2002) alveolar macrophages isolated from BAL] in direct or indirect contact. In co-culture with A549, macrophages differentiated from THP-1 monocytes acquire alveolar macrophage phenotypic characteristics (Stříž *et al.*, 1993), and after exposure to ultrafine nanoparticles, co-culture synergistic effects were observed concerning the release of IL-6 and IL-8 (Wottrich *et al.*, 2004), while no modification of ROS and DNA damage levels were noticed (Jantzen *et al.*, 2012). The defensive role of alveolar

macrophages against particulate matter was proved in co-culture with L132 cells (Abbas *et al.*, 2009). In co-culture, the levels of particulate matter metabolizing enzymes produced were higher than in mono-culture. The significant attenuation of IL-1 β and IL-6 cytokines secretions after exposure to jet fuel on a co-culture of rat alveolar cells and macrophages compared to mono-culture of each cells confirmed that interactions between cells exist (Wang *et al.*, 2002).

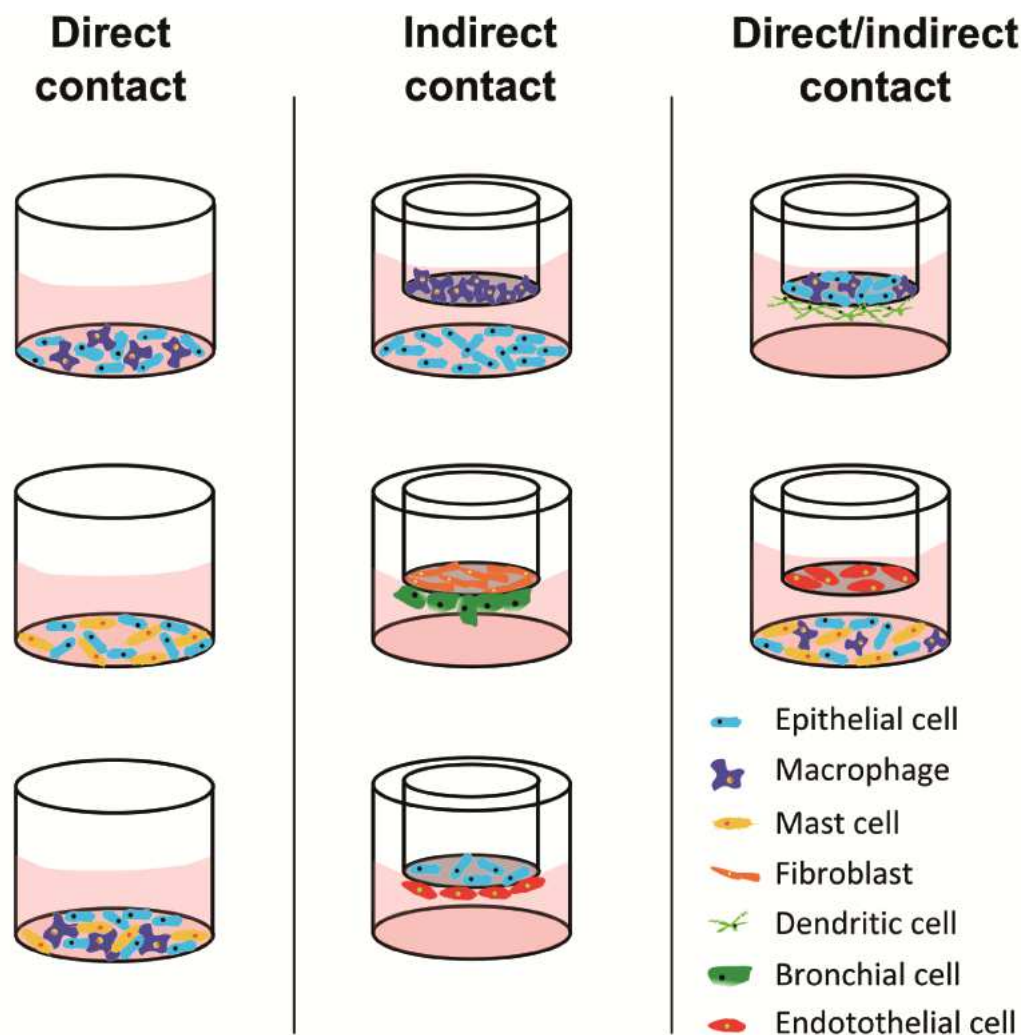


Figure 9. Representation of co-culture models used to mimic the pulmonary tract using Transwell® device, to established co-culture in indirect contact.

Rothen-Rutishauser *et al.* (Rothen-Rutishauser *et al.*, 2005) have established a tri-culture of i) A549 cells seeded on the apical compartment of Transwell®, ii) differentiated dendritic cells seeded on the basal side of the turned insert and iii) differentiated macrophages added on the

apical surface of the epithelial cell monolayer. This tri-culture was used to investigate effects of non biodegradable nanoparticles in alveolar conditions (Müller *et al.*, 2010). Following TEM observations, TiO₂ nanoparticles were found in all cell types, whereas carbon nanotubes were present in epithelial cells. After exposure to carbon nanotubes, ROS production was observed in majority of cells, with a higher level than in mono-culture of epithelial cells, whereas IL-8 and TNF- α quantification (ELISA) did not show any synergistic effect.

In order to deeply understand toxicity mechanisms, and more particularly the inflammatory response after exposure to particulate matter, Alfaro-Moreno and co-workers have deeply investigated mono and co-cultures of epithelial cells (A549), macrophages (differentiated THP-1 monocytes), mast cells (HMC-1) and endothelial cells (EAHY926) (Alfaro-Moreno *et al.*, 2008). Different co-culture combinations were performed: mast cells or macrophages with epithelial cells in direct contact; mast and epithelial cells and macrophages in direct contact, with or without endothelial cells in indirect contact. Cytokine release profile was modified according to the combination and the key role of mast cells and macrophages was demonstrated (large increase of several cytokines in co-culture), as well as the activation of endothelial cells by the co-culture. The cytokine release profile of the system composed of the four cell types was in accordance with *in vivo* profile and correlated to asthmatic patients who were exposed to such particulate matter.

5.3. *Ex-vivo* models

5.3.1. Isolated perfused lungs

The isolated perfused lung (IPL) system represents an interesting alternative when considering all cell-cell interactions that occurred within the isolated organ (Mehendale *et al.*, 1981). This technique consists in extracting the respiratory system (lungs and/or trachea) from rats, guinea pigs or rabbits and keep it as close as possible to the physiological conditions (Byron *et al.*, 1986). The pulmonary circulation (air flow rate, temperature, blood circulation) is maintained in a complex track of pumps to provide isolation, perfusion and ventilation of isolated lungs. IPL are not much used in nanotoxicology even though the radioactive tracking of iridium particles to an isolated perfused rat lung has shown a similar particle distribution to the one occurring *in vivo*, confirming the pertinence of such models (Meiring *et al.*, 2005).

PLGA or branched polyester-based nanoparticles were loaded with a fluorescent compound (Beck-Broichsitter *et al.*, 2009) or salbutamol (Beck-Broichsitter *et al.*, 2010), for the delivery

to the isolated perfused rat lung. Kinetic spectroscopic studies on the IPL have confirmed the presence of nanoparticles in deep lungs up to 2 hours after administration, and the release of active compounds in two phases, the first corresponding to a constant increasing of compounds in the IPL, and the second being the phase of absorption. Similar studies were performed with polystyrene nanoparticles, and confocal laser scanning microscopy imaging of lung slices has shown the presence of such nanoparticles in the deep lung, principally in alveolar macrophages and in free alveolar spaces (Hamoir *et al.*, 2003) (Figure 9), but no evidence of translocation from alveolar to the blood circulation was shown (Nemmar *et al.*, 2005).

IPL studies have certain advantages such as the possibility to achieve complete qualitative and quantitative studies of drug release, by frequent sample collection, but, unfortunately, in a short time duration, because structural and functional integrity of organs will quickly decline (Beck-Broichsitter *et al.*, 2011). Moreover, physiological conditions are not strictly respected, since lymph flow is altered, bronchial perfusion is suppressed, autonomic innervations are disconnected and blood cells are not present (Meiring *et al.*, 2005). In addition, the technique of isolation is hard to control and the perfusion system is expensive.

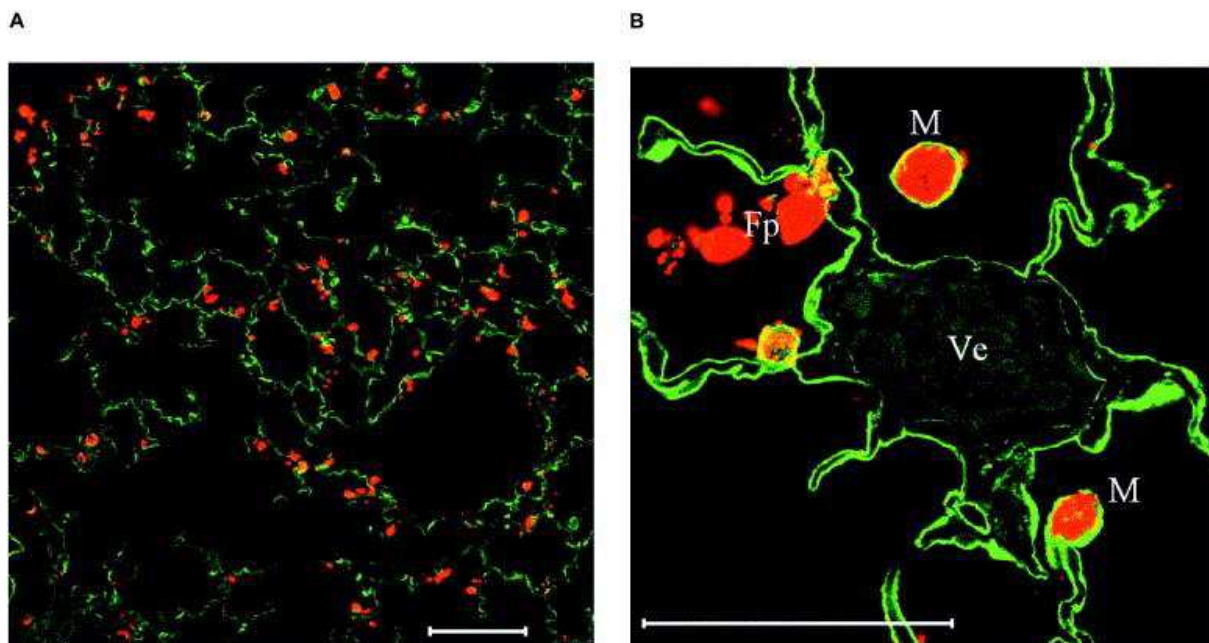


Figure 10. Particle distribution in lungs after intratracheal administration in isolated perfused organs. (A) Microspheres in red were homogeneously distributed into the lungs. (B) Particles were located in macrophages (M) but free particles (Fp) were also observed. No particles were detected in pulmonary vessels (Ve). Bars indicate 50 μm . (Hamoir *et al.*, 2003).

5.3.2. *Ex vitro* mucus models

Because of the rigidity of the mucin and the pore size distribution, mucus penetration is different for each nanoparticles. Indeed, interactions are surface coating-mediated (Kirch *et al.*, 2012). It was, for instance shown that PEG coating decreases mucus-nanoparticles interactions (Schuster *et al.*, 2013), while chitosan coating leads to a strong muco-adhesion (Zaru *et al.*, 2007). Indeed, chitosan-coated nanoparticles displayed more interactions with mucins (confirmed by an increase of zeta potential values), and a more important passage through the mucus than equivalent PVA-coated PLGA nanoparticles (Ungaro *et al.*, 2012, Mura *et al.*, 2011a).

5.4. *In vivo* models

Compared to other models, *in vivo* models present the large advantage to be a whole organism. Moreover, as previously described, *in vitro* lung delivery can be easily performed with specific veterinary devices. However experiments are limited by ethical concerns, and moreover expensive to carry out.

In most cases, small rodents have been employed to follow particle biodistribution and to perform assays on BAL after lung nanoparticle exposure. For example, insulin loaded into liposomes based on hydrogenated soybean phosphatidylcholine and cholesterol (Huang and Wang, 2006) or into SLN (Bi *et al.*, 2009) were administered to diabetic mice or rats by inhalation. In addition of the expected sustained effect, analyses of BAL have shown no immunoreaction nor inflammation (no leukocyte increase). Similarly, liposomes loaded with ciprofloxacin did not induce toxicity after intratracheal delivery to rats (Chono *et al.*, 2006). SLN stabilized with PVA and loaded with several antibiotics were also demonstrated to be interesting for the treatment of tuberculosis in guinea pigs (Pandey and Khuller, 2005). In addition to the sustained effect observed in peripheral organs (until 7 days after delivery), the absence of alteration in serum bilirubin assays has confirmed the safety of the formulations. PVA-coated PLGA nanoparticles loaded with elcatonin have shown a low lung retention in guinea pigs whereas chitosan coated-PLGA nanoparticles were more largely retained. The presence of chitosan causes of high muco-adhesion properties that may open intracellular tight junctions (Yamamoto *et al.*, 2005) and increase the cellular uptake (Yang *et al.*, 2009a). Indeed, positive surface of these nanoparticles induce strong electrostatic interactions with the exacerbated negative charge of cancer cells.

Very few studies relate experiments with non-rodents for lung drug delivery of nanoparticles. Beagle dogs were used to follow X-ray contrast agent nanoparticles, stabilized by Pluronic F68 or F108 (poloxamers) in lung draining lymph nodes, thus detectable with contrast agent radiographs (McIntire *et al.*, 1998). After administration, dogs were in good clinical conditions (good appetite, normal breathing and active/alert behavior) despite the presence of lung lesions detected during the autopsy. These lesions were described as infiltrations of macrophages signaling an inflammatory response, more prevalent with Pluronic F108 than F68. Sheep have shown a good lung dynamic compliance after intratracheal administration of liposomes loaded with amikacin (Schreier *et al.*, 1992) and the therapeutic effect of the liposomal form was higher than the free drug without causing any irritation.

5.5. Compared *in vitro* / *ex vivo* / *in vivo* nanotoxicity studies

Unfortunately, all the models cited previously rapidly reach some limits. Indeed, despite their human origin, *in vitro* cell models are more often immortalized by genetic modifications or originate from tumoral cancer which means they are quite far from the reality. Co-culture models improve traditional *in vitro* cell culture by mimicking cell-cell interactions. *Ex vivo* and *in vivo* models represent an interesting alternative, thanks to the presence of cell interactions or fluid circulation. Yet, the animal physiology is different from the human physiology. In order to improve our understanding of the behavior and interactions of nanoparticles towards human organism, compiling together results obtained on different models may represent a strong interest.

For example, Dailey *et al.* (Dailey *et al.*, 2006) have firstly proved that polymeric nanoparticles (PLGA and branched PLGA) do not induce a significant LDH release after 24 h exposure to A549 cells, whereas after instillation in Balb/c mice, LDH levels in BAL 24 h and 14 days were slightly higher than for non treated animals. In addition, nanoparticles did not provoke PMN recruitment, neither macrophage inflammatory protein secretion. Nassimi *et al.* (Nassimi *et al.*, 2009) have used the same method to investigate the toxicity of SLN: firstly towards A549 cells, then *ex vivo* on isolated lung slices and finally on Balb/c mice. *In vitro* cytotoxicity results have given a higher IC50 than on *ex vivo* experiments, that was explained by the more basic model, and the cell-cell interactions that definitely play a role in *ex vivo* models. The three models have shown the absence of LDH release as well as inflammatory response.

The effect of nanoparticle stabilizers (PVA, chitosan, Pluronic F68) coating PLGA nanoparticles were investigated towards bronchial and alveolar cells (Mura *et al.*, 2011a,b, Grabowski *et al.*, 2013). Pluronic F68-covered PLGA nanoparticles penetrate more deeply the mucus layer on the top of Calu-3 cells than PVA or chitosan-covered nanoparticles (Mura *et al.*, 2011a), without causing more cytotoxicity or inflammatory response (Mura *et al.*, 2011b). However, the same particles induce an increasing inflammatory response on A549 cells with a decrease of the mitochondrial activity, correlated with a higher internalization (Grabowski *et al.*, 2013). Chitosan-coated PLGA nanoparticles are also more cytotoxic than PVA-coated nanoparticles on A549 cells, without inducing other side effects (full membrane integrity, no inflammatory response) (Ungaro *et al.*, 2012). The toxicity of these nanoparticles was explained by the own cytotoxicity of chitosan in aqueous solution. In addition, chitosan-coated nanoparticles caused a decrease which was reversible of TEER, without increasing MUC5AC mRNA expression as well as the other tested nanoparticles (Mura *et al.*, 2011a). Additionally, an increase in cell marker membrane and in the IFN- γ production from dendritic cells after delivery of chitosan nanoparticles to rats was reported (Bivas-Benita *et al.*, 2004b).

In vitro and *in vivo* comparisons were performed in order to evaluate the radiodiagnostic tool potential of hematoporphyrin linked to albumin under nanoparticle form (Yang *et al.*, 2010). Accumulation was shown on A549 cells and correlated to a photodynamic activity after UV exposure, without any toxicity. The accumulation was confirmed in mice-bearing lung tumors and nanoparticles have shown a better half-life in rabbits than the free drug.

As there are in first line to face inhaled nanoparticles, alveolar macrophages should be widely studied, and particularly for phagocytosis (uptake) studies. Rifampicin was encapsulated into PLGA nanoparticles or microparticles (Ohashi *et al.*, 2009). Nanoparticles, or free drug as control, were spray-dried with mannitol to form microparticles. High aerosol performances of rifampicin / PLGA / mannitol microparticles were confirmed with the cascade impactor. In addition, thanks to the immediate mannitol dissolution, rifampicin / PLGA nanoparticles were immediately released. Applied on rat alveolar macrophages (NR8383), PLGA nanoparticles were taken up in significant quantity but less than PLGA microparticles. When rats were intratracheally administered with the three different formulations, the uptake of rifampicin associated to PLGA / mannitol microparticles was higher than from the other preparations. Microscopy observations of rat lungs evidenced that PLGA microparticles were rapidly excreted by the mucociliary clearance, whereas after mannitol dissolution, PLGA nanoparticles were retained in lungs. In comparison, rifampicin was loaded in SLN of 850 nm

and evaluated, *in vitro* on alveolar macrophages, primary epithelial cells (isolated from rats) and cell lines (NR8383 and A549), and delivered *in vivo* to rats (Chuan *et al.*, 2013). As expected, according to the size criteria, alveolar macrophages were specifically targeted (*in vitro* and *in vivo* results), with a sustained effect up to 12 h, and without decreasing the mitochondrial activity. It is also important to highlight that no differences were observed on primary cells and cell lines in terms of uptake and cytotoxicity. Moreover, delivery of PVA-coated PLGA and PLA nanoparticles on rats have shown that the uptake is predominantly achieved by alveolar macrophages compared to epithelial cells, without increasing the immune response (Thomas *et al.*, 2010).

Conclusion

Because of their small size, nanoparticles present a specific potential toxicity towards biological systems. Face to the need to consolidate all toxicity results obtained after nanoparticle exposure, toxicologists have created a new sub-discipline: the nanotoxicology. As shown above, nanoparticle toxicity encompasses several endpoints, and in order to suggest a safe nanomedicine, complete toxicity studies should be performed. For this purpose, to deeply understand interactions between nanomedicine and living organisms, several toxicity endpoints and diverse *in vitro*, *in vivo* and *ex vivo* models should be compared.

The use of nanoparticles in biopharmaceutical applications is constantly increasing. Nanomedicines, obtained through the use of large variety of drugs and nanoparticles, have a promising future in diagnostic and therapeutic (see Tables 2, 3, 4 for summary). Two major types of nanoparticles are currently investigated for the lung drug delivery: lipid and polymeric nanoparticles. Liposomes or SLN have the main advantages to be prepared with natural compounds, and loaded with insulin they have been shown as an interesting alternative to *iv.* administration (Table 2), without causing important toxicity. As far as polymeric nanoparticles are concerned, the stabilizer has a key role in interactions with biological systems (Table 3). According to the present report, lipid and polymeric nanoparticles are good candidates as nanocarriers. Further experimental and clinical studies are expected to understand human organism/nanoparticle interactions, and thus confirm, or not, the therapeutic and diagnostic potential of such nanomedicine.

Finally, a little number of other nanoparticles (Table 4) are proposed for lung delivery. For example, the preparation of contrast agent nanoparticles, stabilized with poloxamers, has revealed a low toxicity and can shown a strong interest in imaging.

Table 2. *In vitro* and *in vivo* pulmonary toxicity endpoints after exposure to **lipid-based nanoparticles**.

Lipid-based nanomedicines				
Nanoparticle	Drug	Model (administration way)	Nanoparticle toxicity endpoints	References
Liposomes				
HPC	Insulin	Normal / diabetic mice	No cell morphology modification, no inflammation	(Huang and Wang, 2006, Schreier <i>et al.</i> , 1992)
Chol	Amikacin	(aerosolization) Sheep (nebulization)	No toxicity, no irritation, good dynamic compliance and lung resistance	
HSPC	Ciprofloxacin	Rat	No toxicity	(Chono <i>et al.</i> , 2006)
PC	Rifampicin	A549 cells	No cytotoxicity	(Zaru <i>et al.</i> , 2007)
DPPC				
6-laurylhexyl lysinate	DNA	A549 cells Rat	Low toxicity	(Li <i>et al.</i> , 2011)
PEG	Manganese	A549 cells	Cytoplasmic uptake, No cytotoxicity	(Howell <i>et al.</i> , 2013)
Phosphatidyl-ethanolamine	DNA	LLC1 cells C57B1/6 mice	High lung retention after 48 h	
Chol				
DOPE				
Solid-lipid nanoparticles				
Lipids	Insulin	rat (diabetic)	No toxicity	(Bi <i>et al.</i> , 2009)
Triglycerides		A549	IC 50 (mg/mL) = 3090 (MTT) – 2090 (neutral red) – 500 (<i>ex vivo</i>)	(Nassimi <i>et al.</i> , 2010)
Phospholipids		Balb/c mice	No increasing of chem. KC, LDH, IL-6, IL-8, TNF- α , total proteins, total cells Toxic effects at 500 μ g/animal (No effect until 200 μ g).	
Lipids	Rifampicin+ Isoniazid + Pyrazinamide	Dunkin Hartley guinea pig	No alteration in serum bilirubin Drug release, with sustained effect, after 45 min	(Pandey and Khuller, 2005)
Lipids	Paclitaxel	A549	PEG and folate enhance cellular uptake without cytotoxicity	(Yuan <i>et al.</i> , 2008)
Soy bean lecithin	Rifampicin	N8383 Primary rat AM A549 Primary rat ATII Sprague-Dawleys rats	Low mitochondrial activity decreasing Better pharmacologic effects than the free drug Sustained effect until 12 h in AM/N8383 SLN fluorescence intensities higher in macrophages than in AEC Macrophage targeting	(Chuan <i>et al.</i> , 2013)

Chem., Chemokine ; *AM*, Alveolar Macrophages ; *AT I*, Alveolar Type II Epithelial cells ; *Chol*, Cholesterol ; *DCP*, dicetylphosphate ; *PC*, Phosphatidylcholine ; *HSPC*, hydrogenated soy phosphatidylcholin ; *DPPC*, 1,2-dipalmitoyl-sn-glycero-3-phosphocholine ; *PEG*, poly(ethyleneglycol) ; *DOPE*, 1,2-Dioleoyl-sn-glycero-3-phosphoethanolamine ; *DNA*, deoxyribonucleic acid.

Table 3. *In vitro* and *in vivo* pulmonary toxicity endpoints after exposure to **polymer-based nanoparticles**.

Polymer-based nanomedicine					
Nanoparticle		Drug	Model (administration mode)	Nanoparticle toxicity endpoints	References
Core	Stabilizer				
PLGA	PVA	Elcatonin Paclitaxel HBsAg	Guinea pig	Low lung retention	(Yamamoto <i>et al.</i> , 2005, Thomas <i>et al.</i> , 2010, Yang <i>et al.</i> , 2009a)
			Mice Rat Sprague-dawley rat	Taken up by alveolar macrophages Basal immune response	
			A549 cells Calu-3 cells HBE cells	Low cytotoxicity and Golgi colocalization	(Ungaro <i>et al.</i> , 2012, Grabowski <i>et al.</i> , 2013, Yang <i>et al.</i> , 2009a, Thomas <i>et al.</i> , 2010, Mura <i>et al.</i> , 2011a,b, Cartiera <i>et al.</i> , 2009)
PLGA	CS	Elcatonin Paclitaxel	Guinea pig	Long lung retention	(Yamamoto <i>et al.</i> , 2005, Yang <i>et al.</i> , 2009a)
			Mice Rat	May opening intracellular tight junctions Strong muco-	
			A549 cells Calu-3 cells	Uptake increase with CS concentration – energy dependent mechanism Medium/high toxicity	(Yang <i>et al.</i> , 2009a, Grabowski <i>et al.</i> , 2013, Mura <i>et al.</i> , 2011a, b)
PLGA	PF68		A549 Calu-3	High uptake – energy dependent mechanism Medium/high toxicity, significant inflammatory response, full membrane integrity	(Mura <i>et al.</i> , 2011a, b, Grabowski <i>et al.</i> , 2013)
PLA	PVA	HBsAg (Thomas <i>et al.</i> , 2010)	Sprague-dawley rat Calu-3	Taken up by alveolar macrophages No immune response	(Thomas <i>et al.</i> , 2010)
CS		DNA	Mice - Dendritic cells	Increasing of CD80, CD86, CD83 expression (LPS levels) and INF- γ production	(Bivas-Benita <i>et al.</i> , 2004b)

PLGA, poly(lactide-co-glycolique) acid ; *PLA*, polylactic acid ; *PVA*, polyvinylque alcoho ;, *CS*, Chitosan ; *PF68*, Pluronic F68 ; *DNA*, deoxyribonucleic acid.

Table 4. *In vitro* and *in vivo* pulmonary toxicity endpoints after exposure to other nanoparticles relevant for biomedical applications.

Nanomedicine					
Nanoparticle					
Core	Shell	Drug	Model (administration way)	Nanomedicine toxicity endpoints	References
Gold	Sodium tribasic dihydrate	LPS	Mice	Slow clearance Biodistribution: heart > thymus > spleen Fast clearance Biodistribution: spleen > thymus > heart	(Hussain <i>et al.</i> , 2013)
Human serum albumin Porcine gelatin	Glutaraldehyde		16HBE14o- cells Primary bronchial cells	Nanoparticle internalized inside cells (energy dependent mechanism) No cytotoxicity, Full membrane integrity, No inflammatory response	(Brzoska <i>et al.</i> , 2004)
Contrast agent	PF68 PF108	Contrast agent	Beagle dog	Good clinical conditions Lung lesions, inflammation Macrophage infiltrations prevalent with PF 108P than PF68	(McIntire <i>et al.</i> , 1998)
Fe ₃ O ₄	PLGA	Quercitin	A549 cells Balb/c mice (nebulization)	No cell morphology modification No cytotoxicity (100 µg/mL) No IL-6 secretion, High GSH levels (transitory)	(Verma <i>et al.</i> , 2013)
Antisense oligonucleotides	Mannose receptor		Rat alveolar macrophages	Full membrane integrity Alveolar macrophages targeting	(Liang <i>et al.</i> , 1996)

LPS = Lipopolysaccharides, PF68 / PF 108 = Pluronic F68 / F108, PLGA = poly(lactide-co-glycolide).

References

- ABBAS, I., SAINT-GEORGES, F., BILLET, S., VERDIN, A., MULLIEZ, P., SHIRALI, P. & GARÇON, G. 2009. Air pollution particulate matter (PM_{2.5})-induced gene expression of volatile organic compound and/or polycyclic aromatic hydrocarbon-metabolizing enzymes in an in vitro coculture lung model. *Toxicology in Vitro*, 23, 37-46.
- AL-HALLAK, M. H. D. K., SARFRAZ, M. K., AZARMI, S., ROA, W. H., FINLAY, W. H., ROULEAU, C. & LÖBENBERG, R. 2012. Distribution of effervescent inhalable nanoparticles after pulmonary delivery: an in vivo study. *Therapeutic Delivery*, 3, 725-734.
- ALFARO-MORENO, E., NAWROT, T. S., VANAUDENAERDE, B. M., HOYLAERTS, M. F., VANOIRBEEK, J. A., NEMERY, B. & HOET, P. H. M. 2008. Co-cultures of multiple cell types mimic pulmonary cell communication in response to urban PM₁₀. *European Respiratory Journal*, 32, 1184-1194.
- ANDUJAR, P., LANONE, S., BROCHARD, P. & BOCZKOWSKI, J. 2009. Effets respiratoires des nanoparticules manufacturées. *Revue des Maladies Respiratoires*, 26, 625-637.
- ANTON, N., JAKHMOLA, A. & VANDAMME, T. F. 2012. Trojan Microparticles for Drug Delivery. *Pharmaceutics*, 4, 1-25.
- BABIOR, B. M. 2000. Phagocytes and oxidative stress. *The American Journal of Medicine*, 109, 33-44.
- BACHAND, G. D., ALLEN, A., BACHAND, M., ACHYUTHAN, K. E., SEAGRAVE, J. C. & BROZIK, S. M. 2012. Cytotoxicity and inflammation in human alveolar epithelial cells following exposure to occupational levels of gold and silver nanoparticles. *Journal of Nanoparticle Research*, 14.
- BEAUCHAMP, C. & FRIDOVICH, I. 1971. Superoxide dismutase: Improved assays and an assay applicable to acrylamide gels. *Analytical Biochemistry*, 44, 276-287.
- BECK-BROICHSITTER, M., GAUSS, J., GESSLER, T., SEEGER, W., KISSEL, T. & SCHMEHL, T. 2010. Pulmonary targeting with biodegradable salbutamol-loaded nanoparticles. *J Aerosol Med Pulm Drug Deliv*, 23, 47-57.
- BECK-BROICHSITTER, M., GAUSS, J., PACKHAEUSER, C. B., LAHNSTEIN, K., SCHMEHL, T., SEEGER, W., KISSEL, T. & GESSLER, T. 2009. Pulmonary drug delivery with aerosolizable nanoparticles in an ex vivo lung model. *International Journal of Pharmaceutics*, 367, 169-178.
- BECK-BROICHSITTER, M., MERKEL, O. M. & KISSEL, T. 2012. Controlled pulmonary drug and gene delivery using polymeric nano-carriers. *Journal of Controlled Release*, 161, 214-224.
- BECK-BROICHSITTER, M., SCHMEHL, T., SEEGER, W. & GESSLER, T. 2011. Evaluating the Controlled Release Properties of Inhaled Nanoparticles Using Isolated, Perfused, and Ventilated Lung Models. *Journal of Nanomaterials*, 2011.
- BÉRUBÉ, K., PRYTHERCH, Z., JOB, C. & HUGHES, T. 2010. Human primary bronchial lung cell constructs: The new respiratory models. *Toxicology*, 278, 311-318.
- BHATTACHARYA, K., DAVOREN, M., BOERTZ, J., SCHINS, R., HOFFMANN, E. & DOPP, E. 2009. Titanium dioxide nanoparticles induce oxidative stress and DNA-adduct formation but not DNA-breakage in human lung cells. *Particle and Fibre Toxicology*, 6, 1-11.

- BI, R., SHAO, W., WANG, Q. & ZHANG, N. 2009. Solid lipid nanoparticles as insulin inhalation carriers for enhanced pulmonary delivery. *J Biomed Nanotechnol*, 5, 84-92.
- BIVAS-BENITA, M., ROMEIJN, S., JUNGINGER, H. E. & BORCHARD, G. 2004a. PLGA-PEI nanoparticles for gene delivery to pulmonary epithelium. *Eur J Pharm Biopharm*, 58, 1-6.
- BIVAS-BENITA, M., VAN MEIJGAARDEN, K. E., FRANKEN, K. L., JUNGINGER, H. E., BORCHARD, G., OTTENHOFF, T. H. & GELUK, A. 2004b. Pulmonary delivery of chitosan-DNA nanoparticles enhances the immunogenicity of a DNA vaccine encoding HLA-A*0201-restricted T-cell epitopes of Mycobacterium tuberculosis. *Vaccine*, 22, 1609-15.
- BIVAS-BENITA, M., ZWIER, R., JUNGINGER, H. E. & BORCHARD, G. 2005. Non-invasive pulmonary aerosol delivery in mice by the endotracheal route. *European Journal of Pharmaceutics and Biopharmaceutics*, 61, 214-218.
- BRUINENBERG, P., SERISIER, D., CIPOLLA, D. & BLANCHARD, J. 2010. Safety, Tolerability And Pharmacokinetics Of Novel Liposomal Ciprofloxacin Formulations For Inhalation In Healthy Volunteers And Non-Cystic Bronchiectasis Patients. *B49. BRONCHIECTASIS: CYSTIC FIBROSIS AND BEYOND*, A3192-A3192.
- BRZOSKA, M., LANGER, K., COESTER, C., LOITSCH, S., WAGNER, T. O. F. & MALLINCKRODT, C. V. 2004. Incorporation of biodegradable nanoparticles into human airway epithelium cells—in vitro study of the suitability as a vehicle for drug or gene delivery in pulmonary diseases. *Biochemical and Biophysical Research Communications*, 318, 562-570.
- BYRON, P. R., ROBERTS, N. S. & CLARK, A. R. 1986. An isolated perfused rat lung preparation for the study of aerosolized drug deposition and absorption. *J Pharm Sci*, 75, 168-71.
- CARTIERA, M. S., JOHNSON, K. M., RAJENDRAN, V., CAPLAN, M. J. & SALTZMAN, W. M. 2009. The uptake and intracellular fate of PLGA nanoparticles in epithelial cells. *Biomaterials*, 30, 2790-8.
- CELL STAINING SIMULATION TOOL LIFE TECHNOLOGIES. *Cell Staining Simulation Tool* [Online]. Available: <http://www.invitrogen.com/site/us/en/home/support/Research-Tools/Cell-Staining-Tool.html?CID=fl-cellstaintool> [Accessed 2013/07/11].
- CHOI, H. S., ASHITATE, Y., LEE, J. H., KIM, S. H., MATSUI, A., INSIN, N., BAWENDI, M. G., SEMMLER-BEHNKE, M., FRANGIONI, J. V. & TSUDA, A. 2010. Rapid translocation of nanoparticles from the lung airspaces to the body. *Nat Biotechnol*, 28, 1300-3.
- CHOI, S. J., OH, J. M. & CHOY, J. H. 2009. Toxicological effects of inorganic nanoparticles on human lung cancer A549 cells. *J Inorg Biochem*, 103, 463-71.
- CHONO, S., TANINO, T., SEKI, T. & MORIMOTO, K. 2006. Influence of particle size on drug delivery to rat alveolar macrophages following pulmonary administration of ciprofloxacin incorporated into liposomes. *J Drug Target*, 14, 557-66.
- CHUAN, J., LI, Y., YANG, L., SUN, X., ZHANG, Q., GONG, T. & ZHANG, Z. 2013. Enhanced rifampicin delivery to alveolar macrophages by solid lipid nanoparticles. *Journal of Nanoparticle Research*, 15, 1-9.
- CONSTANT, S., HUANG, S., CAULFUTY, M., BONFANTE, R., MONACHINO, M., FRAUENFELDER, R. & WISZNIEWSKI, L. 2011a. 28 day repeated dose toxicity test on an in vitro cell model. *Toxicology Letters*, 205, Supplement, S58.

- CONSTANT, S., HUANG, S., CAULFUTY, M., BONFANTE, R., MONACHINO, M., FRAUENFELDER, R. & WISZNIEWSKI, L. 2011b. A simple method for testing the toxicity of nanomaterials on 3D air-liquid interface human airway epithelia (MucilAir™). *Toxicology Letters*, 205, Supplement, S284.
- COONEY, D. J. & HICKEY, A. J. 2011. Cellular response to the deposition of diesel exhaust particle aerosols onto human lung cells grown at the air-liquid interface by inertial impaction. *Toxicology in Vitro*, 25, 1953-1965.
- CRAPO, J. D., BARRY, B. E., GEHR, P., BACHOFEN, M. & WEIBEL, E. R. 1982. Cell number and cell characteristics of the normal human lung. *The American review of respiratory disease*, 126, 332-337.
- CROMWELL, O., HAMID, Q., CORRIGAN, C. J., BARKANS, J., MENG, Q., COLLINS, P. D. & KAY, A. B. 1992. Expression and generation of interleukin-8, IL-6 and granulocyte-macrophage colony-stimulating factor by bronchial epithelial cells and enhancement by IL-1 beta and tumour necrosis factor-alpha. *Immunology*, 77, 330-7.
- DAILEY, L. A., JEKEL, N., FINK, L., GESSLER, T., SCHMEHL, T., WITTMAR, M., KISSEL, T. & SEEGER, W. 2006. Investigation of the proinflammatory potential of biodegradable nanoparticle drug delivery systems in the lung. *Toxicol Appl Pharmacol*, 215, 100-8.
- DESHMANE, S. L., KREMLEV, S., AMINI, S. & SAWAYA, B. E. 2009. Monocyte chemoattractant protein-1 (MCP-1): an overview. *J Interferon Cytokine Res*, 29, 313-26.
- DJOBA SIAWAYA, J. F., ROBERTS, T., BABB, C., BLACK, G., GOLAKAI, H. J., STANLEY, K., BAPELA, N. B., HOAL, E., PARIDA, S., VAN HELDEN, P. & WALZL, G. 2008. An Evaluation of Commercial Fluorescent Bead-Based Luminex Cytokine Assays. *PLoS ONE*, 3, e2535.
- DOMBU, C., CARPENTIER, R. & BETBEDER, D. 2012. Influence of surface charge and inner composition of nanoparticles on intracellular delivery of proteins in airway epithelial cells. *Biomaterials*, 33, 9117-9126.
- DONALDSON, K., STONE, V., TRAN, C. L., KREYLING, W. & BORM, P. J. 2004. Nanotoxicology. *Occup Environ Med*, 61, 727-8.
- DUPONT, N. C., WANG, K., WADHWA, P. D., CULHANE, J. F. & NELSON, E. L. 2005. Validation and comparison of luminex multiplex cytokine analysis kits with ELISA: Determinations of a panel of nine cytokines in clinical sample culture supernatants. *Journal of Reproductive Immunology*, 66, 175-191.
- ELY, L., ROA, W., FINLAY, W. H. & LÖBENBERG, R. 2007. Effervescent dry powder for respiratory drug delivery. *European Journal of Pharmaceutics and Biopharmaceutics*, 65, 346-353.
- EOM, H.-J. & CHOI, J. 2009. Oxidative stress of silica nanoparticles in human bronchial epithelial cell, Beas-2B. *Toxicology in Vitro*, 23, 1326-1332.
- EPTHELIX. *MucilAir™* [Online]. Available: <http://www.epithelix.com/content/view/6/5/lang,en/> [Accessed 2013/09/29].
- FADOK, V. A., VOELKER, D. R., CAMPBELL, P. A., COHEN, J. J., BRATTON, D. L. & HENSON, P. M. 1992. Exposure of phosphatidylserine on the surface of apoptotic lymphocytes triggers specific recognition and removal by macrophages. *The Journal of Immunology*, 148, 2207-16.

- FIEGEL, J., EHRHARDT, C., SCHAEFER, U., LEHR, C.-M. & HANES, J. 2003. Large Porous Particle Impingement on Lung Epithelial Cell Monolayers—Toward Improved Particle Characterization in the Lung. *Pharmaceutical Research*, 20, 788-796.
- FISHER, G. L. & PLACKE, M. E. 1987. In vitro models of lung toxicity. *Toxicology*, 47, 71-93.
- FOGH, J., FOGH, J. M. & ORFEO, T. 1977. One hundred and twenty-seven cultured human tumor cell lines producing tumors in nude mice. *J Natl Cancer Inst*, 59, 221-6.
- FOSTER, K. A., AVERY, M. L., YAZDANIAN, M. & AUDUS, K. L. 2000. Characterization of the Calu-3 cell line as a tool to screen pulmonary drug delivery. *International Journal of Pharmaceutics*, 208, 1-11.
- FOSTER, K. A., OSTER, C. G., MAYER, M. M., AVERY, M. L. & AUDUS, K. L. 1998. Characterization of the A549 cell line as a type II pulmonary epithelial cell model for drug metabolism. *Exp Cell Res*, 243, 359-66.
- GALLEY, H. F. & WEBSTER, N. R. 1996. The immuno-inflammatory cascade. *British Journal of Anaesthesia*, 77, 11-16.
- GÓMEZ-GAETE, C., FATTAL, E., SILVA, L., BESNARD, M. & TSAPIS, N. 2008. Dexamethasone acetate encapsulation into Trojan particles. *Journal of Controlled Release*, 128, 41-49.
- GRABOWSKI, N., HILLAIREAU, H., VERGNAUD, J., ARAGAO, L. S., KERDINE-ROMER, S., PALLARDY, M., TSAPIS, N. & FATTAL, E. 2013. Toxicity of surface-modified PLGA nanoparticles toward lung alveolar epithelial cells. *International Journal of Pharmaceutics*.
- GREEN, L. C., WAGNER, D. A., GLOGOWSKI, J., SKIPPER, P. L., WISHNOK, J. S. & TANNENBAUM, S. R. 1982. Analysis of nitrate, nitrite, and [15N]nitrate in biological fluids. *Analytical Biochemistry*, 126, 131-138.
- GRENHA, A., SEIJO, B. & REMUÑÁN-LÓPEZ, C. 2005. Microencapsulated chitosan nanoparticles for lung protein delivery. *European Journal of Pharmaceutical Sciences*, 25, 427-437.
- GRONEBERG, D. A., EYNOTT, P. R., LIM, S., OATES, T., WU, R., CARLSTEDT, I., ROBERTS, P., MCCANN, B., NICHOLSON, A. G., HARRISON, B. D. & CHUNG, K. F. 2002. Expression of respiratory mucins in fatal status asthmaticus and mild asthma. *Histopathology*, 40, 367-373.
- HAMOIR, J., NEMMAR, A., HALLOY, D., WIRTH, D., VINCKE, G., VANDERPLASSCHEN, A., NEMERY, B. & GUSTIN, P. 2003. Effect of polystyrene particles on lung microvascular permeability in isolated perfused rabbit lungs: role of size and surface properties. *Toxicology and Applied Pharmacology*, 190, 278-285.
- HAYDEN, P., KALUZHNY, Y., KUBILUS, J., AYE HUNIE, S., KANDAROVA, H. & KLAUSNER, M. 2011. Use of normal human 3-dimensional (NHu-3D) tissue models (EpiDerm, EpiAirway) for nanotoxicology applications *Alternative To Experimental Animals*. Montréal, Canada.
- HEIN, S., BUR, M., SCHAEFER, U. F. & LEHR, C.-M. 2011. A new Pharmaceutical Aerosol Deposition Device on Cell Cultures (PADDCCC) to evaluate pulmonary drug absorption for metered dose dry powder formulations. *European Journal of Pharmaceutics and Biopharmaceutics*, 77, 132-138.
- HENSLEY, K., MOU, S. & PYE, Q. 2003. Nitrite Determination by Colorimetric and Fluorometric Griess Diazotization Assays. In: HENSLEY, K. & FLOYD, R. (eds.) *Methods in Biological Oxidative Stress*. Humana Press.

- HERMANN, M. I., UNGER, R. E., KEHE, K., PETERS, K. & KIRKPATRICK, C. J. 2004. Lung epithelial cell lines in coculture with human pulmonary microvascular endothelial cells: development of an alveolo-capillary barrier in vitro. *Lab Invest*, 84, 736-52.
- HILLAIREAU, H. & COUVREUR, P. 2009. Nanocarriers' entry into the cell: relevance to drug delivery. *Cell Mol Life Sci*, 66, 2873-96.
- HOET, P. H., BRUSKE-HOHLFELD, I. & SALATA, O. V. 2004. Nanoparticles - known and unknown health risks. *J Nanobiotechnology*, 2, 12.
- HOWELL, M., MALLELA, J., WANG, C., RAVI, S., DIXIT, S., GARAPATI, U. & MOHAPATRA, S. 2013. Manganese-loaded lipid-micellar theranostics for simultaneous drug and gene delivery to lungs. *J Control Release*, 167, 210-8.
- HUANG, M., MA, Z., KHOR, E. & LIM, L.-Y. 2002. Uptake of FITC-Chitosan Nanoparticles by A549 Cells. *Pharmaceutical Research*, 19, 1488-1494.
- HUANG, Y. Y. & WANG, C. H. 2006. Pulmonary delivery of insulin by liposomal carriers. *J Control Release*, 113, 9-14.
- HUSSAIN, S., VANOIRBEEK, J. A. J., HAENEN, S., HAUFROID, V., BOLAND, S., MARANO, F., NEMERY, B. & HOET, P. H. M. 2013. Prior Lung Inflammation Impacts on Body Distribution of Gold Nanoparticles. *BioMed Research International*, 2013, 6.
- IVERSEN, T.-G., SKOTLAND, T. & SANDVIG, K. 2011. Endocytosis and intracellular transport of nanoparticles: Present knowledge and need for future studies. *Nano Today*, 6, 176-185.
- JÄNICKE, R. U., SPRENGART, M. L., WATI, M. R. & PORTER, A. G. 1998. Caspase-3 Is Required for DNA Fragmentation and Morphological Changes Associated with Apoptosis. *Journal of Biological Chemistry*, 273, 9357-9360.
- JANTZEN, K., ROURSGAARD, M., DESLER, C., LOFT, S., RASMUSSEN, L. J. & MØLLER, P. 2012. Oxidative damage to DNA by diesel exhaust particle exposure in co-cultures of human lung epithelial cells and macrophages. *Mutagenesis*, 27, 693-701.
- KELLEY, J. 1990. Cytokines of the Lung. *American Review of Respiratory Disease*, 141, 765-788.
- KEMP, S. J., THORLEY, A. J., GORELIK, J., SECKL, M. J., O'HARE, M. J., ARCARO, A., KORCHEV, Y., GOLDSTRAW, P. & TETLEY, T. D. 2008. Immortalization of human alveolar epithelial cells to investigate nanoparticle uptake. *Am J Respir Cell Mol Biol*, 39, 591-7.
- KERR, J. F., WYLLIE, A. H. & CURRIE, A. R. 1972. Apoptosis: a basic biological phenomenon with wide-ranging implications in tissue kinetics. *Br J Cancer*, 26, 239-57.
- KIM, I., BYEON, H. J., KIM, T. H., LEE, E. S., OH, K. T., SHIN, B. S., LEE, K. C. & YOUN, Y. S. 2012. Doxorubicin-loaded highly porous large PLGA microparticles as a sustained-release inhalation system for the treatment of metastatic lung cancer. *Biomaterials*, 33, 5574-5583.
- KIRCH, J., SCHNEIDER, A., ABOU, B., HOPF, A., SCHAEFER, U. F., SCHNEIDER, M., SCHALL, C., WAGNER, C. & LEHR, C.-M. 2012. Optical tweezers reveal relationship between microstructure and nanoparticle penetration of pulmonary mucus. *Proceedings of the National Academy of Sciences*, 109, 18355-18360.
- KOOPMAN, G., REUTELINGSPERGER, C. P. M., KUIJTEN, G. A. M., KEEHNEN, R. M. J., PALS, S. T. & VANOERS, M. H. J. 1994. ANNEXIN-V FOR FLOW CYTOMETRIC DETECTION

- OF PHOSPHATIDYLSERINE EXPRESSION ON B-CELLS UNDERGOING APOPTOSIS. *Blood*, 84, 1415-1420.
- KUNZLI, N. & TAGER, I. B. 2005. Air pollution: from lung to heart. *Swiss Med Wkly*, 135, 697-702.
- LABIRIS, N.R & DOLOVICH M. B. 2003, Pulmonary drug delivery. Part I: physiological factors affecting therapeutic effectiveness of aerosolized medications, *British Journal of Clinical Pharmacology*, 56, 588-599.
- LEBEL, C. P., ISCHIROPOULOS, H. & BONDY, S. C. 1992. Evaluation of the probe 2',7'-dichlorofluorescein as an indicator of reactive oxygen species formation and oxidative stress. *Chemical Research in Toxicology*, 5, 227-231.
- LI, N., XIA, T. & NEL, A. E. 2008. The role of oxidative stress in ambient particulate matter-induced lung diseases and its implications in the toxicity of engineered nanoparticles. *Free Radical Biology and Medicine*, 44, 1689-1699.
- LI, P., LIU, D. H., SUN, X. L., LIU, C. X., LIU, Y. J. & ZHANG, N. 2011. A novel cationic liposome formulation for efficient gene delivery via a pulmonary route. *Nanotechnology*, 22.
- LIANG, W., SHI, X., DESHPANDE, D., MALANGA, C. J. & ROJANASAKUL, Y. 1996. Oligonucleotide targeting to alveolar macrophages by mannose receptor-mediated endocytosis. *Biochimica et Biophysica Acta (BBA) - Biomembranes*, 1279, 227-234.
- LIEBER, M., SMITH, B., SZAKAL, A., NELSON-REES, W. & TODARO, G. 1976. A continuous tumor-cell line from a human lung carcinoma with properties of type II alveolar epithelial cells. *Int J Cancer*, 17, 62-70.
- LIN, H., CARLSON, D. M., ST. GEORGE, J. A., PLOPPER, C. G. & WU, R. 1989. An ELISA Method for the Quantitation of Tracheal Mucins from Human and Nonhuman Primates. *American Journal of Respiratory Cell and Molecular Biology*, 1, 41-48.
- LIN, W., HUANG, Y. W., ZHOU, X. D. & MA, Y. 2006. In vitro toxicity of silica nanoparticles in human lung cancer cells. *Toxicol Appl Pharmacol*, 217, 252-9.
- LIU, J., GONG, T., FU, H., WANG, C., WANG, X., CHEN, Q., ZHANG, Q., HE, Q. & ZHANG, Z. 2008. Solid lipid nanoparticles for pulmonary delivery of insulin. *International Journal of Pharmaceutics*, 356, 333-344.
- MACNEE, W. 2001. Oxidative stress and lung inflammation in airways disease. *European Journal of Pharmacology*, 429, 195-207.
- MANSOUR, H. M., RHEE, Y. S. & WU, X. 2009. Nanomedicine in pulmonary delivery. *Int J Nanomedicine*, 4, 299-319.
- MATHIAS, N. R., TIMOSZYK, J., STETSKO, P. I., MEGILL, J. R., SMITH, R. L. & WALL, D. A. 2002. Permeability Characteristics of Calu-3 Human Bronchial Epithelial Cells: In Vitro - In Vivo Correlation to Predict Lung Absorption in Rats. *Journal of Drug Targeting*, 10, 31-40.
- MATSUI, H., RANDELL, S. H., PERETTI, S. W., DAVIS, C. W. & BOUCHER, R. C. 1998. Coordinated clearance of periciliary liquid and mucus from airway surfaces. *J Clin Invest*, 102, 1125-31.
- MATTEK_CORPORATION. *EpiAirway™* [Online]. Available: <http://www.mattek.com/456-an-in-vitro-model-of-human-airway-epithelium-epi-airway-for-in-vitro-metabolism-toxicity-screening-and-drug-delivery-applications> [Accessed 2013/09/29].

- MCCORD, J. M. & FRIDOVICH, I. 1969. Superoxide Dismutase: AN ENZYMIC FUNCTION FOR ERYTHROCUPREIN (HEMOCUPREIN). *Journal of Biological Chemistry*, 244, 6049-6055.
- MCINTIRE, G. L., BACON, E. R., TONER, J. L., CORNACOFF, J. B., LOSCO, P. E., ILLIG, K. J., NIKULA, K. J., MUGGENBURG, B. A. & KETAI, L. 1998. Pulmonary delivery of nanoparticles of insoluble, iodinated CT x-ray contrast agents to lung draining lymph nodes in dogs. *Journal of Pharmaceutical Sciences*, 87, 1466-1470.
- MEHENDALE, H. M., ANGEVINE, L. S. & OHMIYA, Y. 1981. The isolated perfused lung — A critical evaluation. *Toxicology*, 21, 1-36.
- MEIRING, J. J., BORM, P. J., BAGATE, K., SEMMLER, M., SEITZ, J., TAKENAKA, S. & KREYLING, W. G. 2005. The influence of hydrogen peroxide and histamine on lung permeability and translocation of iridium nanoparticles in the isolated perfused rat lung. *Part Fibre Toxicol*, 2, 3.
- MORGAN, E., VARRO, R., SEPULVEDA, H., EMBER, J. A., APGAR, J., WILSON, J., LOWE, L., CHEN, R., SHIVRAJ, L., AGADIR, A., CAMPOS, R., ERNST, D. & GAUR, A. 2004. Cytometric bead array: a multiplexed assay platform with applications in various areas of biology. *Clin Immunol*, 110, 252-66.
- MOSMANN, T. 1983. Rapid colorimetric assay for cellular growth and survival: application to proliferation and cytotoxicity assays. *J Immunol Methods*, 65, 55-63.
- MU, L. & SPRANDO, R. 2010. Application of Nanotechnology in Cosmetics. *Pharmaceutical Research*, 27, 1746-1749.
- MUHLFELD, C., GEHR, P. & ROTHEN-RUTISHAUSER, B. 2008. Translocation and cellular entering mechanisms of nanoparticles in the respiratory tract. *Swiss Med Wkly*, 138, 387-91.
- MÜLLER, L., RIEDIKER, M., WICK, P., MOHR, M., GEHR, P. & ROTHEN-RUTISHAUSER, B. 2010. Oxidative stress and inflammation response after nanoparticle exposure: differences between human lung cell monocultures and an advanced three-dimensional model of the human epithelial airways. *Journal of The Royal Society Interface*, 7, S27-S40.
- MURA, S., HILLAIREAU, H., NICOLAS, J., Kerdine-Romer, S., LE DROUMAGUET, B., DELOMENIE, C., NICOLAS, V., PALLARDY, M., TSAPIS, N. & FATTAL, E. 2011a. Biodegradable nanoparticles meet the bronchial airway barrier: how surface properties affect their interaction with mucus and epithelial cells. *Biomacromolecules*, 12, 4136-43.
- MURA, S., HILLAIREAU, H., NICOLAS, J., LE DROUMAGUET, B., GUEUTIN, C., ZANNA, S., TSAPIS, N. & FATTAL, E. 2011b. Influence of surface charge on the potential toxicity of PLGA nanoparticles towards Calu-3 cells. *Int J Nanomedicine*, 6, 2591-605.
- NASSIMI, M., SCHLEH, C., LAUENSTEIN, H.-D., HUSSEIN, R., LÜBBERS, K., POHLMANN, G., SWITALLA, S., SEWALD, K., MÜLLER, M., KRUG, N., MÜLLER-GOYMANN, C. C. & BRAUN, A. 2009. Low cytotoxicity of solid lipid nanoparticles in in vitro and ex vivo lung models. *Inhalation Toxicology*, 21, 104-109.
- NASSIMI, M., SCHLEH, C., LAUENSTEIN, H. D., HUSSEIN, R., HOYMANN, H. G., KOCH, W., POHLMANN, G., KRUG, N., SEWALD, K., RITTINGHAUSEN, S., BRAUN, A. & MULLER-GOYMANN, C. 2010. A toxicological evaluation of inhaled solid lipid nanoparticles used as a potential drug delivery system for the lung. *Eur J Pharm Biopharm*, 75, 107-16.
- NEMMAR, A., HAMOIR, J., NEMERY, B. & GUSTIN, P. 2005. Evaluation of particle translocation across the alveolo-capillary barrier in isolated perfused rabbit lung model. *Toxicology*, 208, 105-113.

- NEWHOUSE, M. T. 1992. *Powder Inhaler*. USA patent application 484,069.
- NOWACKI, C., HEIGHTS, A. & BRISSON, A. G. 1985. *Metered Dose Inhaler*. USA patent application 574,340.
- NUSSLER, A. K., GLANEMANN, M., SCHIRMEIER, A., LIU, L. & NUSSLER, N. C. 2006. Fluorometric measurement of nitrite/nitrate by 2,3-diaminonaphthalene. *Nat. Protocols*, 1, 2223-2226.
- O'HARE, M. J., BOND, J., CLARKE, C., TAKEUCHI, Y., ATHERTON, A. J., BERRY, C., MOODY, J., SILVER, A. R. J., DAVIES, D. C., ALSOP, A. E., NEVILLE, A. M. & JAT, P. S. 2001. Conditional immortalization of freshly isolated human mammary fibroblasts and endothelial cells. *Proceedings of the National Academy of Sciences*, 98, 646-651.
- OHASHI, K., KABASAWA, T., OZEKI, T. & OKADA, H. 2009. One-step preparation of rifampicin/poly(lactic-co-glycolic acid) nanoparticle-containing mannitol microspheres using a four-fluid nozzle spray drier for inhalation therapy of tuberculosis. *Journal of Controlled Release*, 135, 19-24.
- PANDEY, R. & KHULLER, G. K. 2005. Solid lipid particle-based inhalable sustained drug delivery system against experimental tuberculosis. *Tuberculosis (Edinb)*, 85, 227-34.
- PANYAM, J., SAHOO, S. K., PRABHA, S., BARGAR, T. & LABHASETWAR, V. 2003. Fluorescence and electron microscopy probes for cellular and tissue uptake of poly(d,l-lactide-co-glycolide) nanoparticles. *International Journal of Pharmaceutics*, 262, 1-11.
- PAPRITZ, M., POHL, C., WÜBBEKE, C., MOISCH, M., HOFMANN, H., HERMANN, M. I., THIERMANN, H., KIRKPATRICK, C. J. & KEHE, K. 2010. Side-specific effects by cadmium exposure: Apical and basolateral treatment in a coculture model of the blood-air barrier. *Toxicology and Applied Pharmacology*, 245, 361-369.
- PARK, E.-J., YI, J., CHUNG, K.-H., RYU, D.-Y., CHOI, J. & PARK, K. 2008. Oxidative stress and apoptosis induced by titanium dioxide nanoparticles in cultured BEAS-2B cells. *Toxicology Letters*, 180, 222-229.
- PARK, E.-J., YOON, J., CHOI, K., YI, J. & PARK, K. 2009. Induction of chronic inflammation in mice treated with titanium dioxide nanoparticles by intratracheal instillation. *Toxicology*, 260, 37-46.
- PATTON, J. S. 1996. Mechanisms of macromolecule absorption by the lungs. *Advanced Drug Delivery Reviews*, 19, 3-36.
- PATTON, J. S. & BYRON, P. R. 2007. Inhaling medicines: delivering drugs to the body through the lungs. *Nat Rev Drug Discov*, 6, 67-74.
- PATTON, J. S., FISHBURN, C. S. & WEERS, J. G. 2004. The lungs as a portal of entry for systemic drug delivery. *Proc Am Thorac Soc*, 1, 338-44.
- PHELPS, R. M., JOHNSON, B. E., IHDE, D. C., GAZDAR, A. F., CARBONE, D. P., MCCLINTOCK, P. R., LINNOILA, R. I., MATTHEWS, M. J., BUNN, P. A., CARNEY, D., MINNA, J. D. & MULSHINE, J. L. 1996. NCI-navy medical oncology branch cell line data base. *Journal of Cellular Biochemistry*, 63, 32-91.
- PHILLIPS, J. E., CASE, N. R., CELLY, C., CHAPMAN, R. W., HEY, J. A. & MINNICOZZI, M. 2006. An enzyme-linked immunosorbent assay (ELISA) for the determination of mucin levels in bronchoalveolar lavage fluid. *Journal of Pharmacological and Toxicological Methods*, 53, 160-167.

- POHL, C., HERMANN, M. I., UBOLDI, C., BOCK, M., FUCHS, S., DEI-ANANG, J., MAYER, E., KEHE, K., KUMMER, W. & KIRKPATRICK, C. J. 2009. Barrier functions and paracellular integrity in human cell culture models of the proximal respiratory unit. *European Journal of Pharmaceutics and Biopharmaceutics*, 72, 339-349.
- POLITO, A. J. & PROUD, D. 1998. Epithelial cells as regulators of airway inflammation. *Journal of Allergy and Clinical Immunology*, 102, 714-718.
- RAHMAN, I., KODE, A. & BISWAS, S. K. 2007. Assay for quantitative determination of glutathione and glutathione disulfide levels using enzymatic recycling method. *Nat. Protocols*, 1, 3159-3165.
- RANDALL, T. D. 2010. Chapter 7 - Bronchus-Associated Lymphoid Tissue (BALT): Structure and Function. In: SIDONIA, F. & ANDREA, C. (eds.) *Advances in Immunology*. Academic Press.
- REDDEL, R. R., KE, Y., GERWIN, B. I., MCMENAMIN, M. G., LECHNER, J. F., SU, R. T., BRASH, D. E., PARK, J. B., RHIM, J. S. & HARRIS, C. C. 1988. Transformation of human bronchial epithelial cells by infection with SV40 or adenovirus-12 SV40 hybrid virus, or transfection via strontium phosphate coprecipitation with a plasmid containing SV40 early region genes. *Cancer Res*, 48, 1904-9.
- REPINE, J. E., BAST, A. & LANKHORST, I. D. A. 1997. Oxidative Stress in Chronic Obstructive Pulmonary Disease. *American Journal of Respiratory and Critical Care Medicine*, 156, 341-357.
- REUL, R., TSAPIS, N., HILLAIREAU, H., SANCEY, L., MURA, S., RECHER, M., NICOLAS, J., COLL, J.-L. & FATTAL, E. 2012. Near infrared labeling of PLGA for in vivo imaging of nanoparticles. *Polymer Chemistry*, 3, 694-702.
- ROBERTSON, J., CALDWELL, J. R., CASTLE, J. R. & WALDMAN, R. H. 1976. Evidence for the Presence of Components of the Alternative (Properdin) Pathway of Complement Activation in Respiratory Secretions. *The Journal of Immunology*, 117, 900-903.
- ROTHEN-RUTISHAUSER, B., CLIFT, M. J. D., JUD, C., FINK, A. & WICK, P. 2012. Human epithelial cells in vitro – Are they an advantageous tool to help understand the nanomaterial-biological barrier interaction? . *Euro Nanotox Letters*, 4, 1-20.
- ROTHEN-RUTISHAUSER, B. M., KIAMA, S. G. & GEHR, P. 2005. A Three-Dimensional Cellular Model of the Human Respiratory Tract to Study the Interaction with Particles. *American Journal of Respiratory Cell and Molecular Biology*, 32, 281-289.
- RUBIN, B. K. 2002. Physiology of airway mucus clearance. *Respir Care*, 47, 761-8.
- RUGE, C. A., KIRCH, J., CAÑADAS, O., SCHNEIDER, M., PEREZ-GIL, J., SCHAEFER, U. F., CASALS, C. & LEHR, C.-M. 2011. Uptake of nanoparticles by alveolar macrophages is triggered by surfactant protein A. *Nanomedicine: Nanotechnology, Biology and Medicine*, 7, 690-693.
- SAHAY, G., ALAKHOVA, D. Y. & KABANOV, A. V. 2010. Endocytosis of nanomedicines. *Journal of Controlled Release*, 145, 182-195.
- SAHOO, S. K., PANYAM, J., PRABHA, S. & LABHASETWAR, V. 2002. Residual polyvinyl alcohol associated with poly (d,l-lactide-co-glycolide) nanoparticles affects their physical properties and cellular uptake. *Journal of Controlled Release*, 82, 105-114.
- SAKAGAMI, M. 2006. In vivo, in vitro and ex vivo models to assess pulmonary absorption and disposition of inhaled therapeutics for systemic delivery. *Advanced Drug Delivery Reviews*, 58, 1030-1060.

- SALLUSTO, F., MACKAY, C. R. & LANZAVECCHIA, A. 2000. The role of chemokine receptors in primary, effector, and memory immune responses. *Annu Rev Immunol*, 18, 593-620.
- SAMET, J. M. & CHENG, P. W. 1994. The role of airway mucus in pulmonary toxicology. *Environ Health Perspect*, 102 Suppl 2, 89-103.
- SCHREIER, H., MCNICOL, K. J., AUSBORN, M., SOUCY, D. M., DERENDORF, H., STECENKO, A. A. & GONZALEZROTHI, R. J. 1992. Pulmonary Delivery of Amikacin Liposomes and Acute Liposome Toxicity in the Sheep. *International Journal of Pharmaceutics*, 87, 183-193.
- SCHUSTER, B. S., SUK, J. S., WOODWORTH, G. F. & HANES, J. 2013. Nanoparticle diffusion in respiratory mucus from humans without lung disease. *Biomaterials*, 34, 3439-46.
- SCHWAB, J. A. & ZENKEL, M. 1998. Filtration of particulates in the human nose. *Laryngoscope*, 108, 120-4.
- SCHWARZ, C., MEHNERT, W., LUCKS, J. S. & MÜLLER, R. H. 1994. Solid lipid nanoparticles (SLN) for controlled drug delivery. I. Production, characterization and sterilization. *Journal of Controlled Release*, 30, 83-96.
- SEMMLER-BEHNKE, M., TAKENAKA, S., FERTSCH, S., WENK, A., SEITZ, J., MAYER, P., OBERDORSTER, G. & KREYLING, W. G. 2007. Efficient elimination of inhaled nanoparticles from the alveolar region: evidence for interstitial uptake and subsequent reentrainment onto airways epithelium. *Environ Health Perspect*, 115, 728-33.
- SEMMLER, M., SEITZ, J., ERBE, F., MAYER, P., HEYDER, J., OBERDORSTER, G. & KREYLING, W. G. 2004. Long-term clearance kinetics of inhaled ultrafine insoluble iridium particles from the rat lung, including transient translocation into secondary organs. *Inhal Toxicol*, 16, 453-9.
- SHARMA, K., SOMAVARAPU, S., COLOMBANI, A., GOVIND, N. & TAYLOR, K. M. 2012. Crosslinked chitosan nanoparticle formulations for delivery from pressurized metered dose inhalers. *Eur J Pharm Biopharm*, 81, 74-81.
- SHELLY, M. P., LLOYD, G. M. & PARK, G. R. 1988. A review of the mechanisms and methods of humidification of inspired gases. *Intensive Care Medicine*, 14, 1-9.
- SHERMAN, M. P. & GANZ, T. 1992. Host Defense in Pulmonary Alveoli. *Annual Review of Physiology*, 54, 331-350.
- SHI, L., PLUMLEY, C. J. & BERKLAND, C. 2007. Biodegradable Nanoparticle Flocculates for Dry Powder Aerosol Formulation. *Langmuir*, 23, 10897-10901.
- SHI, Y., WANG, F., HE, J., YADAV, S. & WANG, H. 2010. Titanium dioxide nanoparticles cause apoptosis in BEAS-2B cells through the caspase 8/t-Bid-independent mitochondrial pathway. *Toxicology Letters*, 196, 21-27.
- SHOEMAKER, R. H., WOLPERT-DEFILIPPES, M. K., KERN, D. H., LIEBER, M. M., MAKUCH, R. W., MELNICK, N. R., MILLER, W. T., SALMON, S. E., SIMON, R. M., VENDITTI, J. M. & VON HOFF, D. D. 1985. Application of a Human Tumor Colony-forming Assay to New Drug Screening. *Cancer Research*, 45, 2145-2153.
- SIES, H. 1997. Oxidative stress: oxidants and antioxidants. *Experimental Physiology*, 82, 291-295.
- SIMON-DECKERS, A., GOUGET, B., MAYNE-L'HERMITE, M., HERLIN-BOIME, N., REYNAUD, C. & CARRIERE, M. 2008. In vitro investigation of oxide nanoparticle and carbon

- nanotube toxicity and intracellular accumulation in A549 human pneumocytes. *Toxicology*, 253, 137-46.
- SINGH, N. P., MCCOY, M. T., TICE, R. R. & SCHNEIDER, E. L. 1988. A simple technique for quantitation of low levels of DNA damage in individual cells. *Experimental Cell Research*, 175, 184-191.
- SORG, O. 2004. Oxidative stress: a theoretical model or a biological reality? *Comptes Rendus Biologies*, 327, 649-662.
- SPURR-MICHAUD, S., ARGÜESO, P. & GIPSON, I. 2007. Assay of mucins in human tear fluid. *Experimental Eye Research*, 84, 939-950.
- STEERENBERG, P. A., ZONNENBERG, J. A., DORMANS, J. A., JOON, P. N., WOUTERS, I. M., VAN BREE, L., SCHEEPERS, P. T. & VAN LOVEREN, H. 1998. Diesel exhaust particles induced release of interleukin 6 and 8 by (primed) human bronchial epithelial cells (BEAS 2B) in vitro. *Experimental Lung Research*, 24, 85-100.
- STRÍŽ, I., SLAVČEV, A., KALANIN, J., JAREŠOVÁ, M. & RENNARD, S. I. 2001. Cell-Cell Contacts with Epithelial Cells Modulate the Phenotype of Human Macrophages. *Inflammation*, 25, 241-246.
- STRIZ, I., WANG, Y. M., TESCHLER, H., SORG, C. & COSTABEL, U. 1993. Phenotypic markers of alveolar macrophage maturation in pulmonary sarcoidosis. *Lung*, 171, 293-303.
- SUN, Y., OBERLEY, L. W. & LI, Y. 1988. A simple method for clinical assay of superoxide dismutase. *Clin Chem*, 34, 497-500.
- SUNG, J. C., PULLIAM, B. L. & EDWARDS, D. A. 2007. Nanoparticles for drug delivery to the lungs. *Trends Biotechnol*, 25, 563-70.
- TARNOK, A., HAMBSCH, J., CHEN, R. & VARRO, R. 2003. Cytometric bead array to measure six cytokines in twenty-five microliters of serum. *Clin Chem*, 49, 1000-2.
- TENNANT, J. R. 1964. Evaluation of the Trypan Blue Technique for Determination of Cell Viability. *Transplantation*, 2, 685-694.
- THOMAS, C., RAWAT, A., HOPE-WEEKS, L. & AHSAN, F. 2010. Aerosolized PLA and PLGA Nanoparticles Enhance Humoral, Mucosal and Cytokine Responses to Hepatitis B Vaccine. *Molecular Pharmaceutics*, 8, 405-415.
- TICE, R. R., AGURELL, E., ANDERSON, D., BURLINSON, B., HARTMANN, A., KOBAYASHI, H., MIYAMAE, Y., ROJAS, E., RYU, J. C. & SASAKI, Y. F. 2000. Single cell gel/comet assay: guidelines for in vitro and in vivo genetic toxicology testing. *Environ Mol Mutagen*, 35, 206-21.
- TOMODA, K., OHKOSHI, T., HIROTA, K., SONAVANE, G. S., NAKAJIMA, T., TERADA, H., KOMURO, M., KITAZATO, K. & MAKINO, K. 2009. Preparation and properties of inhalable nanocomposite particles for treatment of lung cancer. *Colloids and Surfaces B: Biointerfaces*, 71, 177-182.
- TOMODA, K., OHKOSHI, T., NAKAJIMA, T. & MAKINO, K. 2008. Preparation and properties of inhalable nanocomposite particles: Effects of the size, weight ratio of the primary nanoparticles in nanocomposite particles and temperature at a spray-dryer inlet upon properties of nanocomposite particles. *Colloids and Surfaces B: Biointerfaces*, 64, 70-76.

- TROUILLER, B., RELIENE, R., WESTBROOK, A., SOLAIMANI, P. & SCHIESTL, R. H. 2009. Titanium Dioxide Nanoparticles Induce DNA Damage and Genetic Instability In vivo in Mice. *Cancer Research*, 69, 8784-8789.
- TSAPIS, N., BENNETT, D., JACKSON, B., WEITZ, D. A. & EDWARDS, D. A. 2002. Trojan particles: large porous carriers of nanoparticles for drug delivery. *Proc Natl Acad Sci U S A*, 99, 12001-5.
- TSENG, C.-L., WU, S. Y.-H., WANG, W.-H., PENG, C.-L., LIN, F.-H., LIN, C.-C., YOUNG, T.-H. & SHIEH, M.-J. 2008. Targeting efficiency and biodistribution of biotinylated-EGF-conjugated gelatin nanoparticles administered via aerosol delivery in nude mice with lung cancer. *Biomaterials*, 29, 3014-3022.
- TSUDA, T., NOGUCHI, H., TAKUMI, Y. & AOCHI, O. 1977. Optimum humidification of air administered to a tracheostomy in dogs: Scanning electron microscopy and surfactant studies. *British Journal of Anaesthesia*, 49, 965-977.
- TSUKAGOSHI, H., SHIMIZU, Y., IWAMAE, S., HISADA, T., ISHIZUKA, T., IIZUKA, K., DOBASHI, K. & MORI, M. 2000. Evidence of oxidative stress in asthma and COPD: potential inhibitory effect of theophylline. *Respiratory Medicine*, 94, 584-588.
- UNGARO, F., D'ANGELO, I., COLETTA, C., D'EMMANUELE DI VILLA BIANCA, R., SORRENTINO, R., PERFETTO, B., TUFANO, M. A., MIRO, A., LA ROTONDA, M. I. & QUAGLIA, F. 2012. Dry powders based on PLGA nanoparticles for pulmonary delivery of antibiotics: modulation of encapsulation efficiency, release rate and lung deposition pattern by hydrophilic polymers. *J Control Release*, 157, 149-59.
- UNGARO, F., GIOVINO, C., COLETTA, C., SORRENTINO, R., MIRO, A. & QUAGLIA, F. 2010. Engineering gas-foamed large porous particles for efficient local delivery of macromolecules to the lung. *European Journal of Pharmaceutical Sciences*, 41, 60-70.
- VANENGLAND, M., RAMAEKERS, F. C. S., SCHUTTE, B. & REUTELINGSPERGER, C. P. M. 1996. A novel assay to measure loss of plasma membrane asymmetry during apoptosis of adherent cells in culture. *Cytometry*, 24, 131-139.
- VARSHOSAZ, J., GHAFFARI, S., MIRSHOJAEI, S. F., JAFARIAN, A., ATYABI, F., KOBARFARD, F. & AZARMI, S. 2013. Biodistribution of Amikacin Solid Lipid Nanoparticles after Pulmonary Delivery. *BioMed Research International*, 2013, 8.
- VERMA, N. K., CROSBIE-STANTON, K., SATTI, A., GALLAGHER, S., RYAN, K. B., DOODY, T., MCATAMNEY, C., MACLOUGHLIN, R., GALVIN, P., BURKE, C. S., VOLKOV, Y. & GUN'KO, Y. K. 2013. Magnetic core-shell nanoparticles for drug delivery by nebulization. *Journal of Nanobiotechnology*. 2013 Jan 23, 11, 1.
- WANG, J. X., CHEN, C. Y., LIU, Y., JIAO, F., LI, W., LAO, F., LI, Y. F., LI, B., GE, C. C., ZHOU, G. Q., GAO, Y. X., ZHAO, Y. L. & CHAI, Z. F. 2008. Potential neurological lesion after nasal instillation of TiO₂ nanoparticles in the anatase and rutile crystal phases. *Toxicology Letters*, 183, 72-80.
- WANG, S., YOUNG, R. S., SUN, N. N. & WITTEN, M. L. 2002. In vitro cytokine release from rat type II pneumocytes and alveolar macrophages following exposure to JP-8 jet fuel in co-culture. *Toxicology*, 173, 211-219.

- WEERS, J., METZHEISER, B., TAYLOR, G., WARREN, S., MEERS, P. & PERKINS, W. R. 2009. A gamma scintigraphy study to investigate lung deposition and clearance of inhaled amikacin-loaded liposomes in healthy male volunteers. *J Aerosol Med Pulm Drug Deliv*, 22, 131-8.
- WEIBEL, E. R. & GOMEZ, D. M. 1962. Architecture of the Human Lung: Use of quantitative methods establishes fundamental relations between size and number of lung structures. *Science*, 137, 577-585.
- WITHERDEN, I. R., VANDEN BON, E. J., GOLDSTRAW, P., RATCLIFFE, C., PASTORINO, U. & TETLEY, T. D. 2004. Primary Human Alveolar Type II Epithelial Cell Chemokine Release. *American Journal of Respiratory Cell and Molecular Biology*, 30, 500-509.
- WÖRLE-KNIRSCH, J. M., PULSKAMP, K. & KRUG, H. F. 2006. Oops They Did It Again! Carbon Nanotubes Hoax Scientists in Viability Assays. *Nano Letters*, 6, 1261-1268.
- WOTTRICH, R., DIABATÉ, S. & KRUG, H. F. 2004. Biological effects of ultrafine model particles in human macrophages and epithelial cells in mono- and co-culture. *International Journal of Hygiene and Environmental Health*, 207, 353-361.
- WRIGHT, J. R. 1997. Immunomodulatory functions of surfactant. *Physiol Rev*, 77, 931-62.
- WRIGHT, J. R. 2005. Immunoregulatory functions of surfactant proteins. *Nat Rev Immunol*, 5, 58-68.
- YAMAMOTO, H., KUNO, Y., SUGIMOTO, S., TAKEUCHI, H. & KAWASHIMA, Y. 2005. Surface-modified PLGA nanosphere with chitosan improved pulmonary delivery of calcitonin by mucoadhesion and opening of the intercellular tight junctions. *J Control Release*, 102, 373-81.
- YANG, R., YANG, S.-G., SHIM, W.-S., CUI, F., CHENG, G., KIM, I.-W., KIM, D.-D., CHUNG, S.-J. & SHIM, C.-K. 2009a. Lung-specific delivery of paclitaxel by chitosan-modified PLGA nanoparticles via transient formation of microaggregates. *Journal of Pharmaceutical Sciences*, 98, 970-984.
- YANG, S. G., CHANG, J. E., SHIN, B., PARK, S., NA, K. & SHIM, C. K. 2010. (99m)Tc-hematoporphyrin linked albumin nanoparticles for lung cancer targeted photodynamic therapy and imaging. *Journal of Materials Chemistry*, 20, 9042-9046.
- YANG, Y., BAJAJ, N., XU, P., OHN, K., TSIFANSKY, M. D. & YEO, Y. 2009b. Development of highly porous large PLGA microparticles for pulmonary drug delivery. *Biomaterials*, 30, 1947-1953.
- YANG, Y., TSIFANSKY, M. D., SHIN, S., LIN, Q. & YEO, Y. 2011. Mannitol-Guided delivery of ciprofloxacin in artificial cystic fibrosis mucus model. *Biotechnology and Bioengineering*, 108, 1441-1449.
- YUAN, H., MIAO, J., DU, Y. Z., YOU, J., HU, F. Q. & ZENG, S. 2008. Cellular uptake of solid lipid nanoparticles and cytotoxicity of encapsulated paclitaxel in A549 cancer cells. *International Journal of Pharmaceutics*, 348, 137-45.
- ZARU, M., MOURTAS, S., KLEPETSANIS, P., FADDA, A. M. & ANTIMISIARIS, S. G. 2007. Liposomes for drug delivery to the lungs by nebulization. *European Journal of Pharmaceutics and Biopharmaceutics*, 67, 655-666.
- ZENG, X.-M., MACRITCHIE, H. B., MARRIOTT, C. & MARTIN, G. P. 2007. Humidity-induced changes of the aerodynamic properties of dry powder aerosol formulations containing different carriers. *International Journal of Pharmaceutics*, 333, 45-55.

Travaux expérimentaux



Ce projet de thèse se propose d'évaluer la toxicité *in vitro* de nanoparticules biodégradables de PLGA, stabilisées ou non par des polymères de surface, vis-à-vis du système pulmonaire.

Comme l'ont démontré les travaux antérieurs, les études de nanotoxicité doivent aborder différents paramètres, afin de comprendre les mécanismes d'interaction entre les nanoparticules et les cellules. Au cours des travaux expérimentaux, les paramètres relatifs à la nanotoxicologie étudiés seront :


- L'activité mitochondriale,
- La viabilité par le test au bleu trypan,
- L'évaluation de la perméabilité de la membrane cellulaire par le dosage de la LDH libérée et le marquage par l'iodure de propidium,
- Le type de mort cellulaire par le marquage à l'Annexine V et le 7-AAD,
- La réponse inflammatoire par le dosage de cytokines sécrétées dans le milieu extracellulaire,
- Le stress oxydant par le dosage des ROS intracellulaires.

Les poumons étant un tissu complexe du point de vue histologique et physiologique, nous avons décidé d'étudier différents modèles *in vitro* : les cellules A549 en mono-culture (Chapitre 1), ou en co-culture avec les macrophages différenciés de monocytes THP-1 (Chapitre 3). Au cours du chapitre 2, le comportement des nanoparticules a été évalué vis-à-vis de macrophages différenciés de monocytes THP-1, qui présentent les caractéristiques des macrophages humains.

Enfin, les résultats seront discutés à la lumière de ceux obtenus précédemment au sein de l'équipe de recherche, d'une part, *in vitro* sur un modèle d'épithélium bronchique, et d'autre part, *in vivo* sur un modèle de souris, afin de dresser un profil de toxicité des nanoparticules selon leurs propriétés physico-chimiques.

Chapitre 1

Toxicité de nanoparticules de PLGA de charge de surface variée vis-à-vis de cellules épithéliales alvéolaires pulmonaires humaines



Article publié dans l'International Journal of Pharmaceutics

Volume 454, Issue 2, Octobre 2013, Pages 686-694

Résumé

Au cours de ce premier chapitre, des nanoparticules biodégradables de polymères ainsi que des nanoparticules non-biodégradables utilisées tout au long des travaux de thèse sont présentées. Ces nanoparticules ont été incubées en présence de cellules A549, lignée de cellules d'épithélium alvéolaire pulmonaire dérivée d'un adénocarcinome humain, afin d'en évaluer l'éventuelle toxicité. Les résultats sont présentés sous forme d'un article scientifique publié.

Au cours de ce travail, des nanoparticules biodégradables à base de (poly-lactide-co-glycolide) (PLGA) ont été formulées par émulsion-évaporation de solvant, ou par nanopréciipitation, en présence d'un agent stabilisant capable de s'associer à la surface des nanoparticules. Les agents qui ont été utilisés sont l'alcool polyvinylique (PVA), le chitosane (CS) ou le Pluronic F68 (PF68) qui aboutissent respectivement à la formation de nanoparticules neutres (PLGA/PVA NPs), positives (PLGA/CS NPs) ou négatives (PLGA/PF68 NPs), ayant toutes une taille moyenne de l'ordre de 230 nm. Les nanoparticules préparées sans agent stabilisant possèdent un potentiel zêta négatif et une taille moyenne de 170 nm.

Parallèlement, des nanoparticules non-biodégradables de polystyrène (PS NPs) ainsi que des nanoparticules de dioxyde de titane (TiO_2), de forme cristalline anatase (anatase TiO_2 NPs) et rutile (rutile TiO_2 NPs) ont été obtenues commercialement. Elles ont été choisies comme contrôle positif car il est décrit dans la littérature qu'elles induisent une certaine toxicité, et particulièrement une réponse inflammatoire (Dailey *et al.*, 2006, Inoue *et al.*, 2008).

Dans un premier temps l'internalisation des nanoparticules par les cellules a été évaluée. Ces expériences menées après exposition aux différents types de nanoparticules de PLGA montrent que les nanoparticules chargées négativement, c'est-à-dire les nanoparticules de PLGA/PF68, sont internalisées plus rapidement et en plus grande quantité que les autres. La microscopie confocale permet de conclure que les nanoparticules sont bien présentes à l'intérieur des cellules, de manière homogène pour les nanoparticules de PLGA/PVA, tandis que les nanoparticules de PLGA/CS et PLGA/PF68 semblent être localisées dans des vacuoles d'endocytose.

La cytotoxicité des nanoparticules a ensuite été évaluée par la mesure de l'activité mitochondriale (tests MTT) ainsi que par l'étude de l'intégrité membranaire (mesure de

l'enzyme lactate deshydrogénase (LDH) libérée dans le milieu extracellulaire, le test au bleu trypan et le marquage à l'iodure de propidium (PI pour Propidium Iodide)) après exposition aux nanoparticules. Les cytotoxicités des nanoparticules de PLGA et de polystyrène sont généralement plus faibles ou équivalentes à celles induites par les nanoparticules de TiO₂, quelque soit la forme cristalline. La toxicité observée après exposition aux nanoparticules de PLGA/CS peut être expliquée par la cytotoxicité propre du chitosane seul en solution aqueuse. Quant à la toxicité des nanoparticules de PLGA/PF68 elle peut être expliquée par l'internalisation en plus grande quantité de ce type de nanoparticules.

La réponse inflammatoire a été quantifiée après exposition aux nanoparticules par le dosage de plusieurs cytokines, notamment l'IL-6, l'IL-8, le MCP-1 et le TNF- α . Exceptées les nanoparticules de PLGA/PF68, les nanoparticules testées induisent une réponse inflammatoire très faible, qui est toujours inférieure à celle induite après exposition au lipopolysaccharides (LPS). En revanche, après exposition aux nanoparticules de PLGA/PF68, les sécrétions des cytokines sont plus importantes que celles obtenues après exposition au LPS, en particulier pour MCP-1. Cette différence dans la réponse inflammatoire peut s'expliquer à nouveau par une internalisation plus importante des nanoparticules PLGA/PF68.

Le stress oxydant causé par les nanoparticules de PLGA et de polystyrène a été quantifié par le dosage des espèces réactives de l'oxygène (ROS pour Reactive Oxygen Species) intracellulaires. Après 1 h, 4 h et 24 h d'exposition, aucune des nanoparticules testées, ni les polymères de surface associés, n'induisent la production de ROS. La combinaison des ces résultats permet de conclure que de manière générale les nanoparticules de PLGA entraînent une faible toxicité vis-à-vis des cellules A549. De plus, nous avons montré que la nature des nanoparticules, ainsi que leur recouvrement de surface, jouent un rôle des plus importants dans la réponse cellulaire, en impactant l'internalisation, la cytotoxicité ou la réponse inflammatoire.

Toxicity of surface-modified PLGA nanoparticles towards lung alveolar epithelial cells

Nadège Grabowski ^{a,b}, Hervé Hillaireau ^{a,b}, Juliette Vergnaud ^{a,b}, Leticia Aragão Santiago ^{a,b},
Saadia Kerdine-Romer ^c, Marc Pallardy ^c, Nicolas Tsapis ^{a,b}, Elias Fattal ^{a,b}

^a. Université Paris-Sud, Faculté de pharmacie, Institut Galien Paris-Sud, LabEx LERMIT, 5 rue JB Clément, 92296 Chatenay-Malabry Cedex, France

^b. CNRS, UMR 8612, 5 rue JB Clément, 92296 Chatenay-Malabry Cedex, France

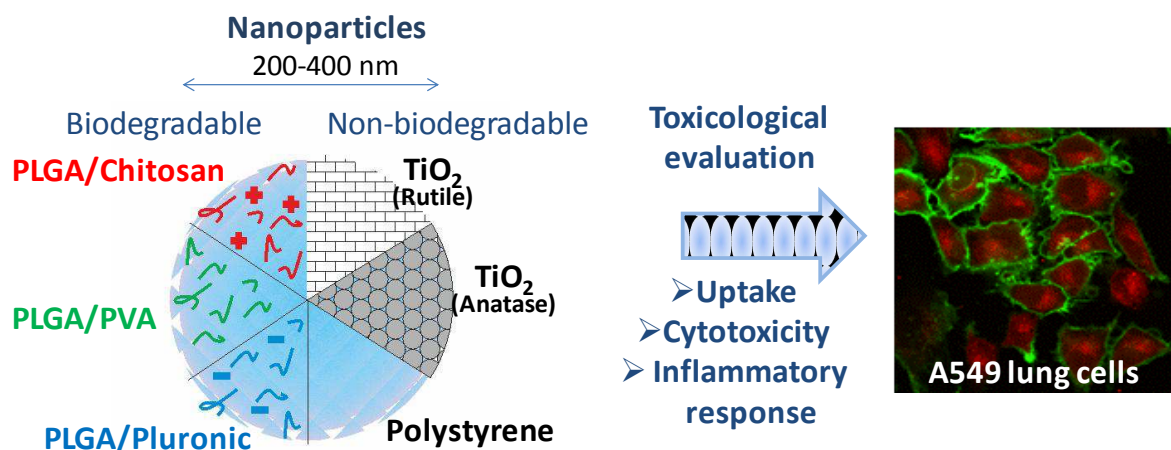
^c. INSERM UMR 996 Cytokines, Chimiokines et Immunopathologie, 5 rue JB Clément, 92296 Chatenay-Malabry Cedex, France

Abstract

In vitro cytotoxicity and inflammatory response following exposure to nanoparticles (NPs) made of poly(lactide-co-glycolide) (PLGA) have been investigated on A549 human lung epithelial cells. Three different PLGA NPs (230 nm) were obtained using different stabilizers (polyvinyl alcohol, chitosan, or Pluronic® F68) to form respectively neutral, positively or negatively charged NPs. Polystyrene NPs were used as polymeric but non-biodegradable NPs, and titanium dioxide (anatase and rutile) as inorganic NPs, for comparison. Cytotoxicity was evaluated through mitochondrial activity as well as membrane integrity (lactate dehydrogenase release, trypan blue exclusion, propidium iodide staining). The cytotoxicity of PLGA-based and polystyrene NPs was lower or equivalent to the one observed after exposure to titanium dioxide NPs. The inflammatory response, evaluated through the release of the IL-6, IL-8, MCP-1, TNF- α cytokines, was low for all NPs. However, some differences were observed, especially for negative PLGA NPs that led to a higher inflammatory response, which can be correlated to a higher uptake of these NPs. Taken together, these results show that both coating of PLGA NPs and the nature of the core play a key role in cell response.

Keywords: Nanoparticles, PLGA, lung cells, cytotoxicity, inflammatory response

Graphical abstract



1. Introduction

The pulmonary route offers several advantages for drug delivery: it is a non-invasive route that can be used not only for local but also systemic treatments, due to a high absorption surface, a high blood flow and a weak enzymatic activity (Patton *et al.*, 2004). Administration of drug-loaded nanoparticles (NPs) into the lungs represents several advantages. NPs can not only transport and protect the drug into the targeted lung cells, but also allow a sustained effect, a decrease of the administering frequency and a diminution of the side effects (Sung *et al.*, 2007).

However, the safety of these NPs should be proved before being used as drug carriers. The poly(lactide-co-glycolide) (PLGA), thanks to its biodegradability and biocompatibility, is already approved for use in medicine and has a promising future in nanomedicine, including through lung delivery (Cartiera *et al.*, 2009). PLGA NPs are popular drug nanocarriers, generally designed as a matrix-like core for drug encapsulation and protection, surrounded by a stabilizer that determines the NP surface charge. Depending on the stabilizer used, uptake and cytotoxicity profiles can change (Win and Feng, 2005, Menon *et al.*, 2012). Since polyvinyl alcohol (PVA) is one of the most used stabilizers, several *in vitro* and *in vivo* studies of PLGA/PVA NP safety have been reported (Dailey *et al.*, 2006, Semete *et al.*, 2010). However, poloxamers, polyacrylic acid or polysaccharides are also good candidates for the formulation of PLGA NPs and the modulation of their properties (Vandervoort and Ludwig, 2002, Nafee *et al.*, 2009).

Many studies have investigated the toxicity of environmental NPs such as particulate matter or inorganic NPs like layered metal hydroxide (Choi *et al.*, 2009), silica (Lin *et al.*, 2006),

titanium dioxide (TiO₂) (Johnston *et al.*, 2009), gold or silver (Bachand *et al.*, 2012) NPs. The pulmonary exposure to these NPs is often unintentional, and could constitute a significant source of toxicity (Nel *et al.*, 2006), inflammation and oxidative stress (Bhattacharya *et al.*, 2009, Limbach *et al.*, 2007).

The aim of this study was to investigate the cytotoxicity and inflammatory response following exposure of A549 alveolar epithelial lung cells to a family of PLGA NPs covered with different polymeric stabilizers, to correlate these effects to the NP uptake kinetics, and to understand the potential own effect of the stabilizers. The cytotoxicity and inflammatory response were compared to those induced by several non biodegradable NPs, either polymeric (polystyrene) or inorganic (TiO₂, in the anatase or rutile form) NPs.

2. Material and methods

2.1. Nanoparticle preparation

PLGA NPs were prepared according to an emulsion/evaporation method. Neutral (PLGA/PVA) and positive (PLGA/CS) NPs were prepared as described before by our group (Mura *et al.*, 2011b). Briefly, PLGA (75:25 Resomer® RG756, Ingelheim) was dissolved in a dichloromethane/acetone (1/1 v/v) mixture and pre-emulsified by vortexing for 1 min, with, respectively, an aqueous solution containing 2.5 mg/mL PVA (87-89 % hydrolyzed, 30-70 kDa, Sigma Aldrich), or an aqueous solution containing 0.6 mg/mL of chitosan (CS) (Protasan® UP CL113, 75-90% deacetylation, 50-150 kDa) and 5 mg/mL PVA (Mowiol®4-88, Kuraray Specialities Europe GmbH). The pre-emulsion was kept on ice and immediately sonicated (Branson Digital Sonifier) at 40 % for, respectively, 1 or 2 min. The purification of NPs (removal of free PVA and CS) was achieved by ultracentrifugation (4 °C, 37 000 x g, 1 h). Pellet resuspension was performed by vortexing.

Negative NPs (PLGA/PF68 NPs) were prepared by dissolving 50 mg PLGA in 5 mL ethyl acetate. The organic phase was added dropwise to 10 mL of a 10 mg/mL poloxamer 188 (Pluronic® F68 (PF68), BASF) aqueous solution under magnetic stirring. After 1 min vortexing, the emulsion was kept on ice and homogenized using an Ultra-Turrax® (IKA works, Inc), equipped with a 18G-stainless steel dispersing tool (10 000 rpm, 2 min). The organic solvent was then evaporated at room temperature under magnetic stirring for 2 h. The

purification of NPs (removal of free PF68) was performed by dialysis during 24 h against 1 L of MilliQ water, using a cellulose ester membrane with a 50 kDa cut off (SpectrumLabs).

All PLGA NPs could be fluorescently labeled, by replacing the total quantity of PLGA by a 90/10 (w/w) mixture of PLGA and Rhodamine B-PLGA conjugate (AV11, Akina, Inc, USA, MW ~30 kDa). The further steps were performed similarly as for unlabeled NPs, but protected from light.

TiO₂ NP suspensions were obtained by thorough dispersion of anatase (spheres, < 25 nm) or rutile (rods, 10 x 40 nm) TiO₂ nanopowders (Sigma-Aldrich) in water. After powders incorporation into water at 1 mg/mL and 1 min vortexing, pH was adjusted to 11 with 1 M sodium hydroxide (previous studies have shown that as soon as sonication of TiO₂ NPs is stopped, re-agglomeration is immediate (Andersson *et al.*, 2011); by adjusting the pH at eleven at the beginning of the process, re-agglomeration was avoided and suspensions are homogenous and stable for few days (He *et al.*, 2007)). Suspensions were then sonicated (40%) on ice during 1.5 h, with 60 s pulsations and 30 s intervals, and subsequently stirred at 24 000 rpm for 5 min on ice using an Ultra-Turrax® equipped with a plastic (polycarbonate/PEEK) dispersing tool (S25D-14G-KS, IKA). Suspensions could be kept at 4 °C, for few days. NP suspensions were vortexed just before use.

Polystyrene (PS) NP aqueous suspensions (0.20 µm, Polysciences Europe GmbH) were briefly vortexed before use.

2.2. Nanoparticle characterization

All NPs were characterized by their size and their zeta potential using a Nano ZS (Malvern instruments, UK). Average hydrodynamic diameters were measured by dynamic light scattering (25 °C, 173° scattering angle) after appropriate dilutions in water. Zeta potential measurements were performed after appropriate dilutions in 1 mM sodium chloride, at 25 °C. NP stability was studied in cell culture medium at the final concentration of 0.1 mg/mL, after 48 h incubation (37 °C). The amount of stabilizers associated to NPs after their purification was assessed through the formation of colored complexes of PVA and CS, or by ¹H NMR in the case of PF68, as previously described (Joshi *et al.*, 1979, Mura *et al.*, 2011a, Mura *et al.*, 2011b, Trimaille *et al.*, 2003, Muzzarelli, 1998).

The fluorescence emission spectra of PLGA-Rhodamine NP suspensions were recorded using an excitation wavelength of 540 nm. The fluorescence intensities of PLGA/PVA and PLGA/PF68 NPs were compared to that of PLGA/CS NPs and expressed as the ratio of the fluorescence intensities collected at the 570 nm maximum emission wavelength (the ratio was set at 1 for PLGA/CS NPs which were the most fluorescent NPs).

Bacterial contaminations of all NPs suspensions were investigated by overnight incubation of 100 μ L of a 0.1 mg/mL suspension at on Luria-Bertani (LB) medium, overnight, at 37 °C. The NP suspensions do not induced any bacterial development.

2.3. Cell culture

The A549 cell line was obtained from ATCC (catalog number CCL-185) and cultured in RPMI-1640 growth medium (Lonza), supplemented with 50 U/mL penicillin, 50 U/mL streptomycin, and 10% fetal bovine serum (Lonza). Cells were maintained at 37 °C in a 5% CO₂ humidified atmosphere. Twice a week, cells were divided at 1/15 ratio, after one rinsing step with PBS, and 4-5 min of trypsin-EDTA 1 X (Lonza). Cells were used from passage 3 to 12 after thawing.

2.4. Nanoparticle uptake kinetics

2.4.1. Flow cytometry

100 000 cells were seeded on 6-well plates, with 2.5 mL of medium. Two days after plating, supernatants were discarded and replaced by a fresh suspension of fluorescent PLGA NPs diluted in medium, at 0.1 mg/mL (final concentration), and incubated at 37 °C or 4 °C. After 2, 6, 24 or 48 h incubation at 37 °C (2 or 6 h at 4 °C), supernatants were discarded, cells rinsed twice with PBS and harvested by 1X trypsin. Cell suspensions were analyzed by flow cytometry (Accuri C6, BD Biosciences), and mean fluorescence intensities were collected on channel FL-2. Results were expressed as the ratio of the mean fluorescence intensity of each sample to the mean fluorescence intensity of non-treated cells. This value was then corrected by the fluorescence factor of each NP suspension. All measurements were performed in triplicate or more.

2.4.2. Confocal microscopy

100 000 cells were seeded on glass coverslips, placed in 6-well plates, with 2.5 mL of medium. Two days after plating, supernatants were discarded and replaced by a fresh suspension of fluorescent PLGA NPs diluted in medium, at 0.1 mg/mL (final concentration), and incubated at 37 °C or 4 °C. After 2, 24 or 48 h supernatants were discarded, cells rinsed twice with serum free-RPMI and once with PBS, and incubated with a 1 % PKH67 (Sigma-Aldrich) solution in PBS, at room temperature for 5 min, protected from light. The membrane labeling was stopped by rinsing twice with complete medium. Cells were fixed with 100 μ L of 4% paraformaldehyde (4 °C, 10 min) after one rinse with PBS. 100 μ L of a 500 μ M NH_4Cl solution was then added (4 °C, 10 min) followed by 3 rinsing steps with PBS. Coverslips were mounted on glass slides with Vectashield (Vector Laboratories, H-100), and sealed with nail polish. Observations were done with a LSM 510 (Zeiss – Meta) confocal microscope equipped with Argon (488 nm, 300 mW) and Helium-Neon (543 nm, 5 mW) lasers, and a plan-apochromat 63X objective. Data were analyzed with the LSM 510 version 3.2 software.

2.5. *In vitro* cytotoxicity

2.5.1. Mitochondrial activity

The *in vitro* mitochondrial activity was evaluated using the 3-[4,5-dimethylthiazol-2-yl]-3,5 diphenyl tetrazolium bromide (MTT) test, adapted from the protocol previously described (Mosmann, 1983). 7 000 cells (in 100 μ L of growth medium) were seeded on 96-well plates (TTP, Zurich, Switzerland) and pre-incubated for 24 h. The medium was then discarded, and 200 μ L of freshly NP preparations dispersed in growth medium were added on cells at various concentrations (0.005 to 3.5 mg/mL). After 48 h of incubation with NPs, 20 μ L of a 5 mg/mL MTT solution was added to each well and incubated for 2 h. Medium was then discarded, and 200 μ L dimethyl sulfoxide (DMSO) was added to dissolve formazan crystals. The absorbance was measured with a micro-plate reader at 540 nm. The fraction of viable cells was calculated as the absorbance ratio between NP-treated cells and untreated cells (control). According to the same protocol, cells were exposed to aqueous solutions of the stabilizing polymers (PVA, CS and PF68) used for the stabilization of NPs, diluted in complete medium, in concentration ranges corresponding to the quantity of stabilizers associated to NPs. In the case of TiO_2 NPs, the sedimentation and opaqueness of the NPs interfere with MTT interpretation. To overcome this obstacle, plates were centrifuged (180 x g, 5 min, 25 °C) after dissolution of the formazan

crystals by DMSO, and 100 μ L of supernatants transferred in new plate (Simon-Deckers *et al.*, 2008). All measurements were performed in triplicate or more.

2.5.2. LDH release test

Lactate dehydrogenase (LDH) released in extracellular medium was quantified using the Cyto Tox 96, Non-radioactive Cytotoxicity Assay (Promega), according to the manufacturer's instructions. 96-well plates seeding and exposure conditions were the same as those described in section 0. Absorbance was measured at 492 nm. The LDH release (%) was calculated as the ratio between the LDH release after NP exposure minus the LDH spontaneously released by non-treated cells, and the intracellular LDH, expressed as the difference of the total LDH measured after cell lysis (Triton X-100, 1/10^e diluted in PBS, 1 h, 37° C) minus the LDH spontaneously released. All measurements were performed in triplicate.

2.5.3. Trypan blue test

Cell viability was also evaluated by trypan blue test. 100 000 cells were seeded in 6-well plates, in 2.5 mL of medium. After 24 hours, supernatants were discarded and replaced by fresh NP dilutions in cell culture medium in range concentration of 0.01 to 2 mg/mL. After 48 hours exposure, supernatants were discarded and cells rinsed twice with PBS. Cells exposed to polymeric NPs (PLGA and polystyrene NPs) were harvested with 1X trypsin, and cells exposed to TiO₂ NPs were scrapped. Cells were mixed with an aqueous solution of trypan blue 0.4%, in 50/50 (v/v) (Eurobio) according to a method previously described (Strober, 2001). Cell counting was performed using Kova counting chambers (Kova Glasstic Slide, Hycor Biomedical) by microscopy. The cell viability was calculated as the ratio between uncolored cells and total cells. All measurements were performed in triplicate.

2.5.4. Propidium iodide/Syto[®] 24 test

Viability was also evaluated with two fluorophores, propidium iodide (Sigma-Aldrich) which binds to nucleic acids of cells with a damaged membrane, and the Syto[®] 24 (Invitrogen), which binds to nucleic acids of all cells. 6-well plates seeding, exposure, and harvesting conditions were the same as those described in part 0. Propidium iodide was first added on cell suspension at final concentration of 1 μ M, and mixing by gentle pipetting homogenization. After 5 min incubation, Syto[®] 24 was added to the cell suspension, at 1 μ M

final concentration, and mixing by gentle pipetting homogenization. After 5 min incubation, cell counting was performed using Kova counting chambers, by fluorescent microscopy, using the range excitation wavelengths of 515-560 nm (band pass filter) for the propidium iodide, and 440-480 nm (band pass filter) for the Syto[®] 24. The cell viability was calculated as the ratio between green cells and total cells. All measurements were performed in triplicate.

2.6. Cytokine quantification after exposure to nanoparticles

Cytokine secretions after exposure to NPs were investigated in supernatants using the multiplexing Cytometric Beads Array (CBA) method proposed by BD Biosciences (Morgan *et al.*, 2004, Tarnok *et al.*, 2003), and performed with the human IL-1 β , IL-6, IL-8, IL-10, IL-12p70, MCP-1 and TNF flex sets and the Human Soluble Protein Master Buffer Kit (BD Biosciences). 40 000 cells were seeded in 12-well plates for 48 hours. Supernatants were then discarded, and replaced by 2 mL of fresh growth medium (non treated cells), with either increasing lipopolysaccharide (LPS) concentrations (0.1, 1, 10 μ g/mL) or NPs at 0.1 mg/mL. After 24 h exposure, supernatants were sampled and cells were rinsed once with PBS and harvested with 1X trypsin, to be counted by flow cytometry. Cytokine results, analyzed with the FACP ArrayTM Software, were obtained as pg/mL concentrations. All measurements were performed in triplicate, or more.

3. Results

3.1. Nanoparticle characterization

A family of PLGA NPs displaying various surface properties was prepared using a selection of hydrophilic polymers as stabilizers (PVA, CS, PF68), as similarly described by our group (Mura *et al.*, 2011b) with some modifications for PLGA/PF68 NPs, the size of which was adjusted to around 230 nm. All PLGA NPs have a similar size in the 210-270 nm range, but differ by their surface charge as shown through zeta potential measurements (around neutrality for PLGA/PVA NPs, around +40 mV for PLGA/CS NPs and -30 mV for PLGA/PF68 NPs). The amount of stabilizers associated to NPs after preparation and purification was found in the range of 10 - 45 mg per 100 mg PLGA. Noteworthy, covalently-labeled, fluorescent counterparts of all these NPs could be obtained without significant alteration of their size and surface charge. Commercially available polystyrene NPs

displaying a similar size were characterized similarly and used as non-biodegradable, polymeric sample NPs (Table 1).

Colloidal suspensions of rutile and anatase TiO₂ were obtained through a controlled dispersion procedure of nanopowders after careful selection of dispersing tools and pH adjustment, without use of any stabilizing agent. The discrepancy between the size of the primary particles (< 50 nm) and the particles in suspension can be due to the aggregation of primary NPs as submicron aggregates (Table 1).

Table 1. Physicochemical properties of NPs. na = not applicable, nd = not determined

NPs	Diameter (nm) (mean ± SD)	Diameter after 48 h in cell culture medium (nm) (mean ± SD)	Polydispersity index	Zeta Potential (mV) (mean ± SD)	Core material	Stabilizer (mg/100mg core)	Crystal form
PLGA/PVA	234 ± 28	212 ± 4	0.099 ± 0.04	- 1.42 ± 1.75	PLGA	PVA (11.5)	
Rhod-PLGA/PVA	247 ± 11	216 ± 11	0.15 ± 0.05	+ 3.7 ± 0.2	PLGA	nd	
PLGA/CS	233 ± 18	269 ± 12	0.210 ± 0.020	+ 39.9 ± 7.2	PLGA	CS (15.3) / PVA (30.4)	na
Rhod-PLGA/CS	195 ± 11	200 ± 7	0.16 ± 0.03	+ 24.3 ± 1.8	PLGA	nd	
PLGA/PF68	229 ± 19	316 ± 16	0.136 ± 0.036	- 32.2 ± 3.5	PLGA	PF 68 (15.5)	
Rhod-PLGA/PF68	227 ± 9	238 ± 9	0.12 ± 0.01	- 31.5 ± 2.6	PLGA	nd	
Polystyrene	250 ± 11	259 ± 21	0.02 ± 0.02	- 48.8 ± 1.5	Polystyrene	Sulfate ester	
Anatase TiO ₂	421 ± 49	625 ± 46	0.42 ± 0.07	- 35 ± 2	TiO ₂	none	Anatase
Rutile TiO ₂	479 ± 184	795 ± 80	0.77 ± 0.25	- 37.2 ± 6	TiO ₂	none	Rutile

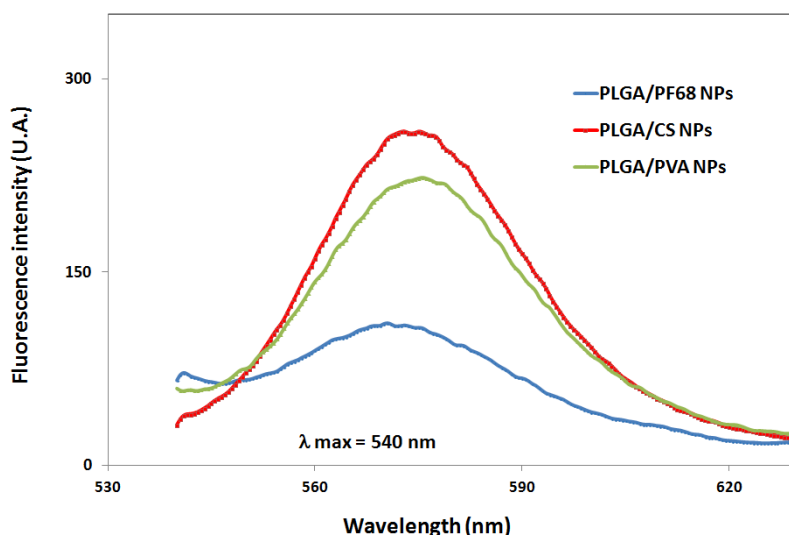


Figure S 1. Fluorescence emission spectra of PLGA-Rhod/PVA (green), PLGA-Rhod/CS (red) and PLGA-Rhod/PF68 (blue) NP suspensions at 540 nm (maximal excitation wavelength).

This NP selection, displaying a variety of core material (polymeric/inorganic, biodegradable or not) and surface coating was then evaluated on the A549 human lung cells.

3.2. Uptake of PLGA nanoparticles

All fluorescent PLGA NPs were taken up according to a similar profile (Figure 1). At 37 °C, NP uptake increased from 2 to 24 h, and then plateaued. At 4 °C, the extent of NP uptake was much lower than at 37 °C, which is characteristic of an energy-dependent uptake mechanism (Figure 2). Confocal microscopy images confirm the progressive uptake from 2 to 24 h at 37 °C, and the differences between 4 °C and 37 °C (Figure 3). Pictures additionally show that PLGA NPs are internalized down to the cytoplasm rather than merely associated to the cell surface. Significant differences are however observed depending on the stabilizer. The negatively-charged PLGA/PF68 NPs display a lower association to cells at 4 °C compared to other NPs (Figure 2). In contrast, some colocalization of NPs (red) and cell membrane (green) is observed in the case of PLGA/CS NPs, showing an adhesion of these positively-charged NPs onto the cell surface (Figure 3).

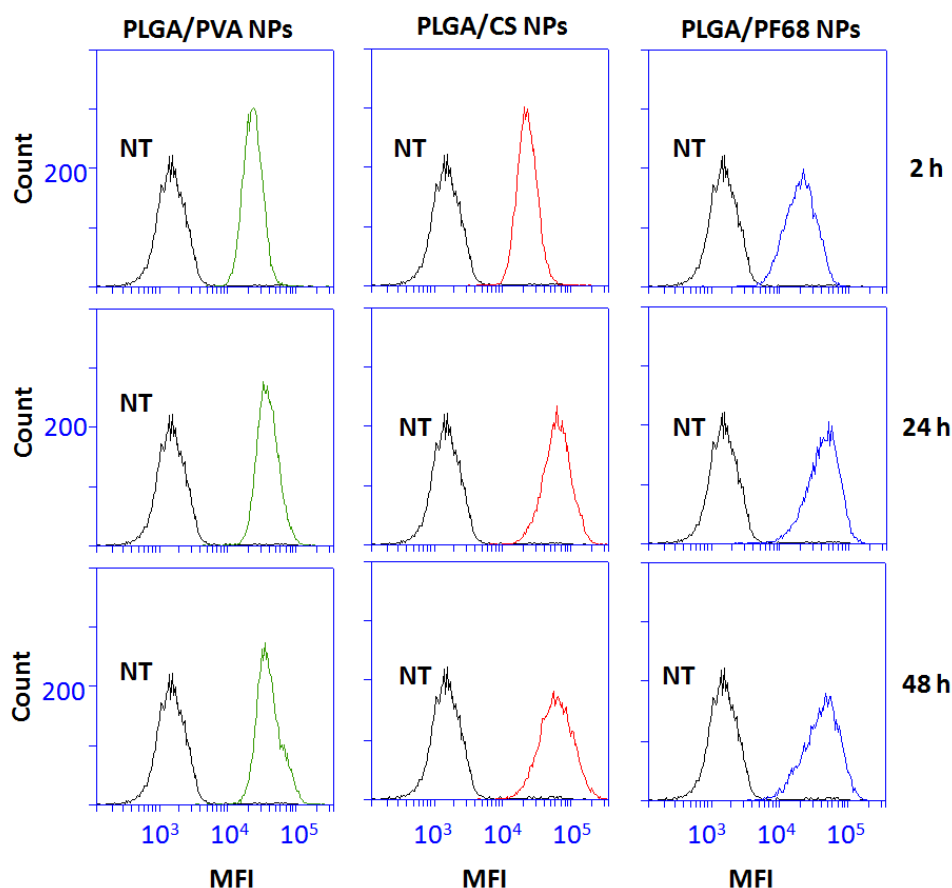


Figure 1. Uptake kinetics of PLGA-Rhod/PVA (green), PLGA-Rhod/CS (red) and PLGA-Rhod/PF68 (blue) NPs by A549 cells after 2, 24 and 48 h incubation at 37 °C, compared to non-treated cells, evaluated by flow cytometry. NT = non treated cells, MFI = mean fluorescence intensity (FL-2 channel).

By measuring the fluorescence intensity of NP suspensions, it appears that the fluorescence ratios, as defined in the material and methods, of PLGA/PVA NPs and PLGA/PF68 NPs are respectively 0.77 and 0.37 (Figure S 2). To truly compare the extent of PLGA NP uptake, the MFI increase (NP-treated cells versus non treated cells) was corrected by the fluorescence intensity ratios accordingly. Results reveal that at 37 °C, after 48 h exposure, PLGA/PF68 NPs are taken up almost twice as much than the PLGA/CS and PLGA/PVA NPs (Figure 4).

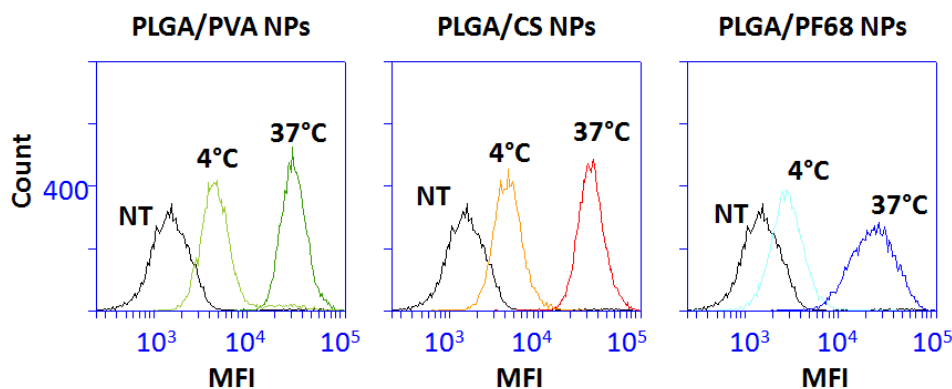


Figure 2. Uptake of PLGA-Rhod/PVA (green), PLGA-Rhod/CS (red) and PLGA-Rhod/PF68 (blue) NPs by A549 cells after 6 h incubation at 4 °C and 37 °C, compared to non-treated (NT) cells, as evaluated by the mean fluorescence intensity (MFI) in flow cytometry.

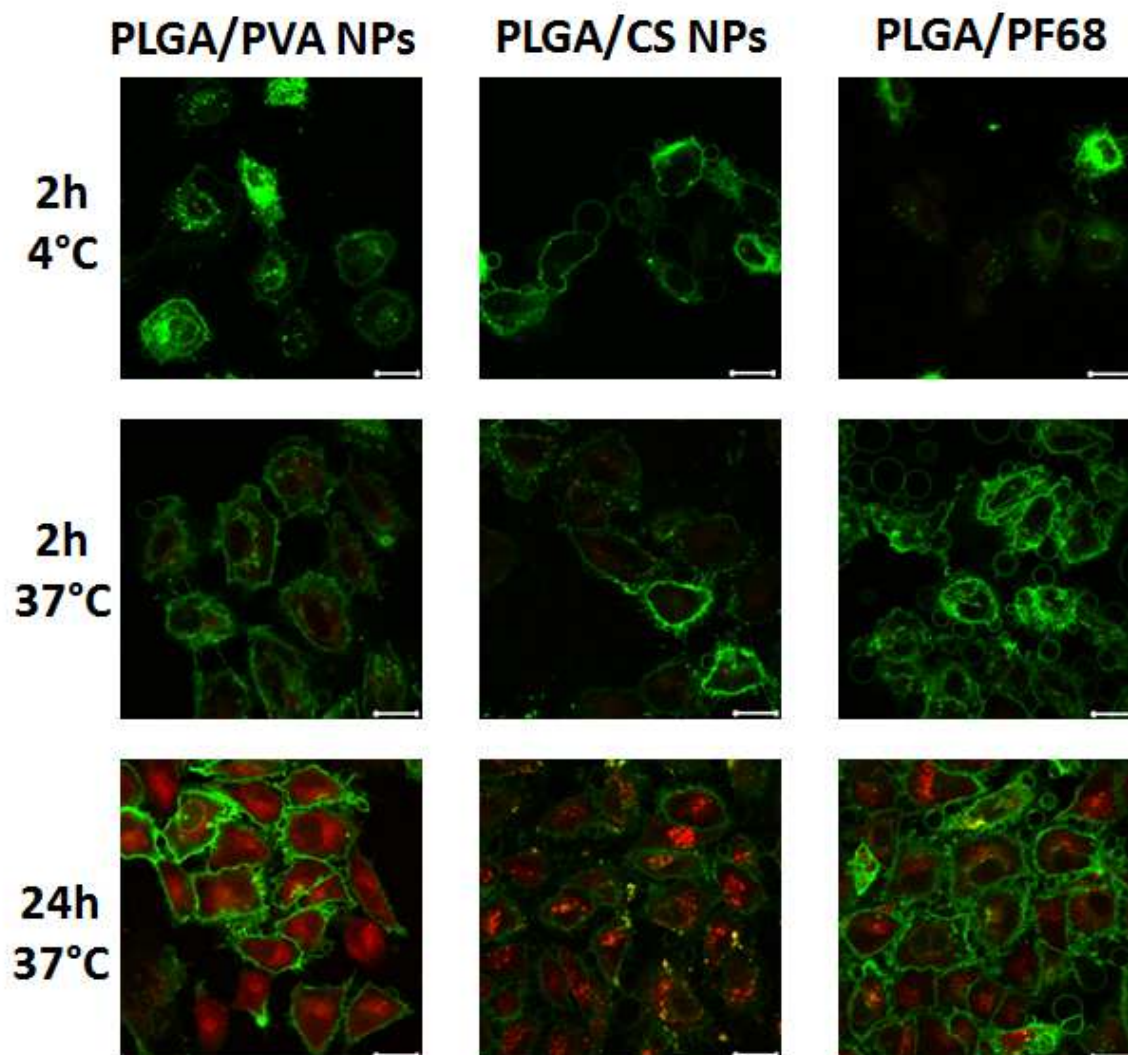


Figure 3. Uptake of PLGA-Rhod/PVA, PLGA-Rhod/CS and PLGA-Rhod/PF68 NPs (red) by A549 cells labeled with PKh67 (green) observed in confocal laser scanning microscopy after 2 h (4 h and 37 °C) and 24 h (37 °C) incubation. Scale bars = 20 μ m.

The cell granularity was also investigated, using the side scattered (SSC) signal in flow cytometry. While PLGA/PVA and PLGA/CS NPs did not entail significant modifications compared to untreated cells, exposure to PLGA/PF68 NPs did increase cell granularity (Figure 5), which can be correlated to the higher uptake of these NPs.

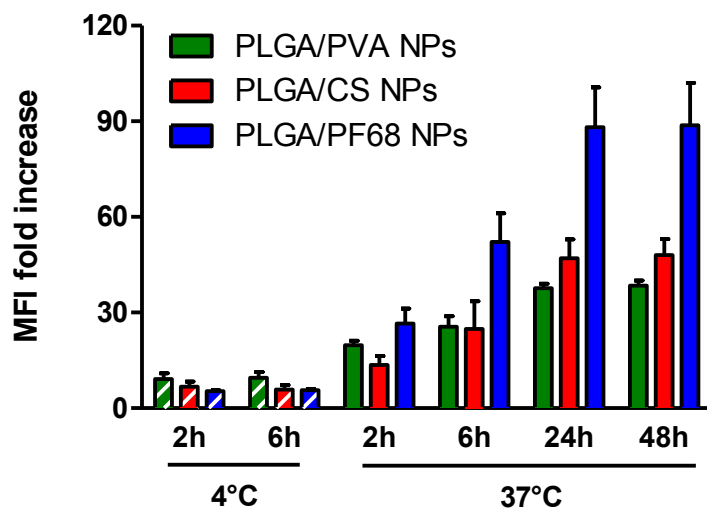


Figure 4. Uptake kinetics of PLGA NPs by A549 cells at 37 °C (full bars) and 4 °C (hatched bars), as evaluated by the mean fluorescence intensity (MFI) in flow cytometry, after correction by relative fluorescence intensity of each NP suspension.

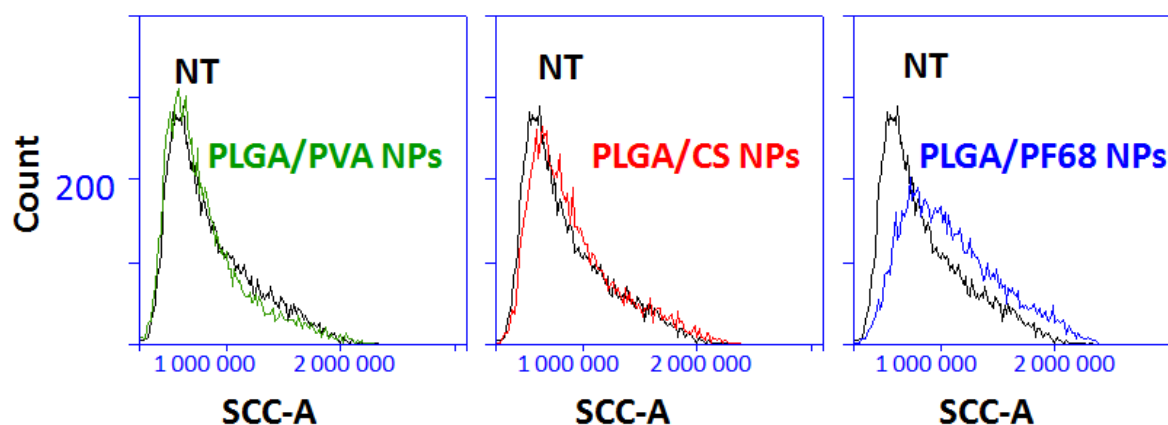


Figure 5. Side-scatter light curves (SSC) of A549 cells after 48 h exposure to PLGA/PVA NPs (green), PLGA/CS NPs (red) and PLGA/PF68 NPs (blue), compared to non treated (NT) cells.

3.3. Cytotoxicity

The cytotoxicity of various NPs was evaluated after exposure of cells to NP concentrations ranging from 0.01 to 4 mg/mL by addressing several reference toxicity endpoints (Eisenbrand *et al.*, 2002): reduced mitochondrial function through MTT test, and alteration of membrane permeability through dye exclusion tests and measurement of released intracellular enzymes. Detailed results are shown in supplementary data (Figure S 1) and summarized in Table 2.

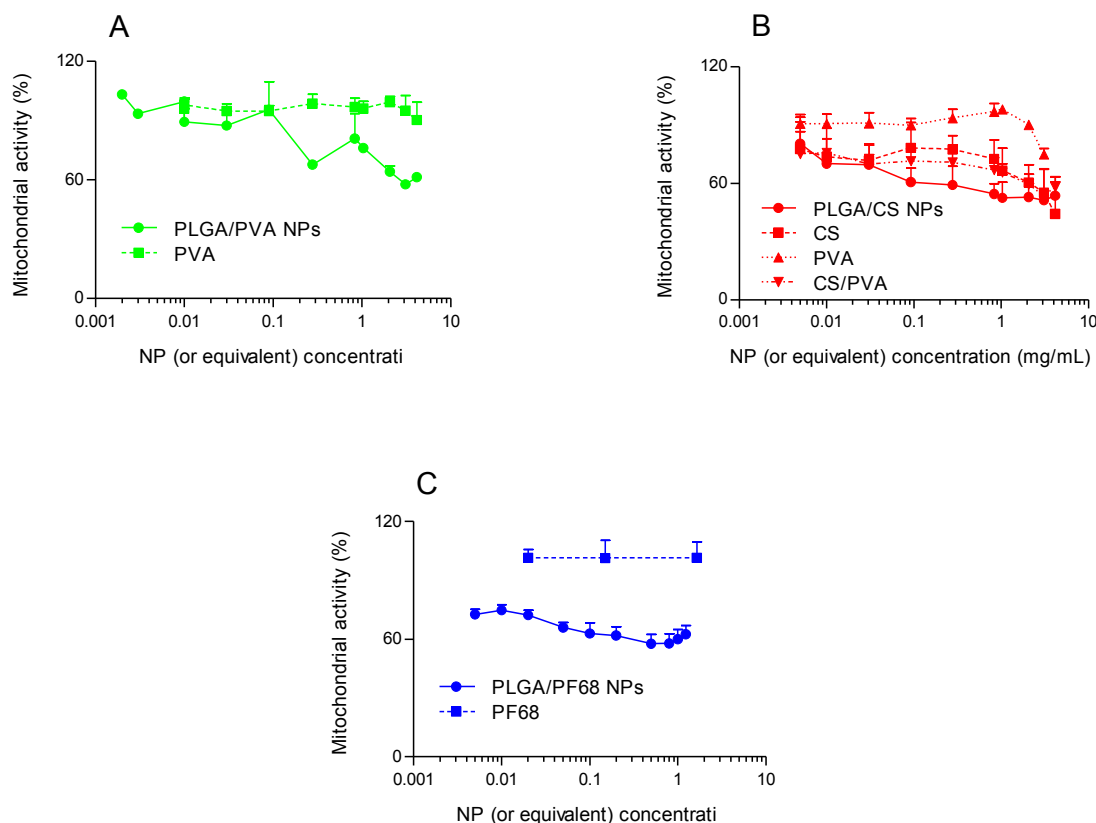


Figure 6. Mitochondrial activity of A549 cells after 48 h exposure to PLGA NPs (plain line) compared to solutions of free stabilizers (dotted line) in equivalent concentrations: PLGA/PVA NPs vs PVA (A), PLGA/CS NPs vs CS/PVA (B) and PLGA/PF68 NPs vs PF68 (C).

The mitochondrial activity measured after 48 h exposure to low concentrations (< 0.1 mg/mL) of PLGA/PVA NPs is higher than after exposure to PLGA/CS and PLGA/PF68 NPs (≥ 90 % vs. ≥ 70 %), whereas at high concentrations (> 0.1 mg/mL), they are similar for all PLGA NPs (around 60 %). Polystyrene NPs induce a similar effect to that of PLGA/PVA NPs. The exposure to TiO_2 nanoparticles reduces mitochondrial activity down to 45 % at high NP concentration (with a slight decrease when concentration increases). At the midpoint concentration of 0.1 mg/mL, all NPs maintain cellular viability around 60 % or above (Figures S 1.A, S 1.E). This concentration was chosen for the study of the inflammatory response.

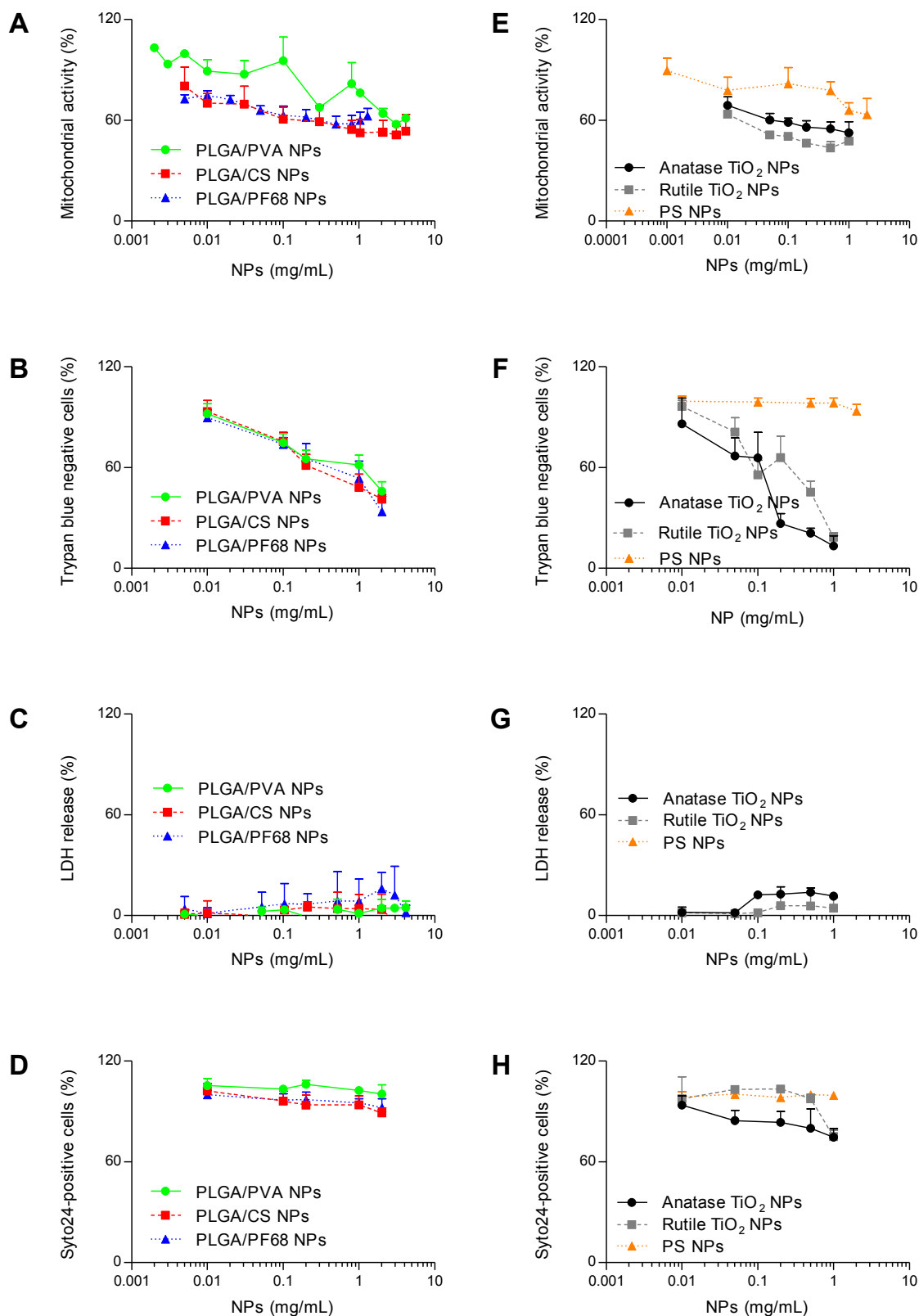


Figure S 2. A549 cell viability estimated with MTT test (A, E), trypan Blue test (B, F), LDH release (C, G) and propidium iodide/Syto[®] 24 staining (D, H) after 48 h exposure to PLGA NPs (A, B, C and D) or polystyrene and TiO₂ NPs (E, F, G and H).

Cell viability estimated by the trypan blue exclusion test shows homogeneous results for all PLGA NPs: a low toxicity at low NP concentration, increasing with the concentration. Cellular viability profile is similar after exposure to TiO₂ NPs, although these particles induce a higher toxicity at high concentrations. Compared to mitochondrial activity, the effect of PLGA and TiO₂ NPs on trypan blue exclusion is more progressive but also more pronounced. In contrast, the effect of polystyrene NPs seems negligible (Figures S 1.B, S 1.F).

The assessment of membrane integrity through the release of LDH, and the staining of nucleic acids with propidium iodide and Syto[®] 24, shows a weak NP effect. High concentrations of TiO₂ NPs are the only conditions leading to a substantial effect, more pronounced for the anatase than rutile form (Figures S 1.C, S 1.D, S 1.G, S 1.H).

Taken together, these results show that low concentrations of PLGA/PVA and polystyrene NPs induce no or mild reduction of cell mitochondrial activity, whereas the impact of PLGA/CS and PLGA/PF68 NPs is more pronounced. The effect on cell membrane integrity is more pronounced for TiO₂ NPs compared to polymeric NPs, especially at high concentrations.

In order to evaluate the potential contribution to cytotoxicity from the hydrophilic polymers used as stabilizers to formulate PLGA NPs, cells were exposed to solutions of the corresponding polymers (PVA, CS and PF68, in the absence of PLGA) in the same range of concentrations as those corresponding to the PLGA NP suspensions (Figure 6). Cell viability was evaluated with the MTT test since it was the most discriminant test to compare the toxicity of PLGA NPs. Results show that solutions of PVA and PF68 do not induce cell mortality, event at high concentration, and thus may not contribute by themselves to the toxicity of PLGA/PVA and PLGA/PF68 NPs. In contrast, solutions containing CS induce a similar toxicity to that of the corresponding PLGA/CS NP suspensions, indicating that the sole presence of CS can induce cytotoxicity as evaluated by mitochondrial activity.

Table 2. Cellular toxicity estimated with various tests (MTT, trypan blue staining, LDH release, Propidium iodide/Syto@24 staining) following exposure (48 h) to low (<1 mg/mL) or high (> 1 mg/mL) concentrations of NPs.

Test	MTT		Trypan Blue		LDH release		Propidium Iodide / Syto@24	
	Low	High	Low	High	Low	High	Low	High
NP concentration								
PLGA/PVA	-	+	-	+	-	-	-	-
PLGA/CS	+	+	-	+	-	-	-	-
PLGA/PF68	+	+	-	+	-	-	-	-
PS	-	+	-	-	-	-	-	-
Anatase TiO ₂	+	+	-	++	-	-	-	+
Rutile TiO ₂	+	+	-	++	-	-	-	+

Toxicity levels (-, +, ++) were assigned according to the following viability intervals: above 75 % (-); between 75 % and 35 % (+); below 35 % (++) . Low concentration corresponds to NP concentration under 0.1 mg/mL; high concentration corresponds to concentration above 0.1 mg/mL. Detailed viability results are shown in figure S 1.

3.4. Inflammatory response following exposure to nanoparticles

Cytokines were quantified in the cell supernatants following exposure to various NPs using the CBA method that allows the dosage of numerous compounds in one sample. We have investigated several cytokines known to be involved in the inflammatory response: IL-1 β , IL-6, IL-8, IL-10, IL-12p70, TNF- α and MCP-1. LPS, a well known Toll-like agonist, was chosen as positive control to induce cytokine secretions from A549 cells. Preliminary results allowed us to select three relevant cytokines: IL6-, IL8 and MCP-1. These cytokines were found to be secreted according to a dose-response profile and reached a maximum in response to 1 μ g/mL LPS (Figure S 3). Other tested cytokines were under the limit detection, even after exposure to 1 μ g/mL LPS. In accordance with the MTT test performed after exposure to PLGA NPs, the NP concentration selected was 0.1 mg/mL. IL-6, IL-8 and MCP-1 secretions following TiO₂ NPs exposure are found to be equivalent or above the basal levels (non-treated cells). PLGA/PVA, PLGA/CS and polystyrene NPs induced cytokine levels between non-treated and LPS-treated cells, or slightly above. In contrast, PLGA/PF68 NPs induced higher cytokine secretions than other polymeric NPs, reaching values equivalent or above LPS-treated cells.

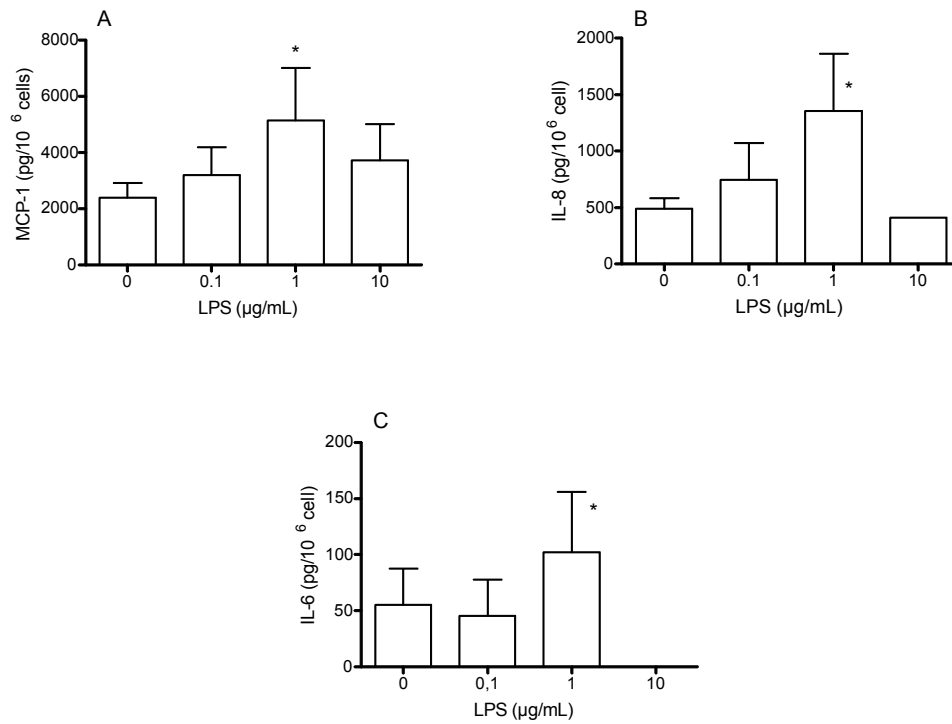


Figure S 3. Secretions of MCP-1 (A), IL-8 (B) and IL-6 (C) cytokines by A549 cells after 24 h exposure to various concentration of LPS. nd = not determined. $n = 3$, * $p < 0.05$ compared to non-treated cells.

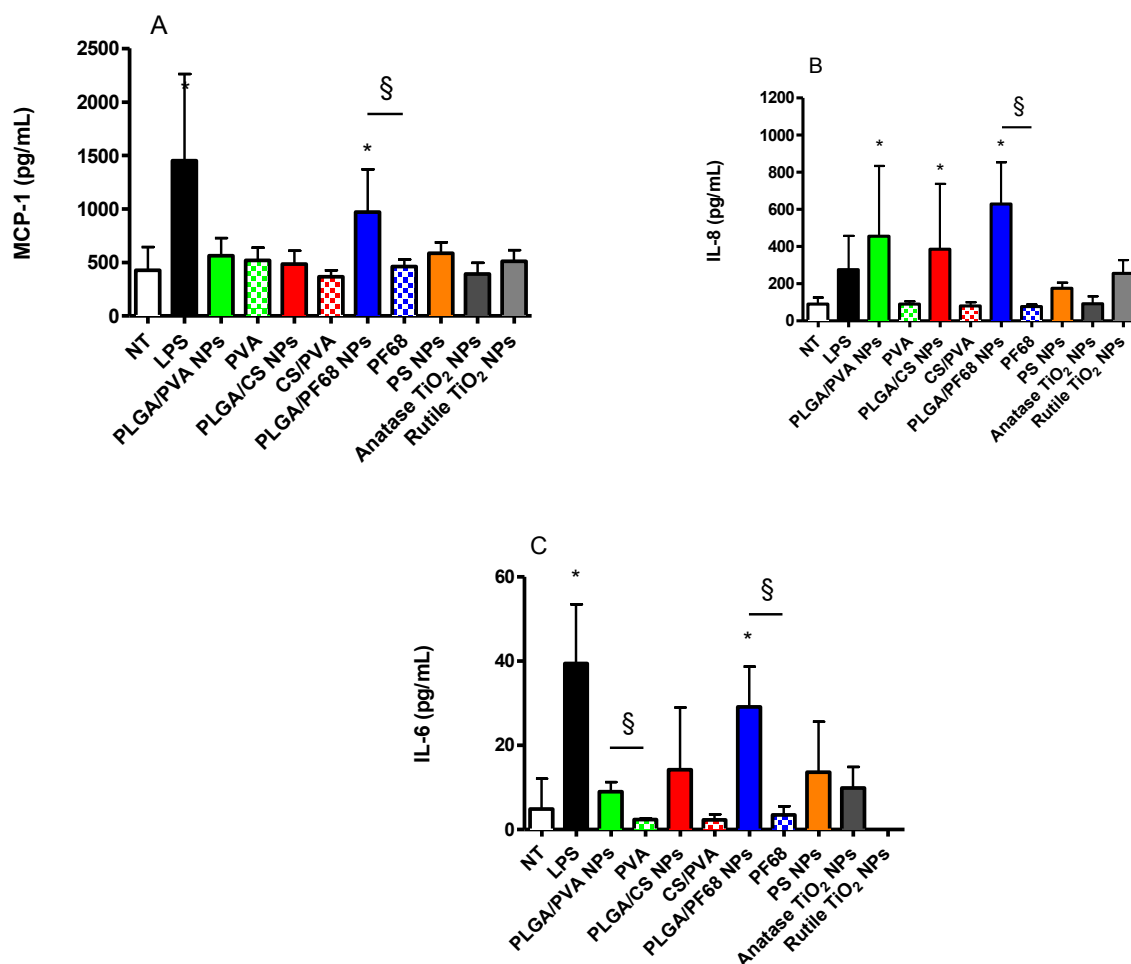


Figure 7. Secretions of MCP-1 (A), IL-8 (B) and IL-6 (C) cytokines after 24 h exposure to 0.1 mg/mL NPs or 1 μ g/mL LPS, quantified with CBA method. NT = non-treated cells, $n \geq 3$, $\star p < 0.05$ compared to non-treated cells, $\S p < 0.05$ for each stabilizer compared to corresponding NP concentration.

4. Discussion

The goal of the present study was to compare the cytotoxicity and inflammatory response following exposure to different types of NPs on A549 cells. The self-designed biodegradable polymeric NPs are comparable in terms of size and size distribution displaying a mean diameter around 230 nm (regardless of the coating agent) that is compatible with cell internalization, with a low polydispersity index. In order to compare the role of the core material and the surface coating of NPs on their toxicity, we have checked in a previous study that the PLGA NPs are not degraded during the short time cytotoxicity studies (Mura *et al.*, 2011b). We have also used polystyrene NPs with an equivalent mean size. Only TiO₂ NPs

displayed a larger mean size but still under 500 nm without the use of any additive that would have changed the behavior of the native NPs.

In this study, the A459 cell line, isolated from a human lung carcinoma (Lieber *et al.*, 1976), was chosen because these cells constitute an appropriate epithelial alveolar model (Rothen-Rutishauser *et al.*, 2012). This model allows an evaluation of the impact of NPs able to reach alveoli, and is complementary to previous studies focused on an *in vitro* Calu-3 model of the bronchial region ((Mura *et al.*, 2011a,b). Among the family of PLGA-based NPs tested in this model, some similarities were observed, such as the uptake mechanism or cytotoxicity at low concentration, but also multiple divergences. Differences observed in NP uptake between 4 and 37 °C characterize an energy-dependent mechanism of internalization consistent with previous studies showing that PLGA NPs are taken up by epithelial cells through an endocytosis pathway in most cases (Cartiera *et al.*, 2009). However, as it was previously shown on Calu-3 cells (Mura *et al.*, 2011a), PLGA/PF68 NPs are internalized in higher amount compared to the two other PLGA NPs. This result confirms that on the one hand the coating plays a role in the uptake (Alexis *et al.*, 2008), and on the other hand explains the granularity increase. Due to the impossibility to use the same labeling technique, we did not explore the internalization of the non-biodegradable PS NPs or the manufactured TiO₂ NPs.

Cell toxicity encompasses various mechanisms, which have been addressed in this study using several toxicity endpoints: modification of cell appearance (size, morphology or granular modifications), reduction of metabolic capacity (mitochondrial activity) and alteration of membrane integrity. Contrary to Calu-3 cells, for which no significant difference in cytotoxicity was observed among the three PLGA NPs, some differences were observed on A549 cells, especially in terms of mitochondrial activity. While at high concentration, all PLGA NPs have a similar impact on mitochondrial activity, at low concentration PLGA/CS NPs have a stronger effect over this activity, which can be correlated to the stronger association to cell membrane as observed by confocal microscopy. Interestingly, the cytotoxicity of PLGA/CS NPs observed was the same as the one induced by CS only, indicating an important contribution in this case of the coating agent to the cytotoxicity, which was not observed for PVA or PF68 (Huang *et al.*, 2004). In the case of PLGA/PF68 NPs, the higher toxicity compared to PLGA/PVA may result from the significantly higher quantity of PLGA/PF68 NPs internalized. Besides these differences, all PLGA NPs were found to induce a low LDH release by the cells, which mostly remained negative to propidium iodide. Taken together, these results suggest that cell exposure to PLGA NPs results in a significant

internalization, which impacts the cell metabolic activity rather than membrane integrity. The cytotoxicity due to polystyrene NPs using all the different assays are similar or lower to those observed with PLGA/PVA NPs. On the contrary, the anatase and rutile TiO₂ NPs tested are more cytotoxic than the polymeric NPs; furthermore the anatase form appears slightly more toxic than the rutile one, as it was previously described (Braydich-Stolle *et al.*, 2009).

The study of the cell inflammatory response constitutes an important indication of what can be expected at the level of the entire living organism when inhaling NPs. Indeed, inflammation is a type of nonspecific immune response and a basic way in which the body reacts to infection or physical and chemical irritation. One indication is the release of inflammatory mediators like the cytokines IL-8 and MCP-1, produced by macrophages or alveolar type-II epithelial-like cells such as A549 cells (Sallusto *et al.*, 2000, Cromwell *et al.*, 1992). MCP-1 and IL-8 are pro-inflammatory chemotactic chemokines that were shown to be involved in the attraction of primarily neutrophils and cells of the innate immune system, to regulate the cell trafficking (Deshmane *et al.*, 2009). In particular, MCP-1 is involved in various diseases, regulating migration and infiltration of monocytes, memory T lymphocytes, and natural killer cells (Polito and Proud, 1998). In our study, the secretion of MCP-1, IL-6 and IL-8 was monitored. PLGA/PVA and PLGA/CS NPs induce cytokine secretions close or lower than those following exposure to 1 µg/mL LPS whereas PLGA/PF68 NPs induce significantly higher secretions of MCP-1, IL-6, and even twice more IL-8. This phenomenon could be explained by the larger amount of NPs taken up by cells compared to the two others, rather than to the sole presence of PF68. Indeed, solutions of any of the three stabilizers did not induce significantly higher cytokine secretions. In comparison, all PLGA NPs induced low cytokine secretions in Calu-3 cells (Mura *et al.*, 2011a,b).

Inflammatory response and cytotoxicity due to polystyrene NPs are similar to those observed with PLGA/PVA NPs as reported by Dailey *et al.* (Dailey *et al.*, 2006) *in vitro* on LDH quantification.

By contrast, none of the TiO₂ NPs induced higher secretions of cytokines compared to untreated cells. A recent study (Andersson *et al.*, 2011) has obtained corroborating results concerning MCP-1 secretions.

Conclusion

In this study we have observed several differences in the cytotoxicity and inflammatory response between inorganic and polymeric NPs. TiO₂ NPs are slightly more cytotoxic than polymeric NPs but do not induce more inflammation. However, important differences among PLGA NPs depending on the surface coating were observed particularly in the cell uptake and induction of inflammatory response. According to those different behaviors, each PLGA NPs could be used for different applications in drug delivery to the lung. PLGA/PF68 NPs display an important potential for intracellular delivery, due to their high internalization into cells. However, a particular attention should be paid to the inflammatory response to these NPs. PLGA/CS NPs could be used when there is a need of adhesion of the nanocarrier to the cell membrane. Finally, PLGA/PVA NPs may provide an interesting compromise between significant cell uptake with limited cytotoxicity and inflammatory response.

These results also show the importance of detailed characterization of the PLGA NPs together with their stabilizing agents, and their potential involvement in the inflammatory response. To gain a deeper understanding, complementary studies are worth being investigated, including complex cell models, and *in vivo* studies.

Acknowledgments

The authors wish to thank Simona Mura (Institut Galien Paris Sud) for her nanoparticle expertise, Valérie Nicolas (IFR IPSIT, Université Paris-Sud) for the confocal laser microscopy observations, Nadia Abed (Institut Galien Paris Sud) for microbiology experiments, Hélène Chacun and Stéphanie Denis (Institut Galien Paris-Sud) for their guidance and assistance in cytotoxicity and cell culture experiments. This study was supported by the ANSES “Emerging risks” program and by ANR (under reference 2009 CESA 011).

References

- ALEXIS, F., PRIDGEN, E., MOLNAR, L. K. & FAROKHZAD, O. C. 2008. Factors affecting the clearance and biodistribution of polymeric nanoparticles. *Mol Pharm*, 5, 505-15.
- ANDERSSON, P. O., LEJON, C., EKSTRAND-HAMMARSTROM, B., AKFUR, C., AHLINDER, L., BUCHT, A. & OSTERLUND, L. 2011. Polymorph- and size-dependent uptake and toxicity of TiO₂ nanoparticles in living lung epithelial cells. *Small*, 7, 514-23.


- BACHAND, G. D., ALLEN, A., BACHAND, M., ACHYUTHAN, K. E., SEAGRAVE, J. C. & BROZIK, S. M. 2012. Cytotoxicity and inflammation in human alveolar epithelial cells following exposure to occupational levels of gold and silver nanoparticles. *Journal of Nanoparticle Research*, 14.
- BHATTACHARYA, K., DAVOREN, M., BOERTZ, J., SCHINS, R. P., HOFFMANN, E. & DOPP, E. 2009. Titanium dioxide nanoparticles induce oxidative stress and DNA-adduct formation but not DNA-breakage in human lung cells. *Part Fibre Toxicol*, 6, 17.
- BRAYDICH-STOLLE, L., SCHAEUBLIN, N., MURDOCK, R., JIANG, J., BISWAS, P., SCHLAGER, J. & HUSSAIN, S. 2009. Crystal structure mediates mode of cell death in TiO₂ nanotoxicity. *Journal of Nanoparticle Research*, 11, 1361-1374.
- CARTIERA, M. S., JOHNSON, K. M., RAJENDRAN, V., CAPLAN, M. J. & SALTZMAN, W. M. 2009. The uptake and intracellular fate of PLGA nanoparticles in epithelial cells. *Biomaterials*, 30, 2790-8.
- CHOI, S. J., OH, J. M. & CHOY, J. H. 2009. Toxicological effects of inorganic nanoparticles on human lung cancer A549 cells. *J Inorg Biochem*, 103, 463-71.
- CROMWELL, O., HAMID, Q., CORRIGAN, C. J., BARKANS, J., MENG, Q., COLLINS, P. D. & KAY, A. B. 1992. Expression and generation of interleukin-8, IL-6 and granulocyte-macrophage colony-stimulating factor by bronchial epithelial cells and enhancement by IL-1 beta and tumour necrosis factor-alpha. *Immunology*, 77, 330-7.
- DAILEY, L. A., JEKEL, N., FINK, L., GESSLER, T., SCHMEHL, T., WITTMAR, M., KISSEL, T. & SEEGER, W. 2006. Investigation of the proinflammatory potential of biodegradable nanoparticle drug delivery systems in the lung. *Toxicol Appl Pharmacol*, 215, 100-8.
- DESHMANE, S. L., KREMLEV, S., AMINI, S. & SAWAYA, B. E. 2009. Monocyte chemoattractant protein-1 (MCP-1): an overview. *J Interferon Cytokine Res*, 29, 313-26.
- EISENBRAND, G., POOL-ZOBEL, B., BAKER, V., BALLS, M., BLAAUBOER, B. J., BOOBIS, A., CARERE, A., KEVEKORDES, S., LHUGUENOT, J. C., PIETERS, R. & KLEINER, J. 2002. Methods of in vitro toxicology. *Food Chem Toxicol*, 40, 193-236.
- HE, Y. R., JIN, Y., CHEN, H. S., DING, Y. L., CANG, D. Q. & LU, H. L. 2007. Heat transfer and flow behaviour of aqueous suspensions of TiO₂ nanoparticles (nanofluids) flowing upward through a vertical pipe. *International Journal of Heat and Mass Transfer*, 50, 2272-2281.
- HUANG, M., KHOR, E. & LIM, L. Y. 2004. Uptake and cytotoxicity of chitosan molecules and nanoparticles: effects of molecular weight and degree of deacetylation. *Pharm Res*, 21, 344-53.
- INOUE, K., TAKANO, H., OHNUKI, M., YANAGISAWA, R., SAKURAI, M., SHIMADA, A., MIZUSHIMA, K. & YOSHIKAWA, T. 2008. Size effects of nanomaterials on lung inflammation and coagulatory disturbance. *International journal of immunopathology and pharmacology*, 21, 197-206.

- JOHNSTON, H. J., HUTCHISON, G. R., CHRISTENSEN, F. M., PETERS, S., HANKIN, S. & STONE, V. 2009. Identification of the mechanisms that drive the toxicity of TiO₂ particulates: the contribution of physicochemical characteristics. *Part Fibre Toxicol*, 6, 33.
- JOSHI, D. P., LAN-CHUN-FUNG, Y. L. & PRITCHARD, J. G. 1979. Determination of poly(vinyl alcohol) via its complex with boric acid and iodine. *Analytica Chimica Acta*, 104, 153-160.
- LIEBER, M., SMITH, B., SZAKAL, A., NELSON-REES, W. & TODARO, G. 1976. A continuous tumor-cell line from a human lung carcinoma with properties of type II alveolar epithelial cells. *Int J Cancer*, 17, 62-70.
- LIMBACH, L. K., WICK, P., MANSER, P., GRASS, R. N., BRUININK, A. & STARK, W. J. 2007. Exposure of engineered nanoparticles to human lung epithelial cells: influence of chemical composition and catalytic activity on oxidative stress. *Environ Sci Technol*, 41, 4158-63.
- LIN, W., HUANG, Y. W., ZHOU, X. D. & MA, Y. 2006. In vitro toxicity of silica nanoparticles in human lung cancer cells. *Toxicol Appl Pharmacol*, 217, 252-9.
- MENON, J. U., KONA, S., WADAJKAR, A. S., DESAI, F., VADLA, A. & NGUYEN, K. T. 2012. Effects of surfactants on the properties of PLGA nanoparticles. *J Biomed Mater Res A*, 100, 1998-2005.
- MORGAN, E., VARRO, R., SEPULVEDA, H., EMBER, J. A., APGAR, J., WILSON, J., LOWE, L., CHEN, R., SHIVRAJ, L., AGADIR, A., CAMPOS, R., ERNST, D. & GAUR, A. 2004. Cytometric bead array: a multiplexed assay platform with applications in various areas of biology. *Clin Immunol*, 110, 252-66.
- MOSMANN, T. 1983. Rapid colorimetric assay for cellular growth and survival: application to proliferation and cytotoxicity assays. *J Immunol Methods*, 65, 55-63.
- MURA, S., HILLAIREAU, H., NICOLAS, J., KERDINE-ROMER, S., LE DROUMAGUET, B., DELOMENIE, C., NICOLAS, V., PALLARDY, M., TSAPIS, N. & FATTAL, E. 2011a. Biodegradable nanoparticles meet the bronchial airway barrier: how surface properties affect their interaction with mucus and epithelial cells. *Biomacromolecules*, 12, 4136-43.
- MURA, S., HILLAIREAU, H., NICOLAS, J., LE DROUMAGUET, B., GUEUTIN, C., ZANNA, S., TSAPIS, N. & FATTAL, E. 2011b. Influence of surface charge on the potential toxicity of PLGA nanoparticles towards Calu-3 cells. *Int J Nanomedicine*, 6, 2591-605.
- MUZZARELLI, R. A. 1998. Colorimetric determination of chitosan. *Anal Biochem*, 260, 255-7.
- NAFEE, N., SCHNEIDER, M., SCHAEFER, U. F. & LEHR, C. M. 2009. Relevance of the colloidal stability of chitosan/PLGA nanoparticles on their cytotoxicity profile. *Int J Pharm*, 381, 130-9.
- NEL, A., XIA, T., MADLER, L. & LI, N. 2006. Toxic potential of materials at the nanolevel. *Science*, 311, 622-7.

- PATTON, J. S., FISHBURN, C. S. & WEERS, J. G. 2004. The lungs as a portal of entry for systemic drug delivery. *Proc Am Thorac Soc*, 1, 338-44.
- POLITO, A. J. & PROUD, D. 1998. Epithelial cells as regulators of airway inflammation. *Journal of Allergy and Clinical Immunology*, 102, 714-718.
- ROTHEN-RUTISHAUSER, B., CLIFT, M. J. D., JUD, C., FINK, A. & WICK, P. 2012. Human epithelial cells in vitro – Are they an advantageous tool to help understand the nanomaterial-biological barrier interaction? . *Euro Nanotox Letters*, 4, 1-20.
- SALLUSTO, F., MACKAY, C. R. & LANZAVECCHIA, A. 2000. The role of chemokine receptors in primary, effector, and memory immune responses. *Annu Rev Immunol*, 18, 593-620.
- SEMETE, B., BOOYSEN, L., LEMMER, Y., KALOMBO, L., KATATA, L., VERSCHOOR, J. & SWAI, H. S. 2010. In vivo evaluation of the biodistribution and safety of PLGA nanoparticles as drug delivery systems. *Nanomedicine*, 6, 662-71.
- SIMON-DECKERS, A., GOUGET, B., MAYNE-L'HERMITE, M., HERLIN-BOIME, N., REYNAUD, C. & CARRIERE, M. 2008. In vitro investigation of oxide nanoparticle and carbon nanotube toxicity and intracellular accumulation in A549 human pneumocytes. *Toxicology*, 253, 137-46.
- STROBER, W. 2001. Trypan blue exclusion test of cell viability. *Curr Protoc Immunol*, Appendix 3, Appendix 3B.
- SUNG, J. C., PULLIAM, B. L. & EDWARDS, D. A. 2007. Nanoparticles for drug delivery to the lungs. *Trends Biotechnol*, 25, 563-70.
- TARNOK, A., HAMBSCHE, J., CHEN, R. & VARRO, R. 2003. Cytometric bead array to measure six cytokines in twenty-five microliters of serum. *Clin Chem*, 49, 1000-2.
- TRIMAILLE, T., PICHOT, C., ELAISSARI, A., FESSI, H., BRIANCON, S. & DELAIR, T. 2003. Poly(D,L-lactic acid) nanoparticle preparation and colloidal characterization. *Colloid and Polymer Science*, 281, 1184-1190.
- VANDERVOORT, J. & LUDWIG, A. 2002. Biocompatible stabilizers in the preparation of PLGA nanoparticles: a factorial design study. *Int J Pharm*, 238, 77-92.
- WIN, K. Y. & FENG, S. S. 2005. Effects of particle size and surface coating on cellular uptake of polymeric nanoparticles for oral delivery of anticancer drugs. *Biomaterials*, 26, 2713-22.

Chapitre 2

Le recouvrement de surface des nanoparticules de polymère joue un rôle clef dans la toxicité vis-à-vis de macrophages dérivés de monocytes humains



Dans cette partie expérimentale de la thèse, des macrophages THP-1 ont été exposés aux différentes nanoparticules de PLGA (PLGA sans stabilisant, PLGA/PVA, PLGA/CS, PLGA/PF68) précédemment détaillées (chapitre 1), afin d'en étudier la toxicité.

La lignée THP-1, est une lignée de monocytes humains dérivés de cellules leucémiques (Tsuchiya *et al.*, 1980). Ces monocytes possèdent les caractéristiques des monocytes humains, de par leur capacité d'internalisation ou encore de par leur capacité à sécréter des composés biologiques impliqués dans la croissance, la communication ou la mort cellulaire. La différenciation en macrophages est généralement réalisée grâce à l'action du phorbol-12-myristate-13-acetate (PMA) (Tsuchiya *et al.*, 1982). Bien qu'il ne soit pas naturel, le PMA conduit à une différenciation complète des monocytes en macrophages (Auwerx, 1991), en augmentant l'expression des marqueurs membranaires CD11b (Mac-1 α , adhérence des cellules immunitaires) et CD14 (antigène des monocytes) (Schwende *et al.*, 1996). Nos résultats ont montré que 24 h d'exposition à 10 nM sont suffisantes pour induire la différenciation (Figure S1).

Lors des études d'internalisation, nous avons montré que les macrophages THP-1 capturaient les nanoparticules de charge de surface négative (*i.e* PLGA sans stabilisant et PLGA/PF68) plus rapidement et en plus grande quantité que les nanoparticules de charge de surface neutre (PLGA/PVA) ou positive (PLGA/CS) (Figure 1). Afin d'étudier la toxicité induite par ces nanoparticules, les macrophages THP-1 ont été exposés aux nanoparticules ainsi qu'aux polymères de surface utilisés en tant que stabilisants. Différents paramètres de toxicité ont été évalués :

- La viabilité cellulaire estimée par l'activité mitochondriale (Figure 2)
- Le type de mort cellulaire (apoptose/nécrose) (Figure 3)
- La sécrétion des cytokines dans le milieu extracellulaire (Figure 4)
- Le stress oxydant par la quantification des ROS et des RNS (espèces réactives de l'oxygène et de l'azote) (Figure 5)

Au cours de cette étude nous avons montré qu'après exposition à de faibles concentrations en nanoparticules (jusqu'à 0,1 mg/mL), aucun signe de toxicité n'a été détecté. Seules les nanoparticules de PLGA/CS se montrent légèrement plus toxiques que les autres, et cette toxicité peut être attribuée à la toxicité propre du chitosane. Les nanoparticules de PLGA ne provoquent ni la libération des cytokines (IL-6, IL-8, MCP-1 et TNF- α) dans le milieu

extracellulaire, ni la production de ROS intracellulaires ou la libération de RNS. Enfin, la mort cellulaire observée est uniquement d'origine nécrotique et non apoptotique.

En revanche, après exposition à des fortes concentrations, les résultats obtenus notamment par des tests MTT, montrent des profils de toxicité différents pour les nanoparticules stabilisées et les nanoparticules sans stabilisant. En effet, au dessus de 1 mg/mL, les nanoparticules de PLGA sans stabilisant n'induisent pas de réduction de l'activité mitochondriale, tandis que les nanoparticules stabilisées induisent une cytotoxicité légèrement plus élevée et cela en dépit d'une pénétration cellulaire équivalente. La toxicité des nanoparticules de PLGA/CS peut à nouveau être attribuée à la toxicité propre du chitosane mais dans le cas du PVA et du PF68, le polymère contribue à la toxicité lorsqu'il recouvre les nanoparticules et jamais de manière isolée. Nous avons conclu que les nanoparticules en étant internalisées vont contribuer à augmenter la toxicité de l'agent de surface qui leur est associé. Il faut cependant noter que d'une manière générale, aucun effet n'a été observé sur le stress oxydant et qu'à une dose thérapeutique pertinente de 0,1 mg/mL, les nanoparticules n'induisent qu'une très faible toxicité vis-à-vis des macrophages.

Surface-coating mediates the toxicity of polymeric nanoparticles towards human-like macrophages

Nadège Grabowski^{a,b}, Hervé Hillaireau^{a,b}, Juliette Vergnaud^{a,b}, Leticia Aragão Santiago^{a,b},
Saadia Kerdine-Römer^c, Marc Pallardy^c, Nicolas Tsapis^{a,b}, Elias Fattal^{a,b}

^a. Université Paris-Sud, Faculté de pharmacie, Institut Galien Paris-Sud, LabEx LERMIT, 5 rue JB Clément, 92296 Chatenay-Malabry Cedex, France

^b. CNRS, UMR 8612, 5 rue JB Clément, 92296 Chatenay-Malabry Cedex, France

^c. Institut d'Innovation thérapeutique (IFR 141), IPSIT, 5 rue JB Clément, 92296 Chatenay-Malabry Cedex, France

^d. INSERM UMR 996 Cytokines, Chimiokines et Immunopathologie, 5 rue JB Clément, 92296 Chatenay-Malabry Cedex, France

To be submitted

Abstract

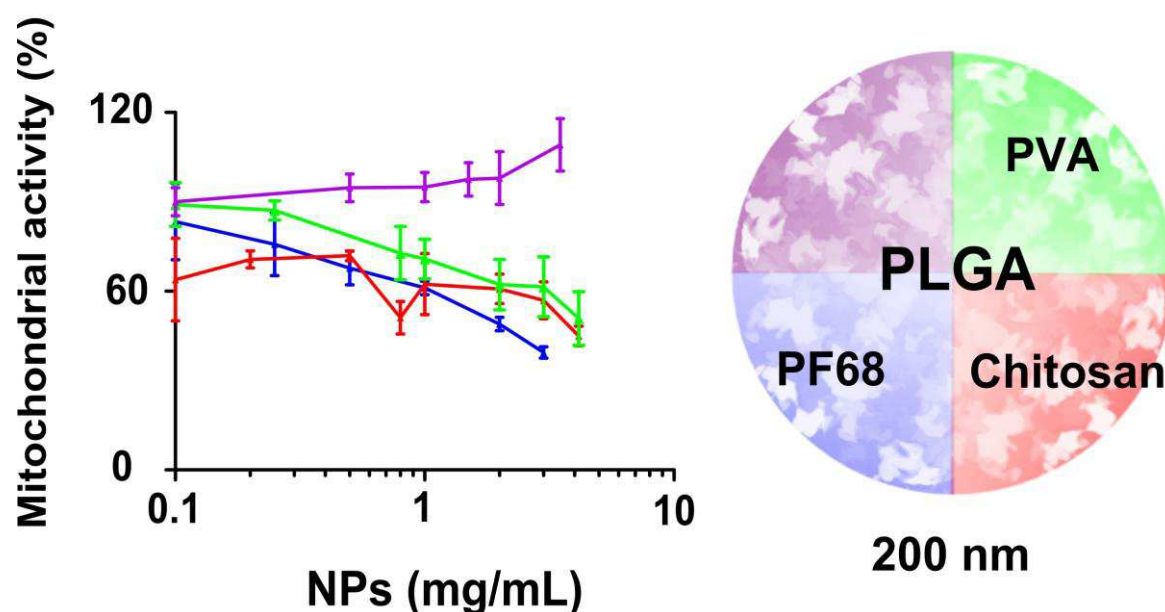
The toxicity of a series of poly(lactide-*co*-glycolic) (PLGA) nanoparticles was investigated on human-like macrophages THP-1. Positively-, negatively-charged and neutral nanoparticles (200 nm) were prepared using chitosan (CS), poloxamer 188 (PF68) and poly(vinyl alcohol) (PVA) respectively as stabilizers, and compared to nude (stabilizer-free) PLGA nanoparticles as well as solutions of stabilizers only.

When used at therapeutically relevant concentrations (up to 0.1 mg/mL *in vitro*), all tested nanoparticles show no or scarce signs of toxicity, as assessed by cell mitochondrial activity, induction of apoptosis and necrosis, production of intracellular ROS and secretion of pro-inflammatory cytokines.

At high concentrations (above 1 mg/mL), toxicity is found to be induced by the presence of stabilizers, whatever the toxicological pattern of the stabilizer itself. While nude PLGA nanoparticles exert no toxicity, the slightly cytotoxic CS polymer confers PLGA nanoparticles significant cytotoxicity when used as nanoparticle stabilizer; more surprisingly, the otherwise innocuous PVA and PF68 also confer a significant cytotoxicity to PLGA nanoparticles.

These results unveil the critical toxicological contribution played by stabilizers used for the formulation of PLGA nanoparticles when used at high concentrations, which may have implications for local toxicities of PLGA-based nanomedicine, and provide additional insight in cytotoxic effects of internalized nanoparticles.

Graphical abstract



Keywords: Nanoparticles, PLGA, stabilizer, macrophage, cytotoxicity, inflammatory response

1. Introduction

Poly(lactide-*co*-glycolide) (PLGA) is a biodegradable and biocompatible polymer used for multiple applications in drug delivery, and particularly for the formation of nanocarriers (Jain, 2000). To do so, PLGA nanoparticles are generally prepared using a hydrophilic polymer such as poly(vinyl alcohol) (PVA), chitosan (CS) or poloxamers (e.g. Pluronic F68 (PF68)) as stabilizers (Yamamoto *et al.*, 2005), while drug molecules may be incorporated into the nanoparticle matrix or adsorbed onto their surface.

While PLGA is widely considered as safe and FDA-approved, a detailed understanding of the potentially deleterious interactions of PLGA nanoparticles with cellular processes, especially at high doses, is still missing. Macrophages are key candidates for such studies, as they stand in frontline in the physiological response to therapeutically relevant nanoparticles. After

intravenous administration, nanoparticles are taken up by macrophages of the mononuclear phagocyte system in most cases; after drug delivery by inhalation, macrophages located in the pulmonary alveolar region also play a key role in the response to nanoparticles (Oberdorster *et al.*, 1992). The potential nanoparticle toxicity can be investigated using a variety of endpoints, such as cytotoxicity, oxidative stress or inflammatory response, which can be correlated. For example, production of cytokines (TNF- α and IL-6) is correlated with an acute toxicity (Arning *et al.*, 1995) while the production of Reactive Oxygen Species (ROS) is involved in apoptosis and cell proliferation (Forman and Torres, 2002, Ott *et al.*, 2007). Finally, it was shown that after ATP stimulation, macrophage response is mediated by ROS production and cytokine secretions (IL-1 and IL-18) (Cruz *et al.*, 2007).

The objective of the present study is to investigate the toxicological pattern of PLGA-based nanoparticles towards macrophages over a wide range of concentrations, and to “pell” such nanoparticles in order to understand the role of the nanoparticle PLGA core as well as the stabilizer shell. To this aim, a series of PLGA-based nanoparticles stabilized with the well-established hydrophilic polymers PVA, CS and PF68 was prepared and characterized, as well as stabilizer-free (‘nude’) PLGA nanoparticles. The effect of nanoparticles was compared to equivalent concentrations of the PVA, CS and PF68 polymers used separately, towards human THP-1 monocyte-derived macrophages, using various toxicity endpoints: impact on mitochondrial activity, induction of oxidative stress (production of ROS), induction of apoptosis/necrosis and inflammatory response (secretion of pro-inflammatory cytokines).

2. Materials and methods

2.1. Materials

Unless otherwise noted, all chemicals were purchased from Sigma-Aldrich. All solvents were of analytical grade. In the following, water refers to purified Milli-Q[®] (Millipore) water (resistivity $\geq 18 \text{ M}\Omega\cdot\text{cm}$).

2.2. Nanoparticle preparation

Stabilized PLGA nanoparticles were prepared according to an emulsion/evaporation method as previously described by our group (Mura *et al.*, 2011a, Mura *et al.*, 2011b, Grabowski *et al.*, 2013).

PLGA (75:25 Resomer® RG756, Ingelheim) was dissolved in a dichloromethane/acetone (1/1 v/v) mixture and pre-emulsified by vortexing for 1 min, with either an aqueous solution containing 2.5 mg/mL PVA (87-89 % hydrolyzed, 30-70 kDa) to prepare PLGA/PVA nanoparticles, or an aqueous solution containing 0.6 mg/mL CS (Protasan® UP CL113, 75-90% deacetylation, 50-150 kDa, FMC Biopolymers) and 5 mg/mL PVA (Mowiol®4-88, Kuraray Specialities Europe GmbH) to prepare PLGA/CS nanoparticles. The pre-emulsion was kept on ice and immediately sonicated (Branson Digital Sonifier) at 40 % for, respectively, 1 or 2 min. The purification of nanoparticles (removal of free PVA and CS) was achieved by ultracentrifugation (4 °C, 37 000 × g, 1 h) and pellet resuspension was performed by vortexing.

PLGA/PF68 nanoparticles were prepared by dissolving 50 mg PLGA in 5 mL ethyl acetate. The organic phase was added dropwise to 10 mL of a 10 mg/mL PF68 (BASF) aqueous solution under magnetic stirring. After 1 min vortexing, the emulsion was kept on ice and homogenized using an Ultra-Turrax® (IKA works, Inc), equipped with a 18G-stainless steel dispersing tool (10 000 rpm, 2 min). The organic solvent was then evaporated at room temperature under magnetic stirring for 2 h. The purification of nanoparticles (removal of free PF68) was performed by dialysis during 24 h against 1 L of MilliQ water, using a cellulose ester membrane with a 50 kDa cutoff (SpectrumLabs).

Stabilizer-free PLGA nanoparticles were prepared by nanoprecipitation using a modified method previously described (Govender *et al.*, 1999). 50 mg PLGA were dissolved in 5 mL acetonitrile. The organic solution was added dropwise under magnetic stirring to 15 mL water. After 5 min magnetic stirring, acetonitrile was removed and the suspension concentrated by evaporation under reduced pressure at 40°C, until a nanoparticle concentration close to 25 mg/mL.

All PLGA nanoparticles were fluorescently labeled, by replacing the total quantity of PLGA by a 99/1 (w/w) mixture of PLGA and a custom-made DY700-PLGA conjugate, obtained by coupling 75:25 PLGA with a NIR (Near Infra Red)-emitting fluorescent dye (DY700, Dyomics) as previously described (Reul *et al.*, 2012). The further steps were performed similarly to unlabeled nanoparticles, protected from light.

The absence of bacterial contaminations of all nanoparticle suspensions was investigated after overnight incubation of 100 µL of a 0.1 mg/mL suspension on a Luria-Bertani gelose at 37 °C. Any bacterial development was observed.

2.3. Nanoparticle characterization

All PLGA nanoparticles were characterized by their size and their zeta potential using a Nano ZS (Malvern instruments, UK). Average hydrodynamic diameters were measured by dynamic light scattering (25 °C, 173° scattering angle) after appropriate dilutions in water. Zeta potential measurements were performed after appropriate dilutions in 1 mM sodium chloride, at 25 °C. Nanoparticle stability was studied in cell culture medium at the final concentration of 0.1 mg/mL, after 48 h incubation (37 °C). The amount of stabilizers associated to nanoparticles after their purification was assessed through the formation of colored complexes with PVA and CS, or by ¹H NMR in the case of PF68, as previously described (Grabowski *et al.*, 2013).

The fluorescence emission spectra of fluorescent nanoparticle suspensions were recorded using an excitation wavelength of 700 nm. The fluorescence intensities of stabilizer free-PLGA, PLGA/PVA and PLGA/PF68 nanoparticles were compared to that of PLGA/CS nanoparticles and expressed as the ratio of the fluorescence intensities collected at the 722 nm emission wavelength (the ratio was set at 1 for PLGA/CS nanoparticles which were the most fluorescent).

2.4. Cell culture

The THP-1 cell line was obtained from ATCC (catalog number TIB-202) and cultured in RPMI-1640 growth medium (Lonza), supplemented with 50 U/mL penicillin, 50 U/mL streptomycin, and 10 % fetal bovine serum (Lonza). Cells were maintained at 37 °C in a 5 % CO₂ humidified atmosphere. Twice a week, cells were passaged at a 1/5 ratio. Cells were used from passage 3 to 12 after thawing.

2.5. Immunocytochemistry

Differentiation of THP-1 monocytes into macrophages was performed using 12-o-tetradecanoylphorbol-13-acetate (PMA). 10⁷ cells were seeded on petri dishes with 10 nM PMA for 24, 48 or 72 h. The supernatant was discarded and replaced by fresh growth medium for 24 h. Cells were then harvested by trypsin, resuspended into PBS and counted on a Malassez counting chamber. 250 000 cells were seeded into eppendorf, and supernatant was discarded after centrifugation (3 min, 1000 x g). Cells were resuspended into PBS containing 0.5 % Bovine Serum Albumine (BSA), referred to as 'PBS/BSA' in the following, and

supernatant was discarded after centrifugation (3 min, 1000 x g). Cells were incubated in PBS/BSA for 20 min at 4 °C with the following monoclonal antibodies: Phycoerythrin (PE)-conjugated anti-CD14, anti-CD11b, anti-CD54, (Bd Biosciences respectively 555398, 555388, 555511, 555665), AlexaFluor (AF)-647-CD68 (Bd Biosciences) or fluorescein-conjugated anti-HLADR (BdBiosciences, 555560). After incubation cells were washed once with PBS/BSA and once with PBS and finally resuspended into PBS to be immediately analyzed by flow cytometry (Accuri C6, BD Biosciences). For each sample, 10 000 events were acquired from a gated homogenous cell population selected from a side- versus forward-scatter plot, fluorescence intensities were collected in the FL-2 channel, and the mean fluorescence intensity (MFI) determined. The MFI fold increase of each sample was determined as the ratio of the sample MFI to the MFI of non labeled cells. In addition, to determine positive cells, histograms with FL-2 parameter against the number of events were used. The marker was placed to the right of the peak to non-treated cells. All experiments were performed in triplicate or more.

2.6. Nanoparticle uptake

The phagocytosis capacity of differentiated THP-1 cells was assessed using fluorescent (fluorescein derivative) latex beads of 200 nm (Invitrogen). 84 000 THP-1 cells were seeded on glass-bottom 35 mm petri dishes (MatTek Corporation) with 10 nM PMA for 24 h. Medium was discarded and replaced by fresh growth medium for 24 h. Fresh medium containing latex beads (0.01 mg/mL) was added. Cells were placed at 37 °C for 2 h and then observed by microscopy (Videomicroscope Axio-Observer Z1 – Colibri – TIRF 3).

For PLGA nanoparticle uptake studies, 84 000 THP-1 cells were seeded on 6-well plates and exposed to 10 nM PMA for 24 h. After medium renewal and 24 h incubation, supernatant was discarded and replaced by a fresh suspension of fluorescent nanoparticles diluted in medium at 0.1 mg/mL (final concentration). After 5 min to 48 h incubation at 37 °C, supernatant was discarded, cells were rinsed twice with PBS and harvested by trypsin. Cell suspensions were analyzed by flow cytometry and MFIs were collected using a NIR-filter. Results were expressed as the ratio of the MFI of each sample to the MFI of non-treated cells. This value was then corrected by the fluorescence factor of each nanoparticle suspension. All experiments were performed in triplicate or more.

2.7. Mitochondrial activity

The mitochondrial activity was evaluated using the 3-[4,5-dimethylthiazol-2-yl]-3,5 diphenyl tetrazolium bromide (MTT) test, as shown previously (Mosmann, 1983). 50 000 cells were seeded on 96-well plates (TTP, Zurich, Switzerland) and incubated with 10 nM PMA for 24 h. After medium renewal and 24 h incubation, supernatants were discarded and 200 μ L of freshly-prepared nanoparticle suspensions dispersed in medium was added on cells at various concentrations (0.005 to 3.5 mg/mL). After 48 h incubation, 20 μ L of a 5 mg/mL MTT solution was added to each well and incubated for 2 h. Supernatants were discarded and 200 μ L dimethyl sulfoxide (DMSO) was added to dissolve formazan crystals. The absorbance at 540 nm was measured with a micro-plate reader. The fraction of viable cells was calculated as the absorbance ratio between nanoparticle-treated and untreated cells. Using the same protocol, cells were exposed to aqueous solutions of the stabilizing polymers (PVA, CS and PF68) used for the stabilization of nanoparticles, diluted in complete medium, in concentration ranges corresponding to the quantity of stabilizers associated to nanoparticles (determined in section 2.3.). All experiments were performed in triplicate or more.

2.8. Apoptosis/necrosis detection

Apoptosis/necrosis detection following exposure to nanoparticles were performed using the annexin-AlexaFluor (AF) 488 (A13201, Life Technologies) / 7-AAD (7-Aminoactinomycin D) (A9400). 84 000 cells were seeded in 12-well plates for 24 h. Supernatants were then discarded, and replaced by 2 mL of fresh growth medium (non treated), with either increasing H₂O₂ (216763) concentrations (250, 750, 1000 μ M), or nanoparticle at 0.1 mg/mL for 24 to 48 h. The cell layer and the supernatants were analyzed separately. In a first step, supernatants were collected in eppendorf, centrifugated (3 min, 1000 \times g) and resuspended into 20 μ L binding buffer that containing 2 μ L of annexin-AF 488 (Life Technologies) and 2 μ L of 7-AAD (Sigma-Aldrich) (10 min, room temperature, darkness). Cells were rinsed once with PBS/BSA, after centrifugation (3 min, 1000 \times g) and kept on ice. In a second step, adherent cell layer were rinsed with cold PBS following by the addition of 200 μ L binding buffer containing 5 μ L annexin-AF488 and 5 μ L of 7-AAD (10 min, room temperature, darkness). Cells were rinsed with PBS and harvested by trypsin, to polled them with pellets obtained in the first step. Cells were immediately analyzed by flow cytometry, and mean fluorescence intensities were collected on FL-1 (AF488) and FL-3 (7-AAD). To perform fluorescence compensations each fluorescent probe was used separately on non treated cells. Cells were

distinguished as: living cells are unlabelled, necrotic cells are 7-AAD positive, early apoptotic cells are annexin V positive and late apoptotic cells are 7-AAD and annexin V positive. All experiments were performed in triplicate or more.

2.9. Cytokine secretions

Cytokine secretions following exposure to nanoparticles were monitored in supernatants using the multiplexed Cytometric Bead Array (CBA) method (BD Biosciences) (Morgan *et al.*, 2004, Tarnok *et al.*, 2003), and performed with the human IL-1 β , IL-6, IL-8, IL-10, IL-12p70, MCP-1 and TNF flex sets. 42 000 cells were seeded in 12-well plates for 48 h. Supernatants were then discarded, and replaced by 2 mL of fresh growth medium (non treated cells), with either increasing lipopolysaccharide (LPS) concentrations (0.1, 1, 10 μ g/mL) or nanoparticles at 0.1 mg/mL. After 24 h exposure, supernatants were sampled and cells were rinsed once with PBS and harvested with trypsin, to be counted by flow cytometry. Cytokines were simultaneously quantified in supernatants according to the manufacturer protocol. To quantify MCP-1 and IL-8, 1/50 dilutions were required. Cytokine results, analyzed with the FACP ArrayTM Software, were obtained as pg/mL concentrations and then expressed as pg/10⁶ cell. All experiments were performed in triplicate or more.

2.10. Oxidative stress

84 000 THP-1 cells were seeded on 6-well plates and exposed to 10 nM PMA for 24 h. After medium renewal and 24 h incubation, supernatant were discarded and cells were incubated with H₂DCFDA (Life Technologies) at the final concentration of 5 μ M in PBS, during 4 min. Supernatant were discarded, 2 mL of fresh medium was added, and plates were placed in the incubator for at least 30 min before use. Fresh PLGA nanoparticle suspensions were then added at the final concentration of 0.1 mg/mL or 1 mg/mL. After 5 min to 48 h incubation at 37 °C, supernatant were discarded, cells were rinsed twice with PBS and harvested by trypsin. Treatment with H₂O₂ (750 μ M, 30 min) was used as a positive control at each time point, in order to confirm that H₂DCFDA was still active. Cell suspensions were immediately analyzed by flow cytometry (Accuri C6, BD Biosciences), and MFIs were collected on the FL-2 channel. Results were expressed as the ratio of the MFI of each sample to the MFIs of non-treated cells. All experiments were performed in triplicate or more.

Statistical analyses

Analyses of variance were performed, using the Dunnett test with a significant value of 0.05.

3. Results

3.1. Nanoparticle characterization

PLGA was used to form biodegradable nanoparticles by the addition or not of hydrophilic polymers as stabilizers. As previously described by our group, PLGA/PVA, PLGA/CS and PLGA/PF68 nanoparticles in the range of 200-230 nm can be obtained with respectively, neutral, positive and negative surface charge, with a precise control of the amount of stabilizers associated to nanoparticles (10-45 mg per 100 mg PLGA) (Mura *et al.*, 2011b, Grabowski *et al.*, 2013). In addition, in this study, stabilizer-free PLGA nanoparticles were prepared with a size of 170 nm and a negative zeta potential. All nanoparticle sizes were stable after 48 h incubation in cell culture medium. The addition of DY700-PLGA to form fluorescent nanoparticles lead to similar sizes and zeta potentials. The fluorescence ratios of DY700 PLGA-based nanoparticles were in the range of 0.68-1 (Table 1).

Table 1. Physicochemical properties of PLGA-based nanoparticles.

Nanoparticles	Mean diameters (nm)		Polydispersity index	Zeta Potential (mV)	Stabilizer (mg/100 mg PLGA)	Fluorescence intensity ratio
	Water	Cell culture medium				
PLGA	171 ± 5	nd	0.044 ± 0.021	-44.8 ± 5.1	None	na
DY700-PLGA	172 ± 15	nd	0.052 ± 0.016	-40.0 ± 7.0	None	0.91
PLGA/PVA	233 ± 28	212 ± 6	0.099 ± 0.050	-1.42 ± 2.19	PVA (11.5)	na
DY700-PLGA/PVA	221 ± 9	nd	0.084 ± 0.018	-4.10 ± 0.75	nd	0.78
PLGA/CS	233 ± 18	269 ± 12	0.210 ± 0.020	+39.9 ± 7.2	CS (15.3), PVA (30.4)	na
DY700-PLGA/CS	234 ± 1	nd	0.182 ± 0.004	+45.3 ± 0.6	nd	1
PLGA/PF68	228 ± 22	316 ± 16	0.133 ± 0.044	-31.3 ± 4.9	PF68 (15.5)	na
DY700-PLGA/PF68	205 ± 27	nd	0.152 ± 0.070	-27.4 ± 7.0	nd	0.68

na: non applicable, nd: not determined

3.2. Cell characterization

Before contact with PMA, THP-1 monocytes are round shaped and in suspension (Tsuchiya *et al.*, 1980). After 24 h PMA exposure, cells are found flattened and adherent, and maintain this phenotype after 48-72 h PMA exposure. Immunocytochemical characterization shows an

increase in the expression of CD11b, CD14 and CD54 from 24 h, which is characteristic of differentiation into macrophages (Striz *et al.*, 1993, Schwende *et al.*, 1996, Daigneault *et al.*, 2010). These changes remain stable after 48 and 72 h (Figure S1, Table S1). The 24 h incubation time was thus chosen for further experiments. CD68 and HLA-DR do not show significant difference compared to untreated THP-1.

The phagocytosis ability of differentiated THP-1 cells was confirmed by microscopy. After 2 h exposure to 200 nm fluorescent latex beads, and several washing steps with cold PBS in order to eliminate the potential nanoparticles adsorbed at the cell surface, cells were found highly loaded with fluorescent nanoparticles (Figure S2).

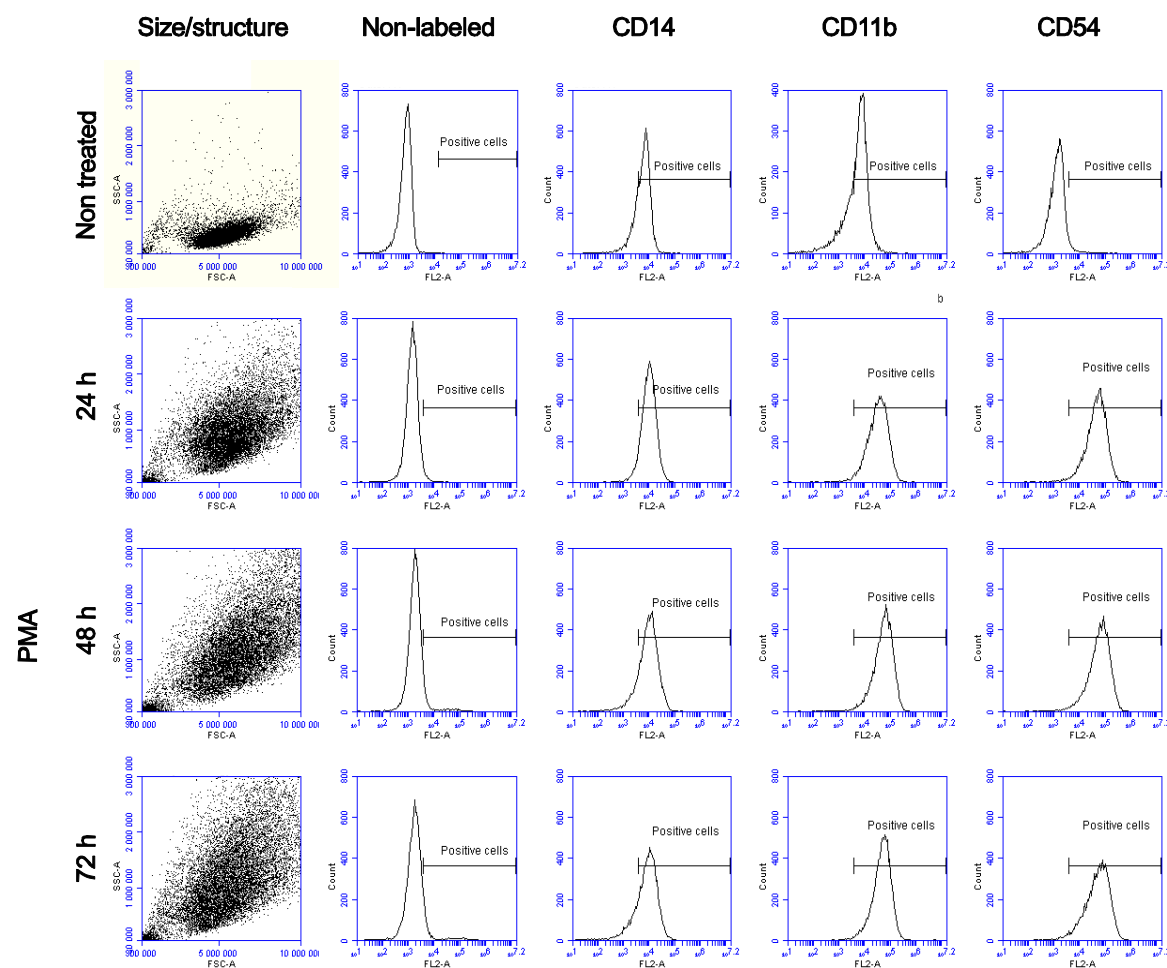


Figure S1. Immunocytochemical characterization of THP-1 cells before and after 24, 48 and 72 h incubation with 10 nM PMA. Evolution of size/structure ratio, CD14, CD11b and CD54 were followed by flow cytometry. To obtain CD14, CD11b, CD54 histograms, cell population was gated on THP-1 undifferentiated cells or THP-1 differentiated cells, according to the corresponding experiment.

Table S1. Fraction of positive cells after 10 nM PMA exposure of THP-1 cells and incubation with antibodies against CD14, CD11b and CD54 followed by flow cytometry. The threshold was defined on non-labeled cells.

Cell marker	Fraction of positive cells (%)			
	Before treatment	PMA (24 h)	PMA (48 h)	PMA (72 h)
CD14	86 ± 2	89 ± 5	63 ± 1	51 ± 4
CD11b	64 ± 1	95 ± 1	96 ± 1	95 ± 1
CD54	17 ± 2	97 ± 1	96 ± 1	92 ± 1

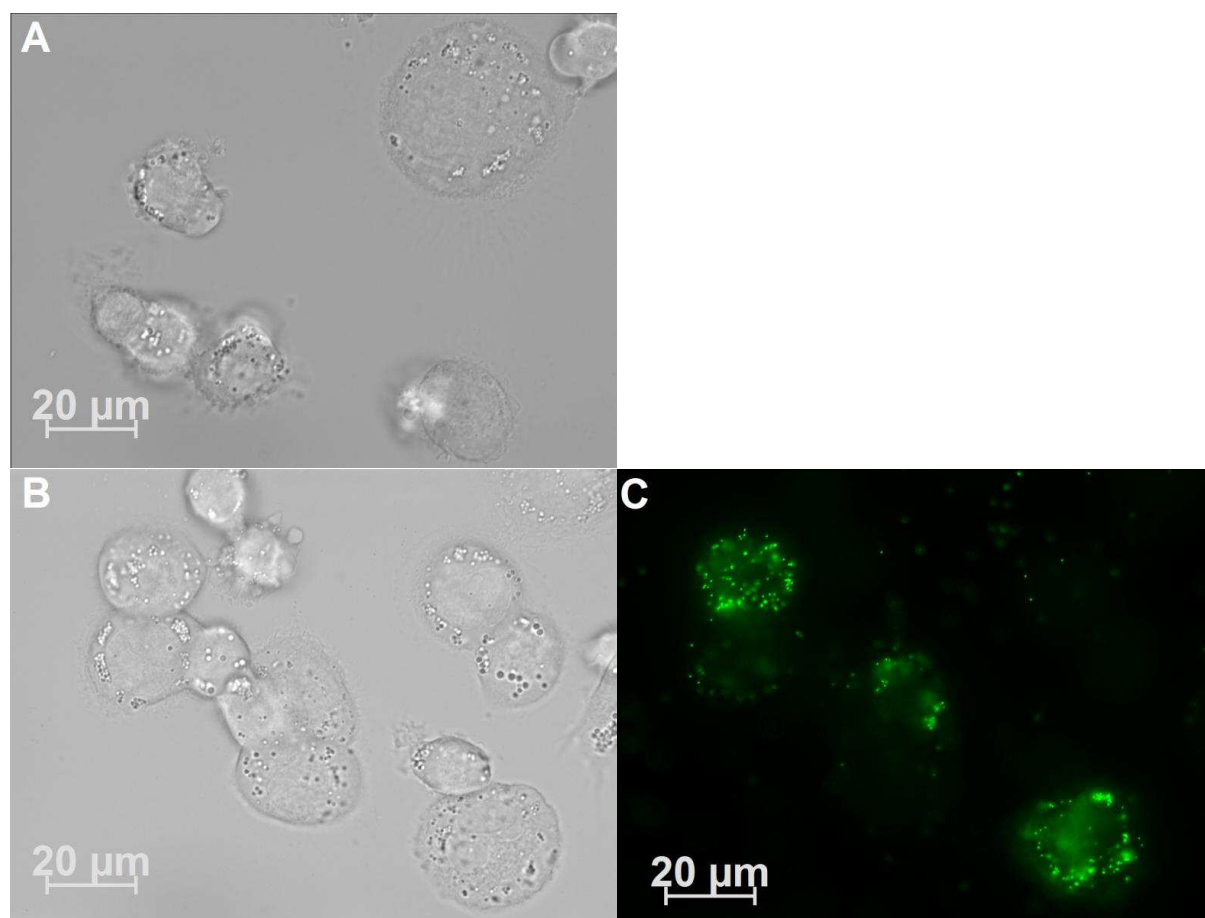


Figure S2. Uptake of fluorescent latex beads (0.01 mg/mL) by human like-macrophages observed in microscopy, after 24 h PMA exposure. Contrast image before exposure (A), contrast image (B) and fluorescent image (C) after 2 h exposure (after two cold PBS washes (B)). Scale bars correspond to 20 µm.

3.3. Uptake of PLGA nanoparticles

All nanoparticles are gradually taken up by THP-1 macrophages until 24 h (Figure 1). Among stabilizer-associated PLGA, the extent of uptake is ranked as: PLGA/PF68 > PLGA/CS > PLGA/PVA, which remains after 48 h although with slight differences. Stabilizer-free PLGA

nanoparticles show a more rapid uptake *versus* PLGA/PF68 nanoparticles after 24 h. The subsequent decrease from 24 h to 48 h could be due to nanoparticle degradation, nanoparticle exocytosis, or on the contrary to nanoparticle accumulation in the cell and fluorescence quenching. On the whole, after 24 h, all nanoparticles are taken up to a significant extent in the same order of magnitude by cells.

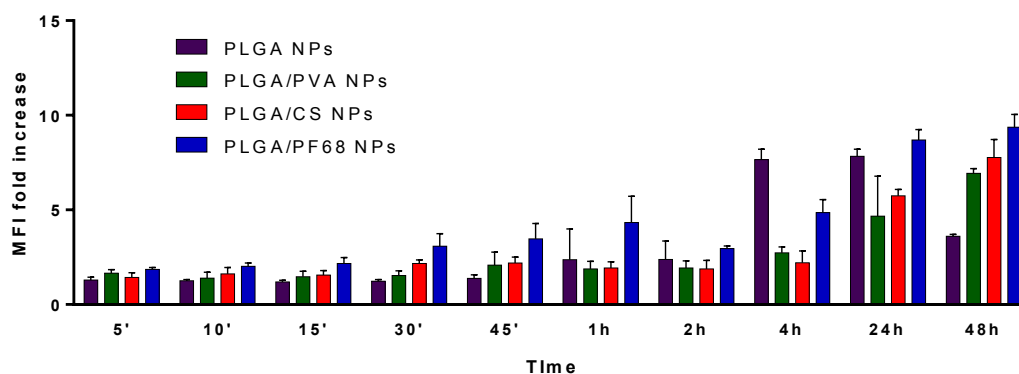


Figure 1. Uptake of DY700-labeled, PLGA-based nanoparticles (NPs) by THP-1 macrophages at 37 °C, as assessed by cell mean fluorescence intensity increase in flow cytometry (mean \pm S.D., $n \geq 3$).

3.4. Impact on mitochondrial activity

The impact of exposure to PLGA-based nanoparticles, nude or associated to stabilizers, on mitochondrial activity was monitored as an evaluation of cell viability (Figure 2 A). For each stabilized nanoparticle, this effect was also compared to the corresponding stabilizer used alone as a solution, at a concentration corresponding to the equivalent amount of stabilizer associated to nanoparticles (Figure 2 B-D).

When exposed to cells at low concentrations (< 0.1 mg/mL), all nanoparticles induce a moderate decrease of cell mitochondrial activity, the effect of PLGA/CS nanoparticles being more pronounced (Figure 2 A). At high concentrations (> 1 mg/mL), sharp differences appear between nude nanoparticles, which do not decrease mitochondrial activity whatever the concentration, and all stabilized nanoparticles, which decrease it by around 50 % at the highest concentration.

The comparison between stabilized nanoparticles and the corresponding stabilizers follows two different trends. In the case of PVA (Figure 2 B) and PF68 (Figure 2 D), the stabilizer alone has no impact on mitochondrial activity, even at the highest concentration, in contrast to

the corresponding stabilized nanoparticles. In the case of CS (Figure 2 C), the stabilizer itself significantly impacts mitochondrial activity (regardless of the small amount of PVA which is also used in the PLGA/CS nanoparticle formulation). This effect is identical to the one of PLGA/CS nanoparticles at all concentrations.

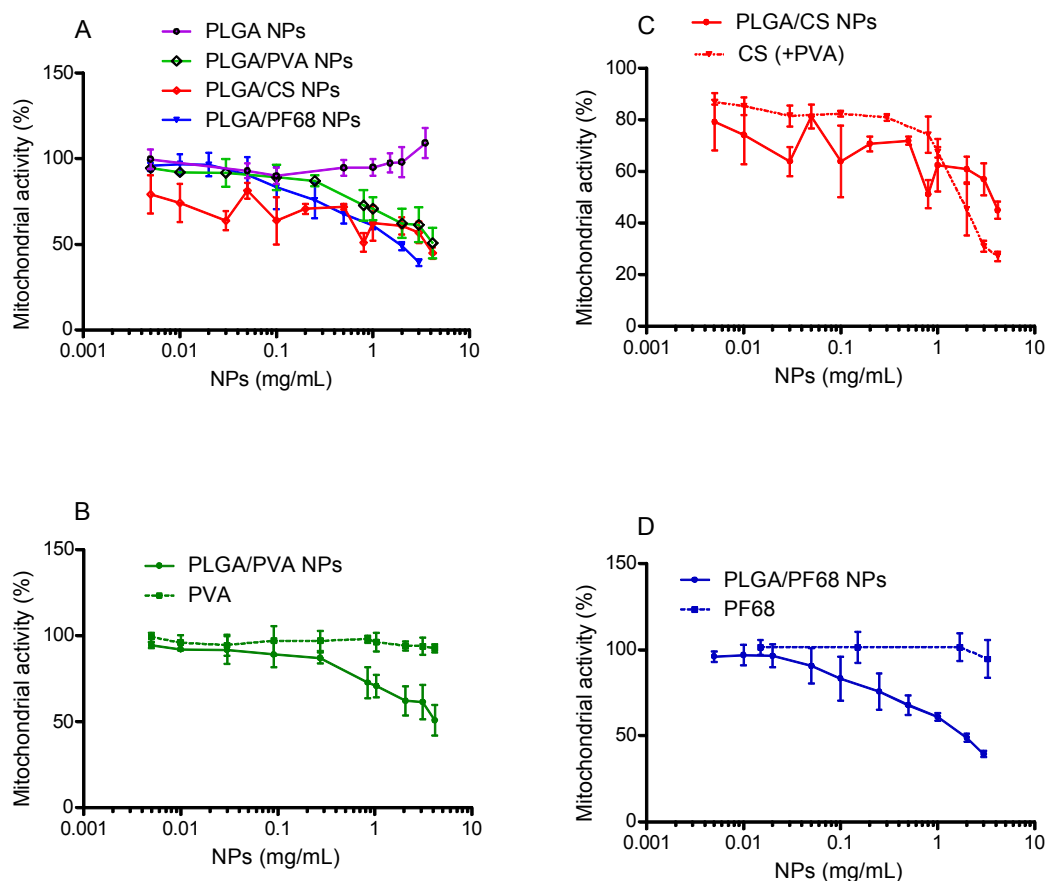


Figure 2. Cell mitochondrial activity after 48 h exposure to PLGA nanoparticles (NPs), nude or stabilized (A), and comparison of stabilized PLGA nanoparticles to their corresponding stabilizer in equivalent nanoparticle concentration: PLGA/PVA vs. PVA (B), PLGA/CS vs. CS (\pm PVA) (C), PLGA/PF68 vs. PF68 (D) (mean \pm S.D., $n \geq 3$).

3.5. Apoptosis/necrosis

The combined use of 7-AAD and annexin V allows to identify living cells (7-AAD and annexin V negative), necrotic cells (7-AAD positive cells), early apoptotic cells (annexin V positive cells) and late apoptotic cells (7-AAD and annexin V positive). Increasing concentrations of H_2O_2 were used as positive controls (Figure S3).

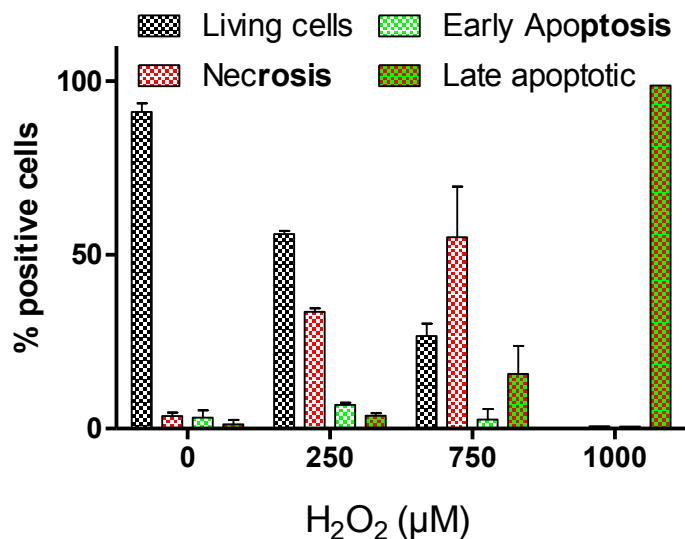


Figure S3. Identification of cell early/late apoptosis and necrosis after 24 h exposure to increasing H₂O₂ concentrations.

Results show that compared to non-treated cells, there is no significant increase of apoptosis after exposure to all nanoparticles, whatever the time and the concentration exposure (Fig. 3). However, significant differences are observed for necrosis. PLGA/CS nanoparticles induce significant necrosis, after 48 h exposure at high concentration (1 mg/mL). This effect can be compared to the CS (+PVA) stabilizer, which also induce significant cell necrosis to a higher extent, this effect occurring earlier (24 h) or at a lower concentration (0.1 mg/mL nanoparticle equivalent).

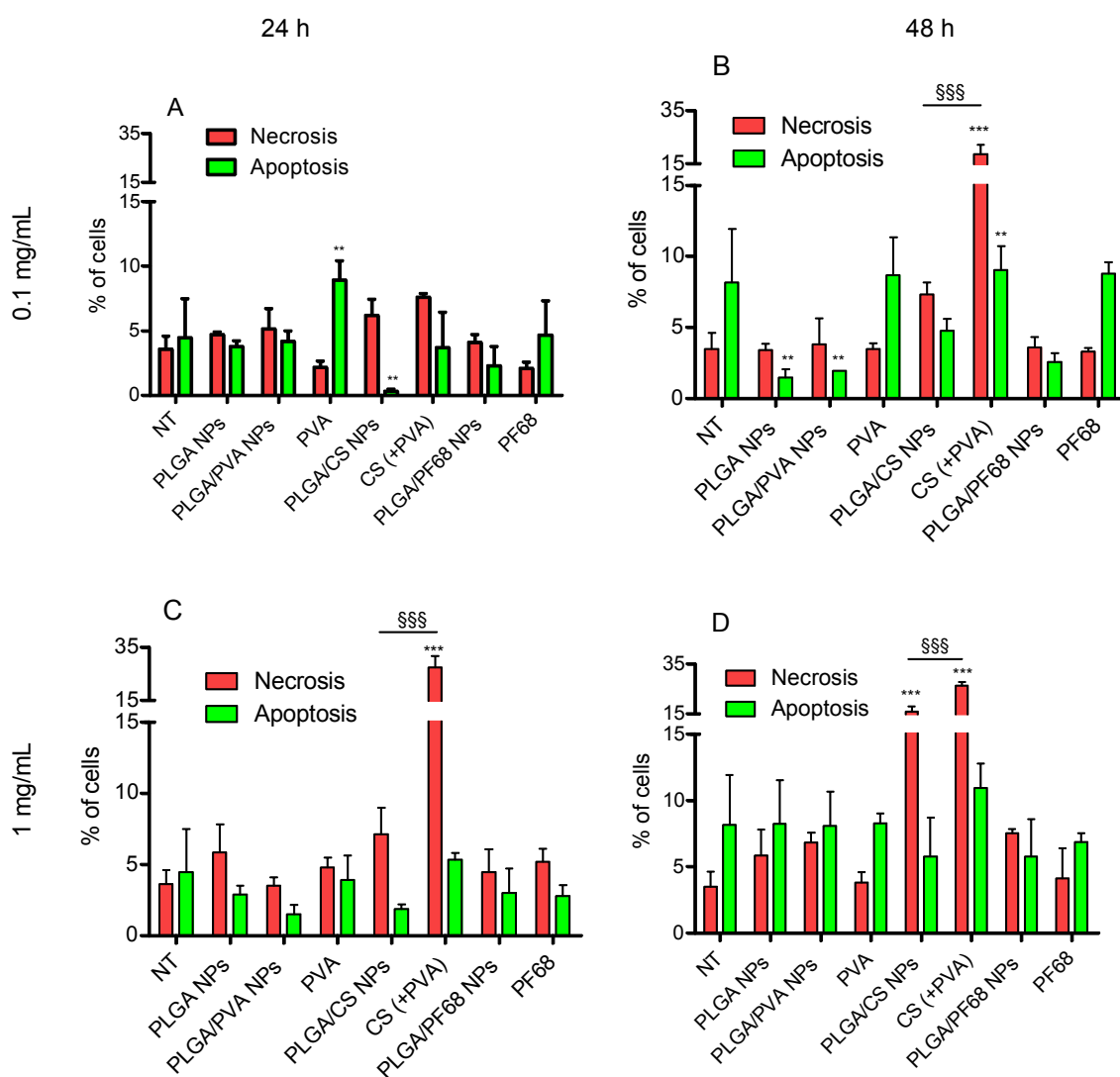


Figure 3. (A-D) Identification of apoptotic and necrotic cells after exposure to PLGA nanoparticles (NPs) and stabilizers at 0.1 mg/mL (A and B) or 1 mg/mL (C and D) (nanoparticle-equivalent concentration) for 24 h (IA-IC) or 48 h (IB-ID) (mean \pm S.D., $n = 3$). NPs=Nanoparticles. ** $p < 0.01$ and *** $p < 0.001$ compared to non treated cells and §§§ $p < 0.001$ for each stabilizer compared to corresponding nanoparticle concentration.

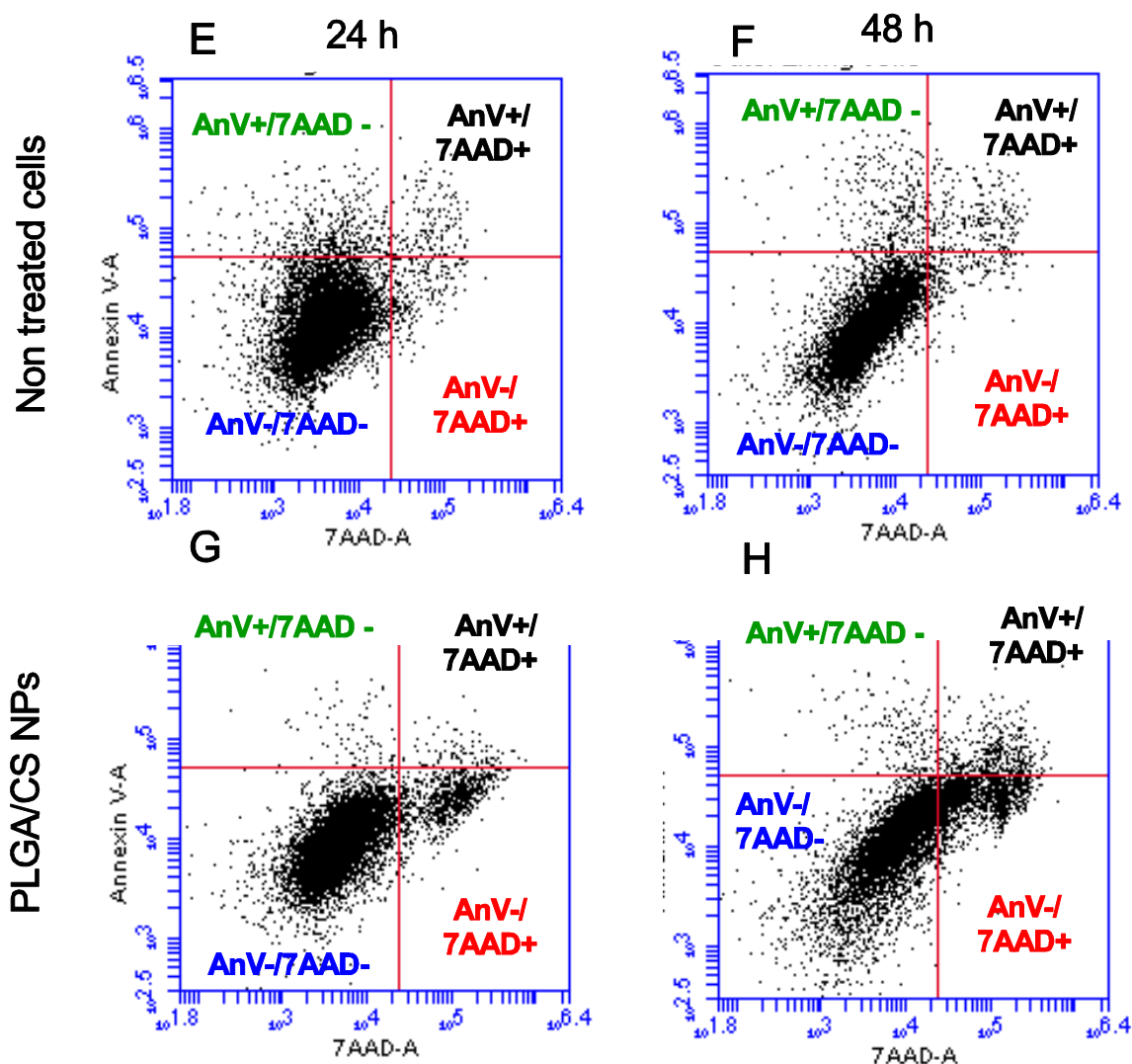


Figure 3. (G-H) Dot-plot representation of necrotic (7-AAD positive cells), early apoptotic (annexin V positive cells) or late apoptotic (7-AAD and annexin V positive cells) cells, without treatment or after 24 and 48 h exposure to PLGA/CS nanoparticles ($n = 1$, representative of 3 independent experiments).

3.6. Inflammatory response

The cytokine secretion was investigated, using the toll-like receptor agonist LPS, known to induce production of pro-inflammatory cytokines, as a positive control. Among all cytokines investigated (IL-1 β , IL-6, IL-8, IL-10, IL-12p70, TNF- α and MCP-1), only IL-6, IL-8, TNF- α and MCP-1 reached significant levels. The effect of LPS was tested in a 0.1-10 μ g/mL concentrations ranging (Figure S4); 1 μ g/mL was chosen in the following.

All PLGA nanoparticles do not induce significantly higher cytokine secretions compare to non-treated cells. Although nanoparticles, in particular PLGA/PF68 nanoparticles, tend to

induce slightly higher levels than the stabilizers themselves, no difference hit statistical significance.

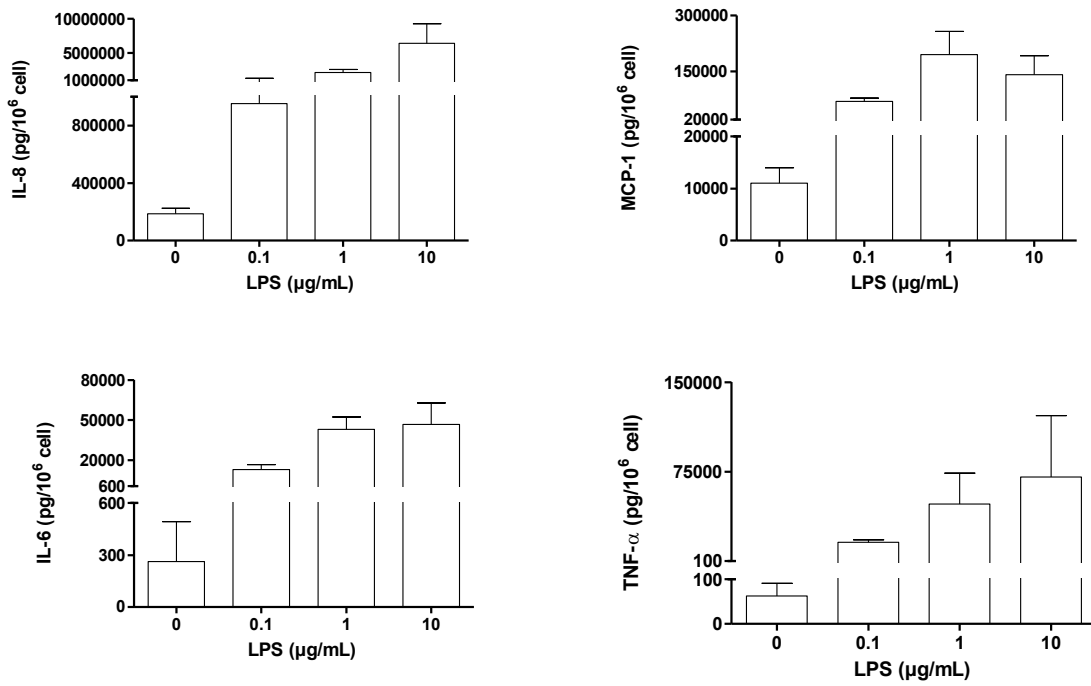


Figure S4. Cytokines secretions (IL-8, MCP-1, IL-6 and TNF- α) evaluated by CBA method after 24 h exposure to increasing LPS concentrations.

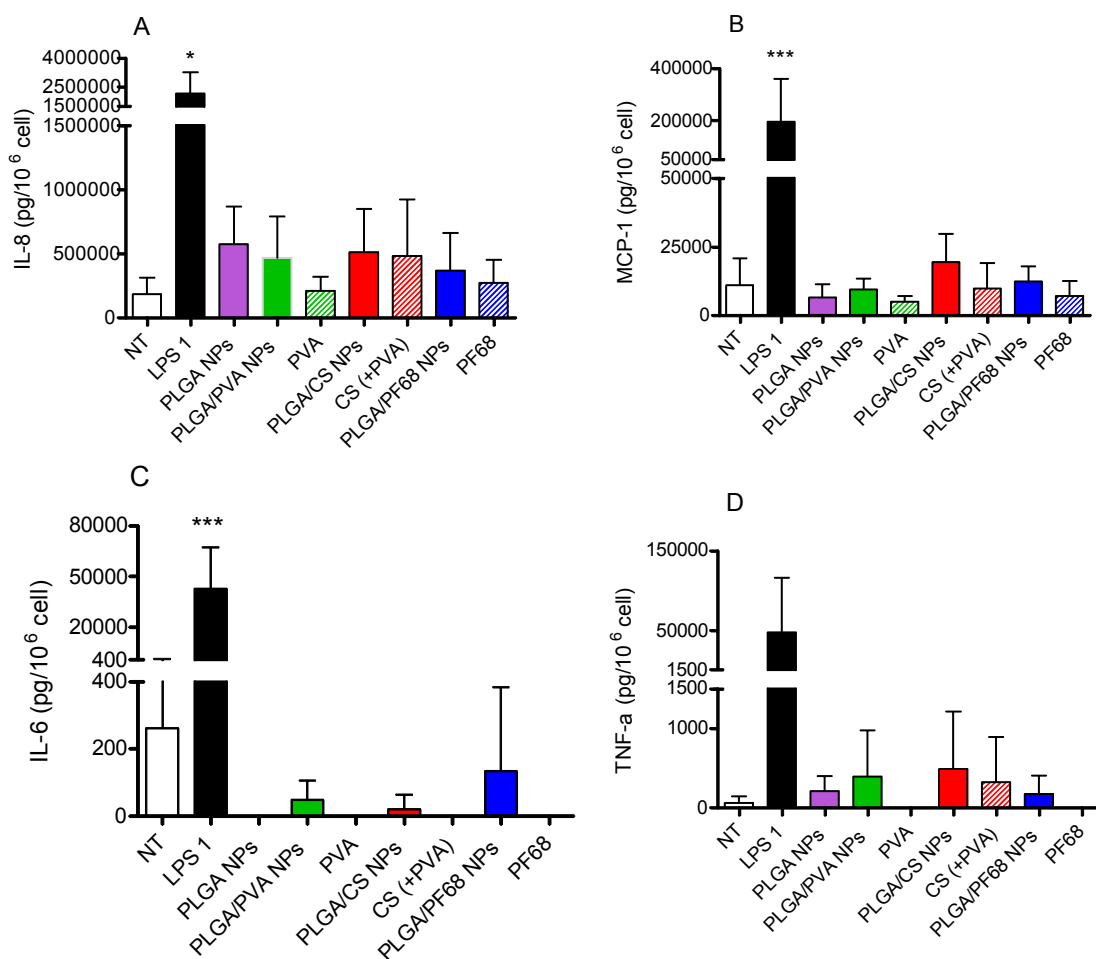


Figure 4. Secretions of IL-8 (A), MCP-1 (B), IL-6 (C) and TNF- α (D) cytokines after 24 h exposure to PLGA nanoparticles (NPs) or the corresponding stabilizers (0.1 mg/mL nanoparticle-equivalent concentration) and comparison to non treated (NT) cells or LPS-treated cells (positive control), quantified with CBA method (mean \pm S.D., $n \geq 3$).

3.7. ROS production

The intracellular production of ROS was investigated using the H₂DCFDA probe, which becomes fluorescent after cellular internalization and oxidation. H₂O₂ was chosen as positive control in such conditions (750 μ M, 30 min preincubation) that cells retain a healthy phenotype using microscope observations. Preincubation with H₂DCFDA allowed satisfactory ROS detection until 4 h exposure to treatment (data not shown).

At 0.1 mg/mL none of the PLGA nanoparticles induce significant ROS production, neither did their stabilizing polymers in equivalent concentrations. At 1 mg/mL, an increase signal occurs for nanoparticles, but this effect is transient. After 15 min, ROS production levels turn back to basal levels.

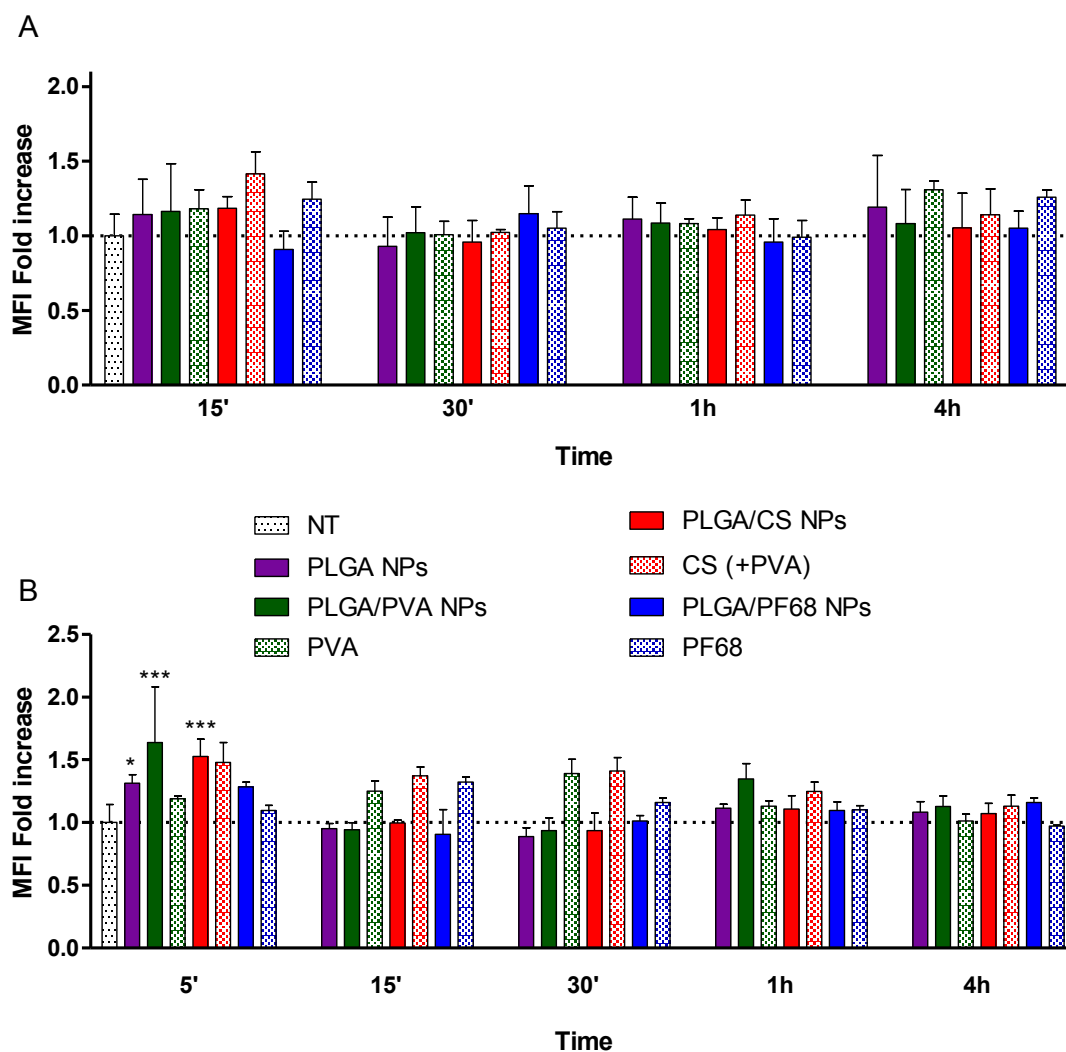


Figure 5. Intracellular ROS production after exposure to PLGA nanoparticles (NPs) or the corresponding stabilizers, at nanoparticle-equivalent concentrations of 0.1 mg/mL (A) or 1 mg/mL (B), quantified with the H₂DCFDA probe (mean ± S.D., $n \geq 3$). * $p < 0.05$, *** $p < 0.001$ compared to non treated cells.

4. Discussion

It was previously shown that the cytotoxicity of solid lipid nanoparticles of similar sizes, towards mouse macrophages, can be mediated by surfactant – the shell – (Schöler *et al.*, 2001) or by the lipid matrix – the core – (Schöler *et al.*, 2002), whereas no influence were detected concerning the inflammatory response neither the oxidative stress. The objective of the present study was to investigate the toxicological profile of a family of PLGA-based nanoparticles towards human-like macrophages, using various cellular toxicity endpoints, in order to understand the role played by the stabilizers most commonly used in their preparation. To do so, PLGA nanoparticles were prepared using the hydrophilic polymers PVA, CS or PF68 as stabilizers, with a homogeneous size (around 200 nm), as previously described by our group (Mura *et al.*, 2011a,b, Grabowski *et al.*, 2013). These nanoparticles are monodisperse (polydispersity index below 0.15) and remain stable after 48 h in cell culture medium. In addition, these PLGA nanoparticles can undergo covalent fluorescent labeling without modifying their physicochemical properties (Reul *et al.*, 2012). In the present study, stabilizer-free ('nude') PLGA nanoparticles have been added to this panel. While such nanoparticles are challenging to prepare (and thus seldom used in the literature), the method previously described leads to a nanoparticle suspension in the same size range with the same stability profile, and can be fluorescently labeled similarly.

Human-like macrophages were obtained by differentiation of a THP-1 monocytes cell line, which has been described as a relevant *in vitro* macrophage model (Tsuchiya *et al.*, 1980, Tsuchiya *et al.*, 1982). This model has been used successfully to investigate the toxicity of nanoparticles, especially in terms of cytotoxicity and cytokine expression (Chellat *et al.*, 2005, Chen *et al.*, 2006). In order to precisely investigate the toxicological profile of nanoparticles, we selected key toxicity endpoints: mitochondrial activity, inflammatory response, oxidative stress, and cell death mechanisms (necrosis, apoptosis).

When exposed to all nanoparticles, human-like macrophages show important differences depending on the nanoparticle concentrations used. On the one hand, few signs of toxicity appear for nanoparticle concentrations below 0.1 mg/mL, either in mitochondrial activity, induction of apoptosis/necrosis, production of intracellular ROS and secretions of pro-inflammatory cytokines. Such concentrations can be considered in the range (or at the higher end) of therapeutically relevant doses – in the case of drug delivery, an *in vitro* concentration 0.1 mg/mL can be correlated to a dose of 370 mg of polymer reaching the total alveoli surface

(70 m²) of adult human lung. These results confirm the safe toxicological pattern shown with the same nanoparticles on other cell models such as Calu-3 (Mura *et al.*, 2011a,b) and A549 (Grabowski *et al.*, 2013).

In contrast, the exposure of macrophages to high concentrations of nanoparticles (above 1 mg/mL) leads to different cellular responses among the nanoparticles. Surprisingly, stabilizer-free PLGA nanoparticles do not decrease cell mitochondrial activity (nor affect other toxicity endpoints), in sharp contrast to all stabilized PLGA nanoparticles. This important result highlights the innocuity of PLGA *alone* in nanoparticle form towards cell viability, even though high concentrations are used and significant cellular uptake occurs. In the case of stabilized PLGA nanoparticles, while PLGA/CS are found to induce a similar toxicity to the CS stabilizer only, the toxicity of PLGA/PVA and PLGA/PF68 nanoparticles contrasts with the innocuity of the PVA and PF68 stabilizers only.

Taken together, these results suggest that the cytotoxic effects of commonly-used stabilized PLGA nanoparticles towards macrophages can be attributed to the stabilizers (PVA, CS or PF68) when they are covering nanoparticles. A slightly toxic polymer like CS would retain its toxicity when carried with nanoparticles, this toxicity occurring through necrosis with limited production of ROS and pro-inflammatory cytokines. Moreover, even if a stabilizer has no effect alone (like PVA, PF68), it may confer toxicity to the nanoparticles. The toxicity mechanism does not seem to involve apoptosis/necrosis nor important ROS and pro-inflammatory cytokines. It could be due to the cellular internalization of the stabilizers when carried by nanoparticles, while these hydrophilic polymers do not interact with cell membranes when used in the free form.

Conclusion

The comparison of routinely-used stabilized PLGA nanoparticles to stabilizer-free nanoparticles and to the corresponding stabilizers used separately shows the importance of precise knowledge of nanoparticle composition, but also that the toxicological profile of stabilized PLGA nanoparticles is very different from the sum of their components studied separately. Although these effects are observed at high concentrations exposed to cells, they can provide an additional understanding of cellular toxicity of such nanoparticles and also have implications for local/cellular toxic effects of PLGA-based nanomedicine.

Acknowledgments

The authors thank Simona Mura (Institut Galien Paris–Sud) for the NP characterization studies, Valérie Nicolas (IFR IPSIT, Université Paris-Sud) for the confocal laser microscopy observations, Nadia Abed (Institut Galien Paris Sud) for microbiology experiments, Claire Merlet (Institut Galien Paris Sud) for her help in nanoparticle preparation. Hélène Chacun and Stéphanie Denis (Institut Galien Paris-Sud) for their guidance and assistance in cell culture and cytotoxicity experiments. This study was supported by the ANSES “Emerging risks” program and by the ANR (under reference 2009 CESA 011).

References

- ARNING, M., KLICHE, K. O., HEER-SONDERHOFF, A. H. & WEHMEIER, A. 1995. Infusion-related toxicity of three different amphotericin B formulations and its relation to cytokine plasma levels. *Mycoses*, 38, 459-465.
- AUWERX, J. 1991. The human leukemia cell line, THP-1: A multifaceted model for the study of monocyte-macrophage differentiation. *Experientia*, 47, 22-31.
- CHELLAT, F., GRANDJEAN-LAQUERRIERE, A., NAOUR, R. L., FERNANDES, J., YAHIA, L. H., GUENOUNOU, M. & LAURENT-MAQUIN, D. 2005. Metalloproteinase and cytokine production by THP-1 macrophages following exposure to chitosan-DNA nanoparticles. *Biomaterials*, 26, 961-970.
- CHEN, H.-W., SU, S.-F., CHIEN, C.-T., LIN, W.-H., YU, S.-L., CHOU, C.-C., CHEN, J. J. W. & YANG, P.-C. 2006. Titanium dioxide nanoparticles induce emphysema-like lung injury in mice. *The FASEB Journal*, 20, 2393-2395.
- CRUZ, C. M., RINNA, A., FORMAN, H. J., VENTURA, A. L. M., PERSECHINI, P. M. & OJCIUS, D. M. 2007. ATP Activates a Reactive Oxygen Species-dependent Oxidative Stress Response and Secretion of Proinflammatory Cytokines in Macrophages. *Journal of Biological Chemistry*, 282, 2871-2879.
- DAIGNEAULT, M., PRESTON, J. A., MARRIOTT, H. M., WHYTE, M. K. & DOCKRELL, D. H. 2010. The identification of markers of macrophage differentiation in PMA-stimulated THP-1 cells and monocyte-derived macrophages. *PLoS One*, 5, e8668.
- FORMAN, H. J. & TORRES, M. 2002. Reactive Oxygen Species and Cell Signaling. *American Journal of Respiratory and Critical Care Medicine*, 166, S4-S8.
- GOVENDER, T., STOLNIK, S., GARNETT, M. C., ILLUM, L. & DAVIS, S. S. 1999. PLGA nanoparticles prepared by nanoprecipitation: drug loading and release studies of a water soluble drug. *Journal of Controlled Release*, 57, 171-185.
- GRABOWSKI, N., HILLAIREAU, H., VERGNAUD, J., SANTIAGO, L. A., Kerdine-Romer, S., PALLARDY, M., TSAPIS, N. & FATTAL, E. 2013. Toxicity of surface-

modified PLGA nanoparticles toward lung alveolar epithelial cells. *International Journal of Pharmaceutics*.

JAIN, R. A. 2000. The manufacturing techniques of various drug loaded biodegradable poly(lactide-co-glycolide) (PLGA) devices. *Biomaterials*, 21, 2475-2490.

MORGAN, E., VARRO, R., SEPULVEDA, H., EMBER, J. A., APGAR, J., WILSON, J., LOWE, L., CHEN, R., SHIVRAJ, L., AGADIR, A., CAMPOS, R., ERNST, D. & GAUR, A. 2004. Cytometric bead array: a multiplexed assay platform with applications in various areas of biology. *Clin Immunol*, 110, 252-66.

MOSMANN, T. 1983. Rapid colorimetric assay for cellular growth and survival: application to proliferation and cytotoxicity assays. *J Immunol Methods*, 65, 55-63.

MURA, S., HILLAIREAU, H., NICOLAS, J., KERDINE-ROMER, S., LE DROUMAGUET, B., DELOMENIE, C., NICOLAS, V., PALLARDY, M., TSAPIS, N. & FATTAL, E. 2011a. Biodegradable nanoparticles meet the bronchial airway barrier: how surface properties affect their interaction with mucus and epithelial cells. *Biomacromolecules*, 12, 4136-43.

MURA, S., HILLAIREAU, H., NICOLAS, J., LE DROUMAGUET, B., GUEUTIN, C., ZANNA, S., TSAPIS, N. & FATTAL, E. 2011b. Influence of surface charge on the potential toxicity of PLGA nanoparticles towards Calu-3 cells. *Int J Nanomedicine*, 6, 2591-605.

OBERDORSTER, G., FERIN, J., GELEIN, R., SODERHOLM, S. C. & FINKELSTEIN, J. 1992. Role of the alveolar macrophage in lung injury: studies with ultrafine particles. *Environ Health Perspect*, 97, 193-9.

OTT, M., GOGVADZE, V., ORRENIUS, S. & ZHIVOTOVSKY, B. 2007. Mitochondria, oxidative stress and cell death. *Apoptosis*, 12, 913-22.

REUL, R., TSAPIS, N., HILLAIREAU, H., SANCEY, L., MURA, S., RECHER, M., NICOLAS, J., COLL, J.-L. & FATTAL, E. 2012. Near infrared labeling of PLGA for in vivo imaging of nanoparticles. *Polymer Chemistry*, 3, 694-702.

SCHÖLER, N., HAHN, H., MÜLLER, R. H. & LIESENFELD, O. 2002. Effect of lipid matrix and size of solid lipid nanoparticles (SLN) on the viability and cytokine production of macrophages. *International Journal of Pharmaceutics*, 231, 167-176.

SCHÖLER, N., OLBRICH, C., TABATT, K., MÜLLER, R. H., HAHN, H. & LIESENFELD, O. 2001. Surfactant, but not the size of solid lipid nanoparticles (SLN) influences viability and cytokine production of macrophages. *International Journal of Pharmaceutics*, 221, 57-67.

SCHWENDE, H., FITZKE, E., AMBS, P. & DIETER, P. 1996. Differences in the state of differentiation of THP-1 cells induced by phorbol ester and 1,25-dihydroxyvitamin D3. *J Leukoc Biol*, 59, 555-61.

STRIZ, I., WANG, Y. M., TESCHLER, H., SORG, C. & COSTABEL, U. 1993. Phenotypic markers of alveolar macrophage maturation in pulmonary sarcoidosis. *Lung*, 171, 293-303.

TARNOK, A., HAMBSCH, J., CHEN, R. & VARRO, R. 2003. Cytometric bead array to measure six cytokines in twenty-five microliters of serum. *Clin Chem*, 49, 1000-2.


TSUCHIYA, S., KOBAYASHI, Y., GOTO, Y., OKUMURA, H., NAKAE, S., KONNO, T. & TADA, K. 1982. Induction of maturation in cultured human monocytic leukemia cells by a phorbol diester. *Cancer Res*, 42, 1530-6.

TSUCHIYA, S., YAMABE, M., YAMAGUCHI, Y., KOBAYASHI, Y., KONNO, T. & TADA, K. 1980. Establishment and characterization of a human acute monocytic leukemia cell line (THP-1). *Int J Cancer*, 26, 171-6.

YAMAMOTO, H., KUNO, Y., SUGIMOTO, S., TAKEUCHI, H. & KAWASHIMA, Y. 2005. Surface-modified PLGA nanosphere with chitosan improved pulmonary delivery of calcitonin by mucoadhesion and opening of the intercellular tight junctions. *J Control Release*, 102, 373-81.

Chapitre 3

Co-culture de cellules épithéliales
alvéolaires pulmonaires humaines et de
macrophages : Un outil *in vitro*
pertinent et efficace en nanotoxicologie



La co-culture de cellules épithéliales pulmonaires (A549) en présence de macrophages (différenciés de monocytes THP-1, et notés THP-1-D) a été établie avec un contact direct entre les deux types cellulaires. Caractérisée par l'identification des récepteurs membranaires CD11b, CD14 et CD54 ainsi qu'en microscopie confocale, la co-existence de 2 populations cellulaires a été confirmée, dont 10 % de macrophages. De plus, le marquage avec CD14 a été utilisé afin d'identifier chaque sous-population cellulaire de la co-culture. Enfin, des interactions entre les deux populations cellulaires ont été mises en évidence, par l'évolution d'une partie du phénotype des cellules A549. Enfin, il est à noter qu'en présence de lipopolysaccharide, des effets synergiques ont été observés concernant la sécrétion des cytokines dans les surnageants de culture, les niveaux de sécrétions des cytokines en co-culture étant supérieurs aux niveaux attendus, c'est-à-dire ceux issus de l'addition des sécrétions obtenues pour chaque type cellulaire en mono-culture.

La co-culture a par la suite été utilisée comme un outil *in vitro* afin d'étudier la toxicité des nanoparticules présentées au cours des précédents chapitres. La concentration en nanoparticules choisie pour cette étude a été de 0,1 mg/mL, concentration à laquelle correspondent 60 à 80 % de viabilité mitochondriale (données MTT) pour chaque type cellulaire en mono-culture (Chapitres 1 et 2). Les différents paramètres de toxicité étudiés ont été l'internalisation des nanoparticules, leur cytotoxicité ainsi que la réponse inflammatoire qu'elles peuvent causer ou augmenter.

L'internalisation des nanoparticules de PLGA a été suivie en cytométrie en flux, spécifiquement par chaque sous-population cellulaire. Les résultats montrent que les nanoparticules de PLGA de potentiel zêta négatifs (dépourvues de stabilisant ou stabilisées par le PF68) sont internalisées en plus grande quantité que les nanoparticules neutres (PLGA/PVA) et positives (PLGA/CS), et ce, quelque soit la population cellulaire. De plus, les macrophages THP-1-D captent plus de nanoparticules que les cellules A549 ce qui démontre leur rôle important dans l'élimination des nanoparticules.

La cytotoxicité des nanoparticules de PLGA a été évaluée par un tri-marquage annexine V/7AAD/CD14, permettant de différencier les différents types de mort cellulaire (apoptose précoce ou avancée et nécrose) et ce, au sein de chaque lignée cellulaire. La co-culture étant un mélange de plusieurs types cellulaires, il ne nous a pas semblé judicieux de réaliser un test MTT classique, qui n'aurait pas fait la distinction entre les deux types de cellules. Les résultats montrent qu'à la concentration de 0.1 mg/mL, les nanoparticules de

PLGA induisent exclusivement la mort par nécrose, et ce, pour chacune des populations cellulaires.

La réponse inflammatoire a été évaluée par les cytokines MCP-1, IL-6, IL-8 et TNF- α (Figure 8). Dans une première étape, les nanoparticules, ainsi que les polymères de surface en solution, ont été appliqués sur la co-culture pendant 24 h, afin de mesurer l'effet inflammatoire des nanoparticules proprement dites. Les nanoparticules de PLGA, en particulier celles préparées sans agent stabilisant, induisent de faibles sécrétions de cytokines. De la même façon, les stabilisants en solution aqueuse n'induisent pas de réponse inflammatoire. Dans une seconde approche, les nanoparticules ont été incubées en présence de LPS, pour déterminer si les nanoparticules peuvent augmenter la réponse inflammatoire, ou encore concentrer les effets du LPS qui, en se fixant sur les nanoparticules, pénétrerait facilement à l'intérieur de la cellule. La réponse inflammatoire après exposition aux nanoparticules de PLGA est à nouveau faible.

L'évaluation du stress oxydant a été entreprise par le dosage des ROS à l'intérieur de chaque population cellulaire, par l'ajout de la sonde H₂DCFDA et un co-marquage avec le CD14, en cytométrie en flux. Malheureusement, la sonde H₂DCFDA émet trop dans le canal du CD14 (PE), et les compensations n'ont pas permis d'obtenir un résultat convenable. Des anticorps CD14 couplés à d'autres sondes fluorescentes ont été testés, mais sans donner de résultats probants.

En conclusion, lors de cette étude, nous avons montré que la co-culture de cellules épithéliales alvéolaires pulmonaires et de macrophages THP-1-D constitue un modèle *in vitro* simple et pertinent pour les études de nanotoxicologie. De plus, une nouvelle fois, nous avons pu démontrer que les nanoparticules de PLGA représentent un intérêt particulier dans la formulation de nanovecteurs pour une application pulmonaire, car elles induisent une faible toxicité ainsi qu'une faible réponse inflammatoire.

Lung epithelial cells and human-like macrophages co-cultures for the evaluation of nanoparticles toxicity

Nadège Grabowski ^{a,b}, Hervé Hillaireau ^{a,b}, Juliette Vergnaud ^{a,b}, Valérie Nicolas ^c,
Saadia Kerdine-Römer ^d, Elias Fattal ^{a,b}

^a. Université Paris-Sud, Faculté de pharmacie, Institut Galien Paris-Sud, LabEx LERMIT, 5 rue JB Clément, 92296 Chatenay-Malabry Cedex, France

^b. CNRS, UMR 8612, 5 rue JB Clément, 92296 Chatenay-Malabry Cedex, France

^c. Institut d'Innovation thérapeutique (IFR 141), IPSIT, 5 rue JB Clément, 92296 Chatenay-Malabry Cedex, France

^d. INSERM UMR 996 Cytokines, Chimiokines et Immunopathologie, 5 rue JB Clément, 92296 Chatenay-Malabry Cedex, France

To be submitted

Abstract

A co-culture of lung alveolar epithelial cells (A459) and macrophages (differentiated THP-1 monocytes) was established by putting in direct contact both cell populations. Using immunocytochemistry and confocal laser scanning microscopy, both cell subpopulations were evidenced. The synergistic effects observed in the co-culture for cytokine secretions confirm cell-cell interactions. The co-culture was thus used as a relevant *in vitro* tool to evaluate the toxicity of polymeric as well as non-biodegradable nanoparticles. Poly(lactide-co-glycolide) (PLGA)-based nanoparticles of 200 nm were prepared, with the addition, or not, of hydrophilic polymers (as stabilizers). Selective uptake kinetics of PLGA nanoparticles by cell subpopulations, as well as apoptosis/necrosis detection, was achieved by using a selective label of each cell type, while cytokine secretions were quantified in culture supernatants. Both cell subpopulations took up PLGA nanoparticles with similar profiles, and induced only necrotic cells. Mild inflammatory response to stabilized nanoparticles was detected (compared to well-known inflammatory compounds), slightly higher than the PLGA and stabilizer components taken individually demonstrating that although biodegradable nanoparticles are safe they can internalize compounds such as the stabilizing agents used here and slightly enhance their toxicity.

Keywords Co-culture, A549, THP-1 macrophages, nanoparticles, toxicology

1. Introduction

In vitro nanotoxicology to the lung must take into account of a large variety of toxicity endpoints as well as the nature of the nanoparticles tested. Indeed, on the one hand, several reviews have detailed the toxicity of inhalable manufactured nanoparticles towards the pulmonary tract, as they could be involved in the induction of inflammation and oxidative stress (Oberdorster *et al.*, 2005, Horie *et al.*, 2012). On the other hand, the pulmonary route offers interesting potentialities for drug delivery. Indeed, it is a non invasive route, that can be used for local or systemic treatments thanks to the high absorption surface, weak enzymatic activity and a high blood supply of the pulmonary region (Patton *et al.*, 2004). A wide range of biodegradable nanocarriers, from liposomes to polymeric nanoparticles, can be considered for lung delivery (Sung *et al.*, 2007, Mansour *et al.*, 2009). Regarding the latter, poly(lactide-co-glycolide) (PLGA)-based nanoparticles present a high interest for drug delivery since this copolymer was approved in many countries for controlled drug delivery implants. In addition, nanoparticles made of such co-polymer can easily be surface-modified for an efficient targeting and several different drugs have been loaded into these particles from small molecules to macromolecules (Danhier *et al.*, 2012).

The majority of *in vitro* studies are driven on mono-culture. Yet, human organism is multi-cellular, and cannot be reduced to a unique cell line. However, for a first approach, the use of a single cell line provides several advantages in terms of cost, convenience, and stability upon splitting. On account of these benefits, the mixture of several cell types (at least two) to create a co-culture represents an important step in the cell culture area. Hence, co-cultures consider cell-cell interactions and are thus an *in vitro* model closer to the physiology than single cell culture. This is reason why co-cultures have been used to mimic different organs or body parts, including the lungs.

From the trachea, to the bronchus and the alveoli, the pulmonary epithelium is composed of multiple cell types (Patton and Byron, 2007, Crapo *et al.*, 1982). The bronchial space was for instance mimicked by a co-culture of bronchial cells (primary or cell lines) and fibroblasts (Pohl *et al.*, 2009). Several co-cultures were used as model of aveoli by co-cultivating alveolar epithelial cells with macrophages (Wottrich *et al.*, 2004, Jantzen *et al.*, 2012, Striz *et al.*, 2011, Striz *et al.*, 2001, Alfaro-Moreno *et al.*, 2008, Hjort *et al.*, 2003). More complex models were reported as the co-culture of alveolar epithelial and dendritic cells as well as macrophages (Rothen-Rutishauser *et al.*, 2005), or the co-culture of macrophages, epithelial,

endothelial and mast cells (Alfaro-Moreno *et al.*, 2008). Co-cultures with alveolar macrophages are particularly interesting, since in lung injury episodes, resident alveolar macrophages release large amounts of biological substances (oxygen radicals, growth-regulating proteins or protease). As a result, alveolar macrophages have shown a dual role by both preventing and contributing to lung injury (Oberdorster *et al.*, 1992) while a defensive role towards epithelial cells has been shown in co-culture (Wang *et al.*, 2002). Up to now, these models, that have been used to investigate the potential harmful effects of non-biodegradable (Müller *et al.*, 2010) or atmospheric nanoparticles (Alfaro-Moreno *et al.*, 2008), have highlighted cooperation effects particularly in the case of inflammatory response and oxidative stress (Jantzen *et al.*, 2012).

In the present study, the co-culture of A549 epithelial cells with human-like macrophages (differentiated from THP-1 monocytes) in direct contact was established, characterized and used to assess the toxicity of PLGA-based nanoparticles, polystyrene and titanium dioxide nanoparticles. Each cell population was distinguished thanks to a specific labeling, in order to determine specific uptake kinetics and specific cytotoxicity of PLGA-based nanoparticles. Furthermore, the secretion of several cytokines upon exposure to different nanoparticles was quantified.

2. Material and methods

2.1. Cell culture & differentiation

The A549 cell line (catalog number CCL-185) and the THP-1 cell line (catalog number TIB-202) were obtained from ATCC and cultured in RPMI-1640 growth medium (Lonza), supplemented with 50 U/mL penicillin, 50 U/mL streptomycin, and 10 % fetal bovine serum (Lonza). Cells were maintained at 37 °C in a 5 % CO₂ humidified atmosphere. Twice a week, A549 cells were passaged at 1:15 ratio and THP-1 at 1:5 ratio. Cells were used from passage 3 to 12 after thawing.

Differentiation of monocytes into macrophages (THP-1 to THP-1-D) was performed using the 12-*o*-tetradecanoylphorbol-13-acetate (PMA) as previously described (Chapter 2). Briefly, 10⁶ cells were seeded on petri dishes with 10 nM PMA for 24 h. The supernatant was then discarded and replaced by fresh medium for 24 h before further use.

2.2. Co-culture

2.2.1. Co-culture establishment

The co-culture was established by direct contact between both cell populations (Figure 1). 10^6 THP-1 monocytes were firstly differentiated into THP-1 macrophages in petri dishes ($t = 0$) as described in section 2.1. The medium was renewed after 24 h. Secondly, 42 000 A549 cells were plated in 12-well plates ($t = 24$ h). Thirdly, THP-1-D macrophages were harvested and centrifuged down ($200 \times g$, 4 min, 4°C). After pellet resuspension in growth medium, 42 000 THP-1-D macrophages were added in direct contact onto the A549 cells in 12-well plates, resulting approximately in a 1:2 ratio (THP-1-D : A549) ($t = 48$ h). The resulting co-culture was incubated for 24 h to allow cell recovery and potential contact establishment between cell types. The co-culture was then characterized, or ready to use (12-well plates) for further studies ($t = 72$ h).

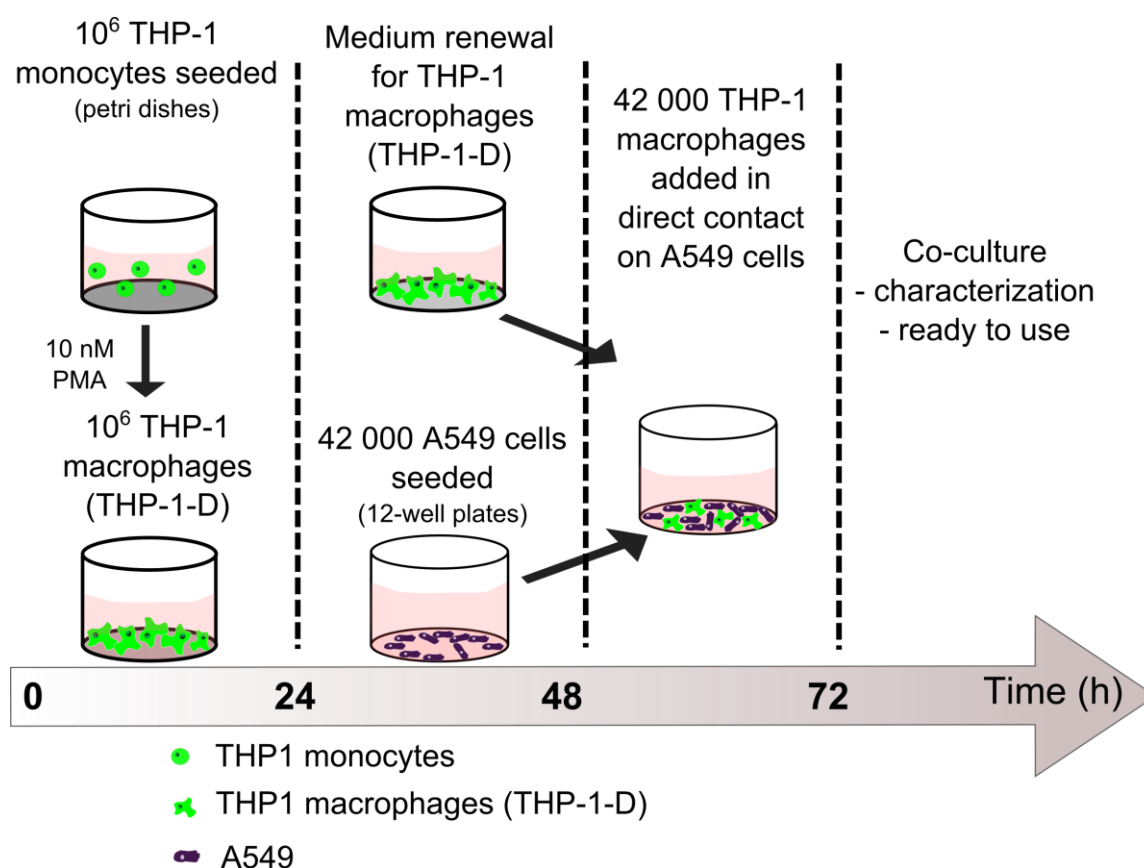


Figure 1. Experimental setup of the establishment of the co-culture of lung epithelial cells (A549) and human-like macrophages (differentiated from THP-1 monocytes) in direct contact.

2.2.2. Immunocytochemistry characterization

After 24 h of direct contact between the two cell populations, the cell layer was rinsed with PBS and harvested with trypsin. 250 000 cells were seeded in 96-well plates with conical bottom. Supernatants were discarded after centrifugation (4 min, $200 \times g$, 4°C), and cells were resuspended in PBS containing 0.5 % Bovine Serum Albumin (BSA) (referred to as 'PBS/BSA' in the following). Supernatants were discarded after centrifugation (4 min, $200 \times g$, 4°C) and cells were incubated in PBS/BSA for 20 min at 4°C (protected from light), with the following monoclonal antibodies: PE (PhycoErythrin)-conjugated anti-CD14, anti-CD11b and anti-CD54 (BD Biosciences respectively 555398, 555388, 555511). After incubation, cells were washed once with PBS/BSA, once with PBS and finally resuspended in PBS, to be immediately analyzed by flow cytometry (FACScalibur, Beckton Dickinson). For each sample 10 000 events were acquired from a gated homogeneous cell population from a side- versus forward-scatter plot. Fluorescence intensities were then collected on the FL-2 channel and mean fluorescence intensities (MFI) determined. The MFI fold increase of each sample was determined as the ratio of the sample MFI to the MFI of non-labeled cells. To determine positive cells, histograms with FL-2 parameter against the number of events were used. The marker was placed to the right of the peak to non-treated cells, to designate positive cells. All experiments were performed in triplicate or more.

2.2.3. Co-culture characterization by confocal laser scanning microscopy

A549 cells were pre-labeled with 5-(and 6)-carboxyfluorescein diacetate succinimidyl ester (CFSE) (Biolegend) according to the protocol provided. Briefly, 10 to 100×10^6 cells were collected, centrifuged (4 min, $200 \times g$, 37°C), and incubated with pre-warmed PBS (37°C) containing CFSE (5 μM) for 10 min at 37°C in a 5 % CO_2 humidified atmosphere. Ice-cold culture medium was added, and cells were centrifuged (4 min, $200 \times g$, 37°C). Supernatants were then discarded and 100 000 of such pre-labeled A549 cells were plated in 6-well plates containing glass coverslips and incubated for 24 h. The day after, pre-differentiated THP-1-D macrophages were harvested, centrifuged ($200 \times g$, 4 min, 37°C) and resuspended in medium containing 0.5 μM Orange Lyotracker (Invitrogen) (5 min, 37°C). Cells were rinsed once with culture medium and 100 000 THP-1-D were added in direct contact with pre-labeled A549 cells. The resulting co-culture was incubated for 24 h. All the protocol was performed in the absence of light. Observations were done with a LSM confocal microscope (Zeiss-Meta) equipped with Argon (488 nm, 300 mV) and Helium-Neon (543 nm, 5 mV) lasers, and

a plan-apochromat 63X objective. During the observation, glass coverslips were kept at 37 °C, using an adapted warming plate, to keep cells alive. Data were analyzed with the LSM 510 software (version 3.2).

2.3. Nanoparticle preparation and characterization

Stabilized PLGA nanoparticles were prepared according to an emulsion/evaporation method as previously described by our group (chapters 1). PLGA (75:25 Resomer[®] RG756, Ingelheim) was dissolved in a dichloromethane/acetone (1/1 v/v) mixture and pre-emulsified by vortexing for 1 min, with either an aqueous solution containing 2.5 mg/mL PVA (87-89 % hydrolyzed, 30-70 kDa) to prepare PLGA/PVA nanoparticles, or an aqueous solution containing 0.6 mg/mL CS (Protasan[®] UP CL113, 75-90% deacetylation, 50-150 kDa, FMC Biopolymers) and 5 mg/mL PVA (Mowiol[®] 4-88, Kuraray Specialities Europe GmbH) to prepare PLGA/CS nanoparticles. The pre-emulsion was kept on ice and immediately sonicated (Branson Digital Sonifier) at 40 % for, respectively, 1 or 2 min. The purification of nanoparticles (removal of free PVA and CS) was achieved by ultracentrifugation (4 °C, 37 000 × g, 1 h) and pellet resuspension was performed by vortexing.

PLGA/PF68 nanoparticles were prepared by dissolving 50 mg PLGA in 5 mL ethyl acetate. The organic phase was added dropwise to 10 mL of a 10 mg/mL PF68 (BASF) aqueous solution under magnetic stirring. After 1 min vortexing, the emulsion was kept on ice and homogenized using an Ultra-Turrax[®] (IKA works, Inc), equipped with a 18G-stainless steel dispersing tool (10 000 rpm, 2 min). The organic solvent was then evaporated at room temperature under magnetic stirring for 2 h. The purification of nanoparticles (removal of free PF68) was performed by dialysis during 24 h against 1 L of MilliQ water, using a cellulose ester membrane with a 50 kDa cutoff (SpectrumLabs).

Stabilizer-free PLGA nanoparticles were prepared by nanoprecipitation as previously described (Chapter 2). 50 mg PLGA 75:25 were dissolved in 5 mL acetonitrile. The organic solution was added dropwise under magnetic stirring to 15 mL water. After 5 min magnetic stirring, acetonitrile was removed and the suspension concentrated by evaporation under reduced pressure at 40 °C, until a nanoparticle concentration close to 25 mg/mL.

All PLGA nanoparticles were fluorescently labeled, by replacing the total quantity of PLGA by a 99/1 (w/w) mixture of PLGA and a custom-made DY700-PLGA conjugate, obtained by coupling 75:25 PLGA with a Near Infra Red (NIR)-emitting fluorescent dye (DY700,

Dyomics) as previously described (Reul *et al.*, 2012). The further steps were performed similarly to unlabeled nanoparticles, protected from light. Particle suspensions were not contaminated by any bacteria.

As previously described (Chapter 1) TiO₂ nanoparticle suspensions were obtained by thorough dispersion of anatase (spheres < 25 nm) or rutile (rods 10 x 40 nm) TiO₂ nanopowders (Sigma-Aldrich) in water. Briefly, powders were incorporated into water at 1 mg/mL and 1 min vortexing, after which pH was adjusted to 11 with 1 M sodium hydroxide. Suspensions were then sonicated (40 %) on ice during 1.5 h, with 60 s pulsations and 30 s intervals, and subsequently stirred at 24 000 rpm for 5 min on ice using an Ultra-Turrax® equipped with a plastic (polycarbonate/PEEK) dispersing tool (S25D-14G-KS, IKA). Nanoparticle suspensions were vortexed just before use. Polystyrene (PS) nanoparticle aqueous suspensions (0.20 µm, Polysciences Europe GmbH) were briefly vortexed before use.

All nanoparticles were characterized by their size and their zeta potential using a Nano ZS (Malvern instruments, UK). Average hydrodynamic diameters were measured by dynamic light scattering (25 °C, 173° scattering angle) after appropriate dilutions in water. Zeta potential measurements were performed after appropriate dilutions in 1 mM sodium chloride, at 25 °C. Nanoparticle stability was studied in cell culture medium at the final concentration of 0.1 mg/mL, after 48 h incubation (37°C). The amount of stabilizers associated to nanoparticles after their purification was assessed through the formation of colored complexes with PVA and CS, or by ¹H NMR in the case of PF68, as previously described (Chapter 1).

The fluorescence emission spectra of fluorescent nanoparticle suspensions were recorded using an excitation wavelength of 700 nm. The fluorescence intensities of stabilizer free-PLGA, PLGA/PVA and PLGA/PF68 nanoparticles were compared to that of PLGA/CS nanoparticles and expressed as the ratio of the fluorescence intensities collected at the 722 nm emission wavelength (the ratio was set at 1 for PLGA/CS nanoparticles which were the most fluorescent). Physicochemical characteristics of PLGA-based nanoparticles and of non-biodegradable nanoparticles are presented on Table 1 and Table 2.

Table 1. Physicochemical properties of PLGA-based nanoparticles.

Nanoparticles	Average diameter (nm)		Polydispersity index	Zeta potential (mV)	Shell (mg/100 mg PLGA)	Fluorescence intensity ratio
	Water	48 h cell culture medium 37 °C				
PLGA	171 ± 5	nd	0.044 ± 0.021	- 44.8 ± 5.1	None	na
DY700-PLGA	172 ± 15	nd	0.052 ± 0.016	- 40.0 ± 7.0	None	0.91
PLGA/PVA	233 ± 28	212 ± 6	0.099 ± 0.050	- 1.42 ± 2.2	PVA (11.5)	na
DY700-PLGA/PVA	221 ± 9	nd	0.084 ± 0.018	- 4.10 ± 0.8	nd	0.78
PLGA/CS	233 ± 18	269 ± 12	0.210 ± 0.020	+ 39.9 ± 7.2	CS (15.3)/PVA (30.4)	na
DY700-PLGA/CS	234 ± 1	nd	0.182 ± 0.004	+ 45.3 ± 0.6	nd	1
PLGA/PF68	228 ± 22	316 ± 16	0.133 ± 0.044	- 31.3 ± 4.9	PF68 (15.5)	na
DY700-PLGA/PF68	205 ± 27	nd	0.152 ± 0.070	-27.4 ± 7.0	nd	0.68

na: non applicable, nd: not determined.

Table 2. Physicochemical properties of non-biodegradable nanoparticles.

Nanoparticles Core	Cristal form	Average diameter (nm)		Polydispersity index	Zeta potential (mV)	Shell
		Water	48 h cell culture medium 37 °C			
TiO ₂	Anatase	421 ± 49	625 ± 46	0.42 ± 0.07	- 35 ± 2	None
TiO ₂	Rutile	479 ± 184	795 ± 80	0.77 ± 0.25	- 37.2 ± 6	None
Polystyrene	na	250 ± 11	259 ± 21	0.02 ± 0.02	- 48.8 ± 1.5	Sulfate ester

na: non applicable

2.4. Selective uptake of nanoparticles

2.4.1. Flow cytometry

After establishment of the co-culture (Figure 1, $t = 72$ h), supernatants were discarded and replaced by a fresh suspension of fluorescent DY700-PLGA nanoparticles diluted in the medium at 0.1 mg/mL (final concentration). After 5 min to 48 h incubation at 37 °C, supernatants were discarded, cells were rinsed twice with PBS and harvested by trypsin. Trypsin was neutralized by PBS/BSA, and cells were labeled with anti-CD14-PE as described above (section 2.2.2). Cell suspensions were immediately analyzed by flow cytometry and MFI was collected on FL-2 (corresponding to PE probe) and FL-3 using a NIR filter (corresponding to DY700 probe). For each sample 10 000 events were acquired from a gated homogenous cell population selected from a side-versus forward-scatter plot. Cell populations were distinguished by gating CD-14 positive cell population and CD-14 negative cell population (Figure 2). For each sample, results were expressed as the ratio of the FL-3 MFI of each gated population to the MFI of corresponding non-treated cells. This value was then corrected by the fluorescence factor of each nanoparticle suspension. All experiments were performed in triplicate or more.

2.4.2. Confocal laser scanning microscopy

After establishment of the co-culture as described in the section 2.2.3 (and Figure 1, $t = 72$ h), supernatants were discarded and replaced by 2 mL of DY700-PLGA nanoparticle suspensions diluted in medium at 0.1 mg/mL (final concentration). After 1 h incubation at 37 °C, coverslips were rinsed with PBS, and fresh medium was added to perform confocal microscopy observations in real time on living cells, using similar setup as described in section 2.2.3, with a supplementary Helium-Neon (633 nm, 5 mV) laser.

2.5. Apoptosis/necrosis detection coupled to CD14 identification

After establishment of the co-culture (Figure 1, $t = 72$ h), supernatants were discarded and replaced by 2 mL of fresh growth medium containing PLGA nanoparticles at 0.1 mg/mL, and incubated for 24 to 48 h. The cell layer and the supernatants were analyzed separately. In a first step, supernatants were collected in eppendorf, centrifugated (3 min, $1000 \times g$) and resuspended into 20 μ L binding buffer that containing 2 μ L of annexin-AlexaFluor (AF) 488 (Life Technologies) and 2 μ L of 7-Aminoactinomycin D (7-AAD) (Sigma-Aldrich) (10 min, room temperature, darkness). Cells were resuspended in with PBS/BSA after centrifugation (3 min, $1000 \times g$) and kept on ice. In a second step, the adherent cell layer was rinsed with ice-cold PBS followed by the addition of 200 μ L binding buffer containing 5 μ L annexin-AF488 and 5 μ L of 7-AAD (10 min, room temperature, darkness). Cells were rinsed with PBS and harvested by trypsin, and pooled them with pellets obtained in the first step. 250 000 cells were then indentified with anti-CD14-PE as described in the section 2.2.2. Cells were immediately analyzed by flow cytometry, and mean fluorescence intensities were collected on FL-1 (AF488 probe), FL-2 (PE probe) and FL-3 (7-AAD) channels (Figure 2). To perform fluorescence compensations each fluorescent probe was used separately on non treated cells.

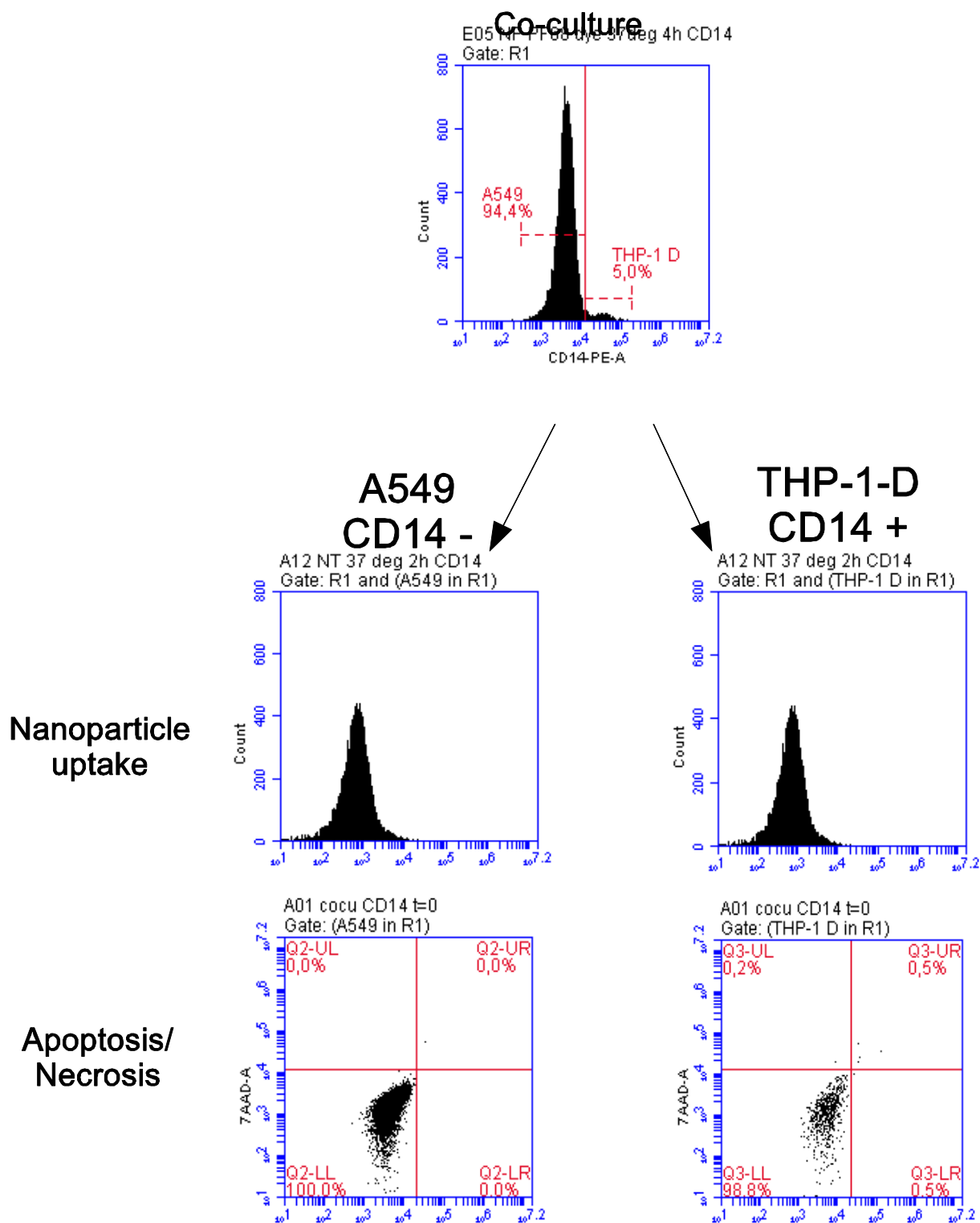


Figure 2. Flow cytometry method employed to identify cell types for uptake and apoptosis/necrosis studies. The total cell population was labeled with CD14-PE (FL-2), A549 cells being CD14-negative and THP-1-D CD14-positive. Then, in the case of uptake kinetics, the MFI of each gated population was followed in FL-3 channel equipped with an NIR-filter, and in the case of apoptosis/necrosis detection, the cellular state was followed in FL-1 (annexin V) and FL-3 (7-AAD) channels.

2.6. Quantification of secreted cytokines

Cytokine secretions following nanoparticle exposure were investigated in supernatants using the multiplexed Cytometric Beads Array (CBA) method (BD Biosciences) (Morgan *et al.*, 2004, Tarnok *et al.*, 2003), and performed with the human IL-1 β , IL-6, IL-8, IL-10, IL-12p70, MCP-1 and TNF flex sets with the Human Soluble Protein Master Buffer Kit (BD Biosciences). After establishment of the co-culture (Figure 1, t = 72 h), supernatant were discarded and replaced by 2 mL of fresh growth medium (non-treated cells), with either increasing lipopolysaccharide (LPS) concentrations (0.1, 1, 10 $\mu\text{g/mL}$) or nanoparticles at 0.1 mg/mL. After 24 h exposure, supernatants were sampled and cells were rinsed once with PBS and harvested with trypsin, to be counted by flow cytometry. To assess a large range of concentrations, each supernatant sample was analyzed without dilution and after a 1:50 dilution in medium. Cytokine results, analyzed with the FACP ArrayTM Software, were obtained as pg/mL. All experiments were performed in triplicate, or more.

3. Results and discussion

3.1. Co-culture establishment and characterization

In order to investigate *in vitro* the pulmonary toxicity of a series of nanoparticles, co-culture models are attractive tools to take into account the diversity of cell populations in the lung tissue and their interactions. In the alveoli, a region expected to interact significantly with deposited nanoparticles after inhalation, pneumocytes and macrophages play an important role, respectively in the maintenance of the epithelial integrity and the inflammatory response. However, the interaction between these cell types should also be taken into account to stay the closest to the physiological response, such as in the case of inflammatory response. In this study, we selected as a model of pneumocytes, A549 cells because they have already been reported as an appropriate epithelial alveolar model (Rothen-Rutishauser *et al.*, 2012). Macrophages have been obtained by controlled differentiation of human THP-1 monocytes, as described previously (chapter 2). They present a phenotype close to alveolar macrophages (Striz *et al.*, 1993). These two cell types were co-cultured in direct contact in order to mimic physiological conditions. While such co-culture conditions have already been described (Wottrich *et al.*, 2004, Jantzen *et al.*, 2012), our goal was (i) to characterize the cell subpopulations and investigate their common interaction, and (ii) to explore the potential of this co-culture for nanotoxicology studies, in particular for the investigation of selective

uptake of nanoparticles, induction of apoptosis and/or necrosis on each subpopulation, and possible synergistic secretion of cytokines.

3.1.1. Phenotype characterization

The phenotype of cell subpopulations in co-culture was investigated and compared to the corresponding cell monocultures, by CLSM and immunocytochemistry. CLSM images on pre-labeled cells show that both cell types exhibit a similar morphology compared to the corresponding mono-cultures (Figure 3). In particular, macrophages retain their surface adhesion capacity despite the transfer step when put into contact with A549 cells. Immunocytochemistry results show that in mono-culture, THP-1-D macrophages are CD11b and CD14 positive, whereas A549 cells are CD11b and CD14 negative (Figure 4). The analysis of the co-culture cell layer shows two populations for the CD11b and CD14 markers: one being CD11b⁺ and CD14⁺ (accounting for approximately 90% of total cells), the other one being CD11b⁻ and CD14⁻ (approximately 10%). This 90/10 ratio is different from the expected 1:4 ratio after 24 h incubation. However, it is worth noting that this final cell ratio is consistent with normal human physiological conditions (Crapo *et al.*, 1982). These profiles also show that anti-CD11b-PE and anti-CD14-PE are good candidates to discriminate both cell subpopulations for further selective uptake studies and moreover apoptosis/necrosis detection in subpopulations.

Some indications of A549/THP-1-D interactions are provided by CLSM images, displaying a close proximity of membranes from the two cell types (Figure 3C). In addition, immunocytochemistry results show that while A549 and THP-1-D cells are respectively CD54⁻ and CD54⁺ in mono-culture, almost all cells are found CD54⁺ in the co-culture (Figure 4), suggesting that contact with THP-1-D cells has induced the expression of CD54 by A549 cells. This receptor, also called ICAM-1, is involved in cell adhesion process. This result is consistent with previous studies showing that A549 cells incubated with conditioned medium of primary monocytes, can express ICAM-1 (Krakauer, 2002).

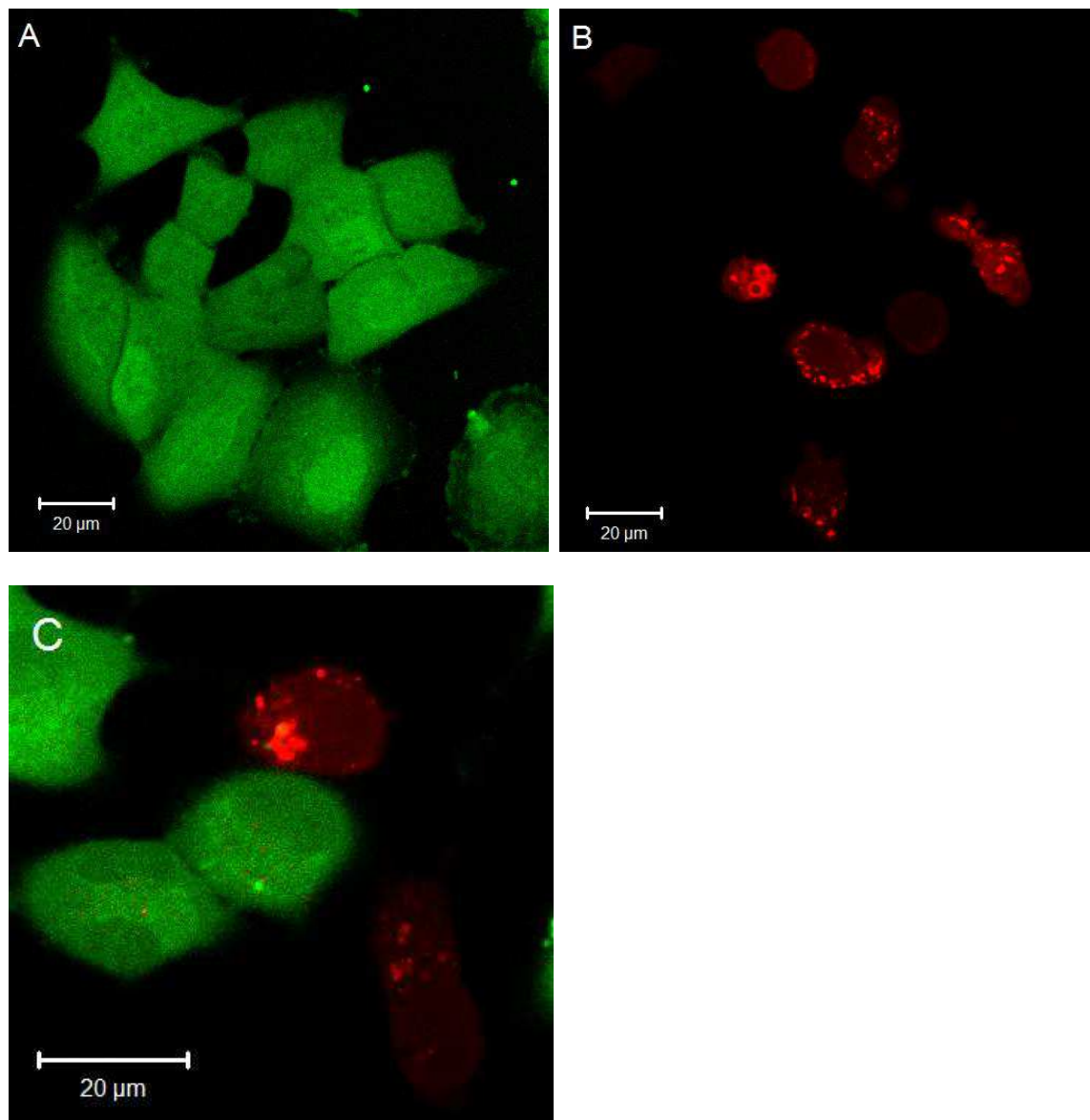


Figure 3. (A) CFSE-labeled A459 cells (green), (B) Orange Lysotracker THP-1-D (red) cells in monoculture, and (C) in a co-culture in direct contact, as observed in confocal laser scanning microscopy (CLSM), in real time with living cells (incubation time shown: 24 h). Scale bar: 20 µm.

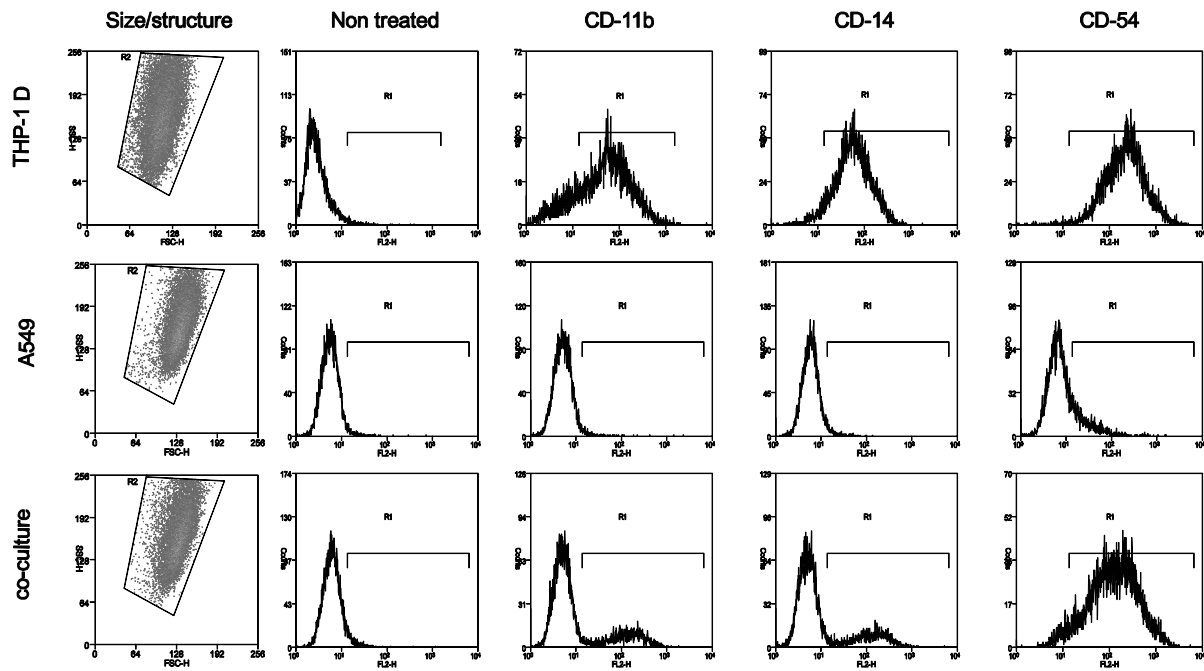


Figure 4. Immunocytochemical characterization of THP-1-D and A549 cells in mono and in co-culture. Cellular morphology and CD-11b, CD-14, CD-54 cell levels were analyzed by flow cytometry. To obtain CD-11b, CD-14, CD-54 histograms, gates were drawn on the major cell population, according to the corresponding experiment. Data shown are representative of 3 independent experiments.

3.1.2. Cytokine secretion

As it was previously shown, interactions between alveolar macrophages and epithelial cells can promote inflammatory response (Tao and Kobzik, 2002). Synergistic effects in cytokine production in the co-culture supernatants were thus investigated after exposure to LPS, and compared to those observed for mono-cultures. Seven cytokines were quantified using the CBA method: IL-1 β , IL-10, IL-6, IL-8, TNF- α , MCP-1 (Figure 5) and IL-12 (data not shown). Four relevant cytokines were found to be secreted in significant levels in mono and co-culture: IL-6, IL-8, MCP-1 and TNF- α . Synergistic effects were observed for IL-6, MCP-1 and IL-8. For example, incubation with 0.1 $\mu\text{g}/\text{mL}$ LPS led to an increase of IL-6 and IL-8 secretion up to 2.5-fold higher in co-culture than the sum of the secretions obtained in mono-cultures (Figure 5 B,C). This increase was even 6-fold higher for MCP-1 (Figure 5 E). As a general trend, cytokine levels peaked upon exposure to 1 $\mu\text{g}/\text{mL}$ LPS and then plateaued or decreased for higher LPS concentrations. Despite their low representation compared to A549 cells, THP-1-D macrophages seem to account for the larger part of IL-6, IL-8 and especially TNF- α secretion, which is consistent with previous studies showing that in co-culture with

A549 cells, PBMC are the main source of –between others cytokines- TNF- α and IL-8 cytokines (Krakauer, 2002). These results show the potential of the A549/THP-1-D co-culture to study the inflammatory response.

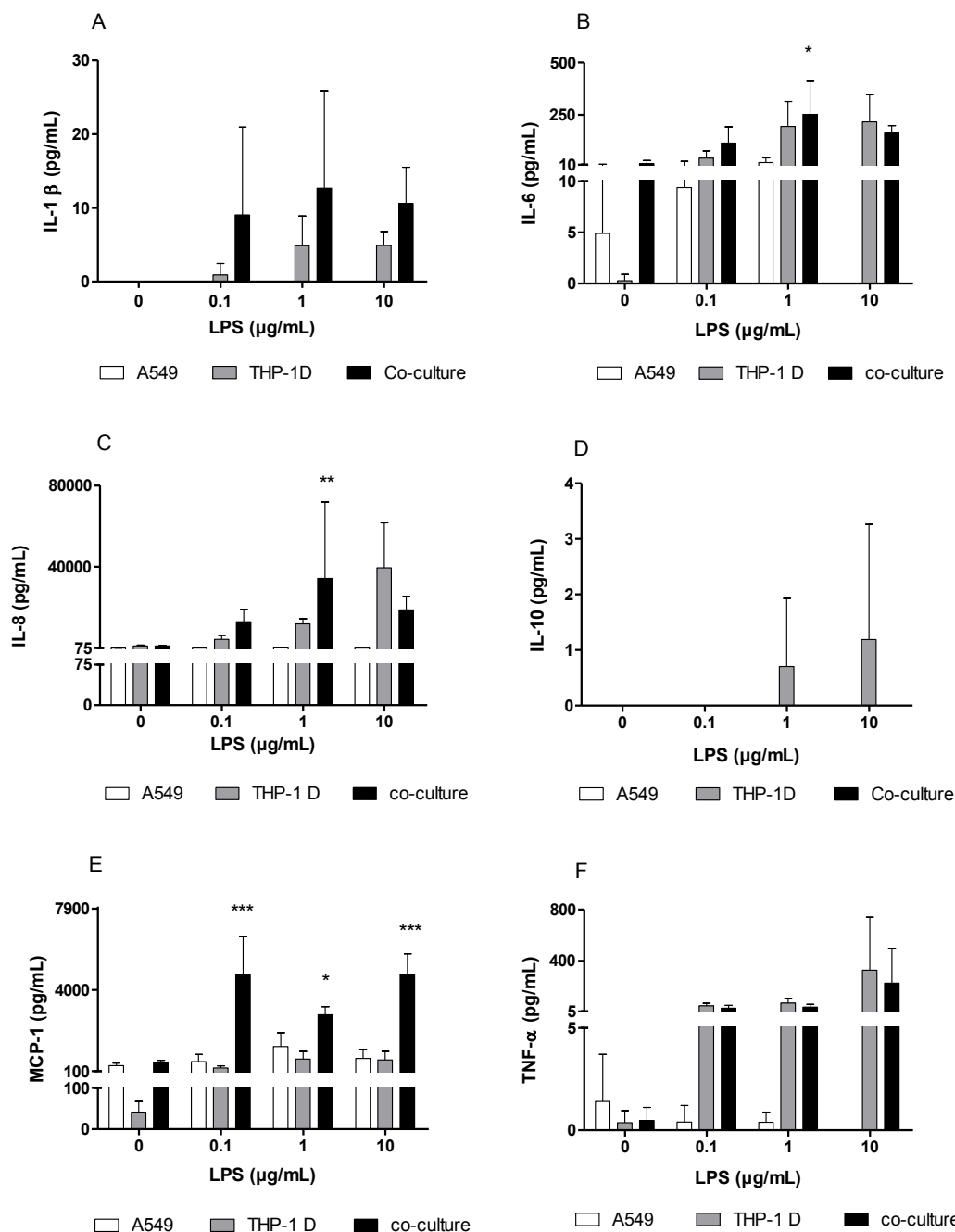


Figure 5. Secretions of IL-1 β (A), IL-6 (B), IL-8 (C), IL-10 (D), MCP-1 (E) and TNF- α (F) cytokines after 24 h exposure to increasing LPS concentrations (0.1, 1, 10 $\mu\text{g/mL}$) in A549 cells (white bars) and THP-1-D cells (grey bars) mono-cultures, or in co-culture (black bars). $n \geq 3$, * $p < 0.05$, ** $p < 0.01$, *** $p < 0.001$ compared to corresponding non treated conditions.

3.2. Comparative toxicological evaluation of nanoparticles

3.2.1. Nanoparticles

The effect of different nanoparticle types has been investigated on the co-culture. In particular, PLGA-based nanoparticles have been selected as it is one the major type of biodegradable polymeric nanoparticles, relevant for the formulation of nanomedicine. A series of custom made PLGA nanoparticles were prepared as previously described by our group (Chapters 1 and 2). Nanoparticles in the range size of 170-230 nm were obtained in the presence of hydrophilic polymers as stabilizers, but also in the absence of any stabilizer. Uncoated PLGA nanoparticles present a negative surface charge, whereas PVA, CS and PF68 form respectively neutral, positive and negative surface charged nanoparticles. The replacement of a low percentage of PLGA by a fluorescent PLGA does not modify physico-chemical properties (Table 1). Moreover, nanoparticle sizes are stable after 48 h in complete culture medium at 37 °C.

PLGA nanoparticles were compared to non-biodegradable nanoparticles, either polymeric (polystyrene) or inorganic (TiO₂). Sulfate ester-stabilized polystyrene nanoparticles were used without modifications and were shown to be stable in culture medium. The diameter of anatase and rutile TiO₂ nanoparticles in suspension was reduced using dispersing tools, without adding any supplementary stabilizer.

3.2.2 Selective uptake of PLGA nanoparticles by cell subpopulations

Uptake kinetic studies (Figure 6) were performed at 37 °C after exposure to fluorescent DY700-PLGA nanoparticles at 0.1 mg/mL. A549 and THP-1-D subpopulations were identified using anti-CD14-PE (Figure 2), which did not alter the detection of nanoparticle fluorescence. All PLGA nanoparticles are taken up with a similar profile by both sub cell populations. Stabilizer-free PLGA and PLGA/PF68 nanoparticles (displaying both a negative zeta potential) are taken up earlier and in higher quantity than PLGA/CS (positive zeta potential) and PLGA/PVA (neutral) nanoparticles, especially by the A549 cells. The same behavior was observed on the same cells in mono-culture (chapters 1 and 2). Another observation is the overall higher uptake of nanoparticles by THP-1-D cells compared to A549 cells. After 24 and 48 h, THP-1-D cells take up twice as much PLGA/PVA nanoparticles than the A549 cells. PLGA nanoparticle uptake by co-culture was also visualized by CLSM in real time on living cells. Both cell populations were fluorescently labeled as described in section

2.2.3 (A549 with CFSE, THP-1-D with Orange LysoTracker), and cultivated in co-culture. The co-culture was finally exposed for 1 h to DY700-PLGA/PF68 nanoparticles and observed by CLSM (Figure 7). PLGA/PF68 nanoparticles were observed within both sub cell populations, but mostly in macrophages, confirming the flow cytometry results. These results come in line with the prominent role of alveolar macrophage in particle clearance from the alveoli region (Wang *et al.*, 2002), although their represent less than 10 % of the cell population, similarly to what is observed here.

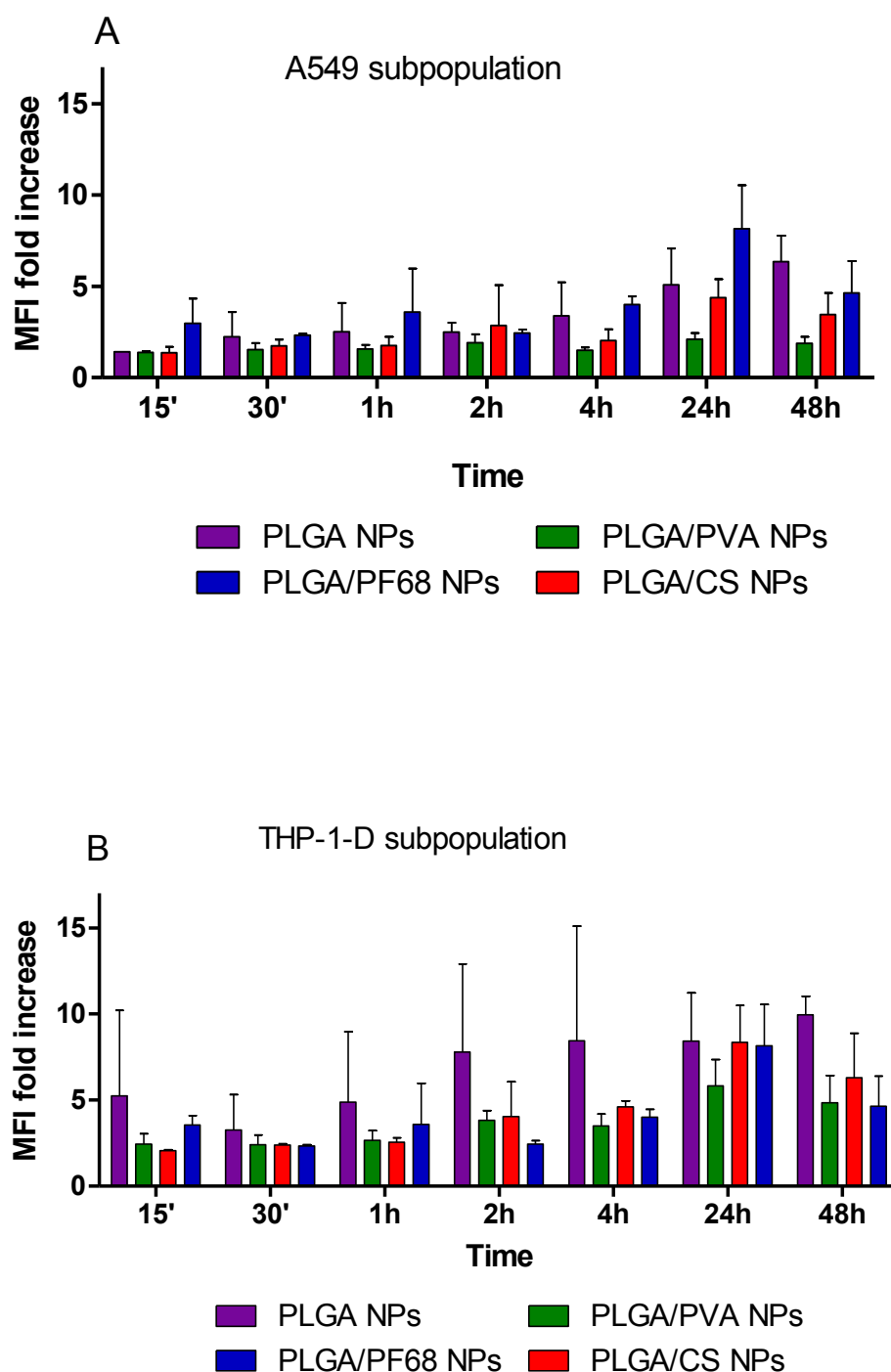


Figure 6. (A) Uptake of PLGA-based nanoparticles by A549 and THP-1-D cells in co-culture at 37 °C, as evaluated by the mean fluorescence intensity (MFI) in flow cytometry after identification of cell subpopulation using anti-CCD14-PE. (B) Co-culture of CFSE-labeled A549 cells (green) and Orange LysoTracker-labeled THP-1-D cells (red) exposed to DY700-PLGA/PF68 nanoparticles (white) for 2 h at 37 °C. Scale bar: 20 µm.

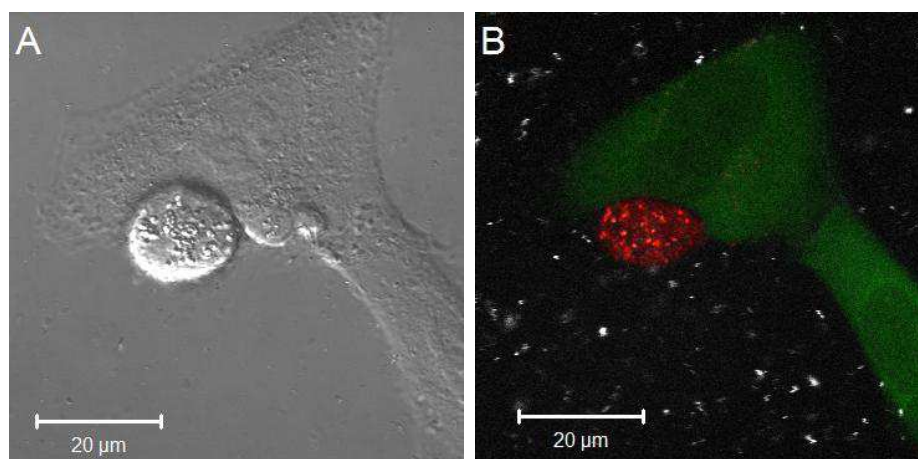


Figure 7. (A) Uptake kinetics of PLGA-based nanoparticles by A549 and THP-1-D cells in co-culture at 37 °C, as evaluated by the mean fluorescence intensity (MFI) in flow cytometry after correction by relative fluorescence factor. (B) Co-culture of A549 cells (green – CFSE) and THP-1-D cells (red – Orange LysoTracker) exposed to DY700-PLGA/PF68 nanoparticles (white) for 2 h at 37 °C. Scale bar: 20 µm.

3.2.3 Effect on apoptosis/necrosis cell subpopulations

For the detection of apoptosis/necrosis, both cell populations were identified using anti-CD14-PE labeling (Figure 2). Based on our previous studies (Chapters 1 and 2) the nanoparticle concentration was set at 0.1 mg/mL corresponding to 60-80 % of viability of single cell lines as evaluated by mitochondrial activity (MTT tests). After exposure to PLGA nanoparticles for 24 h (A, C) and 48 h (B, D), the main cellular death mechanism was shown to be necrosis, and the amount of early/late apoptotic cells was similar in treated and non-treated cells, whatever the formulations tested (Figure 8). Only slight differences among PLGA nanoparticles appear in the co-culture. After 24 h, PLGA/PF68 and PLGA/CS nanoparticles are slightly more toxic on THP-1-D cells than on A549 cells, whereas stabilizer free-PLGA nanoparticles are more toxic on A549 cells than on THP-1-D cells. After 48 h, PLGA/PF68 nanoparticles remain more toxic on THP-1-D cells. Interesting differences appear, though, when comparing the effect of nanoparticles towards the co-culture compared to the mono-cultures (Table 4). In co-culture conditions, PLGA/PF68 nanoparticles show a noticeable toxicity compared to other PLGA nanoparticles (10% necrotic cells among the A549 subpopulation, 21% among THP-1-D), which was not observed in mono-culture (Chapters 1 and 2).

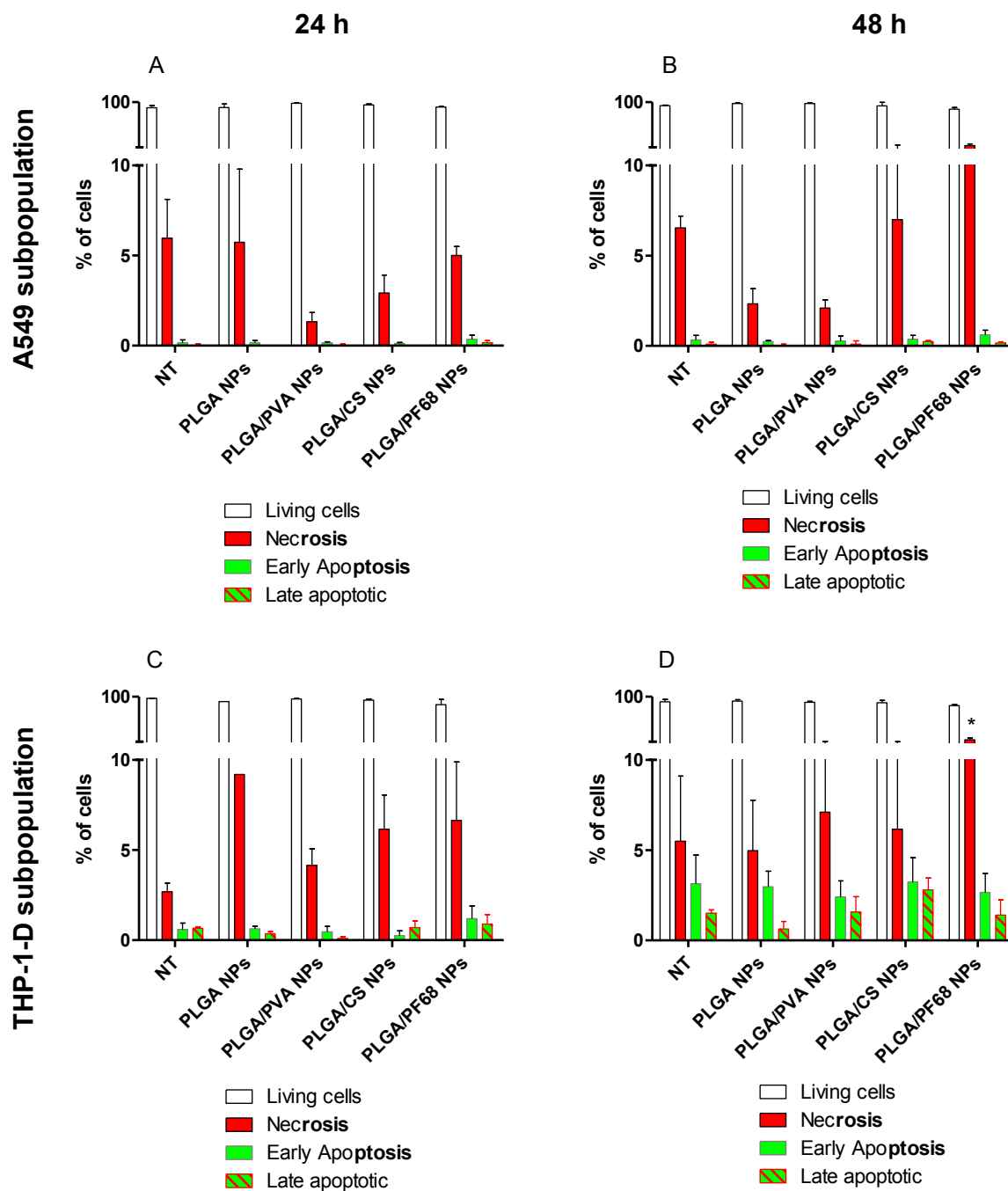


Figure 8. Percentage of living cells, early/late apoptotic cells, and necrotic cells, in the A549 subpopulation (A, B) and THP-1-D subpopulation (C, D) of a co-culture after 24 h (A, C) or 48 h (B, D) exposure to PLGA nanoparticles (NPs). Cells are simultaneously labeled with CD14-PE, 7-AAD and annexin V-AlexaFluor 488. THP-1-D (CD14 positive) and A549 (C14 negative) cells are distinguished as well as necrotic cells (7-AAD positive), early apoptotic cells (Annexin V positive) and late apoptotic cells (both 7-AAD and Annexin V positive). * $p < 0.05$, $n = 3$.

Table 3. Comparison of the percentage of necrotic cells after 48 h exposure to PLGA-based nanoparticle among A549 and THP-1-D cells in mono-culture (Chapters 1 and 2) or as subpopulations in co-culture.

NPs 0.1 mg/mL 48 h	Mono-cultures (Chapters 1 and 2)		Co-culture	
	Necrotic cells (%)		Necrotic cells (%)	
	A549	THP-1-D	A549	THP-1-D
NT	< 1	4	7	3
PLGA NPs	1	3	2	6
PLGA/PVA NPs	1	3	2	8
PLGA/CS NPs	< 1	5	7	8
PLGA/PF68 NPs	3	4	10	21

NPs, nanoparticles ; NT, Non treated

3.2.4 Effect on global cytokine secretions

One of the major interests of a co-culture using macrophages relates to the inflammatory response, as macrophages are able to secrete a large variety of multifunctional biological substances such as cytokines (Nathan, 1987). However, in normal or injured human lungs, all structural cells can secrete cytokines to ensure communication (Kelley, 1990). Quantification of cytokines in co-culture supernatants characterizes not only an inflammatory state, but also cell-cell communications. For example, the quantification of the cytokines of A549 in co-culture with THP-1 monocytes or macrophages has shown that IL-6 and IL-8 significantly increase in co-culture conditions compare to mono-cultures in case of hypoxia (Hjort *et al.*, 2003) or after exposure to ultrafine particles (Wottrich *et al.*, 2004).

The co-culture of A549 and THP-1-D described herein was first used to investigate the own inflammatory potential of nanoparticles, by exposing the co-culture to nanoparticles at 0.1 mg/mL for 24 h. After exposure to stabilizer-free PLGA nanoparticles no increase in cytokine secretion was detected compared to non-treated conditions. Similarly, the aqueous solution of stabilizers did not induce any augmentation in cytokine secretions. On the contrary, stabilized PLGA nanoparticles induced a significant raise in the secretion of several cytokines (IL-8 with PLGA/PVA and PLGA/CS nanoparticles, MCP-1 with PLGA/CS and PLGA/PF68 nanoparticles and IL-6 with PLGA/PF68 nanoparticles) (Figure 9, Table 4). These results highlight the importance of the PLGA/stabilizer combination in the cellular response, as the combination entails significant effect whereas each component is innocuous. Most of the stabilizing agents, being macromolecules, amphiphilic or hydrophilic, does not diffuse by themselves across cell membranes. However, being adsorbed onto nanoparticle

surface, their internalization is enhanced leading to more toxicity. This inflammatory effect remains however limited, much below the cytokine secretions caused by an exposure to 0.1 $\mu\text{g/mL}$ LPS. This co-culture model has thus allowed the detection of mild inflammatory response to stabilized PLGA nanoparticles, slightly higher than the PLGA and stabilizer components individually, but very limited compared to well-known inflammatory compounds.

Table 4. Summary of the *in vitro* inflammatory response after 24 h exposure to polymeric and inorganic nanoparticles on A549 cells and THP-1-D in mono and in co-culture, in presence (co-stimulation) or not of 0.1 $\mu\text{g/mL}$ LPS.

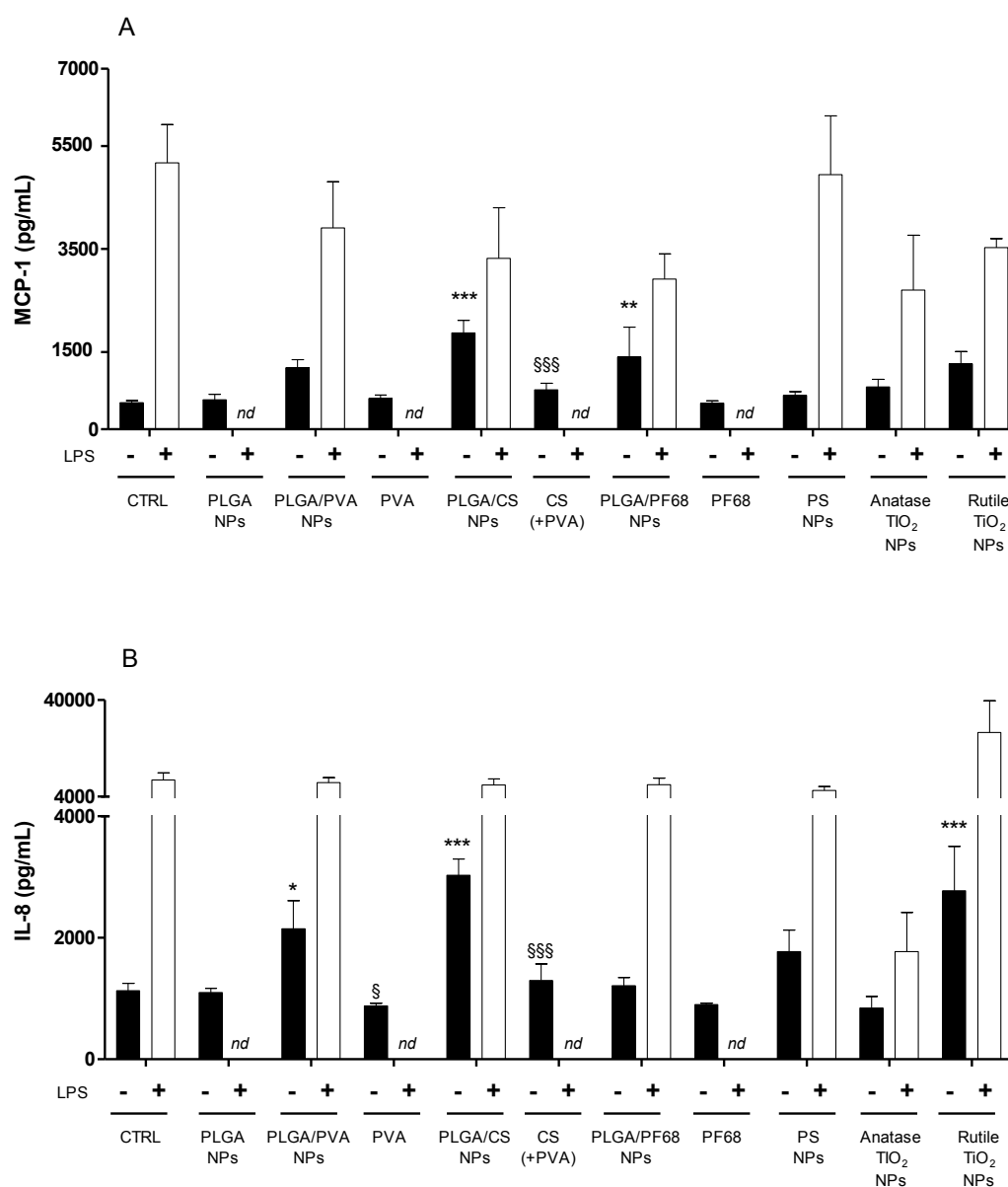
NPs 0.1 mg/mL 24h	Mono-cultures (chapters 1 and 2)				Co-culture	
	A549		THP-1-D		without LPS	with LPS
	without LPS	with LPS	without LPS	with LPS		
PLGA	-	<i>nd</i>	-	<i>nd</i>	-	<i>nd</i>
PLGA/PVA	+ (IL-8)	-	-	-	+ (IL-8)	+ (IL-6)
PLGA/CS	+ (IL-8)	-	-	-	+ (MCP-1 IL-8)	-
PLGA/PF68	+ (MCP-1, IL- 6, IL-8)	-	-	-	+ (MCP-1, IL-6, TNF- α)	+ (IL-6, TNF- α)
PS	-	-	-	-	-	-
Anatase TiO ₂	-	-	-	-	-	-
Rutile TiO ₂	-	-	-	-	+ (IL-8)	-

(+) is defined according to observed significant effects (at least $p < 0.05$) compared to control conditions. *nd*: not determined.

In addition, co-cultures were exposed to nanoparticles in co-stimulation with 0.1 $\mu\text{g/mL}$ LPS, in order to check if nanoparticles can increase the inflammatory response when cells are pre-activated (staggered incubation), or can concentrate LPS that will penetrate the cell easily (simultaneous incubation). Although few statistically significant differences were observed, the relative increase is moderate, and no clear tendency can be drawn regarding a potential effect of nanoparticles on the pro-inflammatory activity of LPS (Figure 9).

These effects were compared to those induced by non-biodegradable nanoparticles, polymeric or inorganic. Unexpectedly, none of the tested nanoparticles induced higher cytokine secretions than PLGA nanoparticles. Such a result is not corroborated by several studies

showing that polystyrene (Dailey *et al.*, 2006) and TiO₂ (Inoue *et al.*, 2008) nanoparticles induce a significant inflammatory response *in vivo*. However, it was previously shown that some particles like carbon black, diesel and TiO₂ nanoparticles tested *in vitro* can adsorb various cytokines, such as IL-6, TNF- α and IL-8, thereby limiting their detection (Val *et al.*, 2009, Kocbach *et al.*, 2008). We observed that the IL-8 secretion following LPS exposure was surprisingly reduced in presence of anatase TiO₂ nanoparticles (Figures 9, S1, S2), which may support this hypothesis.



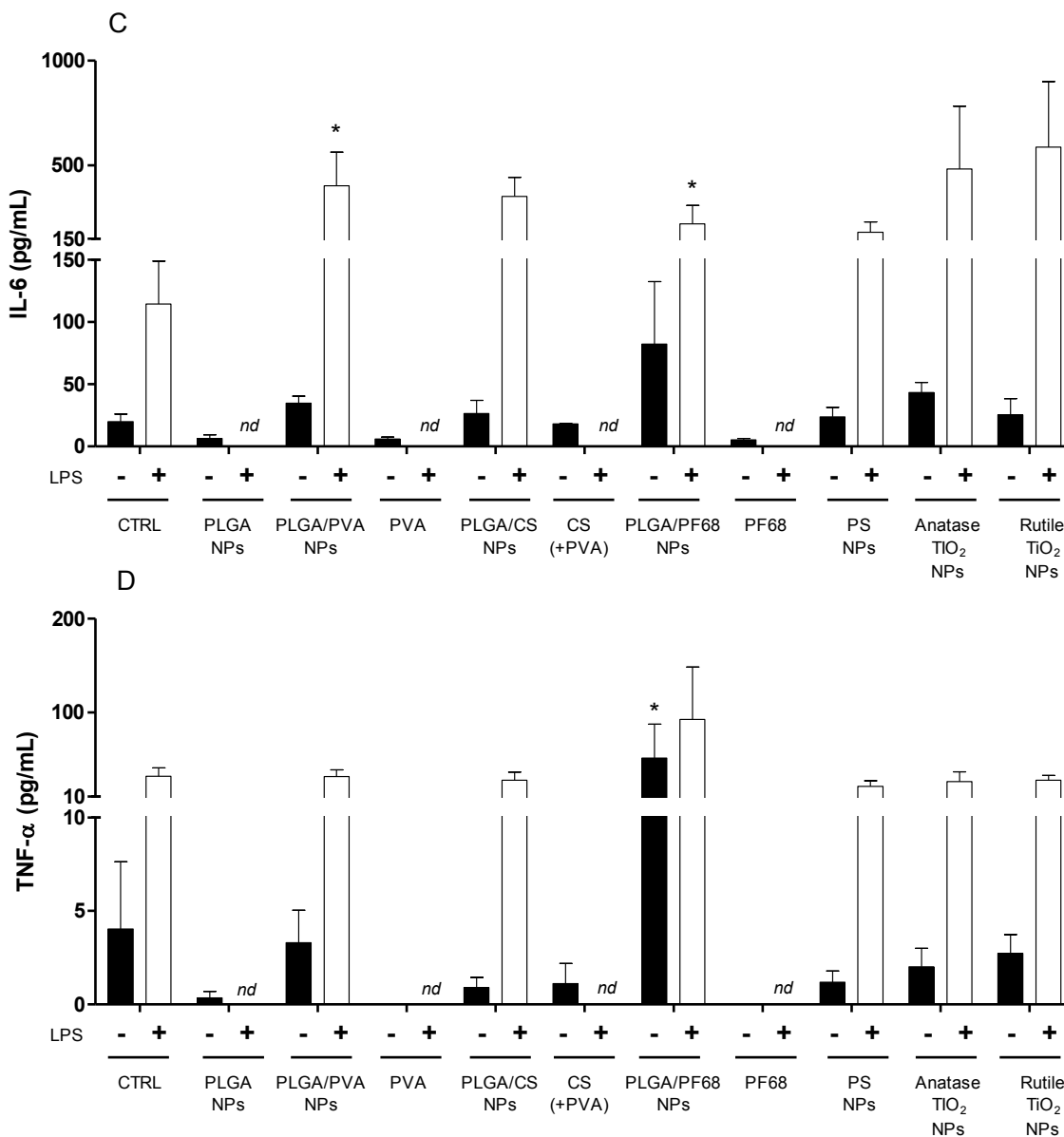


Figure 9. Secretions in co-culture (A549 cells and THP-1-D) of MCP-1 (A), IL-8 (B), IL-6 (C) and TNF- α (D) after 24 h exposure to nanoparticles (NPs) 0.1 mg/mL, or to the corresponding stabilizers used separately in nanoparticle-equivalent concentration, in absence (-) or in presence (+) of 0.1 μ g/mL LPS. CTRL = control, NPs = nanoparticles, $n \geq 3$. * $p < 0.05$, ** $p < 0.01$, *** $p < 0.001$, compared to corresponding untreated conditions. § $p < 0.005$, §§ $p < 0.01$, §§§ $p < 0.001$ for each stabilizer compared to corresponding stabilized nanoparticles.

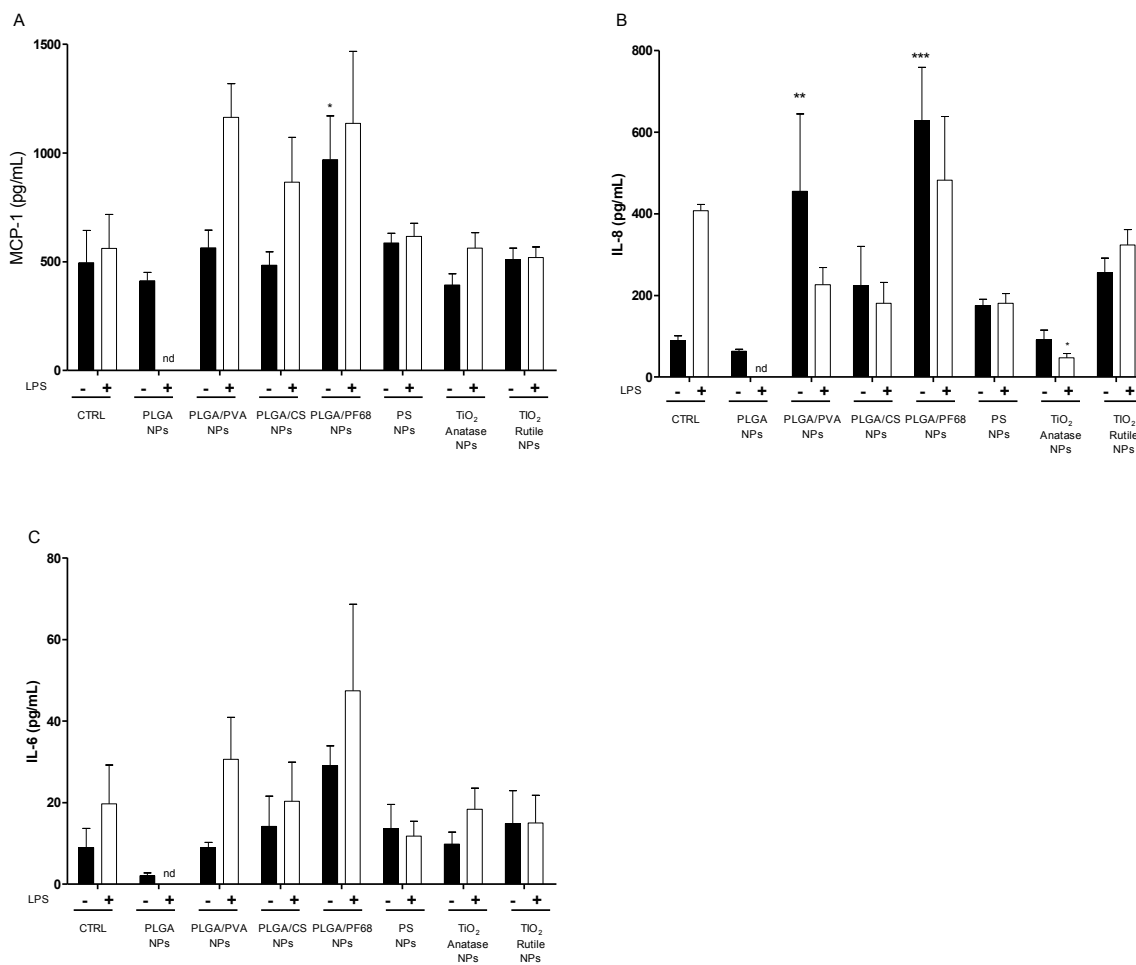


Figure S1. Secretions in mono-culture of A549 cells, of MCP-1 (A), IL-8 (B) and IL-6 (C) after 24 h exposure to nanoparticles (NPs) 0.1 mg/mL or to stabilizers in nanoparticle-equivalent concentration, in absence (-) or in presence (+) of LPS 0.1 μ g/mL, quantified by CBA methods. CTRL = control, NPs = nanoparticles, $n \geq 3$. * $p < 0.05$, ** $p < 0.01$, *** $p < 0.001$, compared to corresponding untreated conditions.

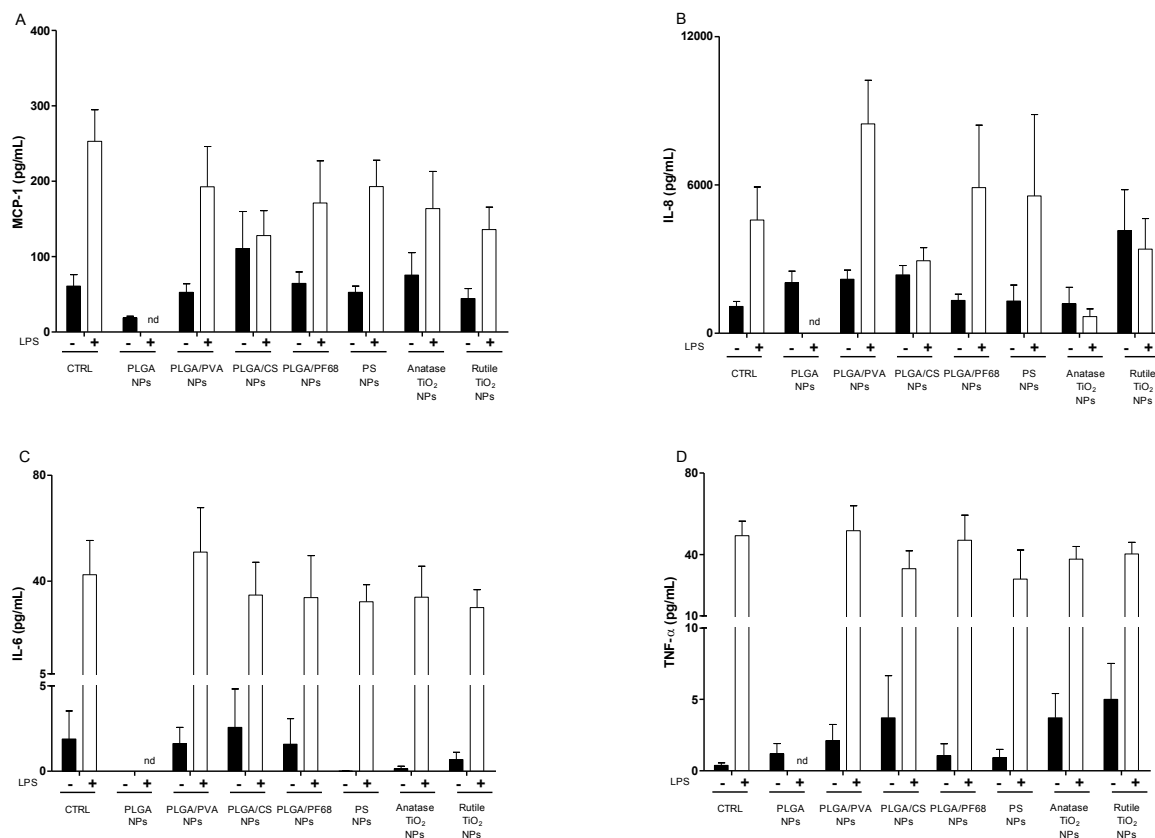


Figure S2. Secretions in mono-culture of THP-1-D cells, of MCP-1 (A), IL-8 (B) and IL-6 (C) after 24 h exposure to nanoparticles 0.1 mg/mL or to stabilizers in nanoparticle-equivalent concentration, in absence (-) or in presence (+) of LPS 0.1 μg/mL, quantified by CBA methods. CTRL = control, NPs = nanoparticles, $n \geq 3$. * $p < 0.05$, ** $p < 0.01$, *** $p < 0.001$, compared to corresponding untreated conditions.

Conclusion

We have shown that a co-culture of A549 epithelial cells and THP-1 macrophages represent an interesting model for *in vitro* pulmonary nanotoxicology studies, in particular for the investigation of selective uptake of nanoparticles, the induction of apoptosis and/or necrosis in each subpopulation, and possible synergistic effect for the secretion of cytokines, even at low levels. This co-culture model has enable the detection of mild inflammatory response to PLGA nanoparticles stabilized by the hydrophilic polymers PVA, CS and PF68, slightly higher than the stabilizer-free PLGA nanoparticles and than stabilizer components individually, but very limited compared to well-known inflammatory compounds.

Acknowledgments

The authors thank Simona Mura (Institut Galien Paris Sud) for her nanoparticle expertise, Nadia Abed (Institut Galien Paris Sud) for microbiology experiments, and Claire Merlet (Institut Galien Paris Sud) for her help. H el ene Chacun and St ephanie Denis (Institut Galien Paris-Sud) for their guidance and assistance in cell culture and cytotoxicity experiments. This study was supported by the ANSES ‘‘Emerging risks’’ program and by the ANR (under reference 2009 CESA 011).

Bibliography

ALFARO-MORENO, E., NAWROT, T. S., VANAUDENAERDE, B. M., HOYLAERTS, M. F., VANOIRBEEK, J. A., NEMERY, B. & HOET, P. H. M. 2008. Co-cultures of multiple cell types mimic pulmonary cell communication in response to urban PM10. *European Respiratory Journal*, 32, 1184-1194.

CRAPO, J. D., BARRY, B. E., GEHR, P., BACHOFEN, M. & WEIBEL, E. R. 1982. Cell number and cell characteristics of the normal human lung. *The American review of respiratory disease*, 126, 332-337.

DAILEY, L. A., JEKEL, N., FINK, L., GESSLER, T., SCHMEHL, T., WITTMAR, M., KISSEL, T. & SEEGER, W. 2006. Investigation of the proinflammatory potential of biodegradable nanoparticle drug delivery systems in the lung. *Toxicology and Applied Pharmacology*, 215, 100-108.

DANHIER, F., ANSORENA, E., SILVA, J. M., COCO, R., LE BRETON, A. & PR  AT, V. 2012. PLGA-based nanoparticles: An overview of biomedical applications. *Journal of Controlled Release*, 161, 505-522.

HJORT, M. R., BRENYO, A. J., FINKELSTEIN, J. N., FRAMPTON, M. W., LOMONACO, M. B., STEWART, J. C., JOHNSTON, C. J. & D'ANGIO, C. T. 2003. Alveolar epithelial cell-macrophage interactions affect oxygen-stimulated interleukin-8 release. *Inflammation*, 27, 137-45.

HORIE, M., KATO, H., FUJITA, K., ENDOH, S. & IWAHASHI, H. 2012. In Vitro Evaluation of Cellular Response Induced by Manufactured Nanoparticles. *Chemical Research in Toxicology*, 25, 605-619.

INOUE, K., TAKANO, H., OHNUKI, M., YANAGISAWA, R., SAKURAI, M., SHIMADA, A., MIZUSHIMA, K. & YOSHIKAWA, T. 2008. Size effects of nanomaterials on lung inflammation and coagulatory disturbance. *International journal of immunopathology and pharmacology*, 21, 197-206.

- JANTZEN, K., ROURSGAARD, M., DESLER, C., LOFT, S., RASMUSSEN, L. J. & MØLLER, P. 2012. Oxidative damage to DNA by diesel exhaust particle exposure in co-cultures of human lung epithelial cells and macrophages. *Mutagenesis*, 27, 693-701.
- KELLEY, J. 1990. Cytokines of the Lung. *American Review of Respiratory Disease*, 141, 765-788.
- KOCBACH, A., TOTLANDSDAL, A. I., LÅG, M., REFSNES, M. & SCHWARZE, P. E. 2008. Differential binding of cytokines to environmentally relevant particles: A possible source for misinterpretation of in vitro results? *Toxicology Letters*, 176, 131-137.
- KRAKAUER, T. 2002. Stimulant-dependent modulation of cytokines and chemokines by airway epithelial cells: cross talk between pulmonary epithelial and peripheral blood mononuclear cells. *Clin Diagn Lab Immunol*, 9, 126-31.
- MANSOUR, H. M., RHEE, Y. S. & WU, X. 2009. Nanomedicine in pulmonary delivery. *Int J Nanomedicine*, 4, 299-319.
- MORGAN, E., VARRO, R., SEPULVEDA, H., EMBER, J. A., APGAR, J., WILSON, J., LOWE, L., CHEN, R., SHIVRAJ, L., AGADIR, A., CAMPOS, R., ERNST, D. & GAUR, A. 2004. Cytometric bead array: a multiplexed assay platform with applications in various areas of biology. *Clin Immunol*, 110, 252-66.
- MÜLLER, L., RIEDIKER, M., WICK, P., MOHR, M., GEHR, P. & ROTHENRUTISHAUSER, B. 2010. Oxidative stress and inflammation response after nanoparticle exposure: differences between human lung cell monocultures and an advanced three-dimensional model of the human epithelial airways. *Journal of The Royal Society Interface*, 7, S27-S40.
- NATHAN, C. F. 1987. Secretory products of macrophages. *J Clin Invest*, 79, 319-26.
- OBERDORSTER, G., FERIN, J., GELEIN, R., SODERHOLM, S. C. & FINKELSTEIN, J. 1992. Role of the alveolar macrophage in lung injury: studies with ultrafine particles. *Environ Health Perspect*, 97, 193-9.
- OBERDORSTER, G., OBERDORSTER, E. & OBERDORSTER, J. 2005. Nanotoxicology: an emerging discipline evolving from studies of ultrafine particles. *Environ Health Perspect*, 113, 823-39.
- PATTON, J. S. & BYRON, P. R. 2007. Inhaling medicines: delivering drugs to the body through the lungs. *Nat Rev Drug Discov*, 6, 67-74.
- PATTON, J. S., FISHBURN, C. S. & WEERS, J. G. 2004. The lungs as a portal of entry for systemic drug delivery. *Proc Am Thorac Soc*, 1, 338-44.
- POHL, C., HERMANN, M. I., UBOLDI, C., BOCK, M., FUCHS, S., DEI-ANANG, J., MAYER, E., KEHE, K., KUMMER, W. & KIRKPATRICK, C. J. 2009. Barrier functions and paracellular integrity in human cell culture models of the proximal respiratory unit. *European Journal of Pharmaceutics and Biopharmaceutics*, 72, 339-349.

- REUL, R., TSAPIS, N., HILLAIREAU, H., SANCEY, L., MURA, S., RECHER, M., NICOLAS, J., COLL, J.-L. & FATTAL, E. 2012. Near infrared labeling of PLGA for in vivo imaging of nanoparticles. *Polymer Chemistry*, 3, 694-702.
- ROTHEN-RUTISHAUSER, B., CLIFT, M. J. D., JUD, C., FINK, A. & WICK, P. 2012. Human epithelial cells in vitro – Are they an advantageous tool to help understand the nanomaterial-biological barrier interaction? . *Euro Nanotox Letters*, 4, 1-20.
- ROTHEN-RUTISHAUSER, B. M., KIAMA, S. G. & GEHR, P. 2005. A Three-Dimensional Cellular Model of the Human Respiratory Tract to Study the Interaction with Particles. *American Journal of Respiratory Cell and Molecular Biology*, 32, 281-289.
- STRIZ, I., BRABCOVA, E., KOLESAR, L., LIU, X. D., BRABCOVA, I., SEKERKOVA, A., POOLE, J. A., JARESOVA, M., SLAVCEV, A. & RENNARD, S. I. 2011. Epithelial cells modulate genes associated with NF kappa B activation in co-cultured human macrophages. *Immunobiology*, 216, 1110-6.
- STRIZ, I., SLAVCEV, A., KALANIN, J., JARESOVA, M. & RENNARD, S. I. 2001. Cell-cell contacts with epithelial cells modulate the phenotype of human macrophages. *Inflammation*, 25, 241-6.
- STRIZ, I., WANG, Y. M., TESCHLER, H., SORG, C. & COSTABEL, U. 1993. Phenotypic Markers of Alveolar Macrophage Maturation in Pulmonary Sarcoidosis. *Lung*, 171, 293-303.
- SUNG, J. C., PULLIAM, B. L. & EDWARDS, D. A. 2007. Nanoparticles for drug delivery to the lungs. *Trends in Biotechnology*, 25, 563-570.
- TAO, F. & KOBZIK, L. 2002. Lung Macrophage–Epithelial Cell Interactions Amplify Particle-Mediated Cytokine Release. *American Journal of Respiratory Cell and Molecular Biology*, 26, 499-505.
- TARNOK, A., HAMBSCH, J., CHEN, R. & VARRO, R. 2003. Cytometric bead array to measure six cytokines in twenty-five microliters of serum. *Clin Chem*, 49, 1000-2.
- VAL, S., HUSSAIN, S., BOLAND, S., HAMEL, R., BAEZA-SQUIBAN, A. & MARANO, F. 2009. Carbon black and titanium dioxide nanoparticles induce pro-inflammatory responses in bronchial epithelial cells: Need for multiparametric evaluation due to adsorption artifacts. *Inhalation Toxicology*, 21, 115-122.
- WANG, S., YOUNG, R. S., SUN, N. N. & WITTEN, M. L. 2002. In vitro cytokine release from rat type II pneumocytes and alveolar macrophages following exposure to JP-8 jet fuel in co-culture. *Toxicology*, 173, 211-219.
- WOTTRICH, R., DIABATÉ, S. & KRUG, H. F. 2004. Biological effects of ultrafine model particles in human macrophages and epithelial cells in mono- and co-culture. *International Journal of Hygiene and Environmental Health*, 207, 353-361.

Discussion générale



Au cours de ces travaux de thèse, la toxicité pulmonaire de nanoparticules biodégradables et non-biodégradables a été étudiée. Ce projet s'inscrit dans un projet global soutenu par l'ANSES (« Emerging risks »), l'ANR (2009 CESA) et le Fond pour la Recherche Respiratoire regroupant des études *in vitro* et *in vivo* menées au sein du laboratoire. Deux précédents articles ont fait état de la toxicité *in vitro* de nanoparticules biodégradables vis-à-vis des cellules d'épithélium bronchiques (Calu-3) (Mura *et al.*, 2011a,b), et un article relatant les effets *in vivo* est en cours de rédaction (Santiago, submitted). Au cours de la présente étude, la toxicité *in vitro* de ces mêmes nanoparticules a été étudiée sur des cellules alvéolaires. Les objectifs de ce travail de thèse étaient (Figure 1) :

- D'enrichir notre bibliothèque de nanoparticules afin d'aboutir à une collection de particules aux caractéristiques physico-chimiques variées et représentatives des nanoparticules les plus couramment rencontrées en nanomédecine et possédant une taille de l'ordre de 200 nm (organiques / inorganiques, biodégradables / non-biodégradables, charges de surface positives, négatives ou neutres),
- D'établir et de caractériser une co-culture mimant les conditions alvéolaires,
- D'étudier la toxicité de nanoparticules sur les cellules en mono et en co-culture, à l'aide de différents tests,
- De tenter de corréler les profils de toxicité des nanoparticules à leurs caractéristiques physico-chimiques afin de proposer un modèle pertinent de nanovecteurs pour l'administration pulmonaire.

Les études portant sur la toxicité pulmonaire de nanoparticules non-biodégradables sont nombreuses. Et pour cause, l'arbre bronchique est exposé à tout type de particules présentes dans l'atmosphère, incluant les nanoparticules non-biodégradables dans l'environnement, telles que les nanoparticules de diesel ou en milieu professionnel, les nanoparticules manufacturées, telles que les nanotubes de carbone. En revanche, assez peu d'études sont disponibles aujourd'hui sur la toxicité pulmonaire de nanoparticules biodégradables, qui entrent dans la fabrication de nanomédicaments. Pourtant, la voie pulmonaire est prometteuse pour l'administration de nanomédicaments, car elle permet d'envisager à la fois des traitements locaux (asthme, broncho-pneumopathie chronique obstructive ou cancer) et des traitements systémiques grâce aux échanges constants entre les alvéoles et la circulation sanguine (diabète, administration de vaccins). Les nanovecteurs qui assurent le transport de ces principes actifs, doivent évidemment faire preuve d'une totale innocuité vis-à-vis de l'organisme.

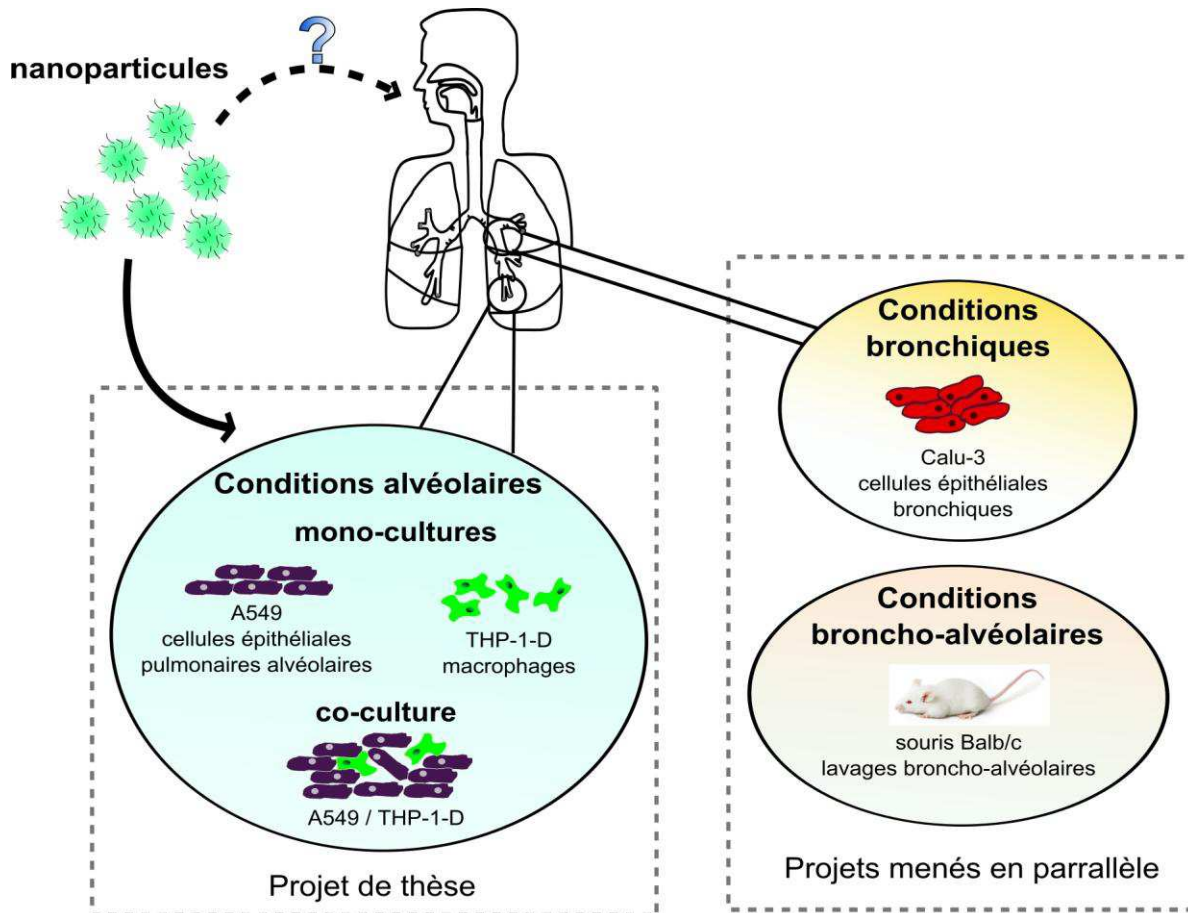


Figure 1. Schéma de l'étude de nanotoxicité menée au sein de l'équipe de recherche. Afin de connaître les effets de nanoparticules vis-à-vis de la voie pulmonaire, la toxicologie *in vitro* de nanoparticules est étudiée sur des cellules épithéliales pulmonaires alvéolaires (A549) et des macrophages (différenciés de monocytes THP-1) en mono et en co-culture (projet de thèse), sur des cellules Calu-3, d'épithélium bronchique, et chez un modèle de souris (Balb/c).

Au sein du projet mené dans l'équipe de recherche (Figure 1), nous étudions la toxicité et le devenir de nanoparticules de poly(lactide(co-glycolide) (PLGA), afin des les proposer en tant que candidats nanomédicaments. Dans le cadre de ce projet de thèse, nous nous sommes particulièrement intéressés à la toxicité de ces nanoparticules vis-à-vis de la région alvéolaire.

1. La bibliothèque de nanoparticules

Des nanoparticules de composition chimique et de charge de surface variées ont été utilisées. Néanmoins, nous avons œuvré dans la formulation pour que la taille des particules reste constante, de l'ordre de 200 nm. Les nanoparticules de PLGA ont été formulées au sein du laboratoire et les nanoparticules de TiO₂ et de polystyrène ont été obtenues commercialement (Figure 2).

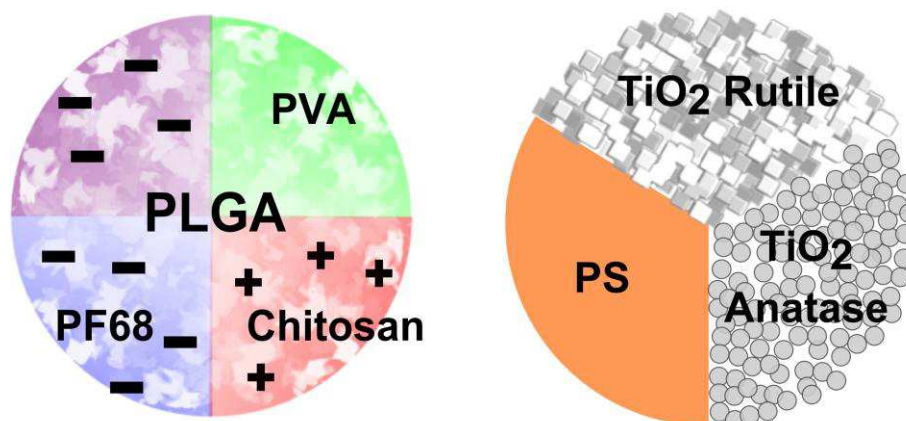


Figure 2. Nanoparticules de PLGA stabilisées ou non stabilisées par l'alcool polyvinylique (PVA), le chitosane ou le pluronic F68 (PF68) et nanoparticules de dioxyde de titane (TiO_2) et de polystyrène (PS) utilisées dans les études de toxicité vis-à-vis de la voie pulmonaire.

Les nanoparticules à base de PLGA ont une taille de l'ordre de 200 nm, et sont formulées par émulsion-évaporation de solvant ou nanopréciipitation. L'introduction au cours de la préparation de polymères hydrophiles en tant qu'agents stabilisants s'adsorbant à la surface des particules, permet de moduler leur charge de surface. L'alcool polyvinylique (PVA) conduit à la formation de nanoparticules neutres, le Pluronic F68 (PF68) permet d'obtenir des nanoparticules négatives, et le chitosane (CS) des nanoparticules positives (Tableau 1). Au cours des précédentes études *in vitro* sur les cellules Calu-3, les nanoparticules stabilisées par le PF68 présentaient une taille de l'ordre de 100 nm, et n'étaient pas purifiées. Suite à une modification du procédé de formulation, nous avons pu obtenir des nanoparticules de l'ordre de 200 nm qui ont ensuite été purifiées. Le diamètre des nanoparticules pouvant influencer sur la toxicité de nanoparticules similaires (Schöler *et al.*, 2002), il était important d'avoir des particules de taille équivalente avant de se focaliser sur la composition de la surface des nanoparticules, qui constitue un paramètre important du point de vue de la nanotoxicité (Schöler *et al.*, 2001). Nous avons, en outre, préparé des nanoparticules de PLGA sans ajouter d'agent stabilisant. Ce type de nanoparticules nous a permis de bien comprendre le rôle des agents stabilisants dans la toxicité des nanoparticules. Enfin, en remplaçant une petite quantité de PLGA par un PLGA lié de façon covalente à une sonde fluorescente, la rhodamine (Mura *et al.*, 2011a) ou le DY700 (Reul *et al.*, 2012), des nanoparticules fluorescentes, dont les caractéristiques physico-chimiques sont identiques aux nanoparticules non-fluorescentes, ont été obtenues. La synthèse d'un polymère lié de façon covalente à une sonde fluorescente permet d'en assurer la stabilité, et d'éviter notamment la libération prématurée de la sonde au

cours du temps. L'intérêt des nanoparticules fluorescentes est de pouvoir étudier leur devenir *in vitro* et *in vivo* en microscopie ou cytométrie en flux (Wu *et al.*, 2008). Des études de stabilité ont montré que les nanoparticules (fluorescentes et non fluorescentes) sont stables plusieurs semaines en milieux aqueux, et au moins jusqu'à 48 h dans les milieux de culture (milieu + sérum non décomplémenté + antibiotiques).

Tableau 1. Bilan des caractéristiques physico-chimiques des nanoparticules formulées à base de PLGA, fluorescentes et non-fluorescentes.

Nanoparticules	Diamètres moyens		Indice de polydispersité	Potentiel zêta	Ratio d'intensité de fluorescence (1 pour NP PLGA/CS)
	Eau	48 h milieu de culture 37 °C			
PLGA					na
DY700-PLGA	~ 170 nm	nd	~ 0,05	~ - 40 mV	0.91
Rhod-PLGA	Impossible à formuler				
PLGA/PVA					na
DY700-PLGA/PVA	~ 230 nm	~ 200 nm	~ 0,05	~ 0 mV	0.78
Rhod-PLGA/PVA					0.77
PLGA/CS					na
DY700-PLGA/CS	~ 200 nm	~ 230 nm	~ 0,15	~ + 40 mV	1
Rhod-PLGA/CS					1
PLGA/PF68					na
DY700-PLGA/PF68	~ 200 nm	~ 250 nm	~ 0,15	~ - 30 mV	0.68
Rhod-PLGA/PF68					0.37

NP: nanoparticules, nd: non déterminé, na: non applicable.

Les nanoparticules de TiO₂ de formes cristallines anatase (sphérique) et rutile (bâtonnet) sont obtenues commercialement sous forme de poudres. Lors de la mise en suspension, les mesures de taille et les analyses microscopiques (données non fournies) montrent la présence de gros agrégats, de tailles disparates. Une étape de sonication suivie d'une agitation par Ultra-Turrax a permis d'homogénéiser et de réduire la taille des agrégats, et ce, de manière reproductible. L'ajustement du pH à 11 en début de procédé permet d'éviter une ré-agglomération qui est *quasi*-immédiate à pH alcalin (He *et al.*, 2007). Nous n'avons pas pu atteindre un diamètre de l'ordre de 200 nm comme nous l'aurions souhaité, mais aucun adjuvant n'a été ajouté dans la formulation. La nature des nanoparticules n'est donc pas modifiée. Cependant, une réaggrégation est observée lors de la dilution dans le milieu de culture cellulaire.

Les nanoparticules de polystyrène sont elles aussi obtenues commercialement. Leurs caractéristiques physico-chimiques sont conformes aux spécifications commerciales, elles ont une taille de 250 nm et sont stables dans le milieu de culture. La présence d'ester de sulfate à leur surface leur confère une charge de surface négative.

2. La co-culture : Un outil *in vitro* pertinent en nanotoxicologie

Les études réalisées *in vitro* constituent une étape indispensable aux études de nanotoxicité. En effet, de nombreux tests permettent de cribler la toxicité de potentiels nanomédicaments, avant de mener des études *in vivo* coûteuses et dont l'éthique peut être remise en question. Néanmoins, l'utilisation de lignées cellulaires classiques ne tient pas compte des interactions qui existent au sein de l'organisme. Afin de prendre en considération certaines des interactions cellulaires, nous avons voulu au cours de cette thèse développer un modèle de co-culture de cellules épithéliales pulmonaires alvéolaires et de macrophages. Le choix des cellules pour l'établissement de la co-culture a été réalisé selon une démarche scientifique bien précise. En effet, les cellules épithéliales constituent un des éléments de défense de l'organisme des plus importants face à tout type de particules présentes dans l'air. De plus, comme nous l'avons précédemment détaillé (Travaux antérieurs), elles se situent en première ligne au cours de l'inhalation. Quant à l'emploi des macrophages, il permet d'étudier la réponse immunitaire mise en place lors de l'exposition aux nanoparticules. En outre, les macrophages sont des cellules particulièrement intéressantes car ils sécrètent une grande variété de substances biologiques impliquées dans les désordres pulmonaires (radicaux de l'oxygène, facteur de croissance, cytokines). Dans la littérature, l'intérêt de la co-culture de cellules A549 (lignée isolée d'épithélium alvéolaire pulmonaire humain) (Lieber *et al.*, 1976) et de macrophages dérivés de monocytes THP-1, notés THP-1-D par la suite, (lignée isolée de sang leucémique humain) a été démontré pour étudier la réponse inflammatoire induite par des nanoparticules manufacturées (Müller *et al.*, 2010), atmosphériques (Alfaro-Moreno *et al.*, 2008) ou ultrafines (Wottrich *et al.*, 2004). De la même manière, au cours de la thèse, la co-culture a été utilisée afin d'évaluer la réponse inflammatoire causée par les nanoparticules que nous avons décrites précédemment. Nous avons également suivi le devenir intracellulaire des nanoparticules ainsi que leur toxicité spécifique grâce à un marquage distinctif de chacune des sous populations cellulaires. Pour valider les résultats obtenus, et les comprendre davantage, les études ont été menées en parallèle sur les mêmes cellules en mono-culture.

Les cultures de cellules A549 utilisées sous des conditions contrôlées, présentent les caractéristiques des cellules épithéliales de type II (Rothen-Rutishauser *et al.*, 2012) et sont aptes à répondre à un stimuli extérieur, en produisant par exemple des cytokines (IL-8, MCP-1) (Cromwell *et al.*, 1992). De par leur stade avancé de maturation, les macrophages humains ne se divisent plus, et n'existent donc pas sous forme de lignée cellulaire. Ils peuvent être obtenus par lavages broncho-alvéolaires de donneurs mais la méthode est compliquée à mettre

en œuvre pour un rendement trop faible. L'alternative consiste à différencier des monocytes primaires ou en lignée, ce qui permet d'obtenir des macrophages en quantité suffisante. L'utilisation des lignées cellulaires présente l'intérêt de réaliser des expériences avec des cellules ayant des caractéristiques phénotypiques stables et reproductibles. En effet, il a été démontré que le phénotype des monocytes humains THP-1 était maintenu plusieurs mois en culture (Tsuchiya *et al.*, 1980), et évoluait lorsqu'ils étaient différenciés en macrophages (expression de CD11b et CD54) (Tsuchiya *et al.*, 1982, Schwende *et al.*, 1996). Parmi les composés disponibles pour différencier les monocytes en macrophages (Park *et al.*, 2007), nous avons choisi le Phorbol-12-myristate-13-acetate (PMA) qui conduit à l'adhésion rapide, à l'arrêt de prolifération des cellules, ainsi qu'à l'expression des récepteurs membranaires CD11b et CD54 (Chapitre 2 – Figure S1). Le CD14, récepteur membranaire exprimé par les cellules immunitaires, est maintenu lors de la différenciation. Le temps d'exposition du PMA est un facteur important dans la différenciation. Bien qu'il soit décrit comme optimal entre 48 et 72 h (Tsuchiya *et al.*, 1982), nos résultats ont pourtant montré qu'après 24 h d'exposition, l'expression des récepteurs membranaires CD11b et CD54 était maximale (Chapitre 2 – Figure S1), et que les macrophages présentaient une bonne capacité de phagocytose (Chapitre 2 – Figure S2). Les macrophages ainsi différenciés présentent un phénotype caractéristique des macrophages humains, ils sont donc utilisés dans de nombreuses études (Auwerx, 1991). Notamment, les macrophages alvéolaires matures humains, issus de lavages broncho-alvéolaires, expriment CD14 et CD11b (Striz *et al.*, 1993). L'utilisation des macrophages THP-1 pour l'établissement de la co-culture est ainsi appropriée. D'autre part, comme toutes les cellules immunitaires, les macrophages THP-1 expriment le récepteur membranaire CD14 (Chapitre 2 – Figure S1), qui sera utilisé dans la suite des études pour distinguer chaque sous population cellulaire au sein de la co-culture.

La co-culture peut être établie en contact direct ou indirect, par l'utilisation d'un insert Transwell® (Figure 3), dont la membrane en polycarbonate présente des pores de 0,4 µm. L'intérêt du modèle en contact indirect est de pouvoir étudier les communications intercellulaires, établies suite à la sécrétion de facteurs solubles, tels que les cytokines, qui peuvent traverser les pores de la membrane. Le modèle en contact direct est quant à lui très proche des conditions physiologiques, mais la distinction entre les différents types cellulaires peut s'avérer compliquée. Au cours de notre travail nous avons tenté de surmonter cette complexité.

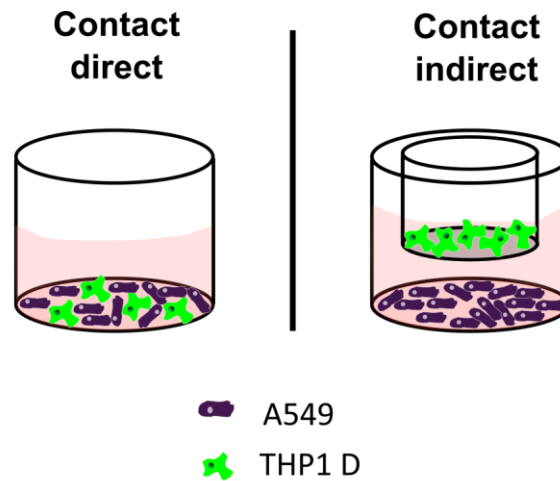


Figure 3. Etablissement de la co-culture de cellules A549 (épithéliales pulmonaires humaines en violet) et de macrophages différenciés de monocytes (THP-1-D en vert) en contact direct ou indirect. L'établissement en contact indirect requiert l'utilisation d'un insert Transwell® (membrane en polycarbonate avec des pores de 0,4 μm)

Lors de l'établissement de la co-culture, certaines études utilisent les THP-1 sous forme monocyttaire (Hjort *et al.*, 2003), et montrent qu'une différenciation complète en macrophages se produit, ce que nous n'avons pas observé (données non présentées). Nous avons donc décidé de pré-différencier les macrophages avant la mise en contact direct. Nous avons établi les deux types de co-culture et avons étudié l'expression des récepteurs membranaires CD11b, CD14 et CD54, après 24 h de contact. Comme détaillé plus haut, les THP-1-D en monoculture expriment ces trois marqueurs membranaires qui ne sont pas présents sur les cellules A549. L'analyse des récepteurs CD11b et du CD14, nous permet de conclure que nous sommes bien en présence de deux populations cellulaires dans le modèle de co-culture, selon un ratio 9 : 1 A549 : THP-1-D, ce qui a été confirmé par l'analyse en microscopie confocale (Chapitre 3 – Figures 2 et 3). En effet, nous retrouvons une population majoritaire négative (90 % – cellules A549) ainsi qu'une population minoritaire négative (10 % – cellules THP-1-D). Un tel ratio est cohérent avec la proportion chez l'homme des cellules alvéolaire épithéliales et des cellules macrophagiques pulmonaires (Crapo *et al.*, 1982). En revanche, lors de l'analyse du CD54, nous observons une unique population cellulaire, positive. Il a été précédemment montré qu'en culture avec du milieu conditionné de monocytes primaires humains, les cellules A549 expriment le CD54, ICAM-1, récepteur de l'adhésion (Krakauer, 2002). Nos données confirment cette observation. De plus, nous observons que le contact direct est nécessaire à cette modification phénotypique, car la quasi totalité des cellules A549

est positive au CD54, tandis que dans le cas du contact indirect, seul 7 % des cellules A549 sont positives (données non présentées).

Les cellules en mono et co-culture ont par la suite été exposées pendant 24 h au LPS (Lipopolysaccharide), composé pro-inflammatoire connu. L'intérêt étant de pouvoir étudier la présence, ou non, d'effets synergiques, en ce qui concerne les sécrétions des cytokines, dosées dans les surnageants de culture, par la méthode CBA (Cytometric Beads Arrays). On parle d'effets synergiques lorsque les niveaux de sécrétions des cytokines en co-culture sont plus élevés que les niveaux théoriques correspondants à la somme de ceux obtenus en monoculture pour chacune des sous populations cellulaires. Parmi les cytokines testées, seules l'IL-6, l'IL-8, MCP-1 et TNF- α ont été sécrétées à des niveaux détectables par les cellules (en mono et co-culture), et la présence d'effets synergiques a été montrée pour l'IL-6, l'IL-8 et le MCP-1 (Figure 4). En effet, en co-culture en contact direct, les niveaux de sécrétion sont de 1,5 (IL-6 et IL-8) à 5 (MCP-1) fois plus élevés que les niveaux théoriques, issus de la somme des sécrétions obtenues pour chaque type cellulaire en monoculture. Les cytokines MPC-1 et IL-8, sont des chimiokines chimiotactiques pro-inflammatoires impliquées dans l'attraction des neutrophiles et la régulation du trafic cellulaire (Deshmane *et al.*, 2009, Polito and Proud, 1998), tandis que l'IL-6, facteur de croissance, et le TNF- α sont impliqués dans la régulation de la réponse immune (Kishimoto, 1989, Akira *et al.*, 1990). De tels effets synergiques confirment la communication intercellulaire. Comme précédemment montré par Krakauer (2002), nos résultats confirment qu'en co-culture, les macrophages constituent la principale source d'IL-6, l'IL-8 et de TNF- α . De plus, nos résultats montrent que les cellules A549 sont, dans la co-culture, la principale source de MCP-1. Dans le cas du contact indirect, les dosages des cytokines ont été réalisés dans les surnageants recueillis dans le compartiment supérieur, contenant les macrophages. Les fortes concentrations en MCP-1 permettent de conclure que la cytokine est capable de passer d'un compartiment à l'autre, et que ce modèle est pertinent dans une approche mécanistique (Figure 4).

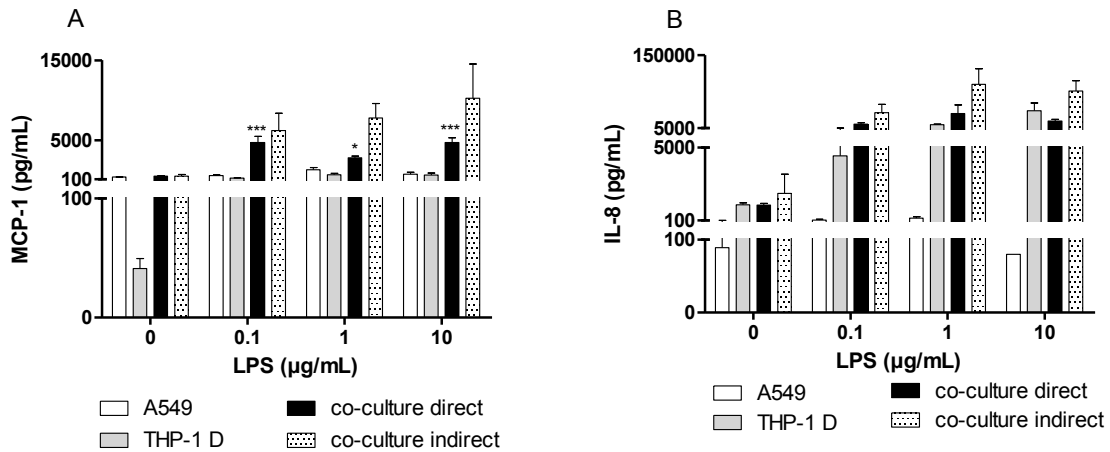


Figure 4. Sécrétions des cytokines MCP-1 (A) et IL-8 (B) par les cellules A549 et THP-1-D en mono et en co-culture (contact direct et indirect), après 24 h d'exposition à des concentrations croissantes (0.1 à 10 µg/mL) de LPS (lypopolysaccharide).

Au cours des études de nanotoxicité qui suivront, seul le modèle en contact direct a été exposé aux nanoparticules. Pour des études futures, l'utilisation de la co-culture en contact indirect permettrait de mieux comprendre les mécanismes de communication cellulaires.

3. Devenir *in vitro* et toxicité des nanoparticules

La toxicité des nanoparticules de PLGA, de TiO₂ et de polystyrène, ainsi que la toxicité des polymères de surface utilisés pour la stabilisation des nanoparticules (en concentrations équivalentes à celles en interactions avec les nanoparticules (Mura *et al.*, 2011b, Grabowski *et al.*, 2013)), ont été évaluées sur les cellules A549 et THP-1-D en mono et en co-culture. Afin d'étudier la pénétration intracellulaire des nanoparticules, les cinétiques d'internalisation ont été réalisées. Par la suite, nous avons choisi d'évaluer différents paramètres de toxicité : l'activité mitochondriale, l'état de la membrane cellulaire (dosage de la LDH libérée, marquage au Bleu Trypan et par l'iodure de propidium/Syto24[®]), la réponse inflammatoire (quantification des cytokines dans les surnageants de culture), et le stress oxydant (quantification des espèces réactives de l'oxygène (ROS)). Les résultats obtenus sont synthétisés dans les tableaux 2, 3 et 4.

3.1. Internalisation des nanoparticules par les cellules en mono et co-culture

Les cinétiques d'internalisation ont été menées après exposition aux nanoparticules de PLGA sur les cellules en mono et co-culture, à la concentration de 0,1 mg/mL. Les nanoparticules de charge de surface négative (PLGA/PF68 et PLGA sans stabilisant) sont internalisées plus rapidement et en plus grande quantité par les cellules en mono et co-culture – jusqu'à 2 fois plus (A549) – que les nanoparticules de charge de surface neutre (PLGA/PVA) et positive (PLGA/CS) (Chapitre 1 – Figure 4, Chapitre 2 – Figure 1, Chapitre 3 – Figure 5). Les observations réalisées en microscopie confocale nous ont permis de confirmer que les nanoparticules sont bien localisées à l'intérieur des cellules A549, mais des différences existent : les nanoparticules de PLGA/PVA sont distribuées dans toute la cellule, tandis que les nanoparticules de PLGA/CS et PLGA/PF68 forment des agrégats qui semblent localisés dans des compartiments subcellulaires que nous pourrions identifier grâce à des marquages spécifiques de chaque organelle (Chapitre 1 – Figure 3). De plus, comme il l'a été précédemment démontré (Cartiera *et al.*, 2009), les cellules A549 internalisent les nanoparticules selon un mécanisme énergie-dépendants, de type endocytose (Chapitre 1 – Figure 2). En revanche, nous n'avons pas pu confirmer que le mécanisme est énergie-dépendant pour les macrophages, car les cellules THP-1-D meurent très rapidement à 4 °C, sous atmosphère non contrôlée. Pour répondre à cette question il faudrait utiliser des inhibiteurs ou des marqueurs des différentes voies d'internalisation. Néanmoins, nous pouvons supposer, que les nanoparticules sont internalisées par phagocytose, principale voie utilisée par les macrophages pour capter des particules d'environ 200 nm (Sahay *et al.*, 2010, Hillaireau and Couvreur, 2009). De plus, en co-culture, les macrophages, internalisent davantage de nanoparticules que les cellules A549 (Chapitre 3 – Figure 5). On remarque notamment que les nanoparticules de PLGA/PVA sont principalement internalisées par les macrophages, tandis que leur internalisation avec les cellules A549 ne varie plus après 15 minutes d'exposition. Le rôle protecteur des macrophages, cellules immunitaires de l'organisme, précédemment avancé (Wang *et al.*, 2002), a ici pu être confirmé. De plus, un tel résultat confirme le rôle clef des macrophages dans l'élimination de nanoparticules. Lors des observations en microscopie confocale, nous avons observé que les nanoparticules de PLGA/PF68 sont bien à l'intérieur des deux types cellulaires après 1 h d'exposition (Chapitre 3 – Figure 7).

En conclusion, les études d'internalisation nous permettent de dire que, quelque soit leur charge de surface, les nanoparticules de PLGA de 200 nm, sont captées en quantité

significative par les cellules épithéliales selon un mécanisme énergie-dépendant. Néanmoins, les nanoparticules chargées négativement, sont internalisées en plus grande quantité et plus rapidement que les autres. Enfin, les macrophages internalisent des quantités plus importantes de nanoparticules que les cellules épithéliales.

L'internalisation des nanoparticules de TiO₂ et de polystyrène n'a pas pu être réalisée quantitativement, car nous ne disposons pas de nanoparticules fluorescentes équivalentes. Cependant, en ce qui concerne les nanoparticules de TiO₂, les analyses en cytométrie en flux, permettent de mettre en évidence une granularité augmentée des cellules, ce qui a été montré comme caractéristique d'une internalisation des nanoparticules par les cellules (Suzuki *et al.*, 2007). L'utilisation d'un cytomètre en flux couplé à la microscopie (Imagestream) nous permettrait d'approfondir ces résultats.

3.2. Toxicologie pulmonaire des nanoparticules

Afin de mieux appréhender les éléments responsables de la cytotoxicité, nous avons testé chacun des éléments qui les constituent séparément (Figure 5). De nombreuses études utilisant les nanoparticules de PLGA stabilisées par des polymères de surface, la valeur ajoutée de ce projet est d'étudier la toxicité de la matrice de PLGA de taille nanométrique, ainsi que les effets de la couche stabilisante de polymère en solution aqueuse.

La cytotoxicité des nanoparticules de PLGA stabilisées, *i.e* PLGA/PVA, PLGA/CS et PLGA/PF68, est le premier paramètre étudié, car il nous permet de définir notre concentration de travail. Suite aux résultats obtenus par les tests MTT, nous avons établi cette concentration à 0.1 mg/mL, pour laquelle l'activité mitochondriale de chaque type cellulaire en mono-culture est d'au moins 60 à 80 % (après 48 h d'exposition). Les nanoparticules de PLGA/PVA sont généralement moins cytotoxiques que les nanoparticules de PLGA/CS et PLGA/PF68. L'étude de la mort cellulaire après une exposition de 0.1 mg/mL de nanoparticules sur les cellules en co-culture, montrent que les nanoparticules de PLGA/PF68 induisent une toxicité beaucoup plus élevée que les autres nanoparticules stabilisées, mais également une toxicité plus forte qu'en mono-culture (Tableau 4). La cytotoxicité des nanoparticules PLGA/PF68 peut être corrélée à la forte internalisation de ces nanoparticules. D'autre part, on remarque que quelque soit le type de cellule étudié, en mono ou en co-culture, les nanoparticules de PLGA stabilisées déclenchent la mort uniquement par nécrose, et n'induisent pas de dommage à la membrane. En ce qui concerne la quantification de la réponse inflammatoire,

seules les nanoparticules de PLGA/PF68 provoquent la libération de cytokines dans le milieu extracellulaire des cellules A549 en mono-culture (Tableau 2). La plus grande internalisation de ces nanoparticules permet à nouveau d'expliquer ces résultats. En revanche, aucun effet inflammatoire significatif n'a été relevé ni après exposition sur les THP-1-D en monoculture, ni sur les cellules en co-culture. De tels résultats laissent penser que la présence des macrophages dans la co-culture régule la sécrétions de cytokines – notamment IL-6, IL-8 et MCP-1 – produites par les cellules A549 lors de l'exposition aux nanoparticules.

Dans le cas des nanoparticules de PLGA sans stabilisant, on remarque qu'à forte concentration, elles n'ont aucun effet cytotoxique sur les THP-1-D en mono-culture (Tableau 3), tandis que leur effet sur les cellules A549 et sur la co-culture (Tableaux 2 et 4), est comparable à celui observé après exposition aux nanoparticules de PLGA stabilisées. De plus, comme les nanoparticules de PLGA stabilisées, elles induisent la mort uniquement par nécrose. En ce qui concerne les niveaux de sécrétions des cytokines après exposition aux nanoparticules de PLGA sans stabilisant, ils sont semblables aux niveaux observés dans les conditions non traitées. La quantification des ROS intracellulaires au sein des cellules A549 et THP-1-D, montrent qu'elles induisent un stress oxydant similaire à celui induit par les nanoparticules de PLGA stabilisées.

Enfin, la toxicité des polymères de surface en solution aqueuse a été étudiée, à des concentrations équivalentes en nanoparticules. Seules les solutions contenant du chitosane induisent une cytotoxicité, vis-à-vis des deux types cellulaires en mono-culture, comme cela a été montré dans la littérature (Huang *et al.*, 2004). Ces résultats permettent d'expliquer la cytotoxicité des nanoparticules PLGA/CS précédemment observée. Polymère naturel, le chitosane, est considéré, parfois à tort (Kean and Thanou, 2010), comme un excipient sûr (Baldrick, 2010). La toxicité qui peut être observée augmente avec le poids moléculaire (Carreño-Gómez and Duncan, 1997), et la dégradation dépend du degré de déacétylation (Verheul *et al.*, 2009). Il est tout de même à l'étude pour la formulation de nombreux médicaments tels que les comprimés, les microcapsules ou les liposomes. D'autre part, l'administration pulmonaire de nanoparticules de PLGA stabilisées par le chitosan a montré que les nanoparticules, ont de fortes propriétés muco-adhésives, et ouvrent les jonctions serrées intracellulaires, et sont ainsi retenues plus longtemps dans les poumons des rats (Yamamoto *et al.*, 2005).

La combinaison de ces résultats nous permet de conclure que la matrice de PLGA, les solutions de PVA et de PF68 n'induisent que peu, voire pas de toxicité pulmonaire, et n'expliquent donc pas directement les toxicités des nanoparticules PLGA/PVA et PLGA/PF68. On peut conclure que les stabilisants PVA et PF68 présentent une toxicité uniquement lorsqu'ils ont été captés par les cellules. De plus, la toxicité des nanoparticules PLGA/PF68 peut être attribuée à la plus grande quantité de nanoparticules internalisées par les cellules. En revanche le chitosane se montrant plus toxique, il permet d'expliquer la toxicité des nanoparticules PLGA/CS.

Nous avons choisi les nanoparticules de polystyrène (Dailey *et al.*, 2006) et de TiO₂ (Inoue *et al.*, 2008) comme contrôles positifs, car il a été notamment montré que lors de l'administration *in vivo* qu'elles sont inductrices de réponse inflammatoire, voire sont capables de l'augmenter. Ces résultats ont été confirmés lors des tests *in vivo* réalisés au sein de notre équipe (Santiago, *submitted*). Pourtant, bien que nous ayons observé une cytotoxicité plus importante (tests MTT, bleu de trypan et libération de la LDH) de la part des nanoparticules de TiO₂, aucune réponse inflammatoire n'a été détectée (Tableaux 2 et 3). Qui plus est, en co-stimulation avec le LPS, après exposition aux nanoparticules de TiO₂ de forme cristalline anatase, la quantité d'Il-8 dans le milieu extracellulaire est plus faible qu'après exposition au LPS seul. Il a été montré que les nanoparticules de diesel, de TiO₂ ou les nanotubes de carbone peuvent adsorber à leur surface certaines cytokines (Val *et al.*, 2009, Kocbach *et al.*, 2008). Les nanoparticules de TiO₂ de forme cristalline anatase semblent confirmer cette hypothèse, et nous pouvons donc conclure, que la méthode utilisée (dosage des cytokines dans le milieu extracellulaire) n'est pas forcément adaptée à ce type de nanoparticules. En revanche, les nanoparticules de PLGA n'adsorbent pas les cytokines à leur surface, puisque en co-stimulation avec le LPS, les niveaux des cytokines sont identiques à ceux de la stimulation du LPS seul. La méthode employée est donc valable. De plus, nous pouvons conclure que les nanoparticules de PLGA n'augmentent pas la réponse inflammatoire de cellules pré-activées, ni ne permettent d'augmenter les effets du LPS.

Tableau 3. Evaluation de la toxicité des nanoparticules de PLGA, de TiO₂ et de polystyrène par différents paramètres après exposition sur les cellules **A549 en mono-culture**.

A549		Toxicité													
Concentration en NP (mg/mL)	Internalisation	MTT		Bleu Trypan		Annexine V / 7-AAD		LDH release		IP / Syto®24		Réponse Inflammatoire (IL6, IL-6, MCP-1, TNF-α)		Stress Oxydant (ROS)	
		≤ 0.1	> 0.1	≤ 0.1	> 0.1	≤ 0.1	> 0.1	≤ 0.1	> 0.1	≤ 0.1	> 0.1	≤ 0.1	> 0.1	≤ 0.1	> 0.1
PLGA	<i>nd</i>	-	+	<i>nd</i>	<i>nd</i>	-	-	<i>nd</i>	<i>nd</i>	<i>nd</i>	<i>nd</i>	-	<i>nd</i>	-	<i>nd</i>
PLGA/PVA	+	-	+	-	+	-	<i>nd</i>	-	-	-	-	-	<i>nd</i>	-	<i>nd</i>
PLGA/CS	+	+	+	-	+	-	<i>nd</i>	-	-	-	-	-	<i>nd</i>	+	<i>nd</i>
PLGA/PF68	++	+	+	-	+	-	<i>nd</i>	-	-	-	-	+	<i>nd</i>	-	<i>nd</i>
PS	<i>nd</i>	-	+	-	-	<i>nd</i>	<i>nd</i>	-	-	-	-	-	<i>nd</i>	-	<i>nd</i>
Anatase TiO ₂	<i>nd</i>	+	+	-	++	<i>nd</i>	<i>nd</i>	-	-	-	+	-	<i>nd</i>	<i>nd</i>	<i>nd</i>
Rutile TiO ₂	<i>nd</i>	+	+	-	++	<i>nd</i>	<i>nd</i>	-	-	-	+	-	<i>nd</i>	<i>nd</i>	<i>nd</i>

Les niveaux d'internalisation (++,+,-) sont établis par rapport aux cellules non traitées. Les niveaux de toxicité (++, + et -) sont définis selon les gammes de viabilité suivantes : supérieure à 75 % (-); entre 75 % et 35 % (+); inférieur à 35 % (++)). Les niveaux de la réponse inflammatoire et du stress oxydant sont définis par rapport aux conditions non traitées, et selon leur différence significative (Anova, $p \leq 0.05$). *nd* = non déterminé.

Tableau 4. Evaluation de la toxicité des nanoparticules de PLGA, de TiO₂ et de polystyrène par différents paramètres après exposition sur les cellules **THP-1-D en mono-culture.**

THP-1-D		Toxicité							
	Internalisation	MTT		Annexine V / 7-AAD		Réponse Inflammatoire (IL6, IL-6, MCP-1, TNF- α)		Stress Oxydant (ROS)	
Concentration en NP (mg/mL)	0.1	≤ 0.1	> 0.1	0.1	1	0.1	1	0.1	1
PLGA	++	-	+	-	-	-	nd	-	-
PLGA/PVA	+	-	+	-	-	-	nd	-	-
PLGA/CS	+	+	+	-	+	-	nd	-	-
PLGA/PF68	++	+	+	-	-	-	nd	-	-
PS	nd	-	+	nd	nd	-	nd	nd	nd
Anatase TiO ₂	nd	+	+	nd	nd	-	nd	nd	nd
Rutile TiO ₂	nd	+	+	nd	nd	-	nd	nd	nd

Les niveaux d'internalisation (++,+,-) sont établis par rapport aux cellules non traitées. Les niveaux de toxicité (MTT, Annexin V/7-AAD) (++, + et -) sont définis selon les gammes de viabilité suivantes : supérieure à 75 % (-); entre 75 % et 35 % (+); inférieure à 35 % (++)). Les niveaux de la réponse inflammatoire et du stress oxydant sont définis par rapport aux conditions non traitées, et selon leur différence significative (Anova, $p \leq 0.05$). nd = non déterminé.

Table 5. Evaluation de la toxicité des nanoparticules de PLGA, de TiO₂ et de polystyrène par différents paramètres après exposition sur les cellules **THP-1-D** et **A549** en co-culture.

	Co-culture		Toxicité		
	Internalisation		Annexine V / 7-AAD		Réponse Inflammatoire (IL6, IL-6, MCP-1, TNF- α)
Nanoparticules à 0.1 mg/mL	A549	THP-1-D	A549	THP-1-D	Surnageants
PLGA	++	++	-	-	-
PLGA/PVA	-	+	-	-	-
PLGA/CS	+	+	-	+	-
PLGA/PF68	++	+	-	-	-
PS	<i>nd</i>	<i>nd</i>	<i>nd</i>	<i>nd</i>	-
Anatase TiO ₂	<i>nd</i>	<i>nd</i>	<i>nd</i>	<i>nd</i>	-
Rutile TiO ₂	<i>nd</i>	<i>nd</i>	<i>nd</i>	<i>nd</i>	-

Les niveaux d'internalisation (++,+,-) sont établis par rapport aux cellules non traitées. Les niveaux de toxicité (MTT, Annexine V/7-AAD) (++, + et -) sont définis selon les gammes de viabilité suivantes : supérieure à 75 % (-); entre 75 % et 35 % (+); inférieur à 35 % (++) . Les niveaux de la réponse inflammatoire sont définis par rapport aux conditions non traitées, et selon leur différence significative (Anova, $p \leq 0.05$). *nd* = non déterminé.

Conclusion : Profil de toxicité et intérêt des nanoparticules de PLGA

Dans l'optique de proposer des nanovecteurs sûrs pour une administration pulmonaire, notre équipe a développé un axe majeur de recherche afin d'évaluer la toxicité *in vitro* et *in vivo* de nanoparticules biodégradables de PLGA (Tableau 6). Il a été montré sur des projets menés en parallèle que les nanoparticules de PLGA induisent une toxicité très faible vis-à-vis des cellules Calu-3 – lignée de cellules épithéliales bronchiques – (Mura *et al.*, 2011a,b), et vis-à-vis des souris (Santiago, submitted). Au cours de ce projet de thèse nous avons également montré que vis-à-vis de cellules épithéliales alvéolaires, et de macrophages, la toxicité des nanoparticules de PLGA est très faible.

La concentration de 0.1 mg/mL choisie lors de ces études, est une dose pertinente en termes de dose thérapeutique, elle représente environ 400 mg de polymère qui atteindraient la surface des alvéoles (70 cm²) chez l'homme (Patton and Byron, 2007).

De manière générale, les nanoparticules de PLGA testées induisent une toxicité faible, toujours inférieure aux composés reconnus toxiques (cytotoxicité plus faible que les

nanoparticules de TIO_2 , réponse inflammatoire plus faible qu'après exposition au LPS). Cependant, les résultats *in vitro* obtenus au cours de ces différentes études montrent que le polymère de surface joue un rôle des plus importants dans le comportement des nanoparticules vis-à-vis des cellules pulmonaires.

Par exemple, l'emploi du PF68 et du chitosane permet d'avoir une très forte internalisation, certes par les macrophages, mais également par les cellules A549. Les nanoparticules de PLGA/PF68 ont montré une facilité à traverser la couche de mucus des cellules Calu-3, et ainsi à être internalisées par ces dernières (Tableau 6). Il est vrai que ces mêmes nanoparticules provoquent une réponse inflammatoire vis-à-vis des cellules A549 en monoculture, mais lors de la co-culture avec les macrophages, cette réponse est régulée. On peut légitimement penser que cet effet sera observé de manière physiologique chez l'homme, comme il l'est observé lors des études *in vitro* (Tableau 6).

En ce qui concerne le chitosane, il n'est pas dénué de toxicité, et confère également une toxicité aux nanoparticules qui lui sont dérivées. Néanmoins, ses propriétés de muco-adhésion en font un candidat prometteur (Yamamoto *et al.*, 2005) pour l'administration de nanomédicaments à libération prolongée ou à effet retard. Nous remarquerons qu'*in vivo*, aucune toxicité n'a cependant été observée.

Quant à l'utilisation du PVA, elle est certes, très intéressante, car les nanoparticules PLGA/PVA sont généralement moins toxiques que les PLGA/CS et PLGA/PF68. En revanche, bien que les nanoparticules PLGA/PVA soient internalisées en quantité significative par les cellules A549 en monoculture, en co-culture, elles sont principalement capturées par les macrophages et non par les cellules A549. Il semble qu'elles aient plus de mal à échapper à la capture macrophagique que les autres nanoparticules, notamment celles ayant une charge de surface négative, ce qui pourrait être un frein à leur emploi lorsque les cellules épithéliales sont ciblées.

Enfin l'emploi des nanoparticules de PLGA sans stabilisant pourrait montrer un très grand intérêt lorsque les cellules cibles sont des macrophages. En effet, elles sont internalisées en grande quantité, et de plus, à très forte concentration, elles ne provoquent aucune toxicité.

Tableau 6. Bilan des résultats des études de nanotoxicité *in vitro* et *in vivo* obtenus après exposition aux nanoparticules biodégradables de PLGA (poly(lactide-co-glycolide), stabilisées, ou non, par l'alcool polyvinylique (PVA), le chitosane (CS) ou le pluronic F68 (PF68).

Nanoparticules de PLGA		<i>In vitro</i>				<i>In vivo</i>
		Cellules épithéliales alvéolaires A549	Macrophages alvéolaires THP-1-D	Co-culture contact direct A549/THP-1-D	Cellules épithéliales bronchiques Calu-3	Souris Balb/c
Avec agents stabilisants	PLGA	Cytotoxicité modérée à forte concentration Pas de réponse inflammatoire	Pas de cytotoxicité Pas de réponse inflammatoire Pas de stress oxydant	Pas de cytotoxicité Pas de réponse inflammatoire	Non étudiées	Non étudiées
	PLGA/PVA	Cytotoxicité modérée à forte concentration Pas de réponse inflammatoire	Cytotoxicité modérée à forte concentration Pas de réponse inflammatoire Pas de stress oxydant	Pas de cytotoxicité Pas de réponse inflammatoire	Très faible cytotoxicité Pas de réponse inflammatoire Pas de stress oxydant	Pas de recrutement des polymorphonucléaires Pas de réponse inflammatoire
	PLGA/CS	Cytotoxicité modérée à forte concentration Pas de réponse inflammatoire		Pas de cytotoxicité Pas de réponse inflammatoire	Très faible cytotoxicité Pas de réponse inflammatoire Pas de stress oxydant	
PLGA/PF68	Cytotoxicité modérée à forte concentration Réponse inflammatoire modérée	Cytotoxicité modérée Pas de réponse inflammatoire		Très faible cytotoxicité Pas de réponse inflammatoire Traverse la couche de mucus → Pénétration intracellulaire plus importante Pas de stress oxydant		
		PLGA/CS : Toxicité attribuée à la toxicité propre du chitosane PLGA/PF68 : Toxicité et réponse inflammatoire attribuée à l'internalisation en plus grande quantité				

Références

- AKIRA, S., HIRANO, T., TAGA, T. & KISHIMOTO, T. 1990. Biology of multifunctional cytokines: IL 6 and related molecules (IL 1 and TNF). *FASEB J*, 4, 2860-7.
- ALFARO-MORENO, E., NAWROT, T. S., VANAUDENAERDE, B. M., HOYLAERTS, M. F., VANOIRBEEK, J. A., NEMERY, B. & HOET, P. H. M. 2008. Co-cultures of multiple cell types mimic pulmonary cell communication in response to urban PM10. *European Respiratory Journal*, 32, 1184-1194.
- AUWERX, J. 1991. The human leukemia cell line, THP-1: A multifaceted model for the study of monocyte-macrophage differentiation. *Experientia*, 47, 22-31.
- BALDRICK, P. 2010. The safety of chitosan as a pharmaceutical excipient. *Regulatory Toxicology and Pharmacology*, 56, 290-299.
- CARREÑO-GÓMEZ, B. & DUNCAN, R. 1997. Evaluation of the biological properties of soluble chitosan and chitosan microspheres. *International Journal of Pharmaceutics*, 148, 231-240.
- CARTIERA, M. S., JOHNSON, K. M., RAJENDRAN, V., CAPLAN, M. J. & SALTZMAN, W. M. 2009. The uptake and intracellular fate of PLGA nanoparticles in epithelial cells. *Biomaterials*, 30, 2790-8.
- CRAPO, J. D., BARRY, B. E., GEHR, P., BACHOFEN, M. & WEIBEL, E. R. 1982. Cell number and cell characteristics of the normal human lung. *The American review of respiratory disease*, 126, 332-337.
- CROMWELL, O., HAMID, Q., CORRIGAN, C. J., BARKANS, J., MENG, Q., COLLINS, P. D. & KAY, A. B. 1992. Expression and generation of interleukin-8, IL-6 and granulocyte-macrophage colony-stimulating factor by bronchial epithelial cells and enhancement by IL-1 beta and tumour necrosis factor-alpha. *Immunology*, 77, 330-7.
- DAILEY, L. A., JEKEL, N., FINK, L., GESSLER, T., SCHMEHL, T., WITTMAR, M., KISSEL, T. & SEEGER, W. 2006. Investigation of the proinflammatory potential of biodegradable nanoparticle drug delivery systems in the lung. *Toxicology and Applied Pharmacology*, 215, 100-108.
- DESHMANE, S. L., KREMLEV, S., AMINI, S. & SAWAYA, B. E. 2009. Monocyte chemoattractant protein-1 (MCP-1): an overview. *J Interferon Cytokine Res*, 29, 313-26.
- GRABOWSKI, N., HILLAIREAU, H., VERGNAUD, J., SANTIAGO, L. A., KERDINE-ROMER, S., PALLARDY, M., TSAPIS, N. & FATTAL, E. 2013. Toxicity of surface-modified PLGA nanoparticles toward lung alveolar epithelial cells. *International Journal of Pharmaceutics*.
- HE, Y. R., JIN, Y., CHEN, H. S., DING, Y. L., CANG, D. Q. & LU, H. L. 2007. Heat transfer and flow behaviour of aqueous suspensions of TiO₂ nanoparticles (nanofluids) flowing upward through a vertical pipe. *International Journal of Heat and Mass Transfer*, 50, 2272-2281.
- HILLAIREAU, H. & COUVREUR, P. 2009. Nanocarriers' entry into the cell: relevance to drug delivery. *Cell Mol Life Sci*, 66, 2873-96.
- HJORT, M. R., BRENYO, A. J., FINKELSTEIN, J. N., FRAMPTON, M. W., LOMONACO, M. B., STEWART, J. C., JOHNSTON, C. J. & D'ANGIO, C. T. 2003. Alveolar epithelial cell-macrophage interactions affect oxygen-stimulated interleukin-8 release. *Inflammation*, 27, 137-45.

HUANG, M., KHOR, E. & LIM, L. Y. 2004. Uptake and cytotoxicity of chitosan molecules and nanoparticles: effects of molecular weight and degree of deacetylation. *Pharm Res*, 21, 344-53.

INOUE, K., TAKANO, H., OHNUKI, M., YANAGISAWA, R., SAKURAI, M., SHIMADA, A., MIZUSHIMA, K. & YOSHIKAWA, T. 2008. Size effects of nanomaterials on lung inflammation and coagulatory disturbance. *International journal of immunopathology and pharmacology*, 21, 197-206.

KEAN, T. & THANOU, M. 2010. Biodegradation, biodistribution and toxicity of chitosan. *Advanced Drug Delivery Reviews*, 62, 3-11.

KISHIMOTO, T. 1989. The biology of interleukin-6. *Blood*, 74, 1-10.

KOCBACH, A., TOTLANDSDAL, A. I., LÅG, M., REFSNES, M. & SCHWARZE, P. E. 2008. Differential binding of cytokines to environmentally relevant particles: A possible source for misinterpretation of in vitro results? *Toxicology Letters*, 176, 131-137.

KRAKAUER, T. 2002. Stimulant-dependent modulation of cytokines and chemokines by airway epithelial cells: cross talk between pulmonary epithelial and peripheral blood mononuclear cells. *Clin Diagn Lab Immunol*, 9, 126-31.

LIEBER, M., SMITH, B., SZAKAL, A., NELSON-REES, W. & TODARO, G. 1976. A continuous tumor-cell line from a human lung carcinoma with properties of type II alveolar epithelial cells. *Int J Cancer*, 17, 62-70.

MÜLLER, L., RIEDIKER, M., WICK, P., MOHR, M., GEHR, P. & ROTHEN-RUTISHAUSER, B. 2010. Oxidative stress and inflammation response after nanoparticle exposure: differences between human lung cell monocultures and an advanced three-dimensional model of the human epithelial airways. *Journal of The Royal Society Interface*, 7, S27-S40.

MURA, S., HILLAIREAU, H., NICOLAS, J., Kerdine-Romer, S., LE DROUMAGUET, B., DELOMENIE, C., NICOLAS, V., PALLARDY, M., TSAPIS, N. & FATTAL, E. 2011a. Biodegradable nanoparticles meet the bronchial airway barrier: how surface properties affect their interaction with mucus and epithelial cells. *Biomacromolecules*, 12, 4136-43.

MURA, S., HILLAIREAU, H., NICOLAS, J., LE DROUMAGUET, B., GUEUTIN, C., ZANNA, S., TSAPIS, N. & FATTAL, E. 2011b. Influence of surface charge on the potential toxicity of PLGA nanoparticles towards Calu-3 cells. *Int J Nanomedicine*, 6, 2591-605.

PARK, E. K., JUNG, H. S., YANG, H. I., YOO, M. C., KIM, C. & KIM, K. S. 2007. Optimized THP-1 differentiation is required for the detection of responses to weak stimuli. *Inflamm Res*, 56, 45-50.

PATTON, J. S. & BYRON, P. R. 2007. Inhaling medicines: delivering drugs to the body through the lungs. *Nat Rev Drug Discov*, 6, 67-74.

POLITO, A. J. & PROUD, D. 1998. Epithelial cells as regulators of airway inflammation. *Journal of Allergy and Clinical Immunology*, 102, 714-718.

REUL, R., TSAPIS, N., HILLAIREAU, H., SANCEY, L., MURA, S., RECHER, M., NICOLAS, J., COLL, J.-L. & FATTAL, E. 2012. Near infrared labeling of PLGA for in vivo imaging of nanoparticles. *Polymer Chemistry*, 3, 694-702.

ROTHEN-RUTISHAUSER, B., CLIFT, M. J. D., JUD, C., FINK, A. & WICK, P. 2012. Human epithelial cells in vitro – Are they an advantageous tool to help understand the nanomaterial-biological barrier interaction? . *Euro Nanotox Letters*, 4, 1-20.

SAHAY, G., ALAKHOVA, D. Y. & KABANOV, A. V. 2010. Endocytosis of nanomedicines. *Journal of Controlled Release*, 145, 182-195.

SANTIAGO, L. A. *submitted*.

SCHÖLER, N., HAHN, H., MÜLLER, R. H. & LIESENFELD, O. 2002. Effect of lipid matrix and size of solid lipid nanoparticles (SLN) on the viability and cytokine production of macrophages. *International Journal of Pharmaceutics*, 231, 167-176.

SCHÖLER, N., OLBRICH, C., TABATT, K., MÜLLER, R. H., HAHN, H. & LIESENFELD, O. 2001. Surfactant, but not the size of solid lipid nanoparticles (SLN) influences viability and cytokine production of macrophages. *International Journal of Pharmaceutics*, 221, 57-67.

SCHWENDE, H., FITZKE, E., AMBS, P. & DIETER, P. 1996. Differences in the state of differentiation of THP-1 cells induced by phorbol ester and 1,25-dihydroxyvitamin D₃. *J Leukoc Biol*, 59, 555-61.

STRIZ, I., WANG, Y. M., TESCHLER, H., SORG, C. & COSTABEL, U. 1993. Phenotypic markers of alveolar macrophage maturation in pulmonary sarcoidosis. *Lung*, 171, 293-303.

SUZUKI, H., TOYOOKA, T. & IBUKI, Y. 2007. Simple and Easy Method to Evaluate Uptake Potential of Nanoparticles in Mammalian Cells Using a Flow Cytometric Light Scatter Analysis. *Environmental Science & Technology*, 41, 3018-3024.

TSUCHIYA, S., KOBAYASHI, Y., GOTO, Y., OKUMURA, H., NAKAE, S., KONNO, T. & TADA, K. 1982. Induction of maturation in cultured human monocytic leukemia cells by a phorbol diester. *Cancer Res*, 42, 1530-6.

TSUCHIYA, S., YAMABE, M., YAMAGUCHI, Y., KOBAYASHI, Y., KONNO, T. & TADA, K. 1980. Establishment and characterization of a human acute monocytic leukemia cell line (THP-1). *Int J Cancer*, 26, 171-6.

VAL, S., HUSSAIN, S., BOLAND, S., HAMEL, R., BAEZA-SQUIBAN, A. & MARANO, F. 2009. Carbon black and titanium dioxide nanoparticles induce pro-inflammatory responses in bronchial epithelial cells: Need for multiparametric evaluation due to adsorption artifacts. *Inhalation Toxicology*, 21, 115-122.

VERHEUL, R. J., AMIDI, M., VAN STEENBERGEN, M. J., VAN RIET, E., JISKOOT, W. & HENNINK, W. E. 2009. Influence of the degree of acetylation on the enzymatic degradation and in vitro biological properties of trimethylated chitosans. *Biomaterials*, 30, 3129-3135.

WANG, S., YOUNG, R. S., SUN, N. N. & WITTEN, M. L. 2002. In vitro cytokine release from rat type II pneumocytes and alveolar macrophages following exposure to JP-8 jet fuel in co-culture. *Toxicology*, 173, 211-219.

WOTTRICH, R., DIABATÉ, S. & KRUG, H. F. 2004. Biological effects of ultrafine model particles in human macrophages and epithelial cells in mono- and co-culture. *International Journal of Hygiene and Environmental Health*, 207, 353-361.

WU, C., BULL, B., SZYMANSKI, C., CHRISTENSEN, K. & MCNEILL, J. 2008. Multicolor Conjugated Polymer Dots for Biological Fluorescence Imaging. *ACS Nano*, 2, 2415-2423.

YAMAMOTO, H., KUNO, Y., SUGIMOTO, S., TAKEUCHI, H. & KAWASHIMA, Y. 2005. Surface-modified PLGA nanosphere with chitosan improved pulmonary delivery of calcitonin by mucoadhesion and opening of the intercellular tight junctions. *J Control Release*, 102, 373-81.

Conclusions & perspectives



Au cours de ce travail, nous avons mis en évidence la pertinence de la co-culture de cellules A549 et de macrophages différenciés de monocytes THP-1 pour les études de nanotoxicologie concernant les nanoparticules biodégradables. De plus, nous avons élargi les tests de toxicité, grâce à un marquage spécifique des macrophages qui nous a permis de distinguer les deux populations cellulaires, et ainsi suivre le devenir de nos nanoparticules de PLGA et étudier leur cytotoxicité au sein de chaque type cellulaire.

D'autre part, au cours des présentes études, nous avons montré que les nanoparticules à base de PLGA induisent une faible toxicité (*in vitro* et *in vivo*) vis-à-vis de cellules pulmonaire. Néanmoins, bien que le poloxamer (PF68) (Kabanov and Alakhov, 2002), le PVA (DeMerlis and Schoneker, 2003) et le chitosan (Baldrick, 2010) soient des excipients pharmaceutiques approuvés, leur ajout en tant que stabilisant de nanoparticules doit faire l'objet d'études approfondies car ils ne sont pas dénués de toxicité. Nous avons également montré que les nanoparticules de PLGA n'augmentent pas la réponse inflammatoire de cellules pré-activées, et pourraient donc être utilisées dans le cas des maladies inflammatoires telles que l'asthme ou la broncho-pneumopathie chronique obstructive. D'autre part, ces différentes études soulignent également le fait que des différences existent *in vitro* et *in vivo*, et qu'elles fournissent des résultats complémentaires afin d'obtenir des informations solides concernant la toxicité de nanoparticules.

Différents types de perspectives peuvent être envisagées à ce travail.

Dans un premier temps, et ce à très court terme, nous avons prévu de compléter la présente étude en testant une concentration plus élevée en nanoparticules de 1 mg/mL.

D'autre part, plusieurs évolutions du modèle de co-culture peuvent être imaginées :

- Pour des études ultérieures, la co-culture en contact indirect permettrait de mieux comprendre les communications intercellulaires. Les nanoparticules pourraient être administrées sélectivement soit aux macrophages soit aux cellules épithéliales, et ainsi nous pourrions étudier les effets d'une internalisation spécifique par une population cellulaire sur l'autre population.
- D'autre part, une co-culture semblable, de cellules épithéliales et de macrophages pourrait être établie avec des cellules primaires humaines, afin de s'approcher d'avantage des conditions physiologiques (Krakauer, 2002, Hermanns *et al.*, 2004).

Les macrophages peuvent être obtenus par lavages-broncho alvéolaires, ou par différenciation de monocytes isolés du sang.

- La co-culture de cellules épithéliales peut être envisagée avec des monocytes (Hjort *et al.*, 2003, Striz *et al.*, 2011, Striz *et al.*, 2001), afin d'observer, ou non, la différenciation des monocytes en macrophages, lors de l'exposition aux nanoparticules. Nous avons montré au cours de ces études, que la seule présence des cellules A549, ou de leur milieu de culture ne suffit pas à obtenir une différenciation complète en macrophages (pas d'adhésion, et l'expression des marqueurs CD11b et CD54 est très faible).
- La co-culture peut être complexifiée par l'ajout d'autres types cellulaires, tels que les cellules dendritiques (Müller *et al.*, 2010), des mastocytes (Alfaro-Moreno *et al.*, 2008), des cellules endothéliales (Hermanns *et al.*, 2004, Papritz *et al.*, 2010, Alfaro-Moreno *et al.*, 2008), ou des cellules alvéolaires de type I.
- Enfin, l'utilisation de cellules épithéliales à l'interface air-liquide permettrait d'étudier les échanges qui opèrent à l'interface air-sang au sein des alvéoles (Jiang *et al.*, 2001, Bitterle *et al.*, 2006) lorsque les nanoparticules se déposent à la surface des cellules.

Finalement, nous avons montré que les nanoparticules de PLGA sont un bon vecteur pour une administration pulmonaire. La prochaine étape est de charger ces nanoparticules d'un principe actif, pour une application locale (par exemple rifampicine pour traiter la tuberculose ou tobramycine pour traiter la mucoviscidose) ou pour une application systémique (par exemple l'insuline pour le traitement du diabète (Klingler *et al.*, 2009)).

Enfin, dans le cadre du projet global mené au sein de l'équipe, l'administration répétée de nanoparticules de PLGA sur un modèle de souris est envisagée. Cela nous permettrait entre autres d'étudier les effets des produits de dégradation sur la réponse inflammatoire à plus long terme.

Références

ALFARO-MORENO, E., NAWROT, T. S., VANAUDENAERDE, B. M., HOYLAERTS, M. F., VANOIRBEEK, J. A., NEMERY, B. & HOET, P. H. M. 2008. Co-cultures of multiple

cell types mimic pulmonary cell communication in response to urban PM10. *European Respiratory Journal*, 32, 1184-1194.

ANTON, N., JAKHMOLA, A. & VANDAMME, T. F. 2012. Trojan Microparticles for Drug Delivery. *Pharmaceutics*, 4, 1-25.

BALDRICK, P. 2010. The safety of chitosan as a pharmaceutical excipient. *Regulatory Toxicology and Pharmacology*, 56, 290-299.

BITTERLE, E., KARG, E., SCHROEPEL, A., KREYLING, W. G., TIPPE, A., FERRON, G. A., SCHMID, O., HEYDER, J., MAIER, K. L. & HOFER, T. 2006. Dose-controlled exposure of A549 epithelial cells at the air-liquid interface to airborne ultrafine carbonaceous particles. *Chemosphere*, 65, 1784-1790.

DEMERLIS, C. C. & SCHONEKER, D. R. 2003. Review of the oral toxicity of polyvinyl alcohol (PVA). *Food and Chemical Toxicology*, 41, 319-326.

HERMANNNS, M. I., UNGER, R. E., KEHE, K., PETERS, K. & KIRKPATRICK, C. J. 2004. Lung epithelial cell lines in coculture with human pulmonary microvascular endothelial cells: development of an alveolo-capillary barrier in vitro. *Lab Invest*, 84, 736-52.

HJORT, M. R., BRENYO, A. J., FINKELSTEIN, J. N., FRAMPTON, M. W., LOMONACO, M. B., STEWART, J. C., JOHNSTON, C. J. & D'ANGIO, C. T. 2003. Alveolar epithelial cell-macrophage interactions affect oxygen-stimulated interleukin-8 release. *Inflammation*, 27, 137-45.

JIANG, X., INGBAR, D. H. & O'GRADY, S. M. 2001. Adrenergic Regulation of Ion Transport Across Adult Alveolar Epithelial Cells: Effects on Cl⁻ Channel Activation and Transport Function in Cultures with an Apical Air Interface. *The Journal of Membrane Biology*, 181, 195-204.

KABANOV, A. V. & ALAKHOV, V. Y. 2002. Pluronic®; Block Copolymers in Drug Delivery: from Micellar Nanocontainers to Biological Response Modifiers. 19, 72.

KLINGLER, C., MÜLLER, B. W. & STECKEL, H. 2009. Insulin-micro- and nanoparticles for pulmonary delivery. *International Journal of Pharmaceutics*, 377, 173-179.

KRAKAUER, T. 2002. Stimulant-dependent modulation of cytokines and chemokines by airway epithelial cells: cross talk between pulmonary epithelial and peripheral blood mononuclear cells. *Clin Diagn Lab Immunol*, 9, 126-31.

MÜLLER, L., RIEDIKER, M., WICK, P., MOHR, M., GEHR, P. & ROTHENRUTISHAUSER, B. 2010. Oxidative stress and inflammation response after nanoparticle exposure: differences between human lung cell monocultures and an advanced three-dimensional model of the human epithelial airways. *Journal of The Royal Society Interface*, 7, S27-S40.

PAPRITZ, M., POHL, C., WÜBBEKE, C., MOISCH, M., HOFMANN, H., HERMANNNS, M. I., THIERMANN, H., KIRKPATRICK, C. J. & KEHE, K. 2010. Side-specific effects by cadmium exposure: Apical and basolateral treatment in a coculture model of the blood-air barrier. *Toxicology and Applied Pharmacology*, 245, 361-369.

STRIZ, I., BRABCOVA, E., KOLESAR, L., LIU, X. D., BRABCOVA, I., SEKERKOVA, A., POOLE, J. A., JARESOVA, M., SLAVCEV, A. & RENNARD, S. I. 2011. Epithelial

cells modulate genes associated with NF kappa B activation in co-cultured human macrophages. *Immunobiology*, 216, 1110-6.

STRIZ, I., SLAVCEV, A., KALANIN, J., JARESOVA, M. & RENNARD, S. I. 2001. Cell-cell contacts with epithelial cells modulate the phenotype of human macrophages. *Inflammation*, 25, 241-6.

WOTTRICH, R., DIABATÉ, S. & KRUG, H. F. 2004. Biological effects of ultrafine model particles in human macrophages and epithelial cells in mono- and co-culture. *International Journal of Hygiene and Environmental Health*, 207, 353-361.

◆ Résumé

La toxicologie pulmonaire *in vitro* de nanoparticules biodégradables, formulées à partir de poly(lactide-co-glycolide) (PLGA), et des nanoparticules non-biodégradables de polystyrène et de dioxyde de titane, est évaluée sur des cellules épithéliales alvéolaires et des macrophages, en mono et co-culture.

◆ Mots-clefs

Nanoparticules, polymères, cellules alvéolaires, macrophages, co-culture

◆ Laboratoire de rattachement

Institut Galien Paris Sud

UMR CNRS 8612

PÔLE : PHARMACOTECHNIE ET PHYSICO-CHIMIE PHARMACEUTIQUE

UNIVERSITÉ PARIS-SUD 11

UFR «FACULTÉ DE PHARMACIE DE CHATENAY-MALABRY »

5, rue Jean Baptiste Clément

92296 CHÂTENAY-MALABRY Cedex